

Bdelloid rotifers (Rotifera, Bdelloidea) of China: diversity and new records

Yue Zeng^{1,2}, Nan Wei³, Qing Wang¹, Nataliia S. Iakovenko^{4,5}, Ying Li¹, Yufeng Yang^{1,2}

1 Institute of Hydrobiology, College of Life Science and Technology, Jinan University, Guangzhou 510632, China **2** Southern Marine Science and Engineering Guangdong Laboratory (Zhuhai), Zhuhai, 519000, China **3** South China Institute of Environmental Sciences, Ministry of Ecology and Environment, Guangzhou 510530, China **4** Czech University of Life Sciences Prague, Faculty of Forestry and Wood Sciences, Kamýcká 129, CZ–16521 Praha 6–Suchbát, Czech Republic **5** Schmalhausen Institute of Zoology NAS of Ukraine, Department of Fauna and Systematics, Bogdana Khmelnyts'kogo 15, 01601 Kyiv, Ukraine

Corresponding author: Yufeng Yang (tyyf@jnu.edu.cn)

Academic editor: Yasen Mutafchiev | Received 26 January 2020 | Accepted 26 March 2020 | Published 16 June 2020

<http://zoobank.org/FDDDD1E54-33F9-4C3B-8CD3-9467D7E2CB79>

Citation: Zeng Y, Wei N, Wang Q, Iakovenko NS, Li Y, Yang Y (2020) Bdelloid rotifers (Rotifera, Bdelloidea) of China: diversity and new records. ZooKeys 941: 1–23. <https://doi.org/10.3897/zookeys.941.50465>

Abstract

Bdelloid rotifers are a group of microscopic invertebrates known for their obligate parthenogenesis and exceptional resistance to extreme environments. Their diversity and distributions are poorly studied in Asia, especially in China. In order to better understand the species distribution and diversity of bdelloid rotifers in China, a scientific surveys of habitats was conducted with 61 samples (both terrestrial and aquatic habitats) from 11 provinces and regions of China, ranging from tropics to subtropics with a specific focus on poorly sampled areas (Oriental) during September 2017 to October 2018. A total of 59 morphospecies (including subspecies) were found, of which, thirty-nine morphospecies (including one genus) are new records for China, almost doubling the number of previous records. Four rare morphospecies (*Adineta* cf. *acuticornis* Haigh, *A. beysunae* Örstan, *Habrotrocha ligula loxoglotta* De Koning and *H. serpens* Donner) are depicted and redescribed, and an updated checklist of Chinese bdelloids with their location and ecological information is presented. This study provides new data from a large region of China, enriching the knowledge of bdelloid biodiversity, and their global biogeography.

Keywords

bdelloids, biogeography, morphospecies, Oriental region, taxonomy

Introduction

Bdelloid rotifers are microscopic invertebrates that constitute a subclass Bdelloidea of the phylum Rotifera, known for their peculiar obligate parthenogenesis (Welch and Meselson 2000; Welch et al. 2004) and outstanding ability to withstand harsh periods through anhydrobiosis (Ricci 1998; Gladyshev and Meselson 2008). The minute size of bdelloids (from less than 160 to 500–600 μm) allows their long-distance dispersal by wind, water, and animals to access to almost all possible habitats (Bohonak and Jenkins 2003; Fenchel 2004; Kellogg and Griffin 2006). They inhabit both aquatic (mainly freshwater lakes, ponds, and streams) and terrestrial habitats (e.g., mosses, lichens, tree barks, soil and litter) (Donner 1965). Rarely, bdelloids are found in marine and brackish waters (Fontaneto et al. 2006; Demirkalp et al. 2010; Song 2014).

Analysis of Bdelloidea taxonomy characteristics is problematic because only observation of living and active specimens allows appropriate identification of species. That is why it has not been widely carried out. Furthermore, there are no readily available reagents that can be used to anesthetize them and preserve their bodies fully extended (Örstan and Plewka 2017). Until recently, only about 460 bdelloid species have been described world-widely (Segers 2007), but there is ample evidence that the total number of bdelloid species is at least several times greater than the current one (Fontaneto et al. 2011; Robeson et al. 2011). In addition, the intensity of taxonomic researches on bdelloid species in different regions of the world was extremely uneven, thus the species diversity varies greatly from region to region. For instance, over 300 species are known from Europe (Fontaneto et al. 2007), while only about 50 species are found in the Oriental region (Segers 2007).

In China, only 48 bdelloid morphospecies have been reported (Zhuge et al. 1998; Koste and Zhuge 1998; Yin and Xu 2016) (Table 1). The first study on the Chinese bdelloid rotifers was reported by Thorpe (1893), who found four species of *Rotaria* in Yangtze River area in Wuhu city, Anhui Province. After that, few fragmental reports from fresh waters and terrestrial environments in a large region of China were presented (Daday 1906; Stewart 1908; Gee 1927; Wang 1961; Bartoš 1963; Wang 1974; Gong 1983; Koste and Zhuge 1996, 1998; Zhuge et al. 1998; Yin and Xu 2016). Up to now, this taxon has not been actively studied in China comparing to Europe or even to Antarctica (Segers 2007), and the biogeography of bdelloids in South Asia is unclear, and their habitat preferences are incomplete. This study aimed to conduct a taxonomic work and evaluate the diversity of bdelloid rotifers in China, especially the poorly investigated tropical zones of the Oriental biogeographic region.

Materials and methods

Sampling area, collection procedures and sample processing

A total of 61 samples was collected during the period from September 2017 to October 2018 in 11 provinces and regions of China across its subtropical and tropical zones at altitudes from 0–2850 m above sea level from four types of terrestrial habitat (soil,

Table 1. Checklist of bdelloid rotifers recorded from China before 2015.

Species	Habitats	EL (m)	WT (°C)	AT (°C)	pH	Distribution and references
<i>Adineta gracilis</i> Janson, 1893	Moss	800–1400	–	–	–	GD (l)
<i>A. oculata</i> (Milne, 1886)	Moss	800–1800	–	–	–	GD (l)
<i>A. vaga</i> (Davis, 1873)	Moss and stream	0–1750 m	16–18	26–28	5	GD (f, l), TB (g, h)
<i>Dissotrocha aculeata</i> (Ehrenberg, 1832)	Pond, river and bog	0–3650	20	20	6	IM (b), HB, SD, ZJ, SC, XJ (e) TB (h), GD (l)
<i>D. macrostyla</i> (Ehrenberg, 1832)	Pond and bog	0–3030	17–20	13.5	6	JS (d), TB (h), HA (i)
<i>D. macrostyla tuberculata</i> (Gosse, 1886)	Puddle on the roadside	–	20	–	7.6	HA(k)
<i>Habrotrocha angusticollis angusticollis</i> (Murray, 1905)	<i>Sphagnum</i> , river, lake branch channel and puddle with aquatic plant	0–4750	14–30	21–25.5	6–8.5	ZJ (e), TB (h), HA (i, k), GD (l)
<i>H. angusticollis attenuata</i> (Murray, 1906)	Moss	–	–	–	–	GD (f)
<i>H. ampulla</i> (Murray, 1911)	River with macrophyte	–	20	–	6.32	HA (i)
<i>H. collaris</i> (Ehrenberg, 1832)	Bog, stream, lake and moss	800–3800	12–19.5	15–25	6–7	TB (h), GD (l)
<i>H. constricta</i> (Dujardin, 1841)	–	–	–	–	–	HA (j)
<i>H. elegans</i> (Milne, 1886)	Lake	3658	13	15	7	TB (h)
* <i>H. flexicollis</i> Bartoš, 1963	Moss	–	–	–	–	GD (f)
<i>H. fusca</i> (Bryce, 1894)	Moss	–	–	–	–	GD (f)
<i>H. insignis</i> Bryce, 1915	Moss	–	–	–	–	GD (f)
<i>H. modesta</i> Bartoš, 1963	Moss	–	–	–	–	GD (f)
<i>H. munda</i> Bryce, 1913	Bog	4200	16.5	13.5	6	TB (h)
<i>H. perforata</i> (Murray, 1906)	Moss	–	–	–	–	GD (f)
<i>H. pulchra</i> (Murray, 1905)	Spring with attachment from meadow, stone and soil, puddle from glacier	5700	17	11	8	TB (g, h)
<i>H. pusilla</i> (Bryce, 1893)	Puddle from spring and wet moss on stone	830–2400	30	25	6	TB (h)
<i>H. thienemanni</i> Hauer, 1924	Puddle with aquatic plant and moss, glacier	830–5550	13–30	15–25	5–7	TB (g, h)
<i>H. tridens</i> (Milne, 1886)	Moss	600–1900	–	–	–	GD (l)
<i>Otostephanos</i> cf. <i>donneri</i> (Bartoš, 1959)	Aquatic ecosystem	–	–	–	–	YN (j)
<i>Macrotrachela bullata</i> (Murray, 1906)	Stream with algae or moss	1668–4150	10–18	19–28	5–6	TB (g, h)
<i>M. ehrenbergii</i> (Janson, 1893)	Moss	4500	–	–	–	TB (h)
<i>M. insolita</i> De Koning, 1947	Moss	1000–1200	–	–	–	GD (l)
<i>M. multispinosa</i> Thompson, 1892	Attachments on aquatic plants, bogs and moss from grass lands	3300	16	17	6	TB (h)
<i>M. muscicola</i> (Milne, 1886)	Springs and wet moss	4150–4500	6	11–19	6	TB (h)
<i>M. plicata</i> (Bryce, 1892)	Puddles	4400–4500	12–14	10–14	7	TB (h)
<i>M. papillosa</i> Thompson, 1892	Moss	–	–	–	–	GD (f)
<i>M. punctata</i> (Murray, 1911)	Attachment from stone and wet grass	3800–3850	12	19	7	TB (h)
<i>M. quadricornifera</i> Milne, 1886	Moss	0–1900	–	–	–	GD (l)
<i>Mniobia tentans</i> Donner, 1949	Stream with algae or moss	1668–1750	16–18	25–28	5	TB (g, h)
<i>Philodina citrina</i> Ehrenberg, 1832	Rice field, puddle, shallow and wet moss	600–4350	12–27	10–28	6–7	TB(c, h), GD (l)
<i>P. erythrophthalma</i> Ehrenberg, 1830	Pond, pool and stream with algae	0–3370	9	12	7	HB (e), TB (c, h)
<i>P. megalotrocha</i> Ehrenberg, 1832	Lake with macrophyte, pond, water reservoir and rice field	–	20–26	–	6–8	HB, SH, JS, ZJ (e) HA(i, k)
<i>P. nemoralis</i> Bryce, 1903	Rice field, bog and moss	2000–2400	36	29	5	TB (h)
<i>P. roseola</i> Ehrenberg, 1832	River, pond, marsh and moss	0–3100	–	–	–	IM (b) TB(c), HB, SH, JS, ZJ, HA (e) GD (l)
<i>P. vorax</i> (Janson, 1893)	Stream, spring and puddle from river or glacier	2400–5500	7–17	–	6–8	TB (g, h)
* <i>Pleuretra similis</i> Bartoš, 1963	Moss	–	–	–	–	GD (f)
<i>Rotaria citrina</i> (Ehrenberg, 1838)	Rice field and pool	0–2400	13–28	–	6	HB (e), TB (h)

Species	Habitats	EL (m)	WT (°C)	AT (°C)	pH	Distribution and references
<i>R. macroceros</i> (Gosse, 1851)	Yangtze River, lake and moss	–	25	–	6	AH (a), HB (e), GD (l), HA(i, k)
<i>R. macrura</i> (Ehrenberg, 1832)	River	–	–	–	–	IM (b)
<i>R. neptunia</i> (Ehrenberg, 1830)	Pond, rice field and puddle	0–3650	18–26	–	6–8.7	AH (a), SH, JS, ZJ, HB, BJ, HL, LN, GS, HN, GD, GX, YN, SC (e), HA (i, k), TB (h)
<i>R. rotatoria</i> (Pallas, 1766)	Pond and rice field	0–830	20–26	–	6–8.7	AH (a), IM (b), SH, HB (e), TB (h), HA (i, k)
<i>R. sordida</i> (Western, 1893)	Moss; polluted lake	–	21	–	7.1	GD (f), HA(i, k)
<i>R. tardigrada</i> (Ehrenberg, 1830)	Lake, polluted river and puddle	0–3658	18–25	–	6–7	AH (a), HA (i, k), HL, SH, GS, JS (e) TB (h)
<i>R. tridens</i> (Montet, 1915)	Bog, wet moss pool and attachment from stone	2900–4550	–	15–18	6	TB (c, h)

Sources: (a) (Thorpe 1893); (b) (Daday 1906); (c) (Stewart 1908); (d) (Gee 1927); (e) (Wang 1961); (f) (Bartoš 1963); (g) (Wang 1974); (h) (Gong 1983); (i) (Koste and Zhuge 1996); (j) (Zhuge 1997); (k) (Koste and Zhuge 1998); (l) (Yin and Xu 2016). 'cf.' is retained for those taxa which have some differences from the nominate morphospecies, requiring further study. *: China only. Abbreviation: AH: Anhui; AT: air temperature; BJ: Beijing; EL: elevation; GD: Guangdong; GS: Gansu; GX: Guangxi; HA: Hainan; HB: Hubei; HL: Heilongjiang; HN: Hunan; IN: Inner Mongolia; JS: Jiangsu; LN: Liaoning; SD: Shandong; SC: Sichuan; SH: Shanghai; TB: Tibet; WT: water temperature; XJ: Xinjiang; YN: Yunnan; ZJ: Zhejiang.

mosses, leaf litter and lichens) and four types of aquatic habitat (plankton, benthos, periphyton and dew) in fresh or brackish waters (Fig. 1, Table 2). Of these samples, eleven were collected from fresh water, six from brackish water, one from dew on leaves, thirty from mosses, ten from leaf litter, two from lichens, and one from soil with mosses.

Based on the definition of boundary between the Palearctic and Oriental biogeographic regions in China (Norton et al. 2010), fifty-seven samples were collected in the Oriental region, while four samples (NX1, NX2, GS1, QH1) were collected in the Palearctic region (Table 2). According to the Geodetector model to partition subtropical and tropical zone in China (Dong 2017), forty-two samples were collected in the subtropical zone, while nineteen samples (GD1–19) were collected in the tropical zone (Table 2).

Samples from terrestrial habitats were placed into firmly closed paper envelopes, then dried at room temperature and stored in the envelopes for several weeks or months. Planktonic samples were obtained by filtering 1 to 5 liters of water through a plankton net with a mesh size 30 µm. Benthic ones were collected by scraping the bottom of water bodies with a 500 ml plastic bottle. Periphytic rotifers were obtained by shaking or scraping aquatic plants, then preserved in plastic bottles.

Samples from aquatic habitats were concentrated by a nylon net of 30 µm mesh size, then examined in lab immediately without fixating or anesthetization. Rotifers from mosses, lichens and leaf litter were extracted by washing the substrate with distilled water following the method of Peters (1993). Soil rotifers were extracted by the method of wet-sieving and centrifugation in a sugar gradient (Freckman 1993).

Light microscopy procedures

Rotifers isolated from waters were transferred into a Petri dish and sorted under a dark field dissecting microscope (SZX10, Olympus, Japan) with a magnification of 64×. Selected specimens were placed onto glass slides by using micropipettes, then

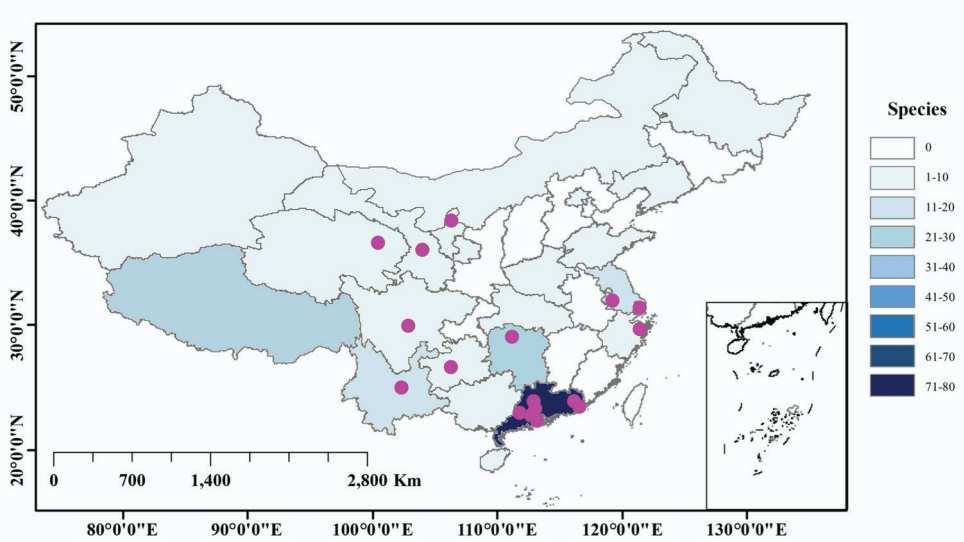


Figure 1. Locations of the sampling sites in this study (purple circles) and species richness of bdelloid rotifers (blue) recorded between 1908 and 2018 in China.

examined alive under a microscope (BX51, Olympus, Japan) with magnification of $\times 200$ – 400 . All living specimens were recorded and photographed using a digital camera (Truechrome Metrics, China) with the software of TCCapture. Photos and digital screenshots from videos were used for species identification and illustrations.

Species identification

Species were identified by both external morphology and anatomy using the keys of Donner (1965) and the original descriptions and redescrptions of specific species (Murray 1906; Song and Kim 2000; Yakovenko 2000a, 2000b; Kutikova 2005; Bielańska-Grajner 2013; Song 2014, 2015; Song and Min 2015; Song and Lee 2017). Drawings of some rare morphospecies were made with Adobe Illustrator CC 2018 and Photoshop CC 2017.

All rotifers were measured from screenshots of digital videos after Iakovenko et al. (2013, 2015) and Örstan (2018). Total length (TL) in the case of adinetid rotifers is the distance between the middle of the anterior rim of the head excluding rostrum, and the posterior rim of the spur pseudosegment; head length (HL) is the distance between the anterior edge of the head (posterior to the rostrum) and the anterior rim of the antennal pseudosegment, i.e., TL and HL do not include the rostrum, because it was usually bent under the head (Iakovenko et al. 2015). The head length in *A. beysunae* is the distance between the anterior edge of the head and an imaginary line passing through the innermost denticles of the rakes to better compare it with the original description (Örstan 2018). The number of denticles on each rake is represented formulaically using an ‘en dash’ (Örstan 2018). We counted the distal foot with the toes as a pseudosegment separate from the one carrying the spurs as Bryce (1894), Donner (1965) and Iakovenko et al. (2013, 2015) did.

Table 2. Sampling locality information of this survey.

Locality codes	Locality	Sampling date	Habitat	GPS coordinates	Elevation (m)
GD1	Chaozhou	18.08.2017	Moss on concrete	23°58'15.13"N, 116°38'12.14"E	1136
GD2	Chaozhou	18.08.2017	Moss on bark	23°58'14.93"N, 116°38'12.08"E	1139
GD3	Chaozhou	18.08.2017	Moss on rock	23°58'14.99"N, 116°38'12.11"E	1138
GD4	Chaozhou	18.08.2017	Moss on soil	23°58'15.02"N, 116°38'12.09"E	1138
GD5	Chaozhou	18.08.2017	Moss on rock	23°55'59.37"N, 116°36'59.84"E	436
GD6	Guangzhou	05.11.2017	Dry moss on bark	23°06'35.11"N, 113°14'21.20"E	10
GD7	Guangzhou	20.09.2017	Lotus pond	23°07'54.80"N, 113°20'39.44"E	16
GD8	Guangzhou	05.11.2017	Lotus pond	23°07'54.80"N, 113°20'39.44"E	16
GD9	Guangzhou	25.10.2018	Lotus pond	23°07'54.80"N, 113°20'39.44"E	16
GD10	Guangzhou	11.06.2018	Moss on concrete	23°08'1.29"N, 113°20'38.81"E	15
GD11	Guangzhou	11.06.2018	Soil	23°07'51.89"N, 113°20'37.45"E	18
GD12	Haiou island	28.10.2017	Water hyacinth root in brackish water	22°58'23.36"N, 113°30'40.95"E	4
GD13	Guangzhou	13.06.2018	Bamboo leaf litter	23°18'4.12"N, 113°26'23.21"E	214
GD14	Guangzhou	13.06.2018	Bamboo leaf litter	23°18'18.99"N, 113°26'56.14"E	152
GD15	Guangzhou	20.06.2017	Bottom of lotic water	23°18'0.59"N, 113°26'27.47"E	226
GD16	Guangzhou	26.10.2018	Urban river	23°03'29.0"N, 113°24' 26.6"E	0.75
GD17	Nanao island	22.04.2018	Puddle	23°25'44.88"N, 117°01'49.56"E	108
GD18	Nanao island	09.01.2018	<i>Gracilaria lichenoides</i> in brackish pond	23°27'18.13"N, 117°7'31.35"E	170
GD19	Nanao island	22.04.2018	Lotic water	23°26'38.29"N, 117°05'22.94"E	124
GD20	Qingyuan	12.05.2018	Moss on concrete	24°36'46.73"N, 112°35'57.02"E	237
GD21	Qingyuan	12.05.2018	Moss on concrete	24°36'40.72"N, 112°35'50.11"E	143
GD22	Qingyuan	12.05.2018	Moss on soil	24°36'40.44"N, 112°36'9.26"E	142
GD23	Qingyuan	12.05.2018	Moss on bark	24°36'41.29"N, 112°36'9.26"E	175
GD24	Qiao island	29.10.2017	Bottom of brackish pool in mangrove	23°27'32.41"N, 117°06'3.59"E	53
GD25	Nanao island	18.11.2018	Leaf litter	22°25'42.45"N, 113°37'51.53"E	137
GD26	Nanao island	18.11.2018	Leaf litter	23°27'18.13"N, 117°7'31.35"E	9
GS1	Lanzhou	07.06.2018	Wet moss near pond	36°08'25.56"N, 103°41'41.18"E	1615
GZ1	Guiyang	24.08.2017	Moss on rock	26°36'1.75"N, 106°41'10.39"E	1213
GZ2	Guiyang	24.08.2017	Moss on rock	26°05'52.74"N, 105°52'55.89"E	1170
HN1	Changde	20.06.2017	Moss on rock	29°3'10.0"N, 111°40'13"E	31
HN2	Changde	15.09.2017	Moss on rock	29°3'10.0"N, 111°40'13"E	31
HN3	Changde	11.12.2017	Moss on rock	29°3'10.0"N, 111°40'13"E	31
HN4	Changde	12.03.2018	Moss on rock	29°3'10.0"N, 111°40'13"E	31
HN5	Changde	11.12.2017	Aquatic plant	29°02'23.49"N, 111°42'33.35"E	35
HN6	Changde	12.12.2017	<i>Lemna minor</i> in river	29°7'20.0"N, 111°39'49"E	57
HN7	Changde	15.09.2017	Water sample from a pond	29°3'10"N, 111°40'13.0"E	30
HN8	Changde	12.03.2018	Moss on soil	29°03'13.78"N, 111°40'12.69"E	31
HN9	Changde	11.12.2017	Lotus pond	29°03'3.68"N, 111°39'57.93"E	35
JS1	Nanjing	15.08.2018	Bamboo leaf litter	32°3'28.63"N, 118°45'27.47"E	39
JS2	Nanjing	15.08.2018	Moss with leaf litter	32°3'28.19"N, 118°45'24.52"E	34
NX1	Yinchuan	02.07.2018	Moss from desert (32 °C of soil surface)	38°33'45.38"N, 106°32'0.37"E	1128
NX2	Yinchuan	01.07.2018	Extremely dry <i>Juniperus</i> litter	38°29'22"N, 106°12'1"E	1109
QH1	Qinghai lake	09.06.2018	Wet moss on bark	36°47'46.11"N, 101°06'18.99"E	2850
SC1	Wawu mountain	23.08.2017	Wet moss on bark	29°40'15.26"N, 102°56'53.92"E	2105

Locality codes	Locality	Sampling date	Habitat	GPS coordinates	Elevation (m)
SC2	Wawu mountain	23.08.2017	Wet moss on bark	29°40'10.36"N, 102°56'53.92"E	2105
SC3	Wawu mountain	23.08.2017	Wet moss on bark	29°40'10.36"N, 102°56'53.92"E	2100
SH1	Chongming island	29.12.2017	Aquatic plants in brackish water	31°31'9.5"N, 121°56'4.3"E	3
SH2	Chongming island	29.12.2017	Moss on soil in brackish marsh	31°29'54"N, 121°55'20.7"E	3
SH3	Chongming island	29.12.2017	Reed root in brackish water	31°30'43.9"N, 121°57'27.9"E	3
SH4	Chongming island	29.12.2017	Aquatic plants in brackish water	31°31'2.9"N, 121°55'3.1"E	2
YN1	Kunming	01.06.2018	Moss on concrete	25°3'20.5"N, 102°42'8.6"E	1889
YN2	Kunming	01.06.2018	Moss on soil	25°3'2.2"N, 102°42'5.1"E	1908
YN3	Kunming	01.06.2018	Moss on concrete	25°3'6.1"N, 102°42'5.41"E	1900
YN4	Kunming	01.06.2018	Lichens on bark	25°8'0.2"N, 102°39'40.6"E	1900
YN5	Kunming	01.06.2018	Moss on rock	24°57'59.4"N, 102°39'35"E	1888
YN6	Kunming	11.10.2018	Lichens on rock	24°57'49.1"N, 102°37'44.6"E	2150
YN7	Kunming	11.10.2018	Leaf litter	24°57'53.2"N, 102°37'44.6"E	2143
YN8	Kunming	11.10.2018	Dew on leaves	24°57'55.5"N, 102°37'44.3"E	2136
ZJ1	Hangzhou	19.11.2017	Dry moss on <i>Torreya grandis</i> bark	30°21'42.0"N, 119°34'28"E	305
ZJ2	Ningbo	03.11.2018	Bamboo leaf litter,	29°52'40.3"N, 121°33'15.55"E	37
ZJ3	Zhoushan	03.11.2018	Leaf litter	–	–

GPS coordinates based on WGS84 system. Abbreviation: GD: Guangdong; GS: Gansu; GZ: Guizhou; HN: Hunan; JS: Jiangsu; NX: Ningxia; QH: Qinghai; SC: Sichuan; SH: Shanghai; XJ: Xinjiang; YN: Yunnan; ZJ: Zhejiang.

Abbreviations

BW	body width (when creeping)	TL	total length
CW	corona width	TrL	trunk and rump length
FL	foot length	RaL	ramus length
FW	foot width	RkW	rake width
HL	head length	RL	rump length
HW	head width	RW	rump width
MinNW	minimal neck width	SL	spur length
MxNW	maximal neck width	SSW	spur pseudosegment width
NL	neck length	TrW	trophi width

Results

Species diversity

Fifty-nine morphospecies (including three subspecies) were identified in this survey (Table 3), and the bdelloids that were unidentifiable to the species level were not included in the list. Of them, thirty-nine taxa (including one genus) are new records for China, and thirty-eight species are new records for the Oriental region. The species list of Chinese bdelloid fauna has been increased from 48 to 87. Detailed information about their distribution and ecological information is reported in Tables 2, 3.

During our survey, five collected bdelloids have a general resemblance to known species, but also showed some dissimilar traits from previously described taxa, and they were qualified with ‘cf.’ and await further analysis. One of these doubtful species, reported as *H. cf. spicula* Bryce, which showed a upturned dorsal protrusion. *Philodina cf. indica* Murray, *P. cf. proterva* Milne and *P. cf. parvicalcar* showed relative wide range of variations in their head proportion, which need further analyses.

Among these new records, some species are very rare, and few were first found out of their type localities or habitats, e.g., *Adineta beysunae* Örstan and *Habrotricha ligula loxoglotta* De Koning; some new morphological characteristics were observed and need to be added to the original descriptions, e.g., *Adineta cf. acuticornis* Haigh and *Habrotricha serpens* Donner, which are redescribed and illustrated in the next section.

Species richness of bdelloids recorded between 1908 and 2018 in different provinces of China is presented in Figure 1, showing that sampling intensity greatly influenced the species diversity in different regions of China. For instance, the provinces of Guangdong, Yunnan and Hunan were the subject of 26, eight, and nine studies, which recorded 33, 18, and 16 morphospecies, respectively, whereas the provinces of Jiangsu, Zhejiang, Guizhou, Sichuan, Shanghai, Qinghai, Ningxia, and Gansu have no more than four investigations, which only recorded up to six morphospecies for each.

Redescriptions of some rare morphospecies

Phylum Rotifera Cuvier, 1817

Class Eurotatoria De Ridder, 1957

Order Adinetida Melone & Ricci, 1995

Family Adinetidae Melone & Ricci, 1995

Genus *Adineta* Hudson & Gosse, 1886

***Adineta cf. acuticornis* Haigh, 1967**

Figure 2; Table 3

Material. Eight specimens found in mosses and two specimens found in lichens, from tropical (GD 6) and subtropical (YN 5–6, SC 2) zones (Table 2).

Description. Body transparent and colorless, with smooth skin. No eyespots. Rostrum rather long when animal creeps and stretches out, distal rostral pseudosegment semi-circular and flattened. Rostral lamella divided into two broad sickles-like lobes, immobile, laterally elongated, no trace of cilia under the present microscope image. Small oval head, HW 63–90% of HL and 11–16% of TL, HL 15–18% of TL. Five rectangular denticles in each rake.

Neck width not distinct from head and trunk. The width of the first two pseudosegments of neck approximately equal to HW, the second neck pseudosegment much wider and swollen than the first one. Antenna of two pseudosegments, with length 56–64% of the bearing pseudosegment width. Trunk oval, BW 15–22% of TL. Rump conical, TrL 54–67% of TL. The stomach lumen very narrow and Z-shaped

Table 3. Bdelloid rotifers found in this study with their updated biogeographic distribution after Segers (2007).

Species	Locality codes	Biogeographic regions
<i>Adineta</i> cf. <i>acuticornis</i> Haigh, 1967	GD6, YN5–6, SC2	AUS, ORI*
<i>A. barbata</i> Janson, 1893	GD10, 14, JS1, ZJ2	AFR, ANT, AUS, NEA, NEO, PAL, ORI*
<i>A. bartosi</i> Wulfert, 1960	GZ2	PAL, ORI*
<i>A. beysunae</i> Örsan, 2018	GD13–14, 25–26, YN7–8, JS1	NEA, ORI*
<i>A. cuneata</i> Milne, 1916	GD1–2, SC2, JS2, YN6–7	AFR, AUS, NEA, PAL, ORI*
<i>A. gracilis</i> Janson, 1893	HN2, QH1, JS1	AFR, ANT, AUS, NEA, ORI, PAL
<i>A. oculata</i> (Milne, 1886)	GD7, YN3, HN1	NEO, PAL, ORI*
<i>A. ricciae</i> Segers & Shiel, 2005	GD23, HN4	AUS, ORI*
<i>A. steineri</i> Bartoš, 1951	GD13	ANT, AUS, NEA, NEO, PAL, ORI*
<i>A. vaga</i> (Davis, 1873)	GZ2, HN2–4, ZJ2, YN1,7, GD5,7,13–14, 20–21,23	AFR, ANT, AUS, NEA, NEO, ORI, PAL
<i>Disotrocha macrostyla</i> (Ehrenberg, 1838)	HN6	AFR, AUS, NEA, NEO, ORI, PAL
<i>Habrotrocha bidens</i> (Gosse, 1851)	ZJ1	AFR, AUS, NEA, NEO, ORI, PAL
<i>H. cf. spicula</i> Bryce, 1913	GD2	AFR, AUS, ORI, PAL
<i>H. constricta</i> (Dujardin, 1841)	HN2	AFR, ANT, AUS, NEA, NEO, PAC, PAL, ORI*
<i>H. insignis</i> Bryce, 1915	GD3	AUS, PAL, ORI*
<i>H. ligula loxoglotta</i> De Koning, 1947	YN5	PAL, ORI*
<i>H. rosa</i> Donner, 1949	GD25	AFR, AUS, NEA, NEO, PAL, ORI*
<i>H. serpens</i> Donner, 1949	GD6	AFR, AUS, PAL, ORI*
<i>Otostephanos regalis</i> Milne, 1916	GD13	AFR, PAL, ORI*
<i>Scapanotrocha semitecta</i> Donner, 1951	SC1	NEO, PAL, ORI*
<i>Macrotrachela bullata</i> (Murray, 1906)	GD3–4, GZ2	AFR, ORI, PAL
<i>M. ehrenbergii</i> (Janson, 1893)	HN7, GZ1	AFR, AUS, NEA, NEO, ORI, PAC, PAL
<i>M. habita</i> (Bryce, 1894)	GD6, 11,20, 22–23, YN1–3, GZ1	AFR, ANT, AUS, NEA, NEO, ORI, PAL
<i>M. heuitti</i> (Murray, 1911)	SH1	AFR, PAL, ORI*
<i>M. inermis</i> Donner, 1965	YN4	PAL, ORI*
<i>M. insolita</i> De Koning, 1947	GD2, HN8	ANT, AUS, NEA, NEO, PAL, ORI*
<i>M. latior</i> Donner, 1951	YN7	PAL, ORI*
<i>M. libera</i> Donner, 1949	HN4	PAL, ORI*
<i>M. multispinosa multispinosa</i> Thompson, 1892	GD6	AFR, AUS, NEA, NEO, ORI, PAL
<i>M. multispinosa brevispinosa</i> (Murray, 1908)	YN5	AFR, AUS, NEO, ORI, PAL
<i>M. nana</i> (Bryce, 1912)	QH1	AFR, AUS, NEA, NEO, PAL
<i>M. plicata</i> (Bryce, 1892)	SC2–3	AFR, AUS, NEA, PAL, ORI*
<i>M. quadricornifera quadricorniferoidea</i> De Koning, 1929	JS1, 2	AFR, ANT, NEO, ORI, PAL
<i>M. quadricornifera scutellata</i> Schulte, 1954	GD13	AUS, PAL, ORI*
<i>M. timida</i> Milne, 1916	SC1–3, YN7	AFR, AUS, PAL, ORI*
<i>Philodina acuticornis</i> Murray, 1902	GD20–21, JS1, ZJ2	AFR, AUS, NEA, NEO, PAL, ORI*
<i>P. cf. indica</i> Murray, 1906	YN4	NEA, PAL, ORI*
<i>P. cf. proterva</i> Milne, 1916	GD5, YN1, 6, ZJ2	AFR, AUS, NEA, PAL, ORI*
<i>P. childi</i> Milne, 1916	GD14, YN7	PAL, ORI*
<i>P. duplicalcar</i> (De Koning, 1947)	NX2	PAL
<i>P. megalotrocha</i> Ehrenberg, 1832	HN5–6, 9, GD9, 12	AFR, AUS, NEA, NEO, ORI, PAL
<i>P. cf. parvicalcar</i> De Koning, 1947	SH2, GD25	PAL, ORI*
<i>P. plena</i> (Bryce, 1894)	QH1, YN7	AFR, ANT, AUS, NEA, NEO, PAL, ORI*
<i>P. rapida</i> Milne, 1916	YN7	AFR, NEO, PAL, ORI*
<i>P. roscola</i> Ehrenberg, 1832	GD19	AFR, AUS, NEA, NEO, PAL, ORI*
<i>P. rugosa</i> Bryce, 1903	GD20–21	AFR, AUS, NEA, NEO, PAL, ORI*
<i>P. tenuicalcar</i> De Koning, 1947	NX1	PAL
<i>P. tranquilla</i> Wulfert, 1942	HN2, GS1	AUS, PAL, ORI*
<i>P. vonax</i> (Janson, 1893)	HN2	AFR, AUS, NEA, NEO, ORI, PAL
<i>Pleuretra africana</i> Murray, 1911	YN2, 6	AFR, NEO, ORI*
<i>P. brycei</i> (Weber, 1898)	GD15, 23	AFR, AUS, NEA, NEO, PAL, ORI*
<i>Rotaria cirrina</i> (Ehrenberg, 1838)	GD16	AFR, AUS, NEA, PAL, ORI*
<i>R. laticeps</i> Wulfert, 1942	GD15, 24	AUS, PAL, ORI*
<i>R. neptunia</i> Ehrenberg, 1830	GD16–17	AFR, AUS, NEA, NEO, ORI, PAL
<i>R. neptunoida</i> Harring, 1913	GD16–17, 19	AFR, AUS, NEA, ORI, PAL
<i>R. rotatoria</i> (Pallas, 1766)	HN5, GD8, 18, SH1, 3	AFR, AUS, NEA, NEO, ORI, PAL
<i>R. sordida</i> (Western, 1893)	HN2, 8, YN2–3, GD13–14,26, JS1	AFR, AUS, NEA, NEO, ORI, PAL
<i>R. tardigrada</i> (Ehrenberg, 1830)	HN9	AFR, AUS, NEA, NEO, ORI, PAL
<i>R. tridens</i> (Montet, 1915)	HN6, 9, GD9, 12	AUS, NEA, NEO, PAL, ORI#

*: Taxa new for China. #: new for ORI. Abbreviations: AFR: Afrotropical region; ANT: Antarctic region; AUS: Australian region; NEA: Nearctic region; NEO: Neotropical region; ORI: Oriental region; PAC: Pacific region; PAL: Palearctic region. 'cf.' is retained for those taxa which have some differences from the nominate morphospecies, requiring further study. Locality codes see Table 2 for sampling information.

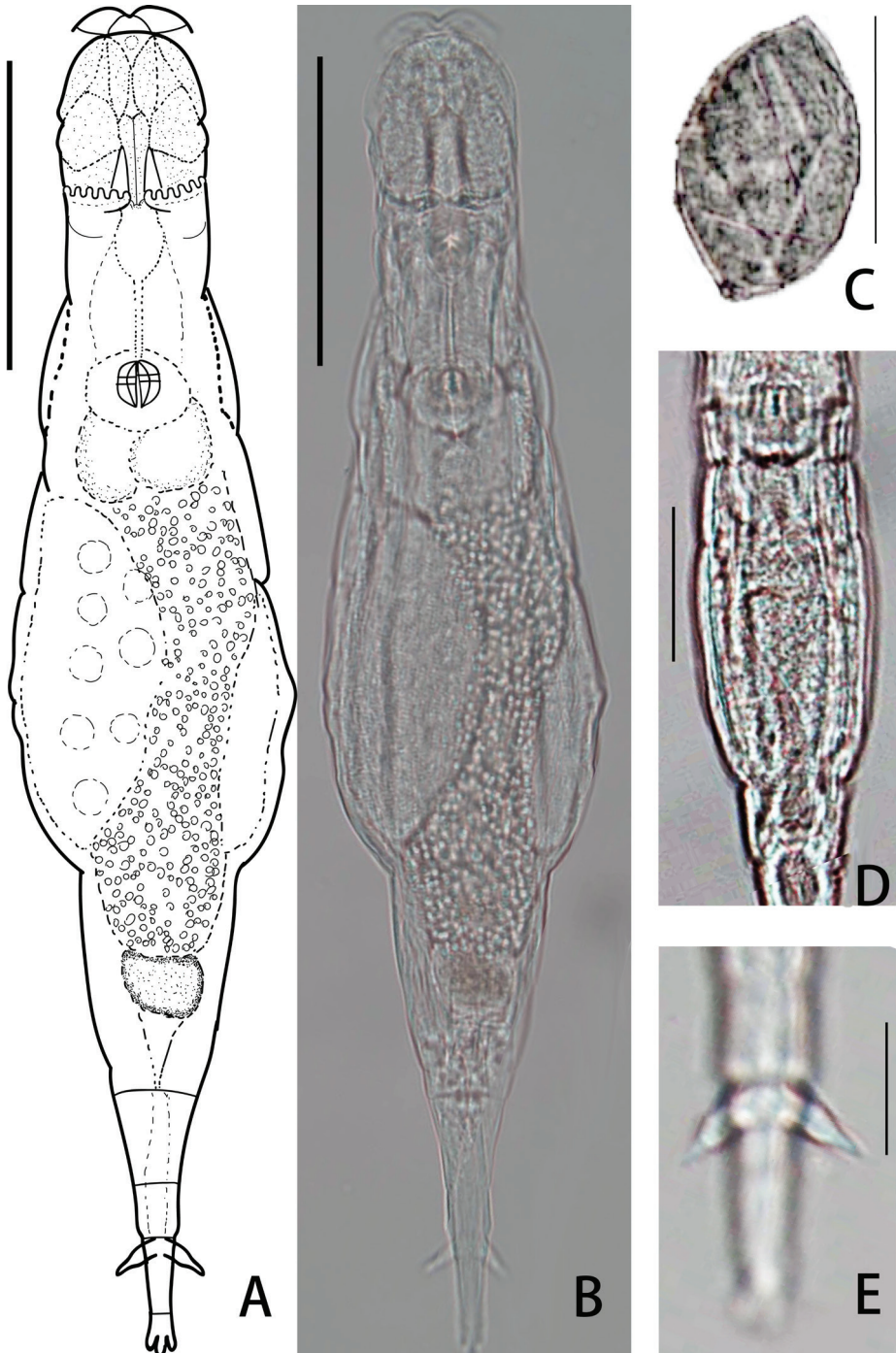


Figure 2. *Adineta cf. acuticornis* Haigh, 1967 **A, B** habitus, ventral view **C** egg **D** stomach lumen **E** spur. Scale bars: 50 μm (**A–D**); 10 μm (**E**).

(Fig. 2D). Oviparous; egg oval and smooth, one knob at each pole (Fig. 2C); Vitellarium large with eight nuclei.

Foot slim and short, of four pseudosegments. Spurs long, the inner edge of the spurs almost parallel to the straight outer edge for two-thirds of its length, then a small bulge followed by a contraction and tapers to a sharp point (Fig. 2E). SL 4–8% of TL, and 143–193% of SSW. Three long and unsegmented toes. Dorsal toe longer than two ventral toes. Trophi small, round. Dental formula 2/2.

Measurements. The detailed measurements are summarized in Table 4 with a comparison of the original data from Haigh (1967).

Remarks. *Adineta acuticornis* has not been found since its original description by Haigh (1967) and was considered as an endemic morphospecies of New Zealand (Shiel and Green 1996). It was found in China for the firstly time also in the Oriental biogeographic region recorded in two provinces of China in 2017 or 2018. It was recorded in damp mosses on soil face in the type locality, whereas in this study, numerous specimens were recorded in both dry and damp mosses, and two specimens in lichens on soil surface.

A distinct characteristic differentiating this morphospecies from *Adineta vaga* Davis is its wide and rostral lamellae which are slightly wider than the anterior head, while the rostral lamellae of *A. vaga* are narrower than the anterior head. It differs from *Adineta glauca* Wulfert by its spur shape, which is short and has a flat base, while *A. glauca* spur with a swollen base. This morphospecies differs from *Adineta longicornis* Murray by its spur shape which has bulge, while *A. longicornis* spur is slender and acute (Murray 1906: 5a, 5b).

The general morphology of the Chinese specimen conforms to the description of the New Zealand population, except the position of the spur contraction is closer to the tip (the contraction is in the middle of the spur in Haigh's description) and the stomach lumen do not have distinct two loops as Haigh's description. A comparison with Haigh's (1967) body dimensions showed a similar body proportion (Table 4). Since there was no genetic evidence to prove its actual systematic status, we assigned 'cf.' (resembling original description) as the status of this find. Besides, we observed three new morphological features missed by Haigh (1967): each rake with five denticles, a larger vitellarium with eight nuclei and egg with one knob on each pole.

Adineta beysunae Örstan, 2018

Figure 3; Table 3

Material. Numerous specimens found in leaf litter from three provinces (GD13–14, 25–26, YN7, JS1) across tropical and subtropical zones. One specimen found in dew on leaves from Southwest of China (YN8) (Table 2).

Description. Body angulate, large and transparent. Sometimes the organs in the trunk show brown coloration. No eyespots. Rostral lamella flat and widened, with two lateral triangular auricular protrusions holding long rostral setae under them (the

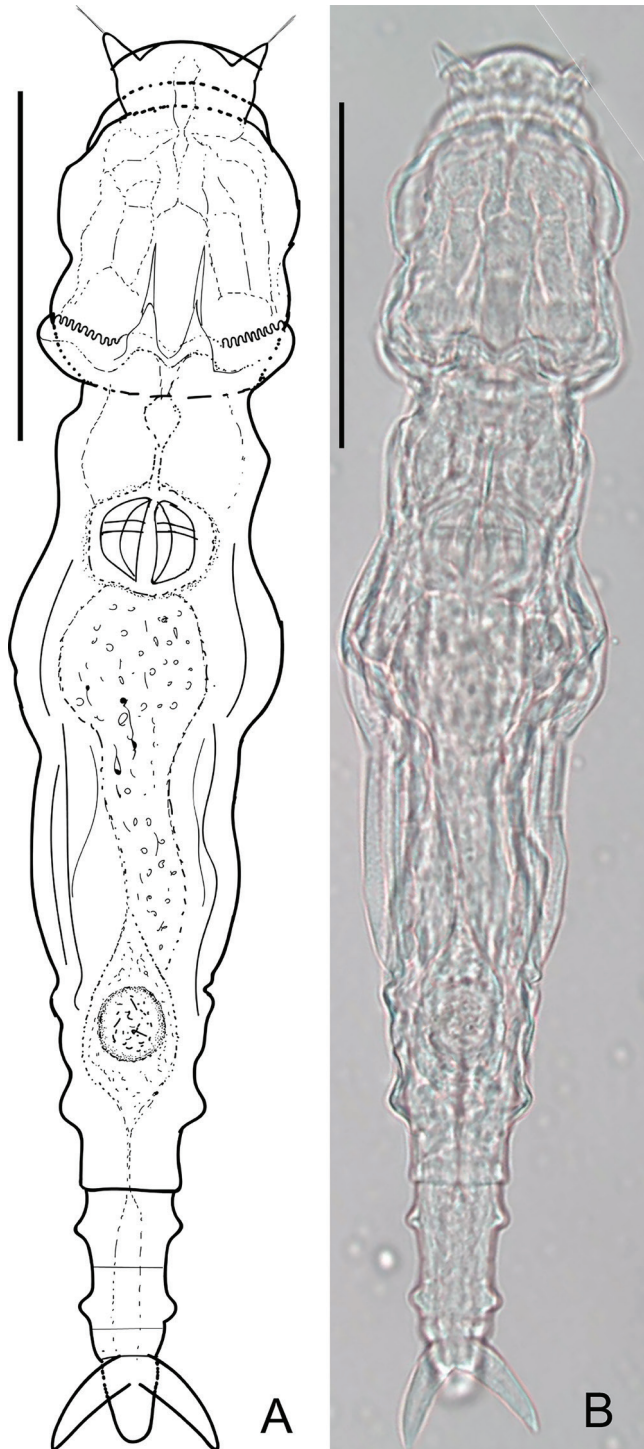


Figure 3. *Adineta beysunae* Örstan, 2018 **A, B** habitus, dorsal view. Scale bars: 50 μm (**A, B**).

Table 4. Comparison the body dimensions of *Adineta acuticornis* between Chinese specimens and the original description.

Measurements	Chinese specimens	Original description
TL	166–266 (227±33)	210
BW	30–61 (44±10)	
HL	30–45 (40±5)	
HW	25–37 (30±4)	30
NL	15–34 (25±6)	
MinNW	16–31 (25±4)	
MxNW	22–42 (31±6)	
RL	20–44 (30±9)	
RW	22–38 (25±7)	
FL	21–32 (28±4)	
FW	11–16 (13±2)	
SL	11–13 (12±1)	12
SSW	6–8 (7±1)	9
RaL	9–12 (10±1)	
TrW	5–6 (5±1)	7.5
Rake	5–5	
TL/SL	14.4–21.6 (18.3±3.4)	17.5
TL/HW	6.6–8.6 (7.5±0.8)	7
Rostral lamella	immobile	immobile
Antenna	1/2 MNW	half neck width
Foot segments	4	4
Stomach lumen	one loop	two loops
Habitats	lichen and moss	damp moss on soil

BW: body width; FL: foot length; FW: foot width; HL: head length; HW: head width; MinNW: minimal neck width; MxNW: maximal neck width; NL: neck length; RaL: ramus length; RL: rump length; RW: rump width; SL: spur length; SSW: spur pseudosegment width; TL: total length; TrW: trophi width. Measurements are given in μm .

number of stiff under each could not be counted under microscope). Setae length varies from 11 to 30 μm . Head trapezoid, rather large and long, HW 80–110% of HL^b, HL^b 17–22% of TL, HW 13–20% of TL. Numbers of U-gaps denticles on rakes: 9–9 ($N = 3$), 10–10 ($N = 4$).

Neck distinct from head, the first two pseudosegments of neck narrower than HW. Trunk oval. Posterior end of the first rump pseudosegment with a pair of lateral angular knobs.

Foot of five pseudosegments with two pairs of lateral knobs on its first two pseudosegments, FL 14–22% of TL. Spurs long and sturdy, with short interspace, SL 6–8% of TL, 172–284% of SSW. Three short unsegmented toes. Ventral toe longer than two dorsal toes. Dental formula 2/2.

Measurements. TL 289±40 μm , HL^b 49±5 μm , HW 45±4 μm , FL 49±8 μm , SL 20±1 μm , SSW 10±1 μm , RkW ($N = 2$, with 9–9 denticles; $N = 4$, with 10–10 denticles) 21±1 μm , RaL ($N = 14$) 15.9±2 μm , TrW 7.3±1 μm .

Remarks. This is the second report of this morphospecies since its original description by Örstan (2018) in rainwater and plant debris from the United States. In the present study, *A. beysunae* was found in leaf litter and dew on leaves. And interestingly, it

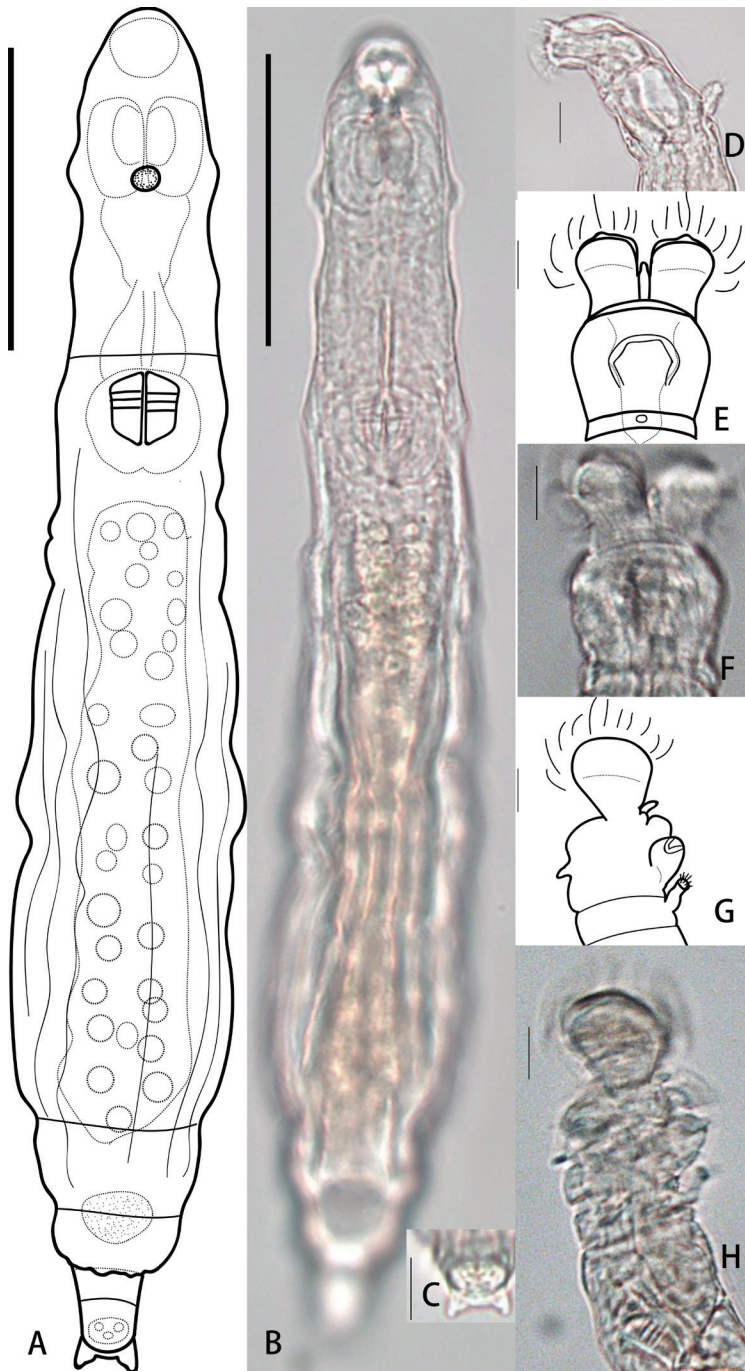


Figure 4. *Habrotrocha ligula loxoglotta* De Koning 1947 **A, B** habitus, creeping, dorsal view **C** rostrum, lateral view **D, E** head, dorsal view **F, G** head, with ligula sloping obliquely to the dorsal side, lateral view. Scale bars: 50 μm (**A, B**), 10 μm (**C–G**).

was abundant in 60% of all leaf litter samples. Our study suggested *A. beysunae* might have a habitat preference for leaf litter and temporary waterbodies.

Family Habrotrochidae Harring, 1913

Genus *Habrotrocha* Ehrenberg, 1838

***Habrotrocha ligula loxoglotta* De Koning, 1947**

Figure 4; Table 3

Materials. Five specimens found in mosses on rock from Southwest China (YN5) (Table 2).

Description. Body slender and transparent, integument smooth. Rostrum long and strongly bent ventrally. Rostral lamellae divided into two semi-circular lobes and wider than the anterior rim of rostrum. Head similar to hexagon, HW 89% of HL. Corona slightly narrower than collar, with papillae clearly seen in the middle of each trochus, CW 97% of HW. Trochal discs separated by a narrow, V-shaped sulcus, in which a cylindrical ligula bends obliquely to the dorsal side (Fig. 4F, G). A slight contraction near the tip which then forms a small papilla on the tip of the ligula, attaining the level of the discs at the inner side (Fig. 4D, E). Upper lip a flat bow. Neck also bent ventrally when animal creeps. The first pseudosegment of neck slightly narrower than the head at the corners of the mouth, not distinct from head and trunk. A pair of lateral cuticular bulges on the dorsal antenna pseudosegment. Antenna with two segments, its length 30–40% of the bearing pseudosegment width.

Trunk slender and cylindrical, TrL 59–67% of TL. Rump conical, with both pseudosegments somewhat swollen and strong arched up dorsally and roofing the foot, the posterior rim of the second pseudosegment creased, RL 8–10% of TL.

Foot short with three pseudosegments, FL 6–8% of TL. Bulbous spurs short and triangular shape, with distinct tips and wide interspace, base swollen. The width of interspace 114% of SL, 97% of the swollen width. Three stout unsegmented toes of the same length. Trophi small, dental formula 3/3.

Measurements. TL 186 ± 43 μm , NL 27 ± 3 μm , TrL 119 ± 37 μm , RL 156 ± 2 μm , RW 22 ± 7 , FL 12 ± 2 μm , SL 4 ± 2 μm , RaL 13 ± 1 μm , TrW 5.6 ± 0.5 μm .

Remarks. *Habrotrocha ligula loxoglotta* was originally described from Holland (De Koning 1947), later reported from beech-oak needle-litter in Germany, from dry mosses in France (Donner 1951) and from mosses in Austria (Kutikova 2005). In this study, it was found for the first time in China (Yunnan Province) as well as in the Oriental region.

***Habrotrocha serpens* Donner, 1949**

Figure 5; Table 3

Materials. Five specimens found in dry mosses on bark from southern China (GD6) (Table 2).

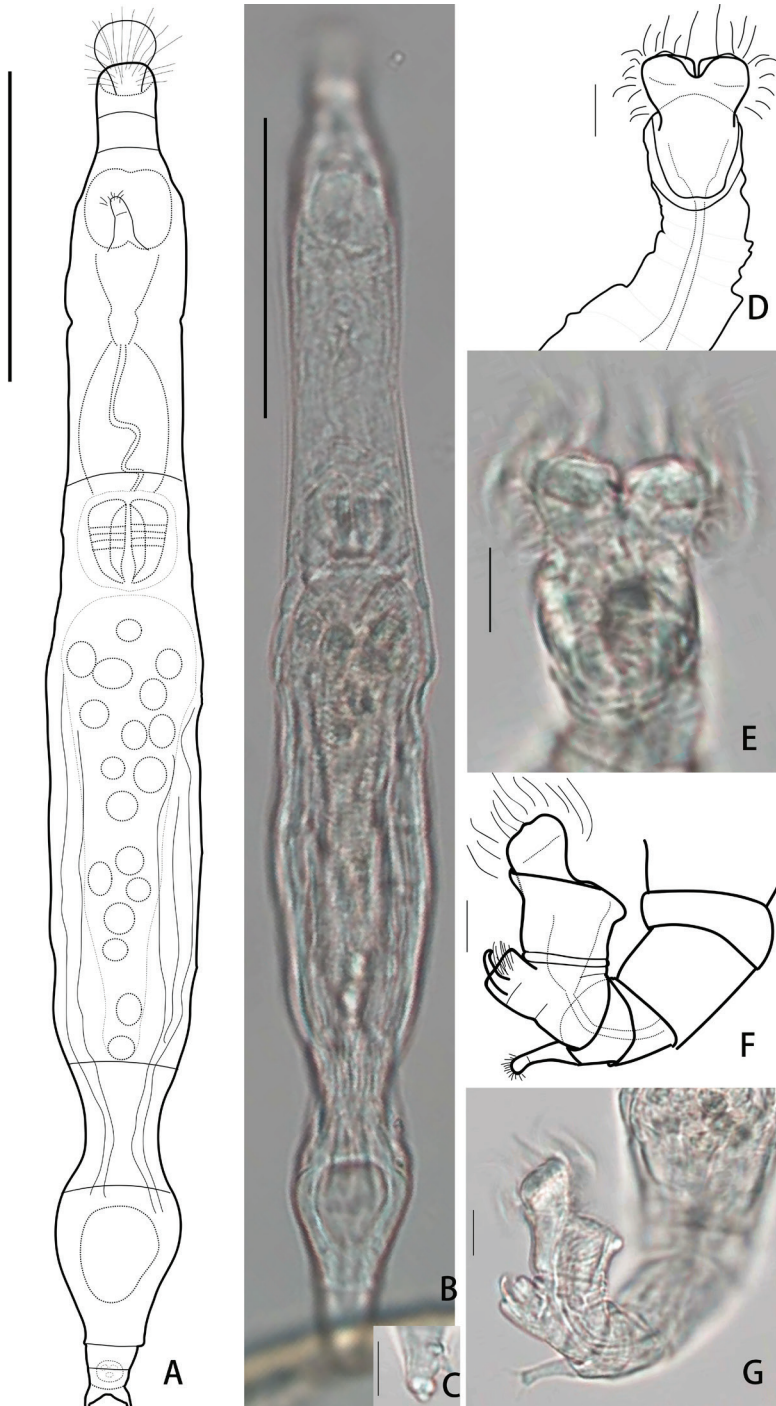


Figure 5. *Habrotrocha serpens* Donner, 1949 **A, B** habitus, creeping (not fully extended), dorsal view **C** three toes, dorsal view **D, E** head, ventral view **F, G** head, lateral view (the second pseudosegment of rostrum contracted). Scale bars: 50 μm (**A, B**); 10 μm (**C–G**).

Table 5. Comparison the body dimensions of *Habrotrocha serpens* between Chinese specimens and the original description from Donner (1949; 1970).

Measurements	Chinese specimens	Donner 1949	Donner 1970
TL	213	193–273	200
BW	18.7		17
HL	42		
HW	18.4		
CW	19.7		
NL	31.2		
MinNW	17.8		
MxNW	19.2		
RL	26.6		
RW	20		
FL	12		
FW	9.9		
SL	3.4		
SSW	5.4		
RaL	14	12.7	14.8
TrW	5.9		
TL/BW	11.4		11.8

BW: body width when creeping; FL: foot length; FW: foot width; HL: head length; HW: head width; CW: corona width; MinNW: minimal neck width; MxNW: maximal neck width; NL: neck length; RaL: ramus length; RL: rump length; RW: rump width; SL: spur length; SSW: spur pseudosegment width; TL: total length; TrW: trophi width. Measurements are given in μm .

Description. Body extremely slender (BW is only about 6% of TL), long and cylindrical, integument transparent and smooth. Rostrum rather long, with two pseudosegments. The first pseudosegment circular and slightly bigger than the second one which often contracted (Fig. 5B). One whole semi-circular lamella not divided into lobes, rather large, broader than the rostrum, covers the long and stiff tactile cilia. Head slender, HW 44% of HL, 22% of TL. Corona also slender, a little wider than the head, CW 107% of HW. Trochal pedicels grown together, central rounded papillae on each separated trochal discs, incline to the dorsal side. Upper lip low, narrow and without lobes, slightly arched, not covered by the incompletely extended rostrum. Lower lip spoon-shaped, strongly protrudes forward.

Neck slender. Throat very short, pharyngeal tube long, undulating before the mastax. Dorsal antenna slender, with two segments, its length 86% of the antennal pseudosegment width. Trunk slender, the two lateral sides of trunk almost parallel when animal fully extended, the last trunk segment often strongly contracted. Rump conical, with both pseudosegments swollen, arched up dorsally and roofing the foot, RL 12% of TL.

Foot very short, of four pseudosegments, FL 5% of TL. Spurs triangular and have swollen base, each with curved inner margins and a very small interspace. SL 63% of SSW. Three short unsegmented and of approximately equal length toes (Fig. 5C). Trophi large, dental formula 4/4.

Measurements. The detailed measurements are summarized in Table 5 with a comparison of the original data from Donner (1949; 1970).

Remarks. The general morphology of our sample conforms with the description of the Austrian population except that the rostrum is not always fully expanded to/ exceeding the upper lip in a feeding position. It may be because of the second pseudosegment of rostrum often contracted. Additionally, we observed three approximately equal-lengthed toes which were not clear in Donner's (1949) description.

This morphospecies was first described from soil from Austria by Donner (1949), and then recorded in moss and soil from Austria and Czechoslovakia (Bartoš 1951); in needle litter, *Calamagrostis* turf, grasses and leaf litter from Austria, Czechoslovakia, Romania, and Spain (Donner 1965, 1970). It is new for China as well as for the Oriental region.

Discussion

Taxonomy and diversity of bdelloid rotifers in China

Only 48 species were recorded in eleven studies conducted in China between 1908 and 2018 (Table 1), which implies that taxonomic and diversity researches on Chinese bdelloids are very limited. Moreover, only 65% (31 of 48) of the recorded morphospecies were illustrated and described (e.g., Wang 1961; Bartoš 1963; Gong 1983), and many of the illustrations are inaccurate, not showing important details and the descriptions are not detailed enough to verify their identity. Besides, there are 17 morphospecies listed in the literature without any illustrations, photographs or descriptions (e.g., Koste and Zhuge 1996; Yin and Xu 2016), which need further verification. Also, some species were recorded out of their specific habitats (e.g., *H. thienemanni* Hauer and *P. roseola* Ehrenberg) and some recorded in unusual environments (e.g., *Habrotrocha pulchra* Murray, *H. thienemanni* Hauer, *Mnionbia tentans* Donner, *Macrotrachela bullata* Murray, and *Philodina vorax* Janson were abundant in glacier over 5500 m a.s.l.) (Table 1). These ecological differences may hide potential cryptic taxa and need further studies combined with new techniques such as DNA taxonomy.

Due to a lack of insufficient taxonomic and diversity research in China, species richness is extremely uneven in different provinces of China. More morphospecies were recorded in the Tibetan Plateau (27 morphospecies) and Guangdong Province (22 morphospecies) with more samples collected (Stewart 1908; Bartoš 1963; Wang 1974; Gong 1983; Yin and Xu 2016). Four new morphospecies were reported in Guangdong, including *Habrotrocha modesta* Bartoš, *H. flexicollis* Bartoš, *Pleuretra proxima* Bartoš, and *P. similis* Bartoš. Unfortunately, they were never found again, and these are considered as disappeared 'endemic morphospecies' in latter researches. Research on different habitats of bdelloids were also uneven. Most studies were only focused on fragmented fresh-water bodies or mosses, but did not pay attention to other habitats such as brackish waters, soil and litter. Therefore, more studies are necessary to explore

the taxonomy and diversity of bdelloid rotifers in China, especially with a focus on the areas and habitats that were not well studied.

Geographical distribution and ecological information of Chinese bdelloids

The high dispersal potential of bdelloids has supposedly led to their generally cosmopolitan distribution (Fenchel and Finlay 2004). The previous extensive sampling of bdelloids confirms that some species can be found in distant areas on different continents, but also some species can only be found in specific area (Donner 1965; Segers 2007). At present, studies of biogeography on these taxa are not comprehensive. For example, *Adineta ricciae* Segers and Shiel, previously considered as an Australia-endemic species, was observed in South China (the Oriental region); *A. beysuanae* has been described in a container filled with plant debris and rain water from the United States (Örstan 2018), and it was then found in similar or drier habitats (dew and leaf litter) from China. These findings imply that the currently described distribution of bdelloids is incomplete and may be strongly influenced by the sampling effort, especially in the poorly investigated areas, such as South Asia.

With study extending to more ecological habitats, some morphospecies were found in a broader range of habitats. We observed five brackish water morphospecies: *Rotaria rotatoria* Pallas, *R. laticeps* Wulfert, *R. tridens* Montet, *Philodina megalotrocha* Ehrenberg and *Macrotrachela hewitti* Murray. They were found among aquatic plants or brackish temporary puddle with sediment in mangrove. Noticeably, *R. rotatoria* was abundant and dominated in *Gracilaria lichenoides* (a red alga) culture ponds, possibly because *G. lichenoides* could provide suitable habitats. These ecological differences seem to represent different ecological niches, which may hide some interesting phenomena of separated evolutionary lineages. For example, *Adineta vaga*, which occurs in the multiple types of habitats, has a large amount of cryptic diversity (Fontaneto et al. 2011).

More extensive surveys of bdelloids in Asia

More than half of the recorded morphospecies from this study (some presumed cosmopolitan) are new records for the Oriental region as well as for South Asia. As there are still considerable gaps in faunistic studies in the Oriental region, we do not yet have sufficient faunistic data to determine the true distributions of bdelloids. Our findings highlight the need for further taxonomic studies on bdelloids in Asia. Furthermore, asexual bdelloids have evolved independently in spite of being effectively sympatric, indicating that they may adapt to different ecological niches, thus the type of habitat is a key player for microscopic species diversity and evolution (Birky et al. 2005). Applications of molecular phylogeny for identification of bdelloid species would be invaluable in uncovering the actual systematic status of some euryoecious or variable morphospecies so that we may better understand the true distribution of bdelloid species.

Acknowledgements

We gratefully acknowledge Prof. Larry Liddle (Long Island University, USA), Dr. Xuejia He (Research Center for Harmful Algae and Aquatic Environment, Jinan University), Dr. Thomas Mesaglio (University of New South Wales, Australia), Dr. Xiao Ma (South China Sea Institute of Oceanology, Chinese Academy of Sciences) and Prof. Zhili He (University of Oklahoma) for their comments on the manuscript and the linguistic help. We also thank Dr. Zhiwei Liu (Jinan University) for helping on the map of the sampling localities. This research was supported by National Natural Science Foundation of China (41673080, 31601840).

References

- Bartoš E (1951) The Czechoslovak Rotatoria of the order Bdelloidea. *Věstník. Československé Zoologické Společnosti* 15: 241–500.
- Bartoš E (1963) Die Bdelloidender Moosprobenaus China und Java. *Věstník. Československé Zoologické Společnosti* 27: 31–42.
- Bielanska-Grajner I, Ejsmont-Karabin J, Iakovenko N (2013) Fauna słdkowodna Polski, Zeszyt 32C: Wrotki (Rotifera, Bdelloidea). Wydawnictwo Uniwersytetu Łódzkiego, Łódź, 153 pp.
- Bohonak AJ, Jenkins DG (2003) Ecological and evolutionary significance of dispersal by freshwater invertebrates. *Ecology Letters* 6 (8): 783–796. <https://doi.org/10.1046/j.1461-0248.2003.00486.x>
- Daday J (1906) Édesvízi mikroskopi állatok Mongoliából. *Mathematikai és Természettudományi Értesítő* 24(2): 34–77.
- De Smet WH (1998) Preparation of rotifer trophi for light and scanning electron microscopy. *Hydrobiologia* 387: 117–121. <https://doi.org/10.1023/A:1017053518665>
- Demirkalp FY, Saygi, Y, Caglar SS, Gunduz E, Kilinc S (2010) Limnological assesment on the Brakish Shallow Liman Lake from Kizilirmak Delta (Turkey). *Journal of Animal and Veterinary Advances* 9(16): 2132–2139. <https://doi.org/10.3923/javaa.2010.2132.2139>
- Dong YX, Xu Q, Yang R, Xu CD, Wang YY (2017) Delineation of the northern border of the tropical zone of China's mainland using Geodetector. *Acta Geographica Sinica* 72(1): 135–147. [in Chinese] <https://doi.org/10.11821/dlxb201701011>
- Donner J (1949) Rotatorien der Humusböden. *Österreichische Zoologische Zeitschrift* 2(1): 117–151.
- Donner J (1951) Rotatorien der Humusböden. III. Teil. *Zoologische Jahrbücher, Abteilung für Systematik, Geographie und Biologie der Tiere* 79: 614–638.
- Donner J (1965) Ordnung Bdelloidea (Rotatoria, Rädertiere). Akademie-Verlag, Berlin, 267 pp.
- Donner J (1970) Rotatorien aus einigen Böden und Moosen Spaniens und seiner Inseln. *Revue d'Écologie et de Biologie du Sol* 7: 501–532.
- Fenchel TOM, Finlay BJ (2004) The ubiquity of small species: patterns of local and global diversity. *BioScience* 54(8): 777–784. [https://doi.org/10.1641/0006-3568\(2004\)054\[0777:TUOSSP\]2.0.CO;2](https://doi.org/10.1641/0006-3568(2004)054[0777:TUOSSP]2.0.CO;2)

- Fontaneto D, Melone G (2003) On some rotifers new for the Italian fauna. *Italian Journal of Zoology* 70(3): 253–259. <https://doi.org/10.1080/11250000309356526>
- Fontaneto D, De Smet WH, Ricci C (2006) Rotifers in saltwater environments, re-evaluation of an inconspicuous taxon. *Journal of the Marine Biological Association of the United Kingdom* 86(4): 623–656. <https://doi.org/10.1017/S0025315406013531>
- Fontaneto D, Ricci C (2006) Spatial gradients in species diversity of microscopic animals: the case of bdelloid rotifers at high altitude. *Journal of Biogeography* 33(7): 1305–1313. <https://doi.org/10.1111/j.1365-2699.2006.01502.x>
- Fontaneto D, Herniou EA, Barraclough TG, Ricci C (2007) On the global distribution of microscopic animals: new worldwide data on bdelloid rotifers. *Zoological Studies* 46(3): 336–346.
- Fontaneto D, Iakovenko N, Eyres I, Kaya M, Wyman M, Barraclough TG (2011) Cryptic diversity in the genus *Adineta* Hudson & Gosse, 1886 (Rotifera: Bdelloidea: Adinetidae): a DNA taxonomy approach. *Hydrobiologia* 662(1): 27–33. <https://doi.org/10.1007/s10750-010-0481-7>
- Freckman DW, Virginia RA (1993) Extraction of nematodes from Dry Valley Antarctic soils. *Polar Biology* 13(7): 483–487. <https://doi.org/10.1007/BF00233139>
- Gee NG (1927) Some Chinese rotifers. *Lingnan Agricultural Review* 4: 43–53.
- Gladyshev E, Meselson M (2008) Extreme resistance of bdelloid rotifers to ionizing radiation. *Proceedings of the National Academy of Sciences* 105(13): 5139–5144. <https://doi.org/10.1073/pnas.0800966105>
- Gong XJ (1983) The rotifers from the High Plateau of Tibet. In: Jiang XZ, Shen YF, Gong XJ (Eds) *Freshwater Invertebrate from Tibet. Series of the Scientific Expedition to Qinghai-Xizang Plateau*. Science Press of China, Beijing, 335–424. [in Chinese]
- Haigh SB (1967) The bdelloid rotifers of New Zealand, Part III. *Journal of the Quekett Microscopical Club* 30: 193–201.
- Iakovenko N S, Kašparová E, Plewka M, Janko K (2013) *Otostephanos* (Rotifera, Bdelloidea, Habrotrochidae) with the description of two new species. *Systematics and Biodiversity* 11(4): 477–494. <https://doi.org/10.1080/14772000.2013.857737>
- Iakovenko N, Smykla J, Convey P, Kašparová E, Kozeretska I, Trokhymets V, Dykyy I, Plewka M, Devetter M, Duriš Z (2015) Antarctic bdelloid rotifers: diversity, endemism and evolution. *Hydrobiologia* 761(1): 5–43. <https://doi.org/10.1007/s10750-015-2463-2>
- Kaya M, Herniou EA, Barraclough TG, Fontaneto D (2009) A faunistic survey of bdelloid rotifers in Turkey. *Zoology in the Middle East* 48(1): 114–116. <https://doi.org/10.1080/09397140.2009.10638379>
- Koste W, Zhuge Y (1996) A preliminary report on the occurrence of Rotifera in Hainan. *Quekett Journal of Microscopy* 37(8): 666–683.
- Koste W, Zhuge V (1998) Zur Kenntnis der Rotatorienfauna (Rotifera) der Insel Hainan, China. Teil 11. *Osnabrücker Naturwissenschaftliche Mitteilungen*, 24: 183–222.
- Kellogg CA, Griffin DW (2006) Aerobiology and the global transport of desert dust. *Trends in Ecology and Evolution* 21(11): 638–644. <https://doi.org/10.1016/j.tree.2006.07.004>
- Kutikova LA (2005) The bdelloid rotifers of the fauna of Russia. Russian Academy of Sciences, *Proceedings of the Zoological Institute, Moscow*, 305 pp.

- Murray J (1906) Some Rotifera of the Sikkim Himalaya. *Journal of the Royal Microscopical Society*: 637–644. <https://doi.org/10.1111/j.1365-2818.1906.tb00619.x>
- Norton CJ, Jin C, Wang Y, Zhang Y (2010) Rethinking the Palearctic-oriental biogeographic boundary in Quaternary China. In: Norton CJ, Braun DR (Eds) *Asian Paleoanthropology*. Springer, Dordrecht, 81–100. https://doi.org/10.1007/978-90-481-9094-2_7
- Örstan A, Plewka M (2017) An introduction to bdelloid rotifers and their study. <http://www.quekett.org/starting/microscopic-life/bdelloid-rotifers/> [accessed 25 February 2019]
- Örstan A (2018) Taxonomic morphology of the genus *Adineta* (Rotifera: Bdelloidea: Adinetidae) with a new species from a suburban garden. *Zootaxa* 4524(2): 187–199. <https://doi.org/10.11646/zootaxa.4524.2.3>
- Peters U, Koste W, Westheide W (1993) A quantitative method to extract moss-dwelling rotifers. *Hydrobiologia* 255(1): 339–341. <https://doi.org/10.1007/BF00025857>
- Ricci C (1998) Anhydrobiotic capabilities of bdelloid rotifers. *Hydrobiologia* 387: 321–326. <https://doi.org/10.1023/A:1017086425934>
- Robeson MS, King AJ, Freeman KR, Birky CW, Martin AP, Schmidt SK (2011) Soil rotifer communities are extremely diverse globally but spatially autocorrelated locally. *Proceedings of the National Academy of Sciences* 108(1): 4406–4410. <https://doi.org/10.1073/pnas.1012678108>
- Segers H (2007) Annotated checklist of the rotifers (Phylum Rotifera), with notes on nomenclature, taxonomy and distribution. *Zootaxa* 1564: 1–104. <https://doi.org/10.11646/zootaxa.1564.1.1>
- Stewart FH (1908) Rotifers and Gastrochicha from Tibet. *Records of the Indian Museum* 2: 316–323.
- Shiel R, Green J (1996) Rotifera recorded from New Zealand, 1859–1995, with comments on zoogeography. *New Zealand Journal of Zoology* 23(2): 191–207. <https://doi.org/10.1080/03014223.1996.9518078>
- Song MO (2014) Eight new records of monogonont and bdelloid rotifers from Korea. *Journal of Species Research* 3(1): 53–62. <https://doi.org/10.12651/JSR.2014.3.1.053>
- Song MO (2015) New records of one monogonont and 5 bdelloid rotifers from Korea. *Korean Journal of Environmental Biology* 33(2): 140–147. <https://doi.org/10.11626/KJEB.2015.33.2.140>
- Song MO, Kim W (2000) Bdelloid rotifers from Korea. *Hydrobiologia* 439(1–3): 91–101. <https://doi.org/10.1023/A:1004181414535>
- Song MO, Lee CH (2017) A new and five rare bdelloids from Korea. *Zootaxa* 4242(3): 529–547. <https://doi.org/10.11646/zootaxa.4242.3.6>
- Song MO, Min GS (2015) A new species and ten new records of bdelloid rotifers from Korea. *Zootaxa* 3964(2): 211–27. <https://doi.org/10.11646/zootaxa.3964.2.3>
- Thorpe SVG (1893) The Rotifera of China. *Journal of the Royal Microscopical Society* 13(2): 145–152. <https://doi.org/10.1111/j.1365-2818.1893.tb01272.x>
- Wang JJ (1961) *Fauna of Freshwater Rotifera of China*. Science Press of China, Beijing, 288 pp. [in Chinese]
- Wang JJ (1974) The preliminary study of Rotifera in Everest Mountain area. In: Tibetan Science Research Team of the Chinese Academy of Sciences (Eds) *Scientific Expedition*

- Reports of Everest Mountain Area, 1966–1968. Vol. 208. Biology and Alpine Physiology. Science Press of China, Beijing, 137–144. [in Chinese]
- Welch DBM, Meselson M (2000) Evidence for the evolution of bdelloid rotifers without sexual reproduction or genetic exchange. *Science* 288(5469): 1211–1215. <https://doi.org/10.1126/science.288.5469.1211>
- Welch JLM, Welch DBM, Meselson M (2004) Cytogenetic evidence for asexual evolution of bdelloid rotifers. *Proceedings of the National Academy of Sciences of the United States of America* 101(6): 1618–1621. <https://doi.org/10.1073/pnas.0307677100>
- Yakovenko N (2000a) New for the fauna of Ukraine rotifers (Rotifera, Bdelloidea) of Adinetidae and Habrotrichidae families. *Vestnik Zoologii* 34(1–2): 11–19.
- Yakovenko N (2000b) New for the fauna of Ukraine rotifers (Rotifera, Bdelloidea) of Philodinidae family. *Vestnik Zoologii* 14: 26–32.
- Yin ZW, Xu RL (2016) The composition and distribution of moss-dwelling bdelloid rotifers in Nanling Forest Park of Guangdong. *Chinese Journal of Applied and Environmental Biology* 22(2): 0307–0312. [in Chinese] <https://doi.org/10.3724/SPJ.1145.2015.07010>
- Zhuge Y, Huang XF, Koste W (1998) Rotifera recorded from China, 1893–1997, with remarks on their composition and distribution. *International Review of Hydrobiology* 83(3): 217–232. <https://doi.org/10.1002/iroh.19980830305>

A new millipede-parasitizing horsehair worm, *Gordius chiashanus* sp. nov., at medium altitudes in Taiwan (Nematomorpha, Gordiida)

Ming-Chung Chiu^{1,2}, Chin-Gi Huang^{3,4}, Wen-Jer Wu⁵,
Zhao-Hui Lin⁶, Hsuan-Wien Chen⁶, Shih-Feng Shiao⁵

1 Department of Biology, Kobe University, Kobe 657-8501, Japan **2** Department of Biology, National Changhua University of Education, Changhua City 55007, Taiwan **3** National Mosquito-Borne Diseases Control Research Center, National Health Research Institutes, Tainan City 704, Taiwan **4** Department of Earth and Life Science, University of Taipei, Taipei 100, Taiwan **5** Department of Entomology, National Taiwan University, Taipei 106, Taiwan **6** Department of Biological Resources, National Chiayi University, Chiayi 300, Taiwan

Corresponding author: Shih-Feng Shiao (sfshiao@ntu.edu.tw)

Academic editor: A. Schmidt-Rhaesa | Received 18 February 2020 | Accepted 8 April 2020 | Published 16 June 2020

<http://zoobank.org/9095718C-8FB0-4618-8F9A-466CD3B0D3BF>

Citation: Chiu M-C, Huang C-G, Wu W-J, Lin Z-H, Chen H-W, Shiao S-F (2020) A new millipede-parasitizing horsehair worm, *Gordius chiashanus* sp. nov., at medium altitudes in Taiwan (Nematomorpha, Gordiida). ZooKeys 941: 25–48. <https://doi.org/10.3897/zookeys.941.49100>

Abstract

Gordius chiashanus sp. nov., a newly described horsehair worm that parasitizes the *Spirobolus* millipede, is one of the three described horsehair worm species in Taiwan. It is morphologically similar to *G. helveticus* Schmidt-Rhaesa, 2010 because of the progressively broadening distribution of bristles concentrated on the male tail lobes, but it is distinguishable from *G. helveticus* because of the stout bristles on the mid-body. In addition, a vertical white stripe on the anterior ventral side and areoles on the inside wall of the cloacal opening are rarely mentioned in other *Gordius* species. Free-living adults emerged and mated on wet soil under the forest canopy in the winter (late November to early February) at medium altitudes (1100–1700 m). Mucus-like structure covering on the body surface, which creates a rainbow-like reflection, might endow the worm with high tolerance to dehydration. Although *Gordius chiashanus* sp. nov. seems to be more adaptive to the terrestrial environment than other horsehair worm species, cysts putatively identified as belonging to this hairworm species found in the aquatic paratenic host, *Ephemera orientalis* McLachlan, 1875, suggest the life cycle of *Gordius chiashanus* sp. nov. could involve water and

land. The free-living adults emerged from the definitive hosts might reproduce in the terrestrial environment or enter an aquatic habitat by moving or being washed away by heavy rain instead of manipulating the behavior of their terrestrial definitive hosts.

Keywords

definitive host, immature stage, parasitic life cycle, terrestrial adaptation

Introduction

In addition to the two previously described species of horsehair worm (Chiu et al. 2011, 2017), *Gordius chiashanus* sp. nov. is the third described species in Taiwan, and one among 90 valid *Gordius* species reported worldwide (Schmidt-Rhaesa 2010, 2014). *Gordius* horsehair worms are characterized by a cuticular fold, known as post-cloacal crescent, on the male tail (Schmidt-Rhaesa 2002). *Gordius* forms a monophyletic group (Gordiidae) with the genus *Acutogordius*, which bears the same characteristics; however, the phylogenetic relationship between these two genera is controversial (Schmidt-Rhaesa 2002). Although *Gordius* is the second most diverse genus, identification of species in the genus *Gordius* is difficult because of the lack of diagnostic characters and our limited understanding of its morphological variables (Schmidt-Rhaesa 2001, 2010). Phylogenetic comparison using DNA sequences with morphological descriptions has become increasingly crucial in detecting the cryptic species (Hanelt et al. 2015; Tobias et al. 2017).

The definitive hosts of *Gordius* cover a wide range of arthropod taxa. Although many host records might be questionable because the genus *Gordius* (*G. aquaticus* Linnaeus, 1758) had been used to represent the entire members of horsehair worms, *Gordius* species might parasitize several insect orders, Chilopoda, Diplopoda, and Araneae as their definitive hosts (Schmidt-Rhaesa 2012; Bolek et al. 2015). The *Gordius* life cycle is highly correlated with the definitive hosts. The freshwater horsehair worm typically exhibits a life cycle that involves aquatic and terrestrial environments; its life cycle comprises a reproduction and paratenic aquatic host phase and a terrestrial definitive host phase (Hanelt et al. 2005). The aforementioned complex life cycle has been reported in multiple *Gordius* species (e.g., *G. robustus* Leidy, 1851 and *G. difficilis* Smith, 1994) (Thorne 1940; Bolek and Coggins 2002); however, it has not been reported in some species that parasitize aquatic definitive hosts (e.g., *G. villoti* Rosa, 1882 and *G. albopunctatus* Müller, 1926) (Valvassori et al. 1988; Schmidt-Rhaesa and Kristensen 2006) or in species that reproduce in terrestrial environments (*G. terrestris* Anaya et al., 2019) (Anaya et al. 2019).

Free-living adults of *Gordius chiashanus* sp. nov. are frequently found in foggy forests situated at altitudes of 1100–1700 m in Taiwan. Their taxonomic status was first examined in the present study by using a description of morphology and phylogenetic comparison of partial mitochondrial DNA cytochrome oxidase subunit I (mtDNA-COI) genes. The definitive host was determined using worms with high sequence

similarity collected from the round-backed millipede, *Spirobolus* sp. nov. (Hsu and Chang, unpublished). Egg strings and larvae were obtained by allowing a field collected adult free-living female worm to oviposit egg string in the laboratory. The cysts which morphologically similar to the laboratory-reared larvae were collected from the field-collected mayfly naiad, *Ephemera orientalis* McLachlan, 1875. Based on our field observations on adult free-living worms, cysts and their hosts, along with our laboratory observations of non-adult stages for this gordiid species, we suggest the possible life history of *Gordius chiashanus* sp. nov.

Materials and methods

Collection and preservation of horsehair worms

Horsehair worm samples were identified visually and collected from the ground. In total, 21 free-living adults (17 male and 4 female adults) were collected for morphological examination and DNA sequencing (detailed information provided in Table 1). All the living worms were killed by treatment with hot water (> 80 °C), fixed in a solution containing 75% alcohol with their hosts for a few days, and preserved in a solution of 95% alcohol. One mated female adult collected from Fenqihu, Zhuqi township, Chiayi county, Taiwan (23°30'12.70"N, 120°41'36.00"E) was placed in 800 mL of aerated tap water in the laboratory and maintained at 15 °C until it oviposited egg strings. The eggs were maintained in aerated water for 49 days until they hatched. One dead worm from a dead round-backed millipede (collected at 17-III-2019) and five immature worms from three of 50 round-backed millipedes (collected at 23-VII-2018 and 28-VII-2018) were collected to confirm the definitive host (detailed information provided in Table 1). All the hosts were preserved at -20 °C until dissection. The infected host and the harbored worms were preserved in a 95% alcohol solution for sequencing. Five cysts photographed from four mayfly naiads of *E. orientalis* collected from Lugu township, Nantou county, Taiwan (23°40'46.00"N, 120°47'18.50"E), where the free-living adult has ever been found in the upstream of less than 1 km, were putatively identified as belonging to this horsehair worm species. All the samples were preserved in a solution of 75% alcohol for morphological examination.

Morphological examination

Free-living adults. Fragments (approximately 0.5 cm in length) of the anterior end, mid-body, and posterior end of the preserved samples were examined and photographed using a stereomicroscope (Leica S8 APO, Leica, Wetzlar, Germany), dehydrated using a series of ethanol and acetone solutions (95% and 100% ethanol (twice) and ethanol/acetone mixtures of 2:1, 1:1, 1:2, and 0:1), dried to the critical point, coated by being sputtered with gold, and examined using a scanning electronic microscope (SEM) (JEOL JSM-5600, Tokyo, Japan) at magnifications ranging from 100× to 15,000×.

Table 1. *Gordius chiashanus* sp. nov. specimen information.

Collection date	GenBank no.	Locality	Longitude and latitude	Collector	Depository	Sex	Status	Length (mm)
20-XI-2017	MN784831 ¹	Dasyueshan (Heping, Taichung, Taiwan)	24°14'47.90"N, 120°56'06.80"E	Ta-Chih Chen	NMNS	M	Free-living adult	430
26-XI-2008	MN784832	Hongshi trail (Haituan, Taiping, Taiwan)	23°04'14.50"N, 121°07'58.30"E	Po-Yen Chen	NMNS	M	Free-living adult	744
22-I-2008	MN784841	Shilijhuo (Zhuqi, Chiayi, Taiwan)	23°29'01.70"N, 120°42'05.90"E	Yu-Hsuan Tsai	NMNS	M	Free-living adult	860
9-II-2007	MN784833	Shilijhuo (Zhuqi, Chiayi, Taiwan)	23°29'01.70"N, 120°42'05.90"E	Yu-Hsuan Tsai	NMNS	F	Free-living adult	707
8-XII-2017	MN784819	Dinghu (Alishan, Chiayi, Taiwan)	23°29'29.10"N, 120°43'19.00"E	Ming-Chung Chiu	LBM	M	Free-living adult	771
8-XII-2017	MN784820	Dinghu (Alishan, Chiayi, Taiwan)	23°29'29.10"N, 120°43'19.00"E	Ming-Chung Chiu	NMNS	M	Free-living adult	734
17-XII-2013	MN784822	Fengqihu (Zhuqi, Chiayi, Taiwan)	23°30'12.70"N, 120°41'36.00"E	Hua-Te Fang	LBM	M	Free-living adult	803
17-XII-2013	MN784823	Fengqihu (Zhuqi, Chiayi, Taiwan)	23°30'12.70"N, 120°41'36.00"E	Hua-Te Fang	LBM	M	Free-living adult	756
17-XII-2013	MN784824	Fengqihu (Zhuqi, Chiayi, Taiwan)	23°30'12.70"N, 120°41'36.00"E	Hua-Te Fang	NMNS	M	Free-living adult	594
17-XII-2013	MN784825	Fengqihu (Zhuqi, Chiayi, Taiwan)	23°30'12.70"N, 120°41'36.00"E	Hua-Te Fang	NMNS	M	Free-living adult	383
17-XII-2013	MN784826	Fengqihu (Zhuqi, Chiayi, Taiwan)	23°30'12.70"N, 120°41'36.00"E	Hua-Te Fang	NMNS	M	Free-living adult	676
17-XII-2013	MN784827	Fengqihu (Zhuqi, Chiayi, Taiwan)	23°30'12.70"N, 120°41'36.00"E	Hua-Te Fang	NMNS	M	Free-living adult	474
18-XII-2017	MN784828	Fengqihu (Zhuqi, Chiayi, Taiwan)	23°30'12.70"N, 120°41'36.00"E	Ming-Chung Chiu	NMNS	M	Free-living adult	749
18-XII-2017	MN784829	Fengqihu (Zhuqi, Chiayi, Taiwan)	23°30'12.70"N, 120°41'36.00"E	Ming-Chung Chiu	NMNS	F	Free-living adult	666
18-XII-2017	MN784830	Fengqihu (Zhuqi, Chiayi, Taiwan)	23°30'12.70"N, 120°41'36.00"E	Ming-Chung Chiu	NMNS	F	Free-living adult	717
18-XII-2016	MN784816	Xitou (Lugu, Nantou, Taiwan)	23°40'21.30"N, 120°47'27.50"E	Ming-Chung Chiu	LBM	M	Free-living adult	498
18-XII-2016	MN784817	Xitou (Lugu, Nantou, Taiwan)	23°40'21.30"N, 120°47'27.50"E	Ming-Chung Chiu	NMNS	M	Free-living adult	403
18-XII-2016	MN784818	Xitou (Lugu, Nantou, Taiwan)	23°40'21.30"N, 120°47'27.50"E	Ming-Chung Chiu	LBM	F	Free-living adult	549
9-II-2008	MN784842	Xitou (Lugu, Nantou, Taiwan)	23°40'21.30"N, 120°47'27.50"E	Ming-Chung Chiu	NMNS	M	Free-living adult	572
10-XII-2011	MN784840	Xitou (Lugu, Nantou, Taiwan)	23°40'21.30"N, 120°47'27.50"E	Ming-Chung Chiu	NMNS	M	Free-living adult	502
17-III-2019	MN784839	Xitou (Lugu, Nantou, Taiwan)	23°40'21.30"N, 120°47'27.50"E	Zhao-Hui Lin	NMNS	-	Dead worm in host	-
23-VII-2018	MN784834	Shilijhuo (Zhuqi, Chiayi, Taiwan)	23°29'01.70"N, 120°42'05.90"E	Yu-Wei Li	NMNS	-	Immature worm	660
28-VII-2018	MN784835	Shilijhuo (Zhuqi, Chiayi, Taiwan)	23°28'22.60"N, 120°41'42.80"E	Yu-Wei Li	NMNS	-	Immature worm	894
28-VII-2018	MN784836	Shilijhuo (Zhuqi, Chiayi, Taiwan)	23°28'22.60"N, 120°41'42.80"E	Yu-Wei Li	NMNS	-	Immature worm	420
28-VII-2018	MN784837	Shilijhuo (Zhuqi, Chiayi, Taiwan)	23°28'22.60"N, 120°41'42.80"E	Yu-Wei Li	NMNS	-	Immature worm	442
28-VII-2018	MN784838	Shilijhuo (Zhuqi, Chiayi, Taiwan)	23°28'22.60"N, 120°41'42.80"E	Yu-Wei Li	NMNS	-	Immature worm	426

LBM: Lake Biwa Museum; NMNS: National Museum of Natural Science.

¹ Holotype.

Eggs and larvae. Eggs and newly hatched larvae (living or treated with hot water (> 80 °C)) were examined and photographed on microslides by using a compound microscope (Olympus BH-2, PM-10AD, Olympus, Tokyo, Japan) at magnifications of 200× and 400×. The eggs examined using the SEM were first fixed using a solution of 75% alcohol, dehydrated, dried to the critical point, and coated with gold sputter. The eggs and larvae were examined at a magnification of 500×. ImageJ 1.47 was used for all morphological measurements (Abràmoff et al. 2004), and spatial calibration was conducted according to the scale included in each picture. The terminology for larval stages used in this study primarily followed that of Schmidt-Rhaesa (2014) and Szymgiel et al. (2014).

Cysts in the paratenic host. The mayflies preserved in 75% alcohol were first treated with Nesbitt's fluid for 15–20 min at 40 °C and a 0.1% KOH solution for 5 min at 40 °C to ensure that the cuticle and muscles had become transparent (Walter and Krantz 2009; Chiu et al. 2016). One of the cysts was further treated with a 5% KOH solution for 6 h at room temperature to release the folded larva inside the cyst wall. The cysts were examined and photographed on microslides by using the compound microscope at 200× magnification.

Phylogenetic analysis

Genomic DNA from a 1-cm mid-body section of each worm was extracted using an ALS Tissue Genomic DNA Extraction Kit (Pharmigene, Kaohsiung, Taiwan). The partial cytochrome c oxidase subunit I (COI) sequence was amplified using universal primers (LCO1490 and HC02198) (Folmer et al. 1994) or a newly designed primer set (GoCOiF-1: TTAGGAAGCTGCTTTAAG, GoCOiR-1: ATAGGGTCAAAGAA-GGAGG). PCR for both primer sets was initiated at 95 °C for 5 min, and amplification was conducted for 35 cycles of 95 °C for 1 min, 50 °C for 1 min, and 73 °C for 1 min, with a final extension at 73 °C for 5 min.

In addition to sequencing three free-living adult worms and six immature worms recovered from millipede hosts (242–457 high-quality base pairs), we obtained high-quality COI sequences (>500 base pairs) from 18 adult free-living individuals to be used in our phylogenetic analysis and estimates of intraspecific genetic distances. Pairwise distance matrices of COI sequence data were calculated using the Kimura 2-parameter model. A phylogenetic tree was reconstructed using the maximum likelihood method by using the General Time Reversible model with the addition of invariant sites and a gamma distribution of rates across sites. For phylogenetic analysis, the COI sequences were first aligned using CLUSTALX 2.0.10 (Thompson et al. 1997). A total of 422 base pairs shared by all the examined sequences, including for our 18 samples, *Gordius/Acutogordius* spp. (as reported by Sato et al. (2012), Hanelt et al. (2015), Chiu et al. (2017), and Tobias et al. (2017)) and *Chordodes formosanus* Chiu, 2011, *Euchordodes nigromaculatus* Poinar, 1991, and *Parachordodes diblastus* (Örley, 1881) (as reported by Chiu et al. (2011) and Tobias et al. (2017)), were analyzed using MEGA 7 (Kumar et al. 2016) (see detailed information in Table 2). One sequence of an un-

Table 2. List of COI sequences obtained from GenBank for phylogenetic analyses in this study.

Accession number	Species/clade	Reference
<i>Gordius/Acutogordius</i>		
KM382317	<i>G. cf. robustus</i> (Clade 8)	Hanelt et al. 2015
KM382316	"	Hanelt et al. 2015
KM382315	"	Hanelt et al. 2015
KM382314	"	Hanelt et al. 2015
KM382313	"	Hanelt et al. 2015
KM382312	"	Hanelt et al. 2015
KM382311	"	Hanelt et al. 2015
KM382310	<i>G. terrestris</i>	Hanelt et al. 2015, Anaya et al. 2019
KM382309	"	Hanelt et al. 2015, Anaya et al. 2019
KM382308	"	Hanelt et al. 2015, Anaya et al. 2019
KM382307	"	Hanelt et al. 2015, Anaya et al. 2019
KM382306	<i>G. cf. robustus</i> (Clade 6)	Hanelt et al. 2015
KM382305	"	Hanelt et al. 2015
KM382304	"	Hanelt et al. 2015
KM382303	"	Hanelt et al. 2015
KM382302	"	Hanelt et al. 2015
KM382301	"	Hanelt et al. 2015
KM382300	"	Hanelt et al. 2015
KM382299	"	Hanelt et al. 2015
KM382297	<i>G. cf. robustus</i> (Clade 5)	Hanelt et al. 2015
KM382296	"	Hanelt et al. 2015
KM382295	"	Hanelt et al. 2015
KM382294	<i>G. cf. robustus</i> (Clade 4)	Hanelt et al. 2015
KM382293	"	Hanelt et al. 2015
KM382292	"	Hanelt et al. 2015
KM382291	"	Hanelt et al. 2015
KM382290	"	Hanelt et al. 2015
KM382289	<i>G. cf. robustus</i> (Clade 3)	Hanelt et al. 2015
KM382288	"	Hanelt et al. 2015
KM382287	"	Hanelt et al. 2015
KM382286	"	Hanelt et al. 2015
KM382285	"	Hanelt et al. 2015
KM382284	"	Hanelt et al. 2015
KM382283	<i>G. cf. robustus</i> (Clade 2)	Hanelt et al. 2015
KM382282	"	Hanelt et al. 2015
KM382281	<i>G. cf. robustus</i> (Clade 1)	Hanelt et al. 2015
KM382280	"	Hanelt et al. 2015
KM382279	"	Hanelt et al. 2015
KM382278	"	Hanelt et al. 2015
KM382277	"	Hanelt et al. 2015
KM382318	<i>G. attoni</i>	Hanelt et al. 2015
KM382319	"	Hanelt et al. 2015
KM382320	<i>G. balticus</i>	Hanelt et al. 2015
KM382321	<i>Gordius</i> sp. N178	Hanelt et al. 2015
KM382322	<i>Gordius</i> sp. N183	Hanelt et al. 2015
KM382323	<i>Gordius</i> sp. N297B	Hanelt et al. 2015
KM382324	<i>Gordius</i> sp. N357	Hanelt et al. 2015
AB647235	<i>Gordius</i> sp. KW-2011-A	Sato et al. 2012
AB647237	<i>Gordius</i> sp. KW-2011-B	Sato et al. 2012
AB647241	<i>Gordius</i> sp. KW-2011-D	Sato et al. 2012
KY172751	<i>Gordius</i> sp. Tobias et al. 2017	Tobias et al. 2017
KY172750	"	Tobias et al. 2017
KY172752	"	Tobias et al. 2017
KY172759	"	Tobias et al. 2017

Accession number	Species/clade	Reference
KY172765	"	Tobias et al. 2017
KY172770*	"	Tobias et al. 2017
KY172777	"	Tobias et al. 2017
KY172749	"	Tobias et al. 2017
KY172792	"	Tobias et al. 2017
KY172789	"	Tobias et al. 2017
KY172791	"	Tobias et al. 2017
KY172799	"	Tobias et al. 2017
KY172801	"	Tobias et al. 2017
KY172802	"	Tobias et al. 2017
KY172804	"	Tobias et al. 2017
KY172753	<i>G. paranensis</i> (Clade2)	Tobias et al. 2017
KY172754	"	Tobias et al. 2017
KY172755	"	Tobias et al. 2017
KY172756	"	Tobias et al. 2017
KY172776	"	Tobias et al. 2017
KY172782	"	Tobias et al. 2017
KY172813	"	Tobias et al. 2017
KY172811	<i>G. paranensis</i> (Clade1)	Tobias et al. 2017
KY172812	"	Tobias et al. 2017
KX591948	<i>Acutogordius taiwanensis</i>	Chiu et al. 2017
KX591947	"	Chiu et al. 2017
KX591946	"	Chiu et al. 2017
KX591945	"	Chiu et al. 2017
KX591944	"	Chiu et al. 2017
KX591943	"	Chiu et al. 2017
KX591942	"	Chiu et al. 2017
KX591941	"	Chiu et al. 2017
KX591940	"	Chiu et al. 2017
KX591939	"	Chiu et al. 2017
KX591938	"	Chiu et al. 2017
KX591937	"	Chiu et al. 2017
KX591936	"	Chiu et al. 2017
KX591935	"	Chiu et al. 2017
KX591934	"	Chiu et al. 2017
KX591933	"	Chiu et al. 2017
KX591932	"	Chiu et al. 2017
KX591931	"	Chiu et al. 2017
KX591930	"	Chiu et al. 2017
KX591929	"	Chiu et al. 2017
KX591928	"	Chiu et al. 2017
KX591927	"	Chiu et al. 2017
KX591926	"	Chiu et al. 2017
KX591925	"	Chiu et al. 2017
KX591924	"	Chiu et al. 2017
KX591923	"	Chiu et al. 2017
KX591922	"	Chiu et al. 2017
MF983649	Myanmar nematomorph	
Out group		
HM044105	<i>Chordodes formosanus</i>	Chiu et al. 2011
HM044124	"	Chiu et al. 2011
KY172780	<i>Euchordodes nigromaculatus</i>	Tobias et al. 2017
KY172803	"	Tobias et al. 2017
KY172747	<i>Parachordodes diblastus</i>	Tobias et al. 2017
KY172778	"	Tobias et al. 2017

* KY172770 was excluded from the analysis since its high difference from the member of *Gordius* and the high similarity with *Euchordodes nigromaculatus*.

determined nematomorph (MF983649) was also included because it exhibited high similarity to *Acutogordius*. The bootstrap method (with 1000 replicates) was used to estimate branch support of the phylogenetic tree.

Seasonal occurrence of free-living adults

Seasonal occurrence of free-living adults was estimated by counting (and removing) free-living adults (living or dead) on the ground in Dinghu, Alishan township, Chiayi county, Taiwan (23°29'29.10"N, 120°43'19.00"E) between October 2017 and May 2018.

Results

Gordius chiashanus Chiu, sp. nov.

<http://zoobank.org/E904851F-6F48-423D-9AC2-5A7BB595FA7B>

Type locality. Dinghu (23°29'29.10"N, 120°43'19.00"E), Alishan township, Chiayi county, Taiwan (holotype). Paratypes were collected from Dasyueshan (Heping district, Taichung city), Xitou (Lugu township, Nantou county), Shihjhuo, Fenqihu (Zhuqi township, Chiayi county), Dinghu (Alishan township, Chiayi county), and Hongshi forest road (Haituan township, Taitung county). Table 1 presents detailed information of the locality.

Type material. Partial bodies of the holotype and allotype were deposited at the National Museum of Natural Science, Taichung, Taiwan. Paratypes were deposited at the National Museum of Natural Science, Taichung, Taiwan and Lake Biwa Museum, Shiga, Japan (Table 1).

Type hosts. *Spirobolus* sp. nov. (Hsu and Chang, unpublished) (Diplopoda: Spirobolidae) (Fig. 5E, F)

Etymology. The specific name is the combination of *chia*, referring to the place (Chiayi county) where the first sample was found, and *shan*, referring to the Chinese word for “mountains.” The word *chia* is also in memory of our friend, Chia-Chih Lin, who died in an accident in a field experiment.

Description. Male adults (N = 11) (Figs 1–3, 5). Body length 627.94 ± 154.75 (383–860) mm, width (widest, after dehydration) 1.30 ± 0.31 (0.81–2.06) mm, light to dark brown, smooth, and covered with mucus-like structure (viscous liquid on live worms with rainbow-like reflection (Fig. 5C, Suppl. material 1: Video S1), and created haze that surrounded the body surface in hot water (Fig. 5A).

Anterior end columnar and spherical; anterior tip white (white cap) with a dark-brown collar and a vertical white stripe on the ventral side (Fig. 1A). Under SEM, surface of anterior end appeared smooth (Fig. 1B) or wrinkled (Fig. 1C) on the tip of one sample; scattered short bristles (11.24 ± 6.57 (4.92–22.24) μm in length) scattered except on tip in most samples (Fig. 1B, D).

Cuticle in mid-body ornamented with a dorsal and a ventral dark pigment line; white spots scattered across entire body surface (Figs 3C, D, 5A). Under SEM, cuticle

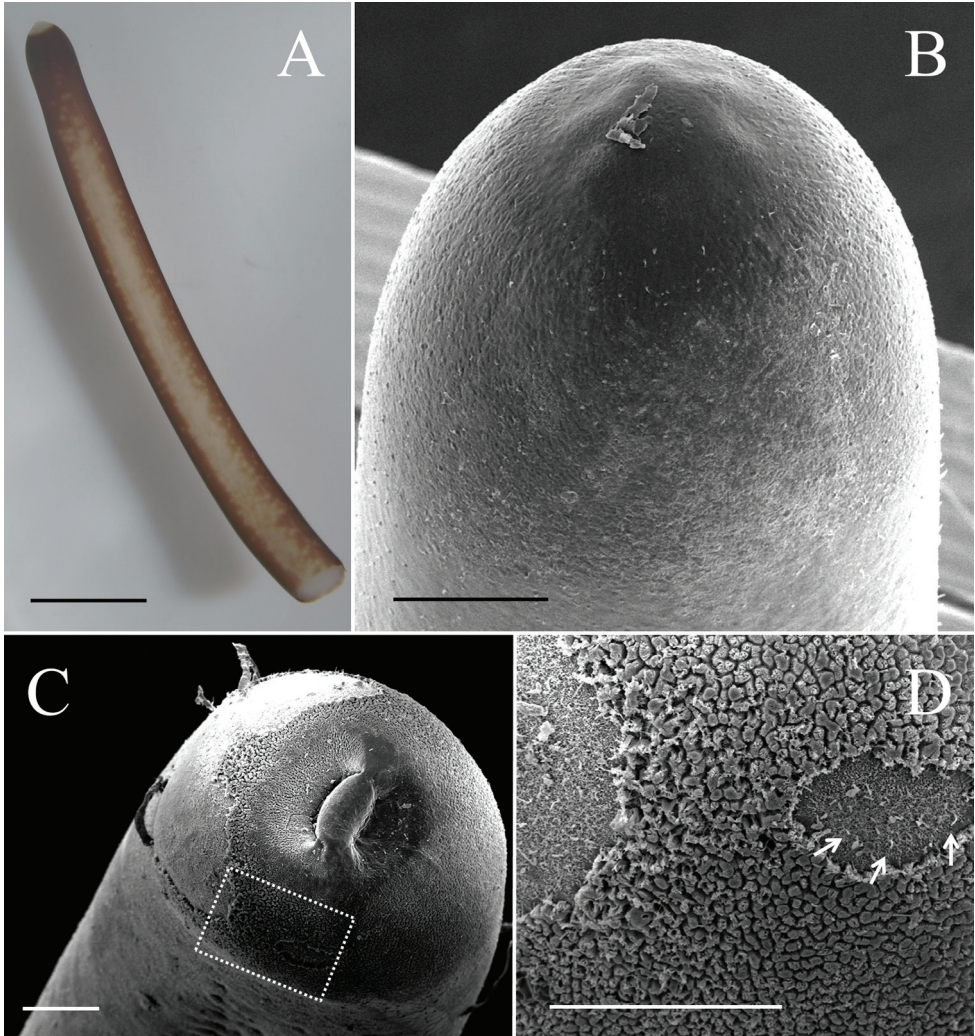


Figure 1. Anterior end of male *Gordius chiashanus* sp. nov. **A** stereomicroscopic image of the ventral side of the anterior end showing a white cap, dark-brown collar, and vertical white stripe on the ventral side **B, C** SEM images of the anterior end surface that is **(B)** smooth with scattered short bristles and **(C)** wrinkled **D** close-up view of the dotted square in C showing the short bristles (arrows) covered by a wrinkled structure. Scale bars: 2 mm **(A)**, 200 μm **(B–D)**.

surface appeared smooth (Fig. 3A) with a few scattered short or cone-like bristles (6.75 ± 2.37 (2.31–10.34) μm in length) (Fig. 3A, B).

Posterior end divided into two tail lobes (Fig. 2A, B), each lobe 855.24 ± 100.89 (658.39–994.88) μm long and 458.55 ± 76.52 (365.95–643.00) μm wide with length-to-width ratio of 1.89 ± 0.26 (1.49–2.42). Inner side of lobe tips white (Fig. 2A). Under SEM, inner side of tail lobes concave in some samples; cuticle surface smooth, but one sample exhibited flat areoles on inner side of lobe tips; short bristles scattered across the surface and concentrated in most samples on lobe tips (Fig. 2C) and on in-

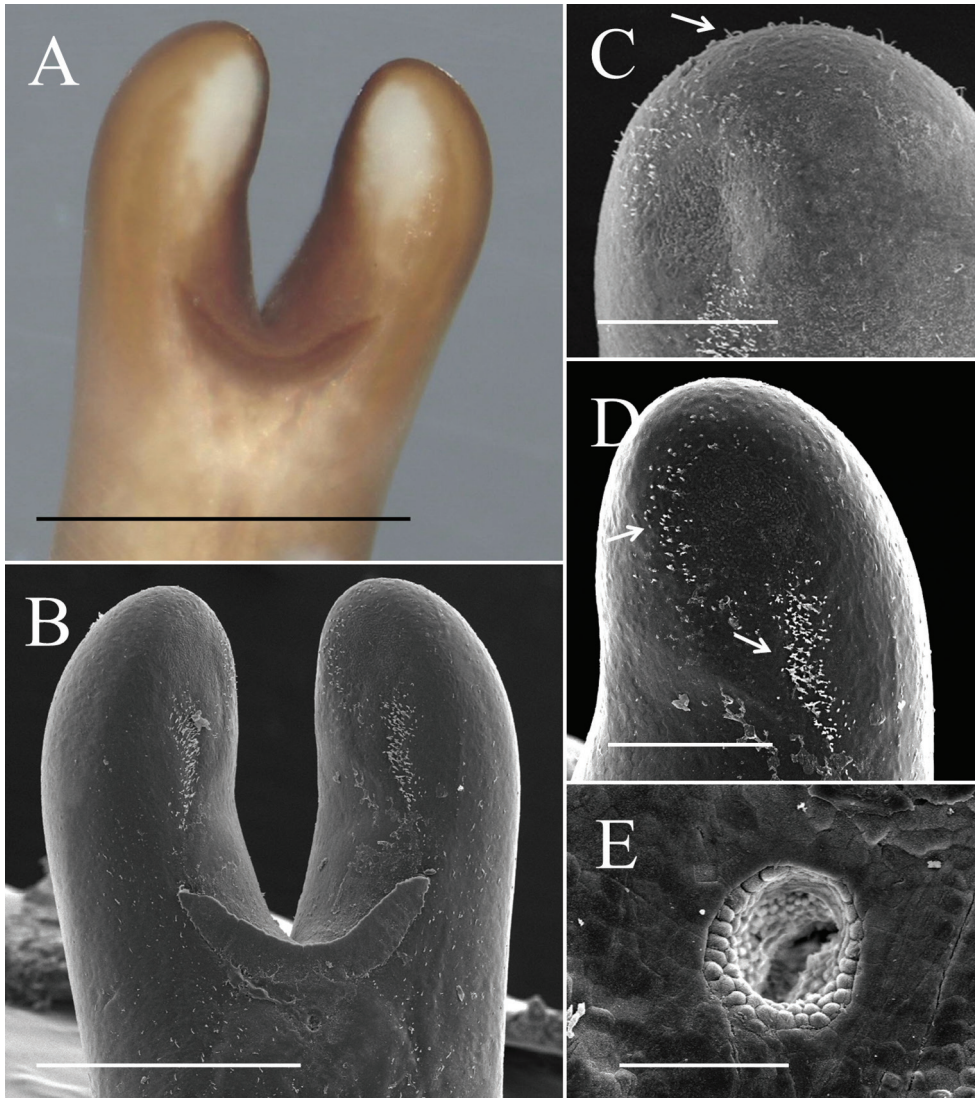


Figure 2. Posterior end of male *Gordius chiashanus* sp. nov. **A** stereomicroscopic image of the posterior end **B–D** SEM images of **(B)** overview of the posterior end with bristles concentrated on the **(C)** lobe tips (arrow), and **(D)** inner side of the lobe tips and the formation of a bristle field on each tail lobe posterior to the tips of the postcloacal crescent (arrows) **E** cloacal opening with areoles on the inside wall. Scale bars: 1 mm **(A)**, 500 µm **(B)**, 200 µm **(C–D)**, 50 µm **(E)**.

ner side of lobe tips forming a bristle field (322.67 ± 99.34 (187.60–412.75) µm long and 71.82 ± 35.49 (44.81–114.54) µm wide) on each of tail lobe posterior to tips of postcloacal crescent (Fig. 2D). Postcloacal crescent (Fig. 2A, B) 718.61 ± 118.77 (536.14–984.34) µm long and 86.7 ± 15.62 (54.73–118.65) µm wide and located on ventral side near base of tail lobes. Crescent generally semicircular or slightly angled,

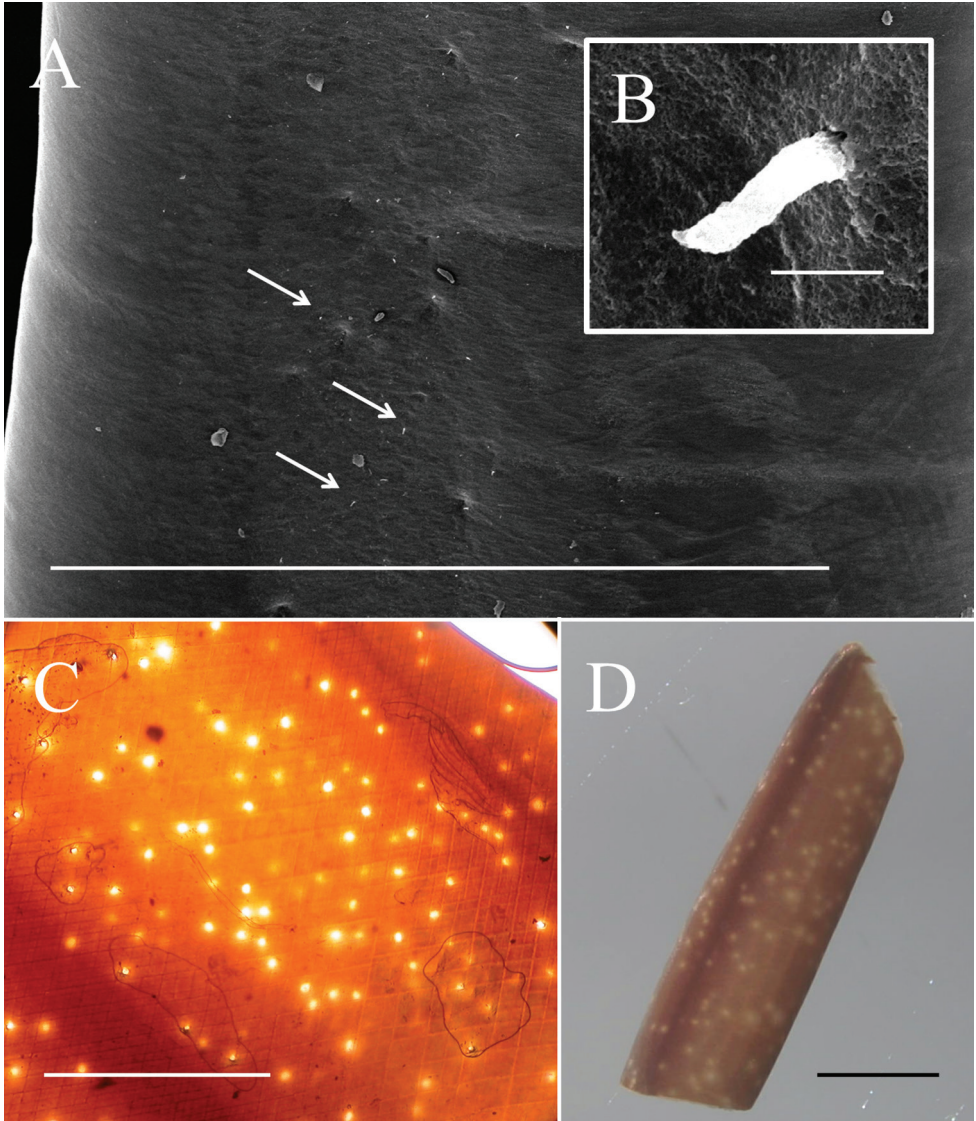


Figure 3. Mid-body of male *Gordius chiashanus* sp. nov. **A, B** SEM images of **(A)** cuticle in the mid-body with scattered short bristles (arrows) and **(B)** close-up view of a short bristle **C, D** white spots and dorsal and ventral dark pigmented line examined using **(C)** a compound microscope and **(D)** a stereomicroscope. Scale bars: 1 mm (**A, C, D**), 5 μ m (**B**).

but a few samples exhibited a straightened form of crescent. Branches of postcloacal crescent usually ended at tail lobes. Cloacal opening circular (40.5 ± 21.87 (27.41–56.14) μ m) and anterior to postcloacal crescent (Fig. 2A, B). Wall inside cloacal opening exhibited areoles (Fig. 2E); no circumcloacal spine or bristles observed in region next to cloacal opening.

Female adults ($N = 4$) (Figs 4, 5). Body length 659.75 ± 77.06 (549–717) mm, width (widest, after dehydration) 1.54 ± 0.54 (1.00–2.03) mm, light to dark brown, smooth, and covered with mucus-like structure. White spots scattered on surface but relatively less obvious than those of male adults (Fig. 4F, G). Anterior end columnar and spherical. Anterior tip white (white cap) with a dark-brown collar and exhibited a vertical white stripe on the ventral side (Fig. 4A). Under SEM, surface of anterior end smooth and exhibited scattered short bristles (16.75 ± 4.60 (13.39–23.56) μm in length) except at tip (Fig. 4B). Cuticle in mid-body ornamented with a dorsal and a ventral dark pigment line (Fig. 4G). Under SEM, cuticle surface smooth with a few short or cone-like bristles (7.24 ± 2.01 (4.94–9.99) μm in length) scattered. Posterior end columnar and rounded at tip (Fig. 4E) and did not exhibit scattered bristles (Fig. 4D). Cloacal opening on terminal end (Fig. 4C, D) circular and 36.56 ± 23.23 (24.68–48.45) μm in diameter.

Eggs ($N = 12$) (Fig. 6C–E). Egg strings (Fig. 6E) 7.41 ± 3.46 (3.78–13.70) mm in length and 1.13 ± 0.12 (0.86–1.25) mm in width; white or light yellow in color, deposited in water as short pieces not adhering to substrate. Eggs round, 54.16 ± 242.89 (49.88–58.61) μm in diameter. Developing embryo surrounded by an inner membrane (Fig. 6C, D) separated by a distinct space from outer egg shell 14.35 ± 1.41 (12.43–17.33) μm .

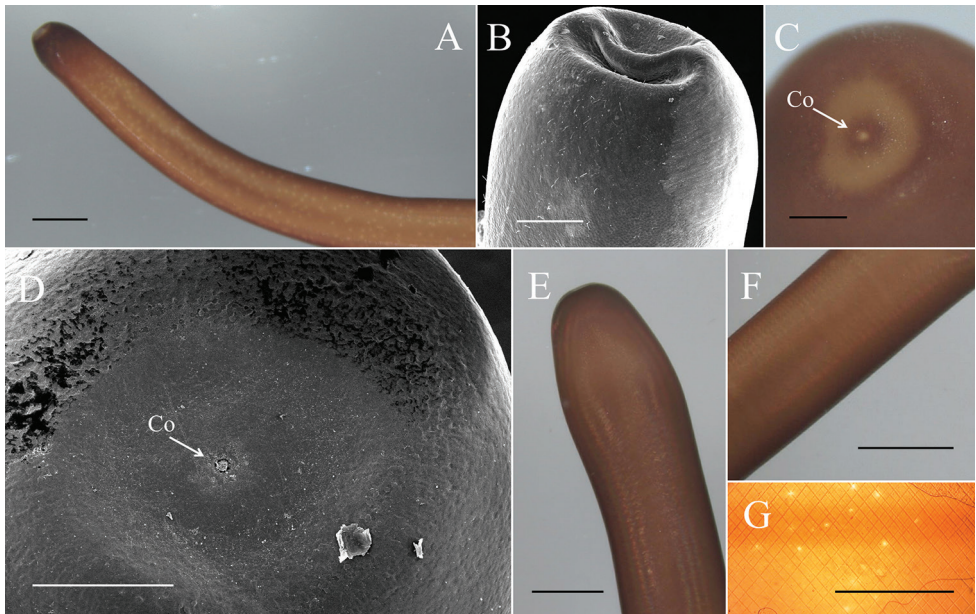


Figure 4. Female *Gordius chiashanus* sp. nov. **A, B** anterior end examined using a **(A)** stereomicroscope and **(B)** SEM **C–E** posterior end with the terminal view examined using a **(C)** stereomicroscope and **(D)** SEM, and the **(E)** lateral view examined using a stereomicroscope **F, G** mid-body examined using a **(F)** stereomicroscope and **(G)** compound microscope. Co, cloacal opening. Scale bars: 1 mm **(A, F, G)**, 200 μm **(B–D)**.



Figure 5. Field observation of *Gordius chiasbanus* sp. nov. **A** hazy appearance (arrows) surrounding the body surface in hot water **B** spermatophore (arrow) on a female collected on the surface of the soil **C** rainbow-like reflection on the body surface **D** free-living adult collected in wet soil **E, F** infected host, *Spirobolus* sp. nov. (Hsu and Chang, unpublished), harboring (**E**) three immature worms (arrow) and (**F**) an adult worm. Photographs courtesy of (**D**) Fang, Hua-Te and (**F**) Hung, Ming-Chin. Scale bars: 1 cm (**E**).

Living larvae ($N = 10$) (Fig. 6B). Eggs developed for approximately 49 days. Hatched larvae remained near egg strings or moved inside eggshells. Under light microscopy, living larvae appeared cylindrical with a single posterior spine. Preseptum length 32.33 ± 4.53 (27.06–40.04) μm , and the width 18.04 ± 0.86 (16.70–19.12) μm . Postseptum length 83.05 ± 8.31 (66.50–92.66) μm , width 15.05 ± 0.73 (14.21–16.10) μm ; proboscis length 14.94 ± 1.99 (12.35–18.48) μm , width 4.11 ± 0.85 (2.77–5.34) μm ; pseudointestine length 60.60 ± 5.40 (54.99–70.12) μm , width 11.66 ± 1.42 (8.84–13.56) μm , unequally subdivided, elongated oval with a depression in anterior end (Fig. 6B).

Larvae treated with hot water ($N = 2$) (Fig. 6A). Larvae treated with hot water similar in morphology but larger than living larvae. Preseptum length 44.57 ± 0.13 (44.48–44.66) μm , width 17.96 ± 0.16 (17.85–18.08) μm . Postseptum length 118.23 ± 1.91 (116.88–119.58) μm , width 15.36 ± 0.68 (14.88–15.84) μm . Proboscis length 12.63 ± 1.18 (11.80–13.47) μm , width 3.26 ± 0.05 (3.23–3.30) μm ; pseudointestine length 77.99 ± 5.22 (74.30–81.68) μm , width 13.99 ± 0.81 (13.41–14.56) μm (Fig. 6A).

Field-collected cysts ($N = 5$) (Fig. 6F–H). Larvae in cysts unfolded ($N = 4$) (Fig. 6F) or exhibited a postseptum folded twice ($N = 1$) (Fig. 6G, H). Unfolded larvae morphologically similar to larvae but larger in size; preseptum length was 60.18 ± 6.72 (50.40–65.18) μm , width 20.87 ± 0.52 (20.28–21.33) μm ; postseptum length

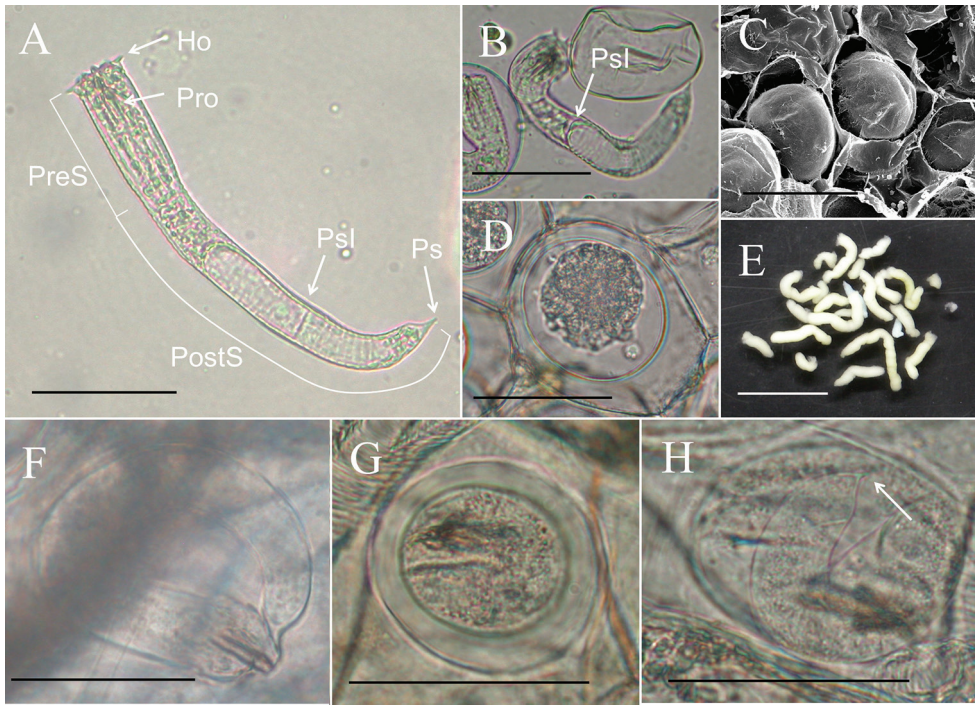


Figure 6. Immature stages of *Gordius chiashanus* sp. nov. **A, B** free-living larva (**A**) treated with hot water and a living larva showing the depression in the anterior end of the pseudointestine (arrow) **C, D** eggs with the inner membrane examined using an (**C**) SEM and (**D**) compound microscope **E** egg strings **F–H** cysts in the paratenic host with (**F**) a unfolded larva and (**G**) a folded larva, showing (**H**) a single posterior spine (arrow) after treatment with a 5% KOH solution. Abbreviations: Ho, hooklet; PostS, post-septum; PreS, preseptum; Pro, proboscis; Psl, pseudointestine. Scale bars: 50 μm (**A–D, F–H**), 1 mm (**E**).

127.33 ± 20.05 (105.10–146.05) μm , width 19.82 ± 2.27 (17.61–22.91) μm ; proboscis length 15.46 ± 1.67 (13.84–17.56) μm , width 4.10 ± 0.68 (3.09–4.52) μm ; pseudointestine not visible (Fig. 6F). Folded larva (length 34.97 μm , width 30.47 μm) fold twice and surrounded by a clear cyst wall, 47.86 μm in total length and 42.40 μm in total width; proboscis length 15.57 μm , width 5.09 μm (Fig. 6G); a single posterior spine visible after treatment with a solution of 5% KOH (Fig. 6H).

Phylogeny. The partial COI sequences of the 18 free-living adults contained 15 haplotypes with 392 invariable sites, nine singletons, and 21 parsimoniously informative sites. The genetic distance among them was 0.0024 within the range of 0.0000–0.0510. The three living adults and six worms inside the hosts were considered conspecific with the 18 free-living adults because of their small genetic distances (0.0000–0.0719). The mean interspecific genetic distances between *Gordius chiashanus* sp. nov. and other *Gordius* species or clades were in the range of 0.2320–0.4242, and that between *Gordius chiashanus* sp. nov. and *Acutogordius taiwanensis* was 0.3648 (Table 3). In addition to short genetic distances, the conspecific status of the 18 free-living

Table 3. Intra- and interspecific mean COI genetic distances of *Gordius/Acutogordius* species or clades under K2P model.

Species/Clade	1	2	3	4	5	6	7	8	9	10	11	12	13	14	15	16	17	18	19	20	21	22	
1 <i>Gordius chiahuanus</i> sp. nov.	0.024																						
2 <i>G. cf. robustus</i> (Clade1)	0.285	0.009																					
3 <i>G. cf. robustus</i> (Clade2)	0.312	0.217	0.015																				
4 <i>G. cf. robustus</i> (Clade3)	0.293	0.297	0.275	0.007																			
5 <i>G. cf. robustus</i> (Clade4)	0.308	0.208	0.249	0.157	0.012																		
6 <i>G. cf. robustus</i> (Clade5)	0.272	0.165	0.211	0.227	0.222	0.003																	
7 <i>G. cf. robustus</i> (Clade6)	0.293	0.257	0.251	0.255	0.228	0.259	0.006																
8 <i>G. terrestris</i>	0.232	0.209	0.265	0.250	0.230	0.222	0.238	0.020															
9 <i>G. cf. robustus</i> (Clade8)	0.265	0.203	0.307	0.338	0.253	0.244	0.251	0.122	0.026														
10 <i>G. attoni</i>	0.277	0.229	0.288	0.337	0.274	0.238	0.289	0.231	0.249	0.010													
11 <i>G. badicus</i>	0.316	0.260	0.298	0.288	0.269	0.274	0.304	0.264	0.323	0.337	–												
12 <i>Gordius</i> sp. N178	0.352	0.260	0.313	0.370	0.289	0.340	0.330	0.256	0.290	0.271	0.323	–											
13 <i>Gordius</i> sp. N183	0.329	0.302	0.290	0.373	0.317	0.344	0.365	0.294	0.336	0.277	0.301	0.246	–										
14 <i>Gordius</i> sp. N297B	0.424	0.416	0.462	0.547	0.441	0.443	0.478	0.375	0.412	0.348	0.455	0.343	0.414	–									
15 <i>Gordius</i> sp. N357	0.332	0.366	0.387	0.420	0.376	0.396	0.302	0.357	0.359	0.379	0.439	0.375	0.434	0.441	–								
16 <i>Gordius</i> sp. KW-2011-A	0.384	0.325	0.327	0.453	0.371	0.336	0.345	0.347	0.348	0.331	0.376	0.332	0.376	0.372	0.424	–							
17 <i>Gordius</i> sp. KW-2011-B	0.334	0.375	0.365	0.370	0.334	0.407	0.364	0.302	0.363	0.333	0.380	0.323	0.358	0.333	0.308	0.290	–						
18 <i>Gordius</i> sp. KW-2011-D	0.375	0.300	0.344	0.393	0.373	0.294	0.388	0.388	0.367	0.369	0.405	0.384	0.390	0.374	0.403	0.312	0.301	–					
19 <i>G. paranensis</i> (Clade1)	0.369	0.405	0.381	0.450	0.381	0.410	0.359	0.373	0.395	0.409	0.398	0.408	0.466	0.426	0.453	0.415	0.386	0.440	0.049				
20 <i>G. paranensis</i> (Clade2)	0.337	0.348	0.391	0.436	0.384	0.372	0.368	0.333	0.368	0.345	0.339	0.334	0.385	0.324	0.404	0.357	0.327	0.344	0.377	0.010			
21 <i>Gordius</i> sp. Tobias et al. 2017	0.335	0.283	0.293	0.436	0.355	0.311	0.366	0.287	0.337	0.347	0.358	0.254	0.308	0.343	0.353	0.304	0.335	0.321	0.354	0.337	0.012		
22 <i>Acutogordius taiwanensis</i>	0.365	0.343	0.327	0.401	0.386	0.368	0.345	0.322	0.375	0.304	0.336	0.270	0.210	0.462	0.469	0.432	0.376	0.366	0.435	0.389	0.311	0.002	

–Indicates a single haplotype whose intraspecific distance could not be calculated.

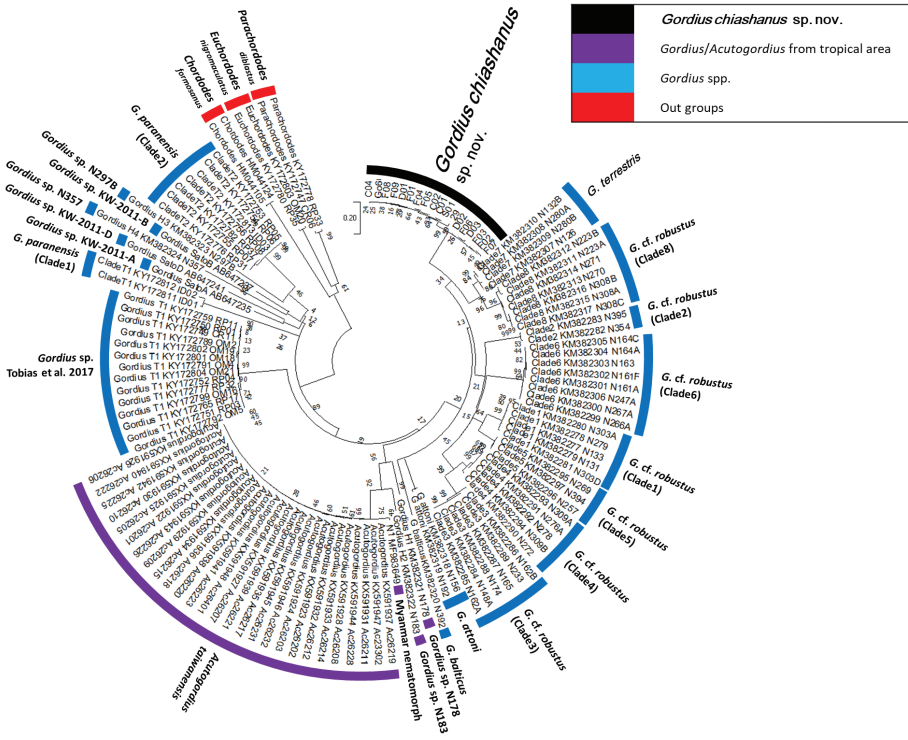


Figure 7. Phylogenetic relationship of *Gordius/Acutogordius* spp. reconstructed using COI partial sequences compared with *C. formosanus*, *E. nigromaculatus*, and *P. diblastus* as out groups. Numbers at the nodes represent the percentage of 1000 bootstrap replicates.

adults was also supported because all the samples were located in a single clade, as indicated by a high bootstrap value. No subgroup was detected because the polytomic topology exhibited low bootstrap values and short genetic distances. The *Gordius* species/clades in the present result were consistent with the results of Hanelt et al. (2015) and Tobias et al. (2017), despite slight differences in the relative relationships among species, which might be attributable to the differences in models used or the shorter sequence adopted in previous studies. The clade of *A. taiwanensis* was located within that of the *Gordius* species, and it did not behave as a sister group (Fig. 7).

Reproductive season. Free-living adult worms frequently aggregate and mate on wet ground (Fig. 5B, C) after rain or fog, and they are sometimes found in water or soil (Fig. 5D). They suddenly emerge in early December, and their number decreases within 1–2 months (Fig. 8). During the reproductive season, no infected host was found. The seasonality and pattern of *Gordius chiashanus* sp. nov. differed from the graph constructed using data from *C. formosanus* (Chiu et al. 2016).

Diagnosis and comments. The 21 free-living *Gordius* adults and six juvenile worms from round-backed millipedes were judged as belonging to the same species in accordance with the results that they all were located in the same clade in the phyloge-

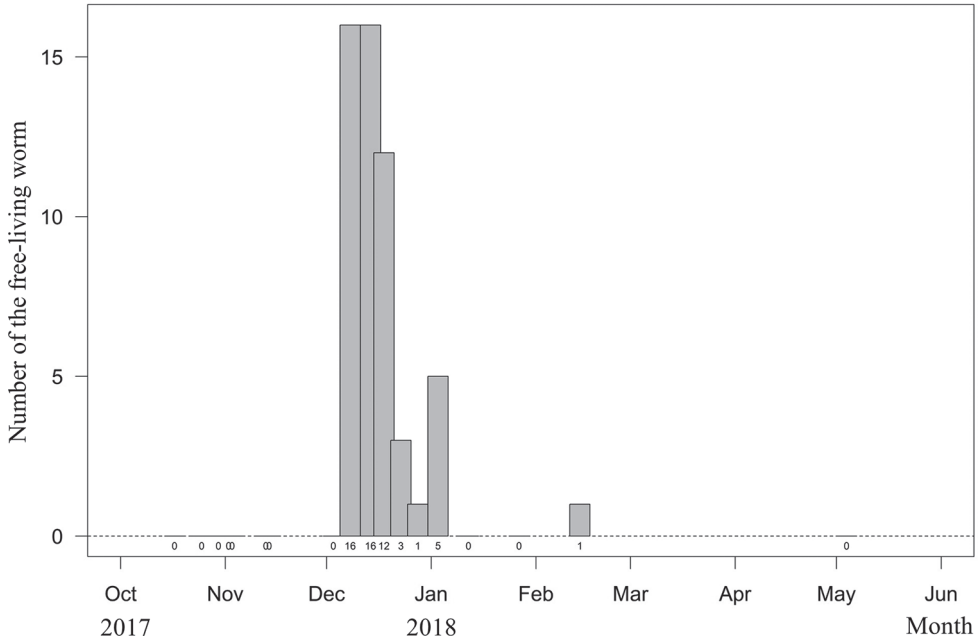


Figure 8. Seasonal occurrence of free-living adults of *Gordius chiashanus* sp. nov. Numbers at the bottom indicate the actual number of each bar.

netic tree and had low genetic distances (Fig. 7, Table 3). These samples were regarded as a new species, *Gordius chiashanus* sp. nov., on the basis of their distribution patterns of bristles on the male tail and presence of a vertical white stripe on the anterior ventral side and areoles on the inside wall of the cloacal opening.

The concentration of bristles and spines on the male tail lobes has been previously described in species from the Palaearctic (Spiridonov 1984; Schmidt-Rhaesa 2010) and Nearctic realms (Anaya et al. 2019). In *Gordius chiashanus* sp. nov., this dense patch of bristles is a stable characteristic that was detected in all samples. The distribution pattern was similar to that of *G. helveticus* (Schmidt-Rhaesa 2010) because the bristles exhibited a progressively broader distribution instead of being concentrated along the row of the ventral border, such as in *G. karwendeli* Schmidt-Rhaesa, 2010 (Schmidt-Rhaesa 2010) and *G. terrestris* (Anaya et al. 2019), or in a circular patch of concentrated spines, such as in *G. spiridonovi* Schmidt-Rhaesa, 2010 (Spiridonov 1984).

Although the distribution pattern of the bristles is similar to that of *G. helveticus*, *G. chiashanus* sp. nov. is morphologically distinct because of the presence of stout bristles on the mid-body, a vertical white stripe on the anterior ventral side, and areoles on the inside wall of the cloacal opening. The vertical white stripe on the anterior ventral side can be easily observed by the naked eye, but it has rarely been mentioned thus far. The presence of a white stripe was previously reported in the terrestrial hairworm, *G. terrestris* (Anaya et al. 2019), which exhibits a broad white patch; however, the patch is likely to be the intensive aggregation of white spots in *Gordius chiashanus* sp. nov. The presence of areoles on the inside wall of the cloacal opening has only been reported in

an unknown *Gordius* (Schmidt-Rhaesa 2012, fig. 3.2.2). Although cloacal openings are usually covered by contamination in many *Gordius* species, as was the case in most of our samples, the areole on the inside wall of cloacal opening might not be a general characteristic of the genus *Gordius* because it is absent in at least some species (e.g., *G. serratus* Schmidt-Rhaesa, 2010, *G. terrestris*, *G. spiridonovi*) (Schmidt-Rhaesa 2010; Schmidt-Rhaesa and Prous 2010; Anaya et al. 2019).

Discussion

Gordius chiashanus sp. nov. and the two previously described species, namely *A. taiwanensis* Chiu et al., 2017 and *C. formosanus* Chiu, 2011 (Chiu et al. 2011, 2017), are the three most frequently sighted horsehair worm species in Taiwan. Unlike the two low-altitude species, *Gordius chiashanus* sp. nov. inhabits medium altitude areas (1100–1700 m), which matches the distribution of its millipede host, *Spirobolus* sp. nov. (Hsu and Chang, unpublished), in Taiwan (1100–1600 m) (Hsu 2008).

Morphology of *Gordius chiashanus* sp. nov. With approximately 90 valid species, *Gordius* is the second most diverse genus of the phylum Nematomorpha (Schmidt-Rhaesa 2012). However, because of the lack of reliable diagnostic characteristics and non-hereditary morphological variation associated with methods of examination, environmental damage, mucus-like structure covering the surface, and different hosts, species identification within this genus is difficult (Schmidt-Rhaesa 2001, 2010; Chiu et al. 2011, 2017; Hanelt et al. 2015). Previously, the white spot has been only found on the male cuticle (Schmidt-Rhaesa 2010). However, we found it, but unexpectedly, in the female *Gordius chiashanus* sp. nov. by examination with a compound microscope. It is clearly necessary to reexamine other species since it might have been ignored especially in the female samples. The mucus-like structure is the structure covering the body surface which might also cause morphological variation. It was first reported in *A. taiwanensis* (Chiu et al. 2017) but not in our observations of *C. formosanus* (Chiu et al. 2011, 2017). In *Gordius chiashanus* sp. nov., it was more obvious than that of *A. taiwanensis* by the bright light reflection on the body surface and the hazy appearance surrounding the worms after treatment with hot water. The mucus-like structure appeared opaque under the SEM; this opacity might hamper the visibility of small structures (Fig. 1C, D), consequently, the reliability of such a diagnostic characteristic is low.

Adult and larval size. The body length of *Gordius* is variable and can be longer than 2 m (Schmidt-Rhaesa 2010). Relative to phylogeny, host size and intensity of infection play more crucial roles in determining worm size (Hanelt 2009; Chiu et al. 2017). Although the adult length is less likely to be a common feature shared among a species, larval size might have been overlooked. Hidden diversity due to large cysts in the paratenic host is often detected (Chiu et al. 2016). Larvae of *Gordius chiashanus* sp. nov. are morphologically similar to *A. taiwanensis* (Chiu et al. 2017) but significantly longer than *A. taiwanensis* larvae (preseptum + postseptum: $162.80 \pm 1.78 \mu\text{m}$ vs. $112.00 \pm 5.52 \mu\text{m}$, larvae treated with hot water). In terms of comparison with other *Gordius* species, although the measurements varied considerably among the untreated larvae, the larval

lengths of *Gordius chiashanus* sp. nov. ($115.38 \pm 12.08 \mu\text{m}$) were similar to those of *G. cf. robustus* # 1 ($110.0 \mu\text{m}$ in Szymgiel et al. 2014) but longer than the unfolded larva of a *Gordius* species ($80.02 \mu\text{m}$ in Fig. 1D, Harkins et al. 2016) and shorter than those of *G. cf. robustus* # 2 ($140.2 \mu\text{m}$ in Szymgiel et al. 2014). The fine structures of larvae are potential to be adopted in distinguishing the close species. By examining with SEM, Anaya et al. (2019) found differences in the number of spines on the proboscis, while *G. terrestris* has seven spines on the distal end of the left lateral and right lateral sides, whereas there are nine in *G. cf. robustus* #1 (Szymgiel et al. 2014). Similarly, the pattern of spines on the proboscis is also different in *C. formosanus* (nine on the distal end of the dorsal and ventral sides (Chiu et al. 2011)) and *C. morgani*, *C. kenyaensis*, and *C. janovyi* (5 on the each side) (Bolek et al. 2010, 2013; Szymgiel et al. 2014). In this study, larvae of *Gordius chiashanus* sp. nov. are failed to be examined by SEM, but it is worth to compare the larval morphology through the horsehair worm species in future studies.

Phylogenetic relationship of *Gordius* and *Acutogordius*. Molecular comparisons have been rarely conducted in the 19 nematomorph genera (Bleidorn et al. 2002; Efeykin et al. 2016), and the present study is the first examination of the phylogenetic relationship of *Acutogordius* and *Gordius* belonging to the family Gordiidae. Because of the shared characteristic of the postcloacal crescent, *Acutogordius* was considered to be phylogenetically close to *Gordius* but distinct because of its pointed tail lobes (Schmidt-Rhaesa 2002). Two hypotheses have suggested that *Acutogordius* might act as a sister group or a subtaxon of *Gordius* (Schmidt-Rhaesa 2002). Our results indicate that the genus *Acutogordius* is a subtaxon of *Gordius* species, although including only one *Acutogordius* species in analysis is insufficient to support a monophyly of the genera *Gordius* and *Acutogordius*. Moreover, our results suggest that *Acutogordius* might be a group of *Gordius* that adapts to tropical habitats. The three clades of tropical horsehair worms are grouped together with the sequences for *A. taiwanensis* from Taiwan, one sequence from Myanmar (Myanmar nematomorph, MF983649), *Gordius* sp. N178 (KM382321) from Nicaragua, and *Gordius* sp. N178 (KM382322) from Malaysia. The adaptation to the tropical habitat of these two genera corresponds with the global distribution. *Acutogordius* species are mostly distributed in the lower latitude regions; by contrast, the *Gordius* species mainly inhabits the Palearctic realm (Schmidt-Rhaesa 2002, 2014; Schmidt-Rhaesa and Geraci 2006; Schmidt-Rhaesa and Schwarz 2016; Chiu et al. 2017). In addition, similar patterns were observed in the altitudinal distribution of these two genera in Taiwan. *Acutogordius taiwanensis* mainly inhabits low-altitude rivers (Chiu et al. 2017), whereas *Gordius chiashanus* sp. nov. is only found in mountains at 1000 m. It is worth to note that *Gordius chiashanus* sp. nov. is in the same clade with *G. terrestris* and *G. cf. robustus* (clade 8). Despite not highly supported by the bootstrap method, these three species show a distinct similarity in biology. The definitive host of *G. cf. robustus* (clade 8) is the millipede, whereas that of most of *G. cf. robustus* (clade 2, 3, 4, 6) are orthopterans (Hanelt et al. 2015). For *Gordius chiashanus* sp. nov. and *G. terrestris*, the egg with a distinct membrane around the larva and the free-living adapting to terrestrial environment have never mentioned in other species. This clade of *Gordius* might represent a unique life history of the horsehair worm.

Definitive host and route of transmission. The millipede has been known to be the host of horsehair worms, including the genera *Gordius* and *Gordionus* (Schmidt-Rhaesa et al. 2009; Schmidt-Rhaesa 2012; Hanelt et al. 2015). As a detritivore, it is less likely to ingest horsehair worm cysts from the paratenic host. In 1930, Dorier suggested water and vegetation possible route of transmission after observing the formation of horsehair worm cysts in the external environment instead of inside the paratenic host (reviewed in Schmidt-Rhaesa et al. 2009). Recent observations of free-living cysts support this hypothesis (Bolek et al. 2015; Chiu et al. 2017). However, a detritivore definitive host can also be infected by ingesting corpses of the infected paratenic hosts. The cysts, which were putatively identified as *Gordius chiashanus* sp. nov., found in the mayfly naiads suggest that this is a possible route of transmission. However, the prevalence was low (3.85 and 8.33% from 26 and 24 hosts collected in Shihjhuo in the end of July). It might suggest the less efficiency in transmission or the under estimation of the prevalence since the samples were collected 4 months before the worm appeared on the soil surface.

Host and host manipulation of horsehair worms. The host and biological characteristics of *Gordius chiashanus* sp. nov. suggest an atypical life history. In general, freshwater horsehair worms (gordiids) develop in terrestrial definitive hosts and reproduce in aquatic environments (Hanelt et al. 2005). Adult worms maturing in terrestrial hosts have long been observed and confirmed through experimentation to manipulate host behavior to facilitate host falling into water, which enables them to reproduce in water (Thomas et al. 2002; Sanchez et al. 2008; Ponton et al. 2011). However, these observations are confined to the gordiids parasitizing a few host taxa (mantids and orthopterans) (Schmidt-Rhaesa and Ehrmann 2001; Thomas et al. 2002), whereas that parasitizing other hosts, crossing several arthropod taxa (Schmidt-Rhaesa 2010; Bolek et al. 2015), is likely to exhibit the different reproductive strategy. The alternative non-manipulative hypotheses include the “chance hypothesis” suggested by observations of adult *C. ferganensis* Kirjanova & Spiridonov, 1989 emerging from mantids that drowned in small puddles formed by heavy rains (Kirjanova and Spiridonov (1989), reviewed by Schmidt-Rhaesa and Ehrmann (2001)). The “aquatic life cycle hypothesis” is suggested by the *Gordius* spp. parasitizing aquatic caddisfly larvae as definitive hosts (Valvassori et al. 1988; Schmidt-Rhaesa and Kristensen 2006), and the “terrestrial life cycle hypothesis” suggested by *G. terrestris* laying eggs in wet soil (Anaya et al. 2019).

In this study, the female adult oviposited in the water. The cysts found in the aquatic paratenic hosts and the eggs developing in water also suggest the life cycle of *Gordius chiashanus* sp. nov. could occur in water and on land. However, the current evidence did not exclude the oviposition in the terrestrial environment because no terrestrial paratenic host was examined for cysts. In addition, the double membraned egg (Anaya et al. 2019) and the mating on the ground both suggest *Gordius chiashanus* sp. nov. might be able to reproduce in the terrestrial environment. Regardless of the scenarios, the adult worm might not be carried to water by manipulating behavior of its millipede host. Alternatively, they may emerge in the terrestrial environment, and move into the water or reproduce in the soil. Free-living adults of *Gordius chiashanus* sp. nov. are frequently found moving and mating on the surface of wet soil during periods of fog and rain. The mucus-like structure, which causes a rainbow-like reflec-

tion, might endow the worm with a high tolerance to dehydration. In the winter (late November to early February), the number of free-living adults sampled from the surface of the soil, suddenly increased and then steadily diminished. The adult *C. formosanus* has a pattern that differs from the bell curve in terms of its presence inside a manipulated host (Chiu et al. 2016, fig. 8) and free-living adults of *G. difficilis* in the water (Bolek and Coggins 2002). This difference suggests that the seasonal occurrence of *Gordius chiashanus* sp. nov. does not represent the time when the worm matures but the time of reproduction after the free-living adult has waited for suitable soil conditions. That worms emerging from the hosts in the soil might explain why infected millipedes are rarely found on the ground.

Acknowledgments

We deeply appreciate the assistance provided by Hua-Te Fang, Po-Yen Chen, Yu-Hsuan Tsai, Ta-Chih Chen, and Yu-Wei Li during sample collection, Wei-Chun Chien during SEM examination, and Masato Nitta, Rui Ueda, Takuya Sato, and Scotty Yang during DNA sequencing. We specially thank Ming-Chin Hung for providing host information. This manuscript was edited by Wallace Academic Editing.

References

- Abràmoff MD, Magalhães PJ, Ram SJ (2004) Image processing with ImageJ. *Biophotonics International* 11: 36–42. <http://imagej.nih.gov/ij/>
- Anaya C, Schmidt-Rhaesa A, Hanelt B, Bolek MG (2019) A new species of *Gordius* (Phylum Nematomorpha) from terrestrial habitats in North America. *ZooKeys* 892: 59–75. <https://doi.org/10.3897/zookeys.892.38868>
- Bleidorn C, Schmidt-Rhaesa A, Garey JR (2002) Systematic relationships of Nematomorpha based on molecular and morphological data. *Invertebrate Biology* 121: 357–364. <https://doi.org/10.1111/j.1744-7410.2002.tb00136.x>
- Bolek MG, Coggins JR (2002) Seasonal occurrence, morphology, and observations on the life history of *Gordius difficilis* (Nematomorpha: Gordioidea) from southeastern Wisconsin, United States. *Journal of Parasitology* 88: 287–294. [https://doi.org/10.1645/0022-3395\(2002\)088\[0287:SOMAOO\]2.0.CO;2](https://doi.org/10.1645/0022-3395(2002)088[0287:SOMAOO]2.0.CO;2)
- Bolek MG, Schmidt-Rhaesa A, Hanelt B, Richardson DJ (2010) Redescription of the African *Chordodes albibarbatulus* Montgomery 1898, and description of *Chordodes janovyi* n. sp. (Gordiida, Nematomorpha) and its non-adult stages from Cameroon, Africa. *Zootaxa* 2631: 36–54. <https://doi.org/10.11646/zootaxa.2631.1.3>
- Bolek MG, Szmygiel C, Kubat A, Schmidt-Rhaesa A, Hanelt B (2013) Novel techniques for biodiversity studies of gordiids and description of a new species of *Chordodes* (Gordiida, Nematomorpha) from Kenya, Africa. *Zootaxa* 3717: 23–38. <https://doi.org/10.11646/zootaxa.3717.1.2>
- Bolek MG, Schmidt-Rhaesa A, De Villalobos LC, Hanelt B (2015) Phylum Nematomorpha. In: Thorp J, Rogers DC (Eds) *Ecology and General Biology: Thorp and Covich's Fresh-*

- water Invertebrates (4th ed.). Academic Press, London, 303–326. <https://doi.org/10.1016/B978-0-12-385026-3.00015-2>
- Chiu MC, Huang CG, Wu WJ, Shiao SF (2011) A new horsehair worm, *Chordodes formosanus* sp. n. (Nematomorpha, Gordiida) from *Hierodula* mantids of Taiwan and Japan with redescription of a closely related species, *Chordodes japonensis*. *ZooKeys* 160: 1–22. <https://doi.org/10.3897/zookeys.160.2290>
- Chiu MC, Huang CG, Wu WJ, Shiao SF (2016) Annual survey of horsehair worm cysts in northern Taiwan, with notes on a single seasonal infection peak in chironomid larvae (Diptera: Chironomidae). *Journal of Parasitology* 102: 319–326. <https://doi.org/10.1645/15-907>
- Chiu MC, Huang CG, Wu WJ, Shiao SF (2017) A new orthopteran-parasitizing horsehair worm, *Acutogordius taiwanensis* sp. n., with a redescription of *Chordodes formosanus* and novel host records from Taiwan (Nematomorpha, Gordiida). *ZooKeys* 683: 1–23. <https://doi.org/10.3897/zookeys.683.12673>
- Dorier A (1930) Recherches Biologiques et Systématiques sur les Gordiacés. *Travaux du Laboratoire d'Hydrobiologie et de Pisciculture de l'Université de Grenoble* 22: 1–183.
- Efeykin BD, Schmatko VY, Spiridonov SE (2016) Comparative phylogenetic informativity of single ribosomal cluster regions in freshwater horsehair worms (Gordieacea, Nematomorpha). *Biology Bulletin* 43: 34–41. <https://doi.org/10.1134/S1062359016010040>
- Folmer O, Black M, Hoen W, Lutz R, Vrijenhoek R (1994) DNA primers for amplification of mitochondrial cytochrome oxidase subunit I from diverse metazoan invertebrates. *Molecular Marine Biology and Biotechnology* 3: 294–299. <https://doi.org/10.1371/journal.pone.0013102>
- Hanelt B (2009) An anomaly against a current paradigm—Extremely low rates of individual fecundity variability of the Gordian worm (Nematomorpha: Gordiida). *Parasitology* 136: 211–218. <https://doi.org/10.1017/S0031182008005337>
- Hanelt B, Thomas F, Schmidt-Rhaesa A (2005) Biology of the phylum Nematomorpha. *Advances in Parasitology* 59: 243–305. [https://doi.org/10.1016/S0065-308X\(05\)59004-3](https://doi.org/10.1016/S0065-308X(05)59004-3)
- Hanelt B, Schmidt-Rhaesa A, Bolek MG (2015) Cryptic species of hairworm parasites revealed by molecular data and crowdsourcing of specimen collections. *Molecular Phylogenetics and Evolution* 82: 211–218. <https://doi.org/10.1016/j.ympev.2014.09.010>
- Harkins C, Shannon R, Papeş M, Schmidt-Rhaesa A, Hanelt B, Bolek MG (2016) Using Gordiid cysts to discover the hidden diversity, potential distribution, and new species of Gordiids (Phylum Nematomorpha). *Zootaxa* 4088: 515–530. <https://doi.org/10.11646/zootaxa.4088.4.3>
- Hsu MH (2008) Taxonomic study of the millipede order Spirobolida (Class Diplopoda) of Taiwan. Master thesis, Kaohsiung, Taiwan: National Sun Yat-sen University. [in Chinese with English abstract]
- Kirjanova ES, Spiridonov SE (1989) Two new species of the nematomorph genus *Chordodes* from mantids. *Parazitologiya* 23: 358–362. [in Russian with English abstract]
- Kumar S, Stecher G, Tamura K (2016) MEGA7: molecular evolutionary genetics analysis version 7.0 for bigger datasets. *Molecular Biology and Evolution* 33: 1870–1874. <https://doi.org/10.1093/molbev/msw054>
- Ponton F, Otálora-Luna F, Lefèvre T, Guerin PM, Lebarbenchon C, Duneau D, Biron DG, Thomas F (2011) Water-seeking behavior in worm-infected crickets and reversibility of parasitic manipulation. *Behavioral Ecology* 22: 392–400. <https://doi.org/10.1093/beheco/arq215>

- Sanchez MI, Ponton F, Schmidt-Rhaesa A, Hughes DP, Misse D, Thomas F (2008) Two steps to suicide in crickets harbouring hairworms. *Animal Behaviour* 76: 1621–1624. <https://doi.org/10.1016/j.anbehav.2008.07.018>
- Sato T, Watanabe K, Tamotsu S, Ichikawa A, Schmidt-Rhaesa A (2012) Diversity of nematomorph and cohabiting nematode parasites in riparian ecosystems around the Kii Peninsula, Japan. *Canadian Journal of Zoology* 90: 829–838. <https://doi.org/10.1139/z2012-048>
- Schmidt-Rhaesa A (2001) Problems and perspectives in the systematics of Nematomorpha. *Organisms Diversity & Evolution* 1: 161–163. <https://doi.org/10.1078/1439-6092-00013>
- Schmidt-Rhaesa A (2002) Are the genera of Nematomorpha monophyletic taxa? *Zoologica Scripta* 31: 185–200. <https://doi.org/10.1046/j.1463-6409.2002.00073.x>
- Schmidt-Rhaesa A (2010) Considerations on the genus *Gordius* (Nematomorpha, horsehair worms), with the description of seven new species. *Zootaxa* 2533: 1–35. <https://doi.org/10.11646/zootaxa.2533.1.1>
- Schmidt-Rhaesa A (2012) Nematomorpha. In: Schmidt-Rhaesa A (Ed.) *Handbook of Zoology. Gastrotricha, Cycloneuralia and Gnathifera* (Vol. 1). Nematomorpha, Priapulida, Kinorhyncha and Loricifera. De Gruyter, Berlin, 29–145. <https://doi.org/10.1515/9783110272536>
- Schmidt-Rhaesa A, Ehrmann R (2001) Horsehair worms (Nematomorpha) as parasites of praying mantids with a discussion of their life cycle. *Zoologischer Anzeiger* 240: 167–179. <https://doi.org/10.1078/0044-5231-00014>
- Schmidt-Rhaesa A, Geraci CJ (2006) Two new species of *Acutogordius* (Nematomorpha), with a brief review of literature data of this genus. *Systematics and Biodiversity* 4: 427–433. <https://doi.org/10.1017/S1477200006001964>
- Schmidt-Rhaesa A, Kristensen P (2006) Horsehair worms (Nematomorpha) from the Baltic island Bornholm (Denmark), with notes on the biology of *Gordius albopunctatus*. *Journal of Natural History* 40: 9–10. <https://doi.org/10.1080/00222930600761803>
- Schmidt-Rhaesa A, Prous M (2010) Records of horsehair worms (Nematomorpha) in Estonia, with description of three new species from the genus *Gordius* L. *Estonian Journal of Ecology* 59: 39–51. <https://doi.org/10.3176/eco.2010.1.03>
- Schmidt-Rhaesa A, Schwarz CJ (2016) Nematomorpha from the Philippines, with description of two new species. *Zootaxa* 4158: 246–260. <https://doi.org/10.11646/zootaxa.4158.2.6>
- Schmidt-Rhaesa A, Farfan MA, Bernard EC (2009) First record of millipeds as hosts for horsehair worms (Nematomorpha) in North America. *Northeastern Naturalist* 16: 125–130. <https://doi.org/10.1656/045.016.0110>
- Spiridonov SE (1984) Two new Nematomorpha species of the family Gordiidae. *Proceedings of the Zoological Institute USSR Academy of Sciences* 126: 97–101.
- Szmygiel C, Schmidt-Rhaesa A, Hanelt B, Bolek MG (2014) Comparative descriptions of non-adult stages of four genera of Gordiids (Phylum: Nematomorpha). *Zootaxa* 3768: 101–118. <https://doi.org/10.11646/zootaxa.3768.2.1>
- Thomas F, Schmidt-Rhaesa A, Martin G, Manu C, Durand P, Renaud F (2002) Do hairworms (Nematomorpha) manipulate the water seeking behaviour of their terrestrial hosts? *Evolutionary Biology* 15: 356–361. <https://doi.org/10.1046/j.1420-9101.2002.00410.x>
- Thompson JD, Gibson TJ, Plewniak F, Jeanmougin F, Higgins DG (1997) The ClustalX windows interface: flexible strategies for multiple sequence alignment aided by quality analysis tools. *Nucleic Acids Research* 25: 4876–4882. <https://doi.org/10.1093/nar/25.24.4876>

- Thorne G (1940) The hairworm *Gordius robustus* Leidy, as a parasite of the Mormon cricket, *Anabrus simplex* Haldeman. Journal of the Washington Academy of Sciences 30: 219–231. <https://www.jstor.org/stable/24529727>
- Tobias ZJC, Yadav AK, Schmidt-Rhaesa A, Poulin R (2017) Intra- and interspecific genetic diversity of New Zealand hairworms (Nematomorpha). Parasitology 144: 1026–1040. <https://doi.org/10.1017/S0031182017000233>
- Valvassori R, Scari G, De Eguileor M, Lernia LD, Magneto P, Melone G (1988) *Gordius villoti* (Nematomorpha) life cycle in relation with caddis fly larvae. Bollettino di Zoologia 55: 1–4. <https://doi.org/10.1080/11250008809386624>
- Walter DE, Krantz GW (2009) Collecting, rearing, and preparing specimens. In: Walter DE, Krantz GW (Eds) A Manual of Acarology (3rd ed.). Texas Tech University Press, Lubbock, 83–96.

Supplementary material 1

Video S1

Authors: Ming-Chung Chiu, Chin-Gi Huang, Wen-Jer Wu, Zhao-Hui Lin, Hsuan-Wien Chen, Shiuh-Feng Shiao

Data type: multimedia

Explanation note: Free-living adult of *Gordius chiashanus* sp. nov. moving on the ground at night, with a rainbow-like reflection on the body surface.

Copyright notice: This dataset is made available under the Open Database License (<http://opendatacommons.org/licenses/odbl/1.0/>). The Open Database License (ODbL) is a license agreement intended to allow users to freely share, modify, and use this Dataset while maintaining this same freedom for others, provided that the original source and author(s) are credited.

Link: <https://doi.org/10.3897/zookeys.941.49100.suppl1>

Supplementary material 2

Fasta 2

Authors: Ming-Chung Chiu, Chin-Gi Huang, Wen-Jer Wu, Zhao-Hui Lin, Hsuan-Wien Chen, Shiuh-Feng Shiao

Data type: molecular data

Explanation note: COI sequences adopted in the phylogenetic analysis, including for *Gordius/Acutogordius* spp. with *Chordodes formosanus*, *Euchordodes nigromaculatus*, and *Parachordodes diblastus* as out groups.

Copyright notice: This dataset is made available under the Open Database License (<http://opendatacommons.org/licenses/odbl/1.0/>). The Open Database License (ODbL) is a license agreement intended to allow users to freely share, modify, and use this Dataset while maintaining this same freedom for others, provided that the original source and author(s) are credited.

Link: <https://doi.org/10.3897/zookeys.941.49100.suppl2>

Population genetics and diversity structure of an invasive earthworm in tropical and temperate pastures from Veracruz, Mexico

Diana Ortíz-Gamino^{1,2}, Josefát Gregorio³, Luis Cunha⁴,
Esperanza Martínez-Romero⁵, Carlos Fragoso⁶, Ángel I. Ortíz-Ceballos¹

1 Instituto de Biotecnología y Ecología Aplicada (INBIOTECA), Universidad Veracruzana. Av. de las Culturas Veracruzanas No. 101, Col. Emiliano Zapata, 91090 Xalapa, Veracruz, México **2** Subdirección de Recursos Naturales y Cambio Climático del H. Ayuntamiento de Xalapa, Calle Volcán de Colima 7, Coapexpan 91070, Xalapa, Veracruz, México **3** Consejo Nacional de Ciencia y Tecnología - Centro de Investigación en Biotecnología Aplicada, Instituto Politécnico Nacional, Av. Insurgentes Sur 1582, Col. Crédito Constructor, Del. Benito Juárez, Ciudad de México, 03940, México **4** School of Applied Sciences, University of South Wales, Pontypridd, UK **5** Centro de Ciencias Genómicas, Universidad Nacional Autónoma de México Campus Morelos, Av. Universidad s/n Col. Chamilpa 62210, Cuernavaca, Morelos, México **6** Instituto de Ecología, A.C., Carretera antigua a Coatepec 351, El Haya 91070, Xalapa, Veracruz, México

Corresponding author: Ángel I. Ortíz-Ceballos (angortiz@uv.mx)

Academic editor: S. James | Received 12 December 2019 | Accepted 13 April 2020 | Published 16 June 2020

<http://zoobank.org/189F5AC3-0F27-4B4E-89A5-74A3F8DBC8FB>

Citation: Ortíz-Gamino D, Gregorio J, Cunha L, Martínez-Romero E, Fragoso C, Ortíz-Ceballos AI (2020) Population genetics and diversity structure of an invasive earthworm in tropical and temperate pastures from Veracruz, Mexico. ZooKeys 941: 49–69. <https://doi.org/10.3897/zookeys.941.49319>

Abstract

Pontoscolex corethrurus (Müller, 1857) is an invasive tropical earthworm, globally distributed. It reproduces through parthenogenesis, which theoretically results in low genetic diversity. The analysis of the population structure of *P. corethrurus* using molecular markers may significantly contribute to understanding the ecology and reproductive system of this earthworm species. This work assessed the genetic diversity and population structure of *P. corethrurus* with 34 polymorphic inter simple sequence repeat markers, covering four populations in tropical and temperate pastures from Veracruz State. Nuclear markers distinguished two genetic clusters, probably corresponding to two distinct genetic lineages. The number of clones detected in the AC population was lower than expected for a parthenogenetic species. Also, the apparent lack of differences in population structures related to the geographic region among the populations studied may indicate that human-mediated transference is prevalent in these areas. Still, most individuals apparently belong to lineage A, and only a few individuals seem to belong to the lineage B. Thus, the admixture signatures

found among the four populations of *P. corethrurus* may have facilitated a successful invasion by directly increasing fitness. In summary, addressing the genetic variation of *P. corethrurus* with ISSR markers was a suitable approach, as it evidenced the genetic diversity and relationships in the populations evaluated.

Keywords

Agroecosystems, asexual reproduction, exotic earthworm, peregrine species, Rhinodrilidae

Introduction

Earthworms are not only ubiquitous ecological engineers of soil that create biogenic structures; they also sustain the functioning of the ecosystem through their fundamental actions (Lavelle et al. 1997; Brown et al. 2001; Barros et al. 2004). Despite the importance of soil organisms in ecosystem functioning, the soil ecosystem seems to be poorly studied (González et al. 2006). In fact, for a long time, little attention has been given to invasive soil organisms such as earthworms (Gates 1954), despite a rise in belowground invasion over the past 30 years (Hendrix et al. 2002; Craven et al. 2016; Cicconardi et al. 2017). In Mexico, the first records regarding exotic earthworms date from 1900–1906, being lumbricids (*Dendrobaena octaedra* Savigny, 1826; *Lumbricus terrestris* Linnaeus, 1758), megascolecids (*Metaphire californica* Kinberg, 1867), benhaminis (*Dichogaster bolau* Michaelsen, 1891), and rhinodrilids (*Pontoscolex corethrurus* Müller, 1857) the earthworms registered (Eisen 1900; Michaelsen 1900; Beddard 1912). Since then, 51 exotic species have been described across the country by classical taxonomy (Fragoso and Rojas 2014). Several factors acting at different temporal and spatial scales are involved in earthworm invasion, but the overall picture is not yet understood (Marinissen and Van den Bosch 1992; Baker et al. 2006; Brown et al. 2006; González et al. 2006; Cameron and Bayne 2009; Marichal et al. 2012). In general, the genetic characteristics of invasive organisms have profound impacts on their establishment capacity, range expansions, and successful invasion (Lee 2002).

Pontoscolex corethrurus, formerly included in Glossoscolecidae but is now placed in Rhinodrilidae (James 2012), is an earthworm species originating in South America, in the Guiana Shield area of the Amazon (Gates 1954; Righi 1984). The global and local distribution of *P. corethrurus* have been addressed, as well as its interspecific interactions (Ortíz-Gamino et al. 2016; Taheri et al. 2018). It has been hypothesized that the successfulness of *P. corethrurus* is based on its genetic plasticity, which in turn is given by high genomic promiscuity associated to its reproductive strategies (Vitturi et al. 2002; Bengtsson 2009; Fernández et al. 2013; Cunha et al. 2014; Pavlíček et al. 2016).

Parthenogenesis is common in earthworms, usually associated with dispersal, where a single propagule is usually sufficient to establish a new population (Terhivuo and Saura 2006). Thus, rapid adaptation of parthenogenetic clonal populations may be an essential mechanism for a successful colonization event, as is the case of *P. corethrurus* (Gates 1973; Lavelle et al. 1987; González et al. 2006; Hendrix et al. 2006; Terhivuo and Saura 2006; Buch et al. 2011). Under such a scenario, the genetic variation of *P. corethrurus* in regions far from its natural geographic range may be low if

only a single or very few individuals were colonizers (Dupont et al. 2012). Through mitochondrial and nuclear markers, 792 earthworms collected recently over 25 countries demonstrated that *P. corethrurus* is a complex of cryptic species. This is represented by a monophyletic clade composed of four morphologically indistinguishable lineages named as L1, L2, L3, L4 (Taheri et al. 2018).

Around the world, *P. corethrurus* is distributed from 0 to 2000 m a.s.l., with an average altitude of 463 m (Fragoso et al. 1999). In Mexico, specifically in Veracruz State, its distribution ranges from 0 to around 1600 m a.s.l., living at an average temperature of 17 °C (Ortíz-Gamino et al. 2016). The distribution of *P. corethrurus* in Mexico seems to be strongly associated with human-mediated dispersal due to agricultural activities (González et al. 2006; Feijoo et al. 2007; Hendrix et al. 2008; Dupont et al. 2012). Moreover, although Taheri and co-workers have determined recently that *P. corethrurus* living in the State of Veracruz correspond to lineages L1 and L3 (Taheri et al. 2018), this finding was based on only a few specimens, which is likely not representing the entire population. For this reason, further research on population genetics may significantly contribute to understanding the ecology of *P. corethrurus* in Mexico. Thus, the objective of this work was to explore the genetic variation and population structure in *P. corethrurus* inhabiting tropical and temperate pastures in Mexico using a molecular approach based on ISSR markers.

Materials and methods

Sampling sites and animal collection

Sampling points were established according to the different attributes of the sites studied in Veracruz State, Mexico (Ortíz-Gamino et al. 2016). In brief, the sampling sites were Laguna Verde (LV), Actopan (AC), Ingenio La Concepción (LC) and Naolinco (NA) (Table 1 and Figure 1), each of them with characteristic ecological attributes. During September 2013, 40 mature (clitellate) individuals of *P. corethrurus* were collected ($N = 10$ per site). Earthworms were kept in plastic boxes with moistened soil and transported to the laboratory at INBIOTECA for taxonomical and anatomical identification (Moreno and Borges 2004). Specimens were rinsed in water to remove soil particles and were fixed with 96% ethanol. All samples were kept at -20 °C until further processing.

Table 1. Attributes of earthworms sampling of four pastures in central Veracruz State, Mexico.

Sampling Site	Altitude (m a.s.l.)	Climate	Grass species	Soil texture (%)		
				Clay	Silt	Sand
Laguna Verde (LV)	24	Aw1(w)g	<i>Paspalum conjugatum</i> , <i>Cynodon nlemfuensis</i>	26.6	28.1	45.3
Actopan (AC)	480	Aw0(w)gw ⁿ	<i>Saccharum officinarum</i> L.	12.8	32.3	54.9
La Concepción (LC)	973–1036	(A)Ca(f)gw ⁿ	<i>Paspalum conjugatum</i> , <i>Cynodon nlemfuensis</i>	26.6	28.2	45.3
Naolinco (NA)	1566–1667	Cb(fm)gw ⁿ	<i>Paspalum conjugatum</i> , <i>Cynodon nlemfuensis</i> , <i>Pennisetum clandestinum</i>	12.8	32.3	54.9

Key: Climate: Aw1(w)g and Aw0(w)gwⁿ are used for warm and sub-humid climate; (A)Ca(f)gwⁿ for warm and humid climate; Cb (fm)gwⁿ, for wet and semi-humid climate. For further details (mean temperature, evapotranspiration, total annual precipitation, etc.), refer to Ortíz-Gamino et al. (2016).

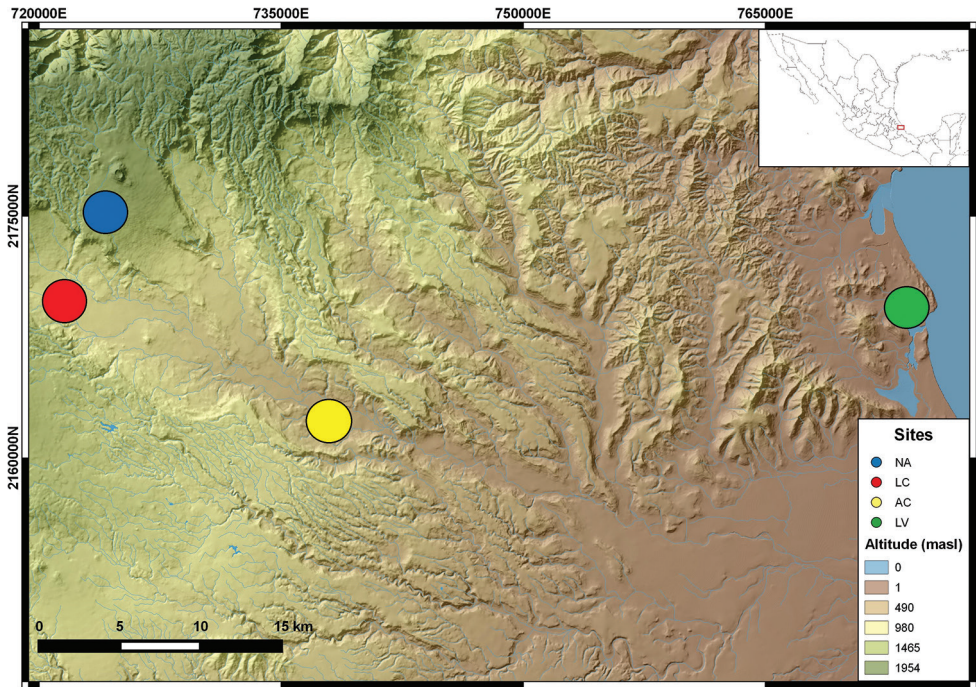


Figure 1. Pastures sampled in the central region of Veracruz State, Mexico. LV, Laguna verde; AC, Actopan; LC, La Concepción; NA, Naolinco. The digital elevation model was created using data provided by Instituto Nacional de Estadística y Geografía, México.

DNA isolation and quantification

Tail-wall tissue was used for extraction of genomic DNA. Total DNA was extracted using the DNeasy Blood & Tissue kit (Qiagen, Mainz, Germany) following the manufacturer's instructions. DNA was checked for quality by gel electrophoresis and quantified using a spectrophotometer (ND-2000, Nanodrop Technologies, Wilmington, DE).

Inter Simple Sequence Repeat (ISSR) protocol

Forty specimens of *P. corethrurus* ($N = 10$ per site) were used for ISSR screening. ISSR screening was based on five primers (Table 2) previously reported to produce polymorphic and reproducible DNA fingerprints for *Eudrilus eugeniae* (Kinberg, 1867) and *Eisenia fetida* (Savigny, 1826) (Sharma et al. 2011). Each PCR reaction contained 1X PCR buffer, 2 mM $MgCl_2$, dNTPs at 100 μ M each, primers at 0.8 μ M each, 1.5 U of Taq DNA polymerase, 1 μ g/ μ l BSA and 30 ng template DNA. The PCR reaction mix was brought to a final volume of 10 μ L with water. PCR amplifications were performed in an Eppendorf Mastercycler (Eppendorf, Hamburg, Germany) according to the following conditions: an initial step at 95 °C for 3 minutes, followed by 35 denaturation cycles at 95 °C for 30 seconds, annealing at primer-specific temperature

Table 2. Primers used for PCR amplification of *Pontoscolex corethrurus* genomic DNA.

Primer	Sequence	T _a (°C)	Maximum number of bands	Estimated size (bp)
840	GAGAGAGAGAGAGAYT	59.5	8	2000-200
834	AGAGAGAGAGAGAGAYT	61	7	2000-300
866	CTCCTCCTCCTCCTCCTC	70	6	2000-400
810	GAGAGAGAGAGAGAT	52.4	6	2000-400
807	AGAGAGAGAGAGAGAT	54.4	7	2000-300

for 30 seconds, and elongation at 72 °C for 1 minute. A final extension was performed at 72 °C for 10 minutes. The PCR products were visualized in 2% agarose gels (with ethidium bromide at 1ul/ml). Although the initial screening used a total of 18 primers, only those primers that were polymorphic and reproducible were selected for subsequent analysis (Table 2).

Data analysis

The amplified DNA fragments were transformed into a binary matrix (1 = presence, 0 = absence), as reported previously (Abbot 2001). A multilocus genotype (MLG) was constructed for each individual by pooling data of single ISSR fingerprints using the procedure available in the POPPR package in R for genetic analysis of populations (Kamvar et al. 2014). Isolates with the same MLG were considered clones, and some analyses were conducted for the original and clone-corrected datasets (Gramaje et al. 2014). The POPPR package in R was used to calculate dissimilarity distance matrices and generate a minimum spanning network from these matrices (Kamvar et al. 2014). To assess the potential evolutionary relationships among MLGs, a minimum spanning network was constructed using the genotypes of earthworm from each sampling location. Bootstrapping was performed with 1000 bootstrap resampling. Genotypic diversity, genetic richness and the evenness index were calculated for each population. The 'rarecurve' function from the VEGAN package in R (Oksanen et al. 2007) was used to generate rarefaction curves. Curves were calculated to determine whether the sampling intensity was adequate to detect most of the MGLs in each *P. corethrurus* population. Additionally, the minimum number of loci needed to distinguish all MGLs was also calculated. Given that sample size varied among populations, we employed rarefaction to explore the effect of sample size on observed MLGs.

Genetic differentiation, structure, and clustering analyses

The genetic variance for all MLGs was estimated through an analysis of molecular variance (AMOVA) using the GenAlEx v.6.5 software (Peakall and Smouse 2006). Genetic variance relative to total variance was calculated as PhiPT (analog of the F_{st} fixation index) for all populations, as well as regarding within-population genetic variance (Peakall and Smouse 2006). The significance was computed by using 9,999 permutations, and the confidence interval at 95%, by 10,000 re-samplings. For this

analysis, only single copies of the different genotypes were used to give identical weight to MLGs. The Mantel test was used to explore the potential correlation between the matrix of genetic differentiation between pairs of MLGs and the matrix of spatial distances between populations, using Arlequin v.3.5 (Excoffier and Lischer 2010). The association between *P. corethrurus* individuals was assessed initially using a Principal Components Analysis (PCA) implemented in GenAlEx v. 6.51 (Peakall and Smouse 2006). As PCA is independent of any genetic hypotheses it is suitable for the analysis of partially clonal species. Additionally, Unweighted Pair Group Method with Arithmetic Mean (UPGMA) dendrograms were also created using the POPPR package (Kamvar et al. 2014). Bootstrapping was performed with the PVCLUST package in R using 10,000 bootstrap re-samplings (Suzuki and Shimodaira 2006).

Population structure was explored using the Bayesian clustering method implemented in STRUCTURE v.2.3.4 (Pritchard et al. 2000), as well as a distance-based approach using a discriminant analysis of principal components (DAPC) (Jombart et al. 2010). STRUCTURE v.2.3.4 was used to identify the number of genetic clusters within the dataset, and to assign individuals to the clusters defined using an admixture model. To this end and to confirm consistency, 15 replicate runs were carried out for each K (1–8). The most likely value of K was determined with “BestK” implemented in CLUMPAK (Evanno et al. 2005), which uses the ΔK method of Evanno et al. (2005). The results from the 15 replicate runs were pooled using CLUMPAK online version (Evanno et al. 2005). Relative dissimilarity distances were calculated according to the index of association (Brown et al. 1980; Smith et al. 1993). The approach returns a distance reflecting a ratio of the number of observed differences to the number of possible differences.

The hybridization status of individuals according to the Bayesian genetic clusters defined in Structure (defined as putative Lineage A and Lineage B) was further investigated using NEWHYBRIDS v1.1 (Anderson and Thompson 2002), which also uses a Bayesian assignment by implementing a multilocus allele frequency model-based approach. This approach clusters together MGLs without *a-priori* knowledge of parental allele frequencies, and also has the advantage of specifically assuming a mixture of parental and several hybrid classes (F1's, F2's, and various backcrosses as B1 and B2 hybrids) to assign them into categories. Individual posterior probabilities belonging to each hybrid category were estimated using the MCMC method in a Bayesian framework using Jeffreys-type priors and a burn-in period of 100000 iterations followed by 50000 sweeps from the posterior distribution sampling (Anderson and Thompson 2002). Linkage disequilibrium as an indication of random mating was calculated and tested for significance with 1,000 randomizations using the POPPR package in R (R core team 2004). The measures of gametic disequilibrium tested were the index of association (I_A) (Brown et al. 1980; Smith et al. 1993) and a standardized alternative of the I_A (\bar{r}_d) (Agapow and Burt 2001). The null hypothesis for this test is that there is a random association among alleles at different loci and $I_A=0$; the null hypothesis for random mating is rejected where if $I_A>0$.

Results

Beyond the ecological relevance of *P. corethrurus*, information on genetic variability is relevant to determine the selective forces that act on the reproductive system of this species. In that sense, the survey carried out in this study was aimed to reveal the population genetic structure of *P. corethrurus* in natural landscapes covering tropical and temperate pastures. For this, a set of ISSR markers were used to assess the genetic diversity and population structure of *P. corethrurus* genotypes from four locations in Veracruz State, Mexico.

Genotypic diversity of *P. corethrurus* populations

Following a PCR-based approach, ISSR primers produced bands on agarose gel that were suitable for assessing the genetic diversity and genetic relationship between and across populations of *P. corethrurus*. The PCR products ranged between ~200 and ~2000 bp from genomic DNAs of *P. corethrurus*. The total number of bands and polymorphism rates are shown in Table 3. A total of 33 MLGs among the 35 *P. corethrurus* individuals yielded reliable products. Overall, one MLG corresponding to AC was observed twice, whereas the rest of MLGs (31) were detected only once. As regards MLG diversity (H), this parameter varied across populations, with no correlation to any specific geographic location (Table 3). On the other hand, in contrast to AC, evenness values (E_5) were higher for LV, LC, and NA, in agreement with the fact that all genotypes found were unique to these populations (Table 3). Nei's unbiased gene diversity (H_{exp}) values varied from the highest (LC = 0.39) to the lowest (NA = 0.29). Most populations exhibit low genetic diversity (Table 3), except for the NA population, which displays a higher genetic diversity. This was supported by the rarefaction curves, which indicated that NA had a higher number of sampled loci, as well as higher MGLs, than the other three populations (Figure 2A). Interestingly, the minimum number of loci needed to define the total number of MLGs found reached a plateau after 18 loci (Figure 2B). Moreover, the variation among and within populations assessed with AMOVA resulted in values of 25% and 75%, respectively (Table 4). Altogether, all populations showed high genotypic diversity, and according to the PhiPT

Table 3. Parameters of genetic variation in four *Pontoscolex corethrurus* populations living in central Veracruz State, Mexico.

Sampling Site	N	MLG	eMLG	Pb	Tb	H	G	E_5	H_{exp}	Ia	rbarD
LV	9	9	9	20	34	2.20	9	1	0.30	1.98*	0.10*
AC	10	8	8	22	34	2.03	7.14	0.93	0.30	3.23*	0.15*
LC	6	6	6	27	34	1.79	6	1	0.39	1.16*	0.04*
NA	10	10	10	24	34	2.30	10	1	0.29	4.08*	0.18*
Total	35	33	9.85			3.48	31.41	0.97	0.40	1.65	0.05

Abbreviations: N, samples; MLG, Multilocus genotypes; eMLG, estimated MLG; H, genetic diversity; G, Evenness index; E_5 , evenness values; H_{exp} , Nei's unbiased gene diversity; Ia, Index of Association; rbarD, standardized index of association.

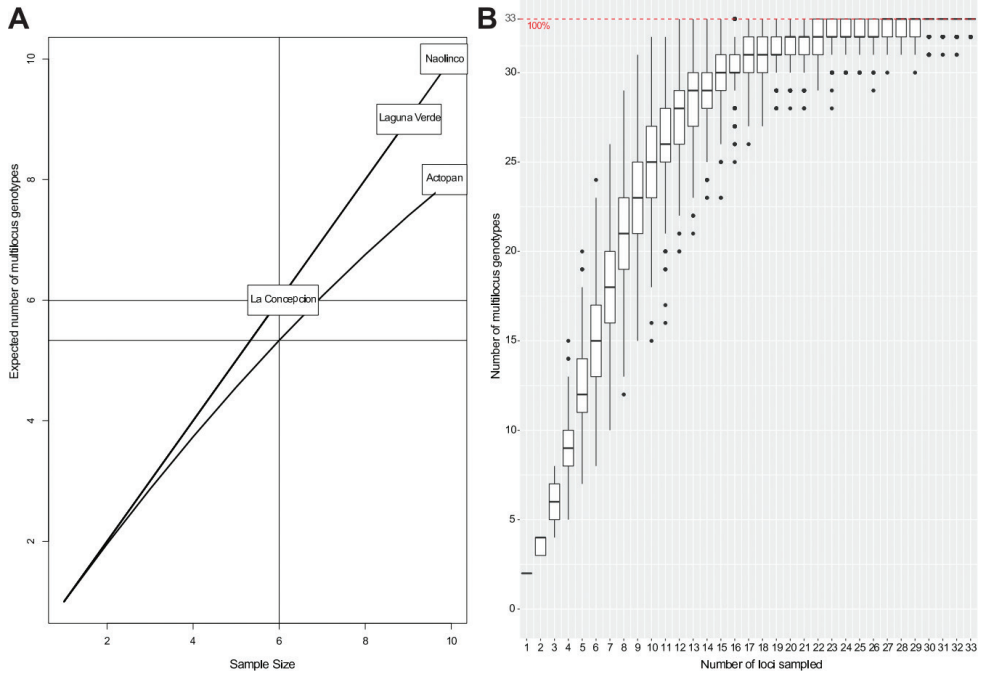


Figure 2. Rarefaction curve of expected number of MLGs captured per earthworm of *Pontoscolex corethrurus* sampled (A), and a MLG accumulation curve according to the number of loci sampled (B).

Table 4. Analysis of molecular variance (AMOVA) testing for genetic differentiation between four populations of *Pontoscolex corethrurus* living in central Veracruz State, Mexico (A), and PhiPT pairwise comparisons (B).

	Level of variation	d.f.	SS	MS	Est. Var.	Proportion (%)
A)	Among Populations	3	59.079	19.693	1.760	25%
	Within Populations	29	154.497	5.327	5.327	75%
	Total	32	213.576		7.088	100%
B)	Population	Laguna Verde	Actopan	La Concepcion	Naolinco	
	Laguna Verde	0.000				
	Actopan	0.229**	0.000			
	La Concepcion	0.069	0.161**	0.000		
	Naolinco	0.335**	0.347**	0.199*	0.000	

Abbreviations: d.f., degrees of freedom; SS, sum of squares; MS, mean squares; Est. Var., estimated variance; %, proportion of molecular variation. Significance levels as follows: * p < 0.05 and ** p < 0.01.

value (analog of F_{st} fixation index), there were significant differences between the LV, AC, and NA populations were found (Table 4).

Clustering of MLGs: relationships between- and within *P. corethrurus* populations

Although some individuals cluster together according to site (e.g., animals in NA), most of the individuals scattered in a non-uniform clustering (Figure 3A). As shown

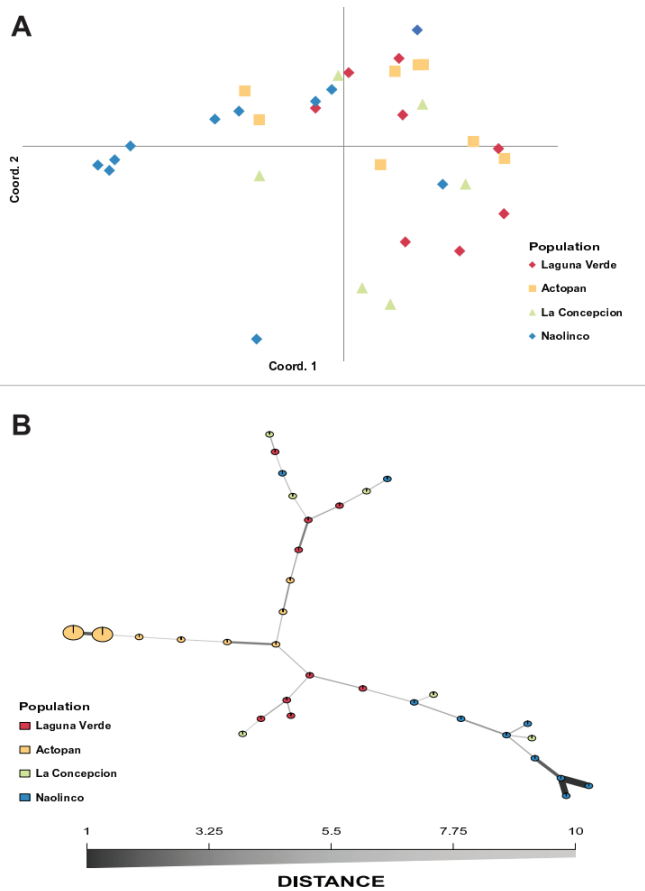


Figure 3. A Principal Components Analysis, where colors indicate specimens of the population (**A**) and a Minimum Spanning Network where each node denotes a different MLG, with size matching the number of individuals. Edge thickness and color are proportional to absolute genetic distance. Edge lengths are arbitrary (**B**). Both analyses show the relationship between multilocus genotypes (MLGs) for four different earthworm populations of *Pontoscolex corethrurus* living in central Veracruz State, Mexico.

in Figure 3A, axes 1 and 2 of the PCA scatter plot accounted for 26% and 15% of total genetic variability, respectively. On the other hand, the global minimum spanning network showed that all populations have MLGs that are closely related (Figure 3B). The comparison of the matrix of Euclidian genetic distance with the matrix of geographic distances using the Mantel test showed that there is no correlation between these two matrices. Thus, data in the genetic distance matrix is not explained by the geographic positioning of the populations (Figure 3). Moreover, the genetic distance between MLGs and between populations indicate no evident correlation with geographic locations, even though LC and LV appeared to be genetically related (Figure 4A, B, respectively). In summary, the clustering analysis shows no clear association with geographic distances.

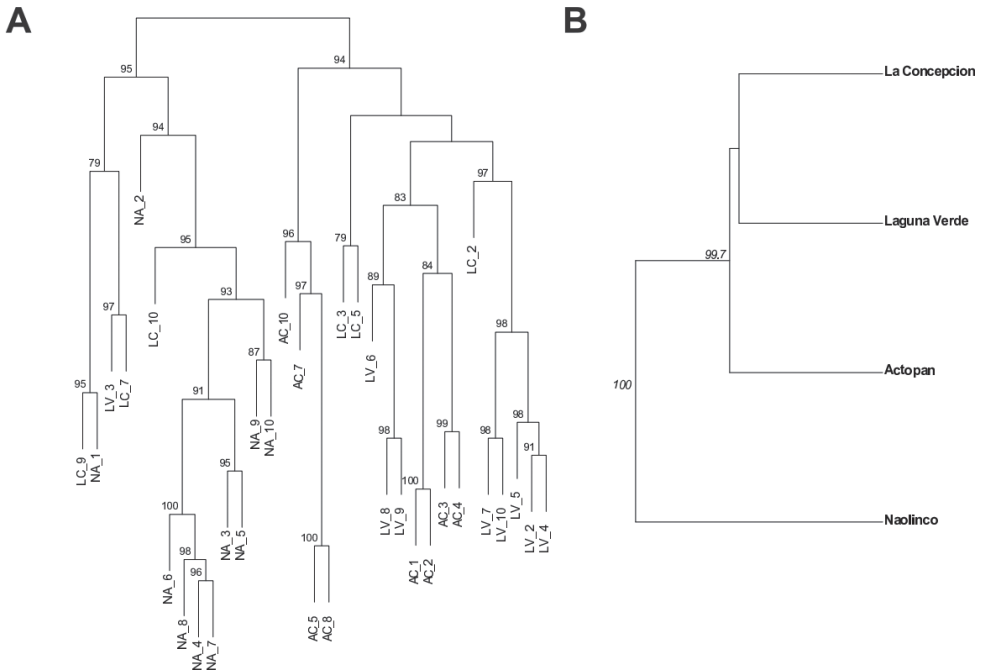


Figure 4. UPGMA dendrogram of genetic distance between MGLs (A) and between populations (B) observed in the distinct populations of *Pontosclex corethrurus* collected in central Veracruz State, Mexico. Only bootstrap values higher than or equal to 70% are shown.

Estimation of population structure according to genetic clusters

The Bayesian analysis of population structure estimated two distinct genetic clusters ($K = 2$, $\ln P(D) = -557.89 \pm 0.31$) distributed across the four geographic locations (Figure 5). Similar to the results obtained by the PCA and dendrogram analyses, the Bayesian analysis revealed no apparent structure that could be associated with geographic location (Figure 5). Nevertheless, the NA population seems to belong mostly to cluster 2 and the one from LV to cluster 1, whereas AC and LC appear to be strongly admixed (Figure 5). From this analysis, two distinct genetic lineages can be identified among populations, henceforth defined as lineages A (mostly LV individuals) and lineage B (mostly NA individuals). Besides, the DAPC analysis confirmed the above genetic relationship between LC and LV, even when they belong to distant geographic locations (Figure 6). On the other hand, similar to the results of the Bayesian analysis, AC (lineage A) and NA (lineage B) are detached (Figure 7). Notably, both clone-corrected ($N = 33$) and uncorrected ($N = 35$) reject the hypothesis of no linkage among markers (Table 3), supporting asexuality in all populations (Suppl. material 1: Figure S1). Altogether, the assessment of genetic diversity in the four populations of *P. corethrurus* suggests that they belong to two different lineages, with some relationships among them despite their distribution in different locations.

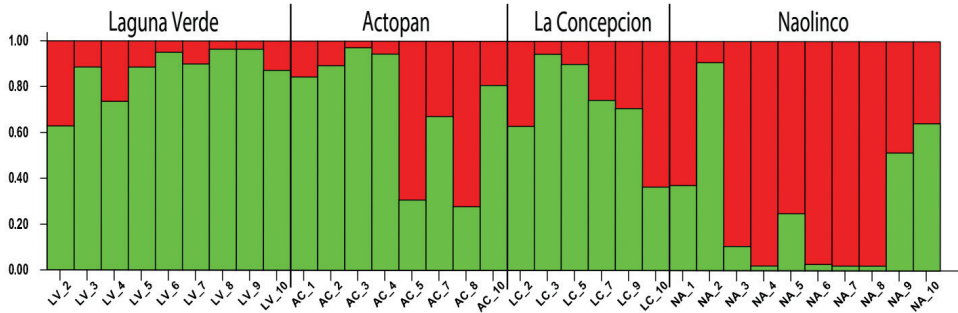


Figure 5. Estimated population genetic structure with a summary plot of Q estimates based on the ISSR data observed for four populations of *Pontoscolex corethrurus* in central Veracruz State, Mexico. Each individual is shown by a vertical line, which is partitioned into colored segments representing the fraction of the number of members in cluster K (%).

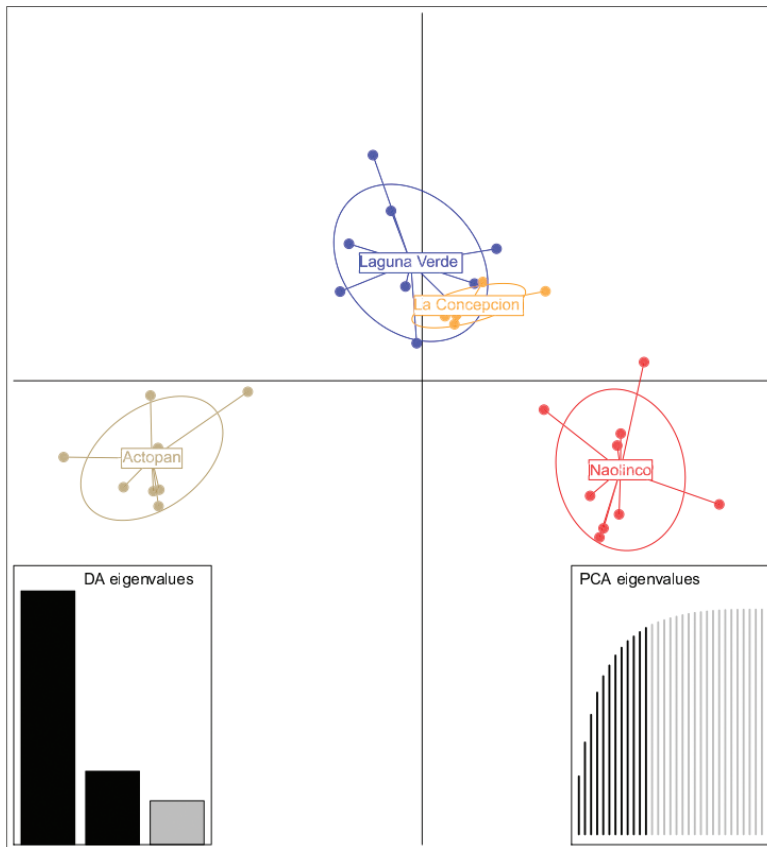


Figure 6. Genetic structure using ISSR data for 35 *Pontoscolex corethrurus* individuals based on discriminant analysis of principal components (DAPC). Proportion of eigenvalues in discriminant analysis (bottom left plot) and PCA eigenvalues (bottom right), with the first 12 significant principal components highlighted in black.

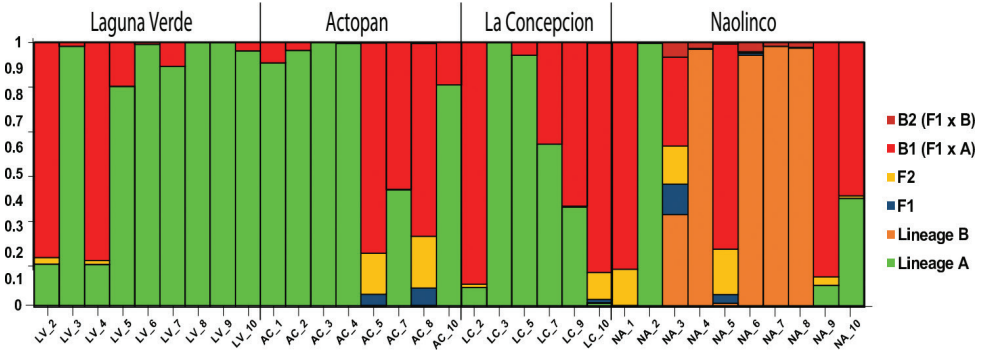


Figure 7. Classification of *Pontoscolex corethrurus* individuals according to a Bayesian assignment algorithm implemented in NEWHYBRIDS (Anderson and Thompson 2002) to detect gene flow. Each unit represents an individual corresponding to parental lineages (Lineage A and Lineage B), F1 generation, F2 (F1 x F1) and later generation or introgressive hybrids B1 (Lineage A x F1) and B2 (e.g., Lineage B x F1).

Discussion

Soil texture and chemical composition are among the key environmental variables that play a role in the invasion process of earthworms (Hendrix and Bohlen 2006; Marichal et al. 2012; Craven et al. 2016). On the other hand, traits intrinsic to this species, such as dispersal capacity, life history, and reproduction mode, are known to influence the genetic structure of earthworms (González et al. 2006; Cameron et al. 2008; Marichal et al. 2012). All these features can contribute to the isolation of populations, favoring intra-specific relationships that determine the population structure (Baker 1998; Novo et al. 2010; Fernández et al. 2013). Thus, determining the genetic variability in asexual organisms, such as the earthworm *P. corethrurus*, is of interest, since it may influence population structure and therefore, putative evolutionary bottlenecks.

In this work, the study of genetic diversity and population structure of four populations living in Mexican tropical and temperate pasture was carried out through a molecular approach using ISSR markers. The use of ISSR markers is well supported by several studies since it produces a high percentage of polymorphic loci (Abbot 2001; Dušínský et al. 2006; Luan et al. 2006; Sharma et al. 2011; Seyedimoradi and Talebi 2014; Ng and Tan 2015; Buczkowska et al. 2016). Also, ISSR markers potentially discriminate isolated populations by geographic conditions and are able to differentiate cryptic species ((Dušínský et al. 2006; Buczkowska et al. 2016). Finally, since ISSR markers only amplify nuclear regions of eukaryotic genomes, it avoids the amplification of bacterial DNA fragments, i.e., members of the phylum Bacteroidetes, commonly associated with *P. corethrurus* (Bernard et al. 2012; Seyedimoradi and Talebi 2014).

According to PhiPT values, there were significant differences between the LV, AC, and NA populations, meaning that most populations possess high genotypic diversity (Figure 2 and Table 4). In this regard, the AMOVA analyses showed that most genetic diversity (75%) was found within populations, and only 25% among populations.

This finding is similar to those reported by Cameron et al. (2008) and Cunha et al. (2014) for *Dendrobaena octaedra* and *P. corethrurus*, respectively. In both cases, most of the genetic variability was found within populations, and only a minor proportion occurred between populations (Cameron et al. 2008; Cunha et al. 2014). The high levels of genotypic diversity observed in this study could be expected because there is evidence of high diversity in populations of *P. corethrurus* using AFLPs (Cunha et al. 2014). It is also likely that the high genotypic diversity observed in the populations of *P. corethrurus* studied is due to the high evolutionary rate of change within ISSR regions compared to other nuclear regions tackled by AFLPs, RAPD or URPs (Sharma et al. 2011; Gramaje et al. 2014; Seyedimoradi and Talebi 2014; Ng and Tan 2015).

As regards the movement of MLGs across the different sites, a conspicuous behavior was observed, particularly in LV, AC, and LC. Such observation may be explained only by an intense human-mediated transference of *P. corethrurus* through road networks or activities associated with agriculture (Lapied and Lavelle 2003; Baker et al. 2006; González et al. 2006; Feijoo et al. 2007; Dupont et al. 2012; Ortíz-Gamino et al. 2016). On the other hand, clustering analyses through PCA and a dendrogram identified a significant admixture across all populations; however, it was possible to identify at least two divergent and well-differentiated genetic clusters (lineages A and B). It is likely that the lineages identified potentially correspond to those previously reported by Taheri and co-workers, namely lineages L1 and L3 (Taheri et al. 2018). It is important to highlight that both our sampling sites and the molecular approach, are different from the work done by Taheri et al. (2018). Their research involved specimens collected in different years, covering an extended period (from 1996 to 2016; Taheri et al. 2018, Suppl. material 1: Figure S1). Despite these differences, our results are consistent with those reported by Taheri et al. (2018), namely, the identification of two lineages in the *P. corethrurus* populations.

Lineage A seems to be widespread, covering LC and LV sites (Figure 6). Such distribution may indicate wide ecological tolerance, with populations probably well adapted to warm temperatures and poor soils. The distribution of lineage A may suggest that this lineage corresponds to L1 (Taheri et al. 2018), since it was found in most of the places sampled. Moreover, our results are similar to those reported for other species, such as *Octolasion tyrtaeum* (Savigny, 1826), for which a single haplotype was found in all sampling stations (Terhivuo and Saura 1993). Hence, for peregrine species, the evidence indicates that human activities are strongly shaping the dispersal pattern of MLGs through incidental transfer in crops soil or fishing (Cameron et al. 2008; Dupont et al. 2012; Ortíz-Gamino et al. 2016). However, there are also reports of the intentional introduction of earthworm species for commercial applications like waste management and land bioremediation (Hendrix 2006).

In contrast to lineage A, lineage B (mostly NA specimens) showed the best distinct cluster of individuals (Figure 5). This cluster is likely associated with the contrasting environmental conditions that predominate in NA, namely higher altitude, three types of grass (*Paspalum conjugatum* P.J. Bergius, *Cynodon nlemfuensis* Vanderyst, *Pennisetum clandestinum* Hochst. ex Chiov.), soil rich in organic matter, or even interactions

with other soil organisms (Ortíz-Gamino et al. 2016). All these characteristics could be acting as an environmental screen that results in the clustering of NA individuals (Figure 3). Remarkably, a similar finding has been reported for *Aporrectodea trapezoides* (Dugés, 1828), in which clonal lineages seem to remain close to their original areas, indicative of some level of local adaptation or strong interspecific relationships (Fernández et al. 2013). Thus, the lineage described as L2 by Taheri et al. (2018) could correspond to lineage B in this work. If so, this lineage is likely well-adapted to micro conditions including habitat, feeding habits and biotic interactions. As proposed earlier, another barrier to the dispersal of lineage B may be temperature (Janzen 1967). This could be the case for the NA population, in which the mean annual temperature (17 °C) may be acting as the main barrier to MGL dispersion (Ortíz-Gamino et al. 2016). Importantly, under a global-change scenario, namely intensive land-use change and alarming global warming, this barrier could become weaker, thus enabling the invasion of pantropical earthworm species (Jiménez and Decaëns 2000; Eisenhauer et al. 2014; Gutiérrez and Cardona 2014).

On the other hand, sexual reproduction is a rare event in *P. corethrurus* (Gates 1973), as it is widely accepted that its reproduction occurs mainly by parthenogenesis (Gates 1973). The standardized index of association (\bar{r}_d) supported the hypothesis of clonal population structure (Suppl. material 1: Figure S1). In this sense, \bar{r}_d values suggest a widespread dispersal of MLGs across populations. This contrasts with the linkage disequilibrium tests, in which the null hypothesis of random mating was rejected for all populations. Nevertheless, these results should be interpreted with caution, as it is challenging to demonstrate the presence of linkage disequilibrium with small sample sizes (Hagenblad et al. 2006; Du et al. 2007; Gramaje et al. 2014). In earthworms, parthenogenesis has been associated with polyploidy, as well as with high levels of DNA methylation (Regev et al. 1998). Therefore, it is also plausible that methylation may be fostering the epigenetic control of phenotypic plasticity, which could be crucial for a successful colonization (Stürzenbaum et al. 2009). It is tempting to claim that temperature affects *P. corethrurus* and impacts its reproduction rate, which also may be regulated by polyploidy and epigenetic control (Ortíz-Gamino et al. 2016). Further studies regarding the number of chromosomes or genomic rearrangements are needed to address whether or not these features are linked to environmental features.

In summary, the screening of genetic diversity is helpful to monitor the dynamics of population structure and its relationships to ecological and environmental features and to contribute valuable information about the isolation of invasive earthworm species. In this sense, our work provides evidence of the existence of two lineages of *P. corethrurus* in Veracruz State, Mexico, showing different distribution patterns according to the prevailing environmental conditions found in regions studied. Therefore, our data represent an relevant contribution to know the movement dynamics and diversification of *P. corethrurus*, which will be useful information for planning successful strategies aimed to control or prevent the biological invasion of this species in Mexico.

Conclusions

Despite being random, biological invasions are intriguing events, mainly because they involve populations of organisms with certain features and particular habits. Intriguingly, a parthenogenic species such as *P. corethrurus* has been successful in colonizing areas all over the world. The interaction of *P. corethrurus* genetics with the environment should drive its selection and distribution pattern.

In this work, we assessed populations of *P. corethrurus* inhabiting tropical and temperate pastures of Veracruz, Mexico, in terms of genetic variation through ISSR markers. Our results revealed the existence of at least two well-differentiated genetic clusters, corresponding to different lineages (lineages A and B). The lineages identified in this work likely correspond to lineages L1 and L3 identified previously by Taheri et al. (2018). Although further research is needed to discern why *P. corethrurus* populations occur in some sites but not in others, our work suggests that genetic variation is playing a key role in the invasion process. The association between the genetic variability of *P. corethrurus* and its success in invading new sites is counter-intuitive due to its parthenogenic reproduction, i.e., clonal multiplication. Additional genotyping of *P. corethrurus* individuals inhabiting diverse environments or different States like Tabasco, Puebla, and Tamaulipas, will be necessary, not only to confirm our results, but to track the dynamics of dispersal and diversification of lineages, as well as to identify new dominant genotypes or newly introduced lineages. All this information should be gathered before using *P. corethrurus* in biotechnology research, remediation, or fishing, or before estimating its effects on local crops, plants, or organisms.

Acknowledgements

We would like to thank to Norma Flores-Estévez and Wilberth A. Poot-Poot for the support and help at INBIOTECA, Ernesto Ormeño-Orrillo for his help at Ciencias Genómicas, and to Rogelio Lara González and Katia J. Martínez Velázquez for their help during fieldwork. We are thankful to Alejandra Velázquez Lobo for valuable comments and careful revision of the manuscript and Alberto Ortiz Brito for proving the sampling map. Diana Ortiz-Gamino was supported by a scholarship (No. 251818) by Consejo Nacional de Ciencia y Tecnología (CONACYT).

References

- Abbot P (2001) Individual and population variation in invertebrates revealed by Inter-simple Sequence Repeats (ISSRs). *Journal of Insect Science* 1: 1–8. <https://doi.org/10.1673/031.001.0108>
- Agapow PM, Burt A (2001) Indices of multilocus linkage disequilibrium. *Molecular Ecology Notes* 1: 101–102. <https://doi.org/10.1046/j.1471-8278.2000.00014.x>

- Anderson EC, Thompson EA (2002) A model-based method for identifying species hybrids using multilocus genetic data. *Genetics* 160(3): 1217–1229.
- Baker GH (1998) The ecology, management, and benefits of earthworms in agricultural soils, with particular reference to southern Australia. In: Edwards CA (Ed.) *Earthworm Ecology*. St Lucie Press, Boca Raton, 1229–1257.
- Baker GH, Brown G, Butt K, Curry JP, Scullion J (2006) Introduced earthworms in agricultural and reclaimed land: their ecology and influences on soil properties, plant production and other soil biota. *Biological Invasions* 8: 1301–1316. <https://doi.org/10.1007/s10530-006-9024-6>
- Barros E, Grimaldi M, Sarrazin M, Chauvel A, Mitja D, Desjardins T, Lavelle P (2004) Soil physical degradation and changes in macrofaunal communities in Central Amazon. *Applied Soil Ecology* 26: 157–168. <https://doi.org/10.1016/j.apsoil.2003.10.012>
- Beddard FE (1912) *Earthworms and Their Allies*. University Press, Cambridge, 150 pp. <https://doi.org/10.5962/bhl.title.17625>
- Bernard L, Chapuis-Lardy L, Razafimbelo T, Razafindrakoto M, Pablo AL, Legname E, Bröls T, O'Donohue M, Brauman A, Chotte J-L, Blanchart E (2012) Endogeic earthworms shape bacterial functional communities and affect organic matter mineralization in a tropical soil. *The ISME Journal* 6(1): 213–222. <https://doi.org/10.1038/ismej.2011.87>
- Bengtsson BO (2009) Asex and Evolution: A very Large-Scale Overview. In: Schön I, Martens K, Van Dijk P (Eds) *Lost Sex: The Evolutionary Biology of Parthenogenesis*. Springer, New York, 615 pp. https://doi.org/10.1007/978-90-481-2770-2_1
- Brown GG, Fragoso C, Barois I, Rojas P, Patrón JC, Bueno J, Moreno AG, Lavelle P, Ordaz V, Rodríguez C (2001) Diversidad y rol funcional de la macrofauna edáfica en los ecosistemas tropicales mexicanos. *Acta Zoológica Mexicana* (n.s.) 1: 79–110.
- Brown AHD, Feldman MW, Nevo E (1980) Multilocus structure of natural populations of *Hordeum spontaneum*. *Genetics* 96(2): 523–536.
- Brown GG, James SW, Pasini A, Nunes DH, Benito NP, Trigo P, Sautter KD (2006) Exotic, Peregrine, and Invasive Earthworms in Brazil: Diversity, Distribution, and Effects on Soils and Plants. *Caribbean Journal of Science* 42: 339–358.
- Brown GG, Moreno A, Barois I, Fragoso C, Rojas P, Hernández B, Patrón JC (2004) Soil macrofauna in SE Mexican pastures and the effect of conversion from native to introduced pastures. *Agriculture, Ecosystems & Environment* 103(2): 313–327. <https://doi.org/10.1016/j.agee.2003.12.006>
- Buch A, Brown GG, Niva CC, Sautter KD, Lourençato LF (2011). Life cycle of *Pontoscolex corethrurus* (Müller, 1857) in tropical artificial soil. *Pedobiologia* 54 Supplement: S19–S25. <https://doi.org/10.1016/j.pedobi.2011.07.007>
- Buczowska K, Rabska M, Gonera P, Pawlaczyk EM, Wawrzyniak P, Czolpinska M, Bączkiewicz A (2016) Effectiveness of ISSR markers for determination of the *Aneura pinguis* cryptic species and *Aneura maxima*. *Biochemical Systematics and Ecology* 68: 27–35. <https://doi.org/10.1016/j.bse.2016.06.013>
- Cameron E, Bayne EM, Coltman DW, Coltman DW (2008) Genetic structure of invasive earthworms *Dendrobaena octaedra* in the boreal forest of Alberta: insights into introduction mechanisms. *Molecular Ecology* 17: 1189–1197. <https://doi.org/10.1111/j.1365-294X.2007.03603.x>

- Cameron EK, Bayne EM (2009) Road age and its importance in earthworm invasion of northern boreal forest. *Journal of Applied Ecology* 46: 28–36. <https://doi.org/10.1111/j.1365-2664.2008.01535.x>
- Cicconardi F, Borges PA, Strasberg D, Oromí P, López P, Pérez-Delgado H, Casquet AJ, Caujapé-Castells J, Fernández-Palacios J, Thébaud B, Emerson BC (2016) MtDNA metagenomics reveals large-scale invasion of belowground arthropod communities by introduced species. *Molecular Ecology*. <https://doi.org/10.1111/mec.14037>
- Cuatrecasas J (1964) Cacao and its allies: a taxonomic revision of the genus *Theobroma*. *Contributions from the United States National Herbarium* 35: 379–614.
- Cunha L, Montiel R, Novo M, Orozco-terWengel P, Rodrigues A, Morgan AJ, Kille P (2014) Living on a volcano's edge: genetic isolation of an extremophile terrestrial metazoan. *Heredity* 112: 132–142. <https://doi.org/10.1038/hdy.2013.84>
- Craven D, Thakur MP, Cameron EK, Frelich LE, Beauséjour R, Blair RB, Blossey B, Burtis J, Choi A, Dávalos A, Fahey TJ, Fisichelli NA, Gibson K, Handa IT, Hopfensperger K, Loss SR, Nuzzo V, Maerz JC, Sackett T, Scharenbroch BC, Smith SM, Vellend M, Umek LG, Eisenhauer N (2016) The unseen invaders: introduced earthworms as drivers of change in plant communities in North American forests (a meta-analysis). *Global Change Biology* 23(3): 1065–1074. <https://doi.org/10.1111/gcb.13446>
- Du FX, Clutter AC, Lohuis MM (2007) Characterizing Linkage Disequilibrium in Pig Populations. *International Journal Biological Sciences* 3(3): 166–178. <https://doi.org/10.7150/ijbs.3.166>
- Dupont L, Decaëns T, Lapied E, Chassany V, Marichal R, Dubs F, Maillot M, Ro V (2012) Genetic signature of accidental transfer of the peregrine earthworm *Pontoscolex corethrurus* (Clitellata, Glossoscolecidae) in French Guiana. *European Journal of Soil Biology* 53: 70–75. <https://doi.org/10.1016/j.ejsobi.2012.09.001>
- Dušinský R, Kúdela M, Stloukalová V, Jedlička L (2006) Use of inter-simple sequence repeat (ISSR) markers for discrimination between and within species of blackflies (Diptera: Simuliidae). *Biologia* 61(3): 299–304. <https://doi.org/10.2478/s11756-006-0055-3>
- Eisenhauer N, Stefanski A, Fisichelli NA, Rice K, Rich R, Reich PB (2015) Warming shifts 'worming': effects of experimental warming on invasive earthworms in northern North America. *Scientific Reports* 4: 1–6890. <https://doi.org/10.1038/srep06890>
- Eisen G (1900) Researches in the American Oligochaeta, with special reference to those of the Pacific coast and adjacent islands. *Proceedings of California Academy of Science* 2: 85–276.
- Evanno G, Regnaut S, Goudet J (2005) Detecting the number of clusters of individuals using the software STRUCTURE: a simulation study. *Molecular Ecology* 14(8): 2611–2620. <https://doi.org/10.1111/j.1365-294X.2005.02553.x>
- Excoffier L, Lischer HEL (2010) Arlequin suite ver 3.5: a new series of programs to perform population genetics analyses under Linux and Windows. *Molecular Ecology Resources* 10(3): 564–567. <https://doi.org/10.1111/j.1755-0998.2010.02847.x>
- Feijoo A, Zúñiga M, Quintero H, Lavelle P (2007) Relaciones entre el uso de la tierra y las comunidades de lombrices en la cuenca del río La Vieja, Colombia. *Pastos y Forrajes* 30(2): 235–249.
- Fernández R, Almodóvar A, Novo M, Gutiérrez M, Díaz Cosín DJ (2011) A vagrant clone in a peregrine species: Phylogeography, high clonal diversity and geographical distribution

- in the earthworm *Aporrectodea trapezoides* (Dugès, 1828). *Soil Biology & Biochemistry* 43(10): 2085–2093. <https://doi.org/10.1016/j.soilbio.2011.06.007>
- Fernández R, Almodóvar A, Novo M, Simancas B, Díaz Cosín DJ (2012) Adding complexity to the complex: New insights into the phylogeny, diversification and origin of parthenogenesis in the *Aporrectodea caliginosa* species complex (Oligochaeta, Lumbricidae). *Molecular Phylogenetics and Evolution* 64(2): 368–379. <https://doi.org/10.1016/j.ympev.2012.04.011>
- Fernández R, Almodóvar A, Novo M, Gutiérrez M, Díaz Cosin DJ (2013) Earthworms, good indicators for palaeogeographical studies? Testing the genetic structure and demographic history in the peregrine earthworm *Aporrectodea trapezoides* (Dugès, 1828) in southern Europe. *Soil Biology & Biochemistry* 58: 127–135. <https://doi.org/10.1016/j.soilbio.2012.10.021>
- Fragoso C, Coria-Martínez ML, Camarena LM (2009) An update of the earthworm fauna of Los Tuxtlas Ver. and adjacent regions: are native species in the risk of extinction? In: Barois I, Huisin EJ, Okoth P, Trejo D, De los Santos M (Eds) *Below-Ground Biodiversity in Sierra San Marta, Los Tuxtlas, Veracruz, México*. Instituto de Ecología, A.C., Xalapa, Mexico, 219–228.
- Fragoso C, Rojas P (2014) Biodiversidad de lombrices de tierra (Annelida: Oligochaeta: Crassiditellata). *Revista Mexicana de Biodiversidad, Supl.* 85: S197–S207. <https://doi.org/10.7550/rmb.33581>
- Gates GE (1954) Exotic earthworms of the United States. *Bulletin of the Museum of Comparative Zoology at Harvard College* 111: 217–258.
- Gates GE (1973) Contributions to North American Earthworms (Annelida) No. 6 Contributions to a revision of the earthworm family Glossoscolecidae. I. *Pontoscolex corethrurus* (Müller, 1857). *Bulletin of Tall Timbers Research Station* 14: 1–12.
- Gramaje D, León M, Santana M, Crous PW, Armengol J (2014) Multilocus ISSR Markers Reveal Two Major Genetic Groups in Spanish and South African Populations of the Grapevine Fungal Pathogen *Cadophora luteo-olivacea*. *PLoS ONE* 9(10): e110417. <https://doi.org/10.1371/journal.pone.0110417>
- González G, Huang CY, Zou X, Rodríguez C (2006) Earthworm invasions in the tropics. In: Hendrix PF (Ed.) *Biological Invasions Belowground: Earthworms as Invasive Species*. Springer, Dordrecht, 47–56. <https://doi.org/10.1007/s10530-006-9023-7>
- Hagenblad J, Bechsgaard J, Charlesworth D (2006) Linkage Disequilibrium Between Incompatibility Locus Region Genes in the Plant *Arabidopsis lyrata*. *Genetics* 173(2): 1057–1073. <https://doi.org/10.1534/genetics.106.055780>
- Hendrix PF (2006) Biological invasions belowground—earthworms as invasive species. In: Hendrix PF (Ed.) *Biological Invasions Belowground: Earthworms as Invasive Species*. Springer, Netherlands, 4 pp. <https://doi.org/10.1007/978-1-4020-5429-7>
- Hendrix PF, Bohlen PJ (2002) Exotic Earthworm Invasions in North America: Ecological and Policy Implications Expanding global commerce may be increasing the likelihood of exotic earthworm invasions, which could have negative implications for soil processes, other animal and plant species, and importation of certain pathogens. *Bioscience* 52(9): 801–811. [https://doi.org/10.1641/0006-3568\(2002\)052\[0801:EEIINA\]2.0.CO;2](https://doi.org/10.1641/0006-3568(2002)052[0801:EEIINA]2.0.CO;2)
- Hendrix P, Baker G, Callahan M, Damof G, Fragoso C, Gonzalez G, James S, Lachnicht S, Winsome T, Zou X (2006) Invasion of exotic earthworm into inhabited by native earthworm. *Biological Invasions* 8: 1287–1300. <https://doi.org/10.1007/s10530-006-9022-8>

- Hendrix PF, Callaham Jr. MA, Drake JM, Huang ChY, James SW, Snyder BA, Zhang W (2008) Pandora's box contained bait: the global problem of introduced earthworm. *Annual Review of Ecology Evolution, and Systematics* 39: 593–613. <https://doi.org/10.1146/annurev.ecolsys.39.110707.173426>
- James SW (2012) Re-erection of *Rhinodrilidae* Benham, 1890, a senior synonym of *Pontoscolocidae* James, 2012 (Annelida: Clitellata). *Zootaxa* 3540: 67–68. <https://doi.org/10.11646/zootaxa.3540.1.6>
- Janzen DH (1967) Why Mountain Passes are Higher in the Tropics? *The American Naturalist* 101(919): 233–249. <https://doi.org/10.1086/282487>
- Jiménez JJ, Decaëns T (2000) Vertical distribution of earthworms in grassland soils of the Colombian Llanos. *Biology and Fertility of Soils* 32: 463–473. <https://doi.org/10.1007/s003740000277>
- Jombart T, Devillard S, Balloux F (2010) Discriminant analysis of principal components: a new method for the analysis of genetically structured populations. *BMC Genetics* 11: 1–94. <https://doi.org/10.1186/1471-2156-11-94>
- Kamvar ZN, Tabima JF, Grünwald NJ (2014) Poppr: an R package for genetic analysis of populations with clonal, partially clonal, and/or sexual reproduction. *PeerJ* 2: e281. <https://doi.org/10.7717/peerj.281>
- Lapied E, Lavelle P (2003) The peregrine earthworm *Pontoscolex corethrurus* in the East coast of Costa Rica. *Pedobiologia* 47: 471–474. <https://doi.org/10.1078/0031-4056-00215>
- Lavelle P, Barois I, Cruz I, Fragoso C, Hernández A, Pineda A, Rangel P (1987) Adaptive strategies of *Pontoscolex corethrurus* (Glossoscolecidae, Oligochaeta), a peregrine geophagous earthworm of the humid tropics. *Biology and Fertility of Soils* 5: 188–194. <https://doi.org/10.1007/BF00256899>
- Lavelle P, Bignell D, Lepage M, Wolters V, Roger P, Ineson P, Heal OW, Dhillon S (1997) Soil Function in a changing world: the role of invertebrate ecosystem engineers. *European Journal of Soil Science* 33: 159–193.
- Luan S, Chiang T-Y, Gong X (2006) High Genetic Diversity vs. Low Genetic Differentiation in *Nouelia insignis* (Asteraceae), a Narrowly Distributed and Endemic Species in China, Revealed by ISSR Fingerprinting. *Annals of Botany* 98(3): 583–589. <https://doi.org/10.1093/aob/mcl129>
- Lee CE (2002) Evolutionary genetics of invasive species. *Trends in Ecology & Evolution* 17(8): 386–391. [https://doi.org/10.1016/S0169-5347\(02\)02554-5](https://doi.org/10.1016/S0169-5347(02)02554-5)
- Narayanan SP, Sathrumithra S, Christopher G, Thomas AP, Julka JM (2016) Current distribution of the invasive earthworm *Pontoscolex corethrurus* (Müller, 1857) after a century of its first report from Kerala state, India. *Opuscula Zoologica (Budapest)* 47(1): 101–107. <https://doi.org/10.18348/opzool.2016.1.101>
- Ng WL, Tan SG (2015) Inter-Simple Sequence Repeat (ISSR) Markers: Are We Doing It Right? *ASM Science Journal* 9(1): 30–39.
- Marichal R, Grimaldi M, Mathieu J, Brown GG, Desjardins T, Lopes da Silva Jr. M, Praxedes C, Martins MB, Velasquez E (2012) Is invasion of deforested Amazonia by earthworm *Pontoscolex corethrurus* driven by soil texture and chemical properties? *Pedobiologia* 55(5): 233–240. <https://doi.org/10.1016/j.pedobi.2012.03.006>

- Mantel N (1967) The detection of disease clustering and a generalized regression approach. *Cancer Research* 27(2): 209–220.
- Marinissen JCY, Van den Bosch F (1992) Colonization of new habitats by earthworms. *Oecologia* 91: 371–376. <https://doi.org/10.1007/BF00317626>
- Moreno AG, Borges S (2004) Avances en taxonomía de lombrices de tierra (Annelida: Oligochaeta). Editorial Complutense. Madrid, 428 pp.
- Nei M (1978) Estimation of average heterozygosity and genetic distance from a small number of individuals. *Genetics* 89(3): 583–590.
- Novo M, Almodóvar A, Fernández R, Trigo D, Díaz Cosín DJ (2010) Cryptic speciation of hormogastrid earthworms revealed by mitochondrial and nuclear data. *Molecular Phylogenetics and Evolution* 56: 507–512. <https://doi.org/10.1016/j.ympev.2010.04.010>
- Ortíz-Gamino D, Pérez-Rodríguez P, Ortiz-Ceballos AI (2016) Invasion of the tropical earthworm *Pontoscolex corethrurus* (Rhinodrilidae, Oligochaeta) in temperate grasslands. *PeerJ* 4: e2572. <https://doi.org/10.7717/peerj.2572>
- Oksanen J, Kindt R, Legendre P, O'Hara RB, Simpson GL, Solymos P, Henry M, Stevens MHH, Szoecs E, Wagner H (2007) The vegan package. *Community Ecology Package* 10: 631–637.
- Pavliček T, Cohen T, Yadav S, Glasstetter M, Král P, Pearlson O (2016) Aneuploidy Occurrence in Oligochaeta. *Ecology and Evolutionary Biology* 1(3): 57–63.
- Peakall ROD, Smouse PE (2006) GENALEX 6: Genetic analysis in Excel. Population genetic software for teaching and research. *Molecular Ecology Notes* 6: 288–295. <https://doi.org/10.1111/j.1471-8286.2005.01155.x>
- Pritchard JK, Stephens M, Donnelly P (2000) Inference of population structure using multilocus genotype data. *Genetics* 155(2): 945–959. <https://doi.org/10.1111/j.1471-8286.2007.01758.x>
- Regev A, Lamb MJ, Jablonka E (1998) The role of DNA methylation in invertebrates: developmental regulation or genome defense? *Molecular Biology and Evolution* 15: 880–891. <https://doi.org/10.1093/oxfordjournals.molbev.a025992>
- Righi G (1984) *Pontoscolex* (Oligochaeta, Glossoscolecidae), a new evaluation. *Studies on Neotropical Fauna and Environment* 19(3): 159–177. <https://doi.org/10.1080/01650528409360653>
- R Core Team (2014) R: A language and environment for statistical computing. R Foundation for Statistical Computing, Vienna. Available: <https://www.R-project.org/>
- Schultes RE (1984) Amazonian cultigens and their northward and westward migrations in pre-Columbian times. In: Stone D (Ed.) *Pre-Columbian Plant Migration*. Cambridge: Papers of the Peabody Museum of Archaeology and Ethnology (Vol. 76). Harvard University Press, 19–38.
- Seyedimoradi H, Talebi R (2014) Detecting DNA polymorphism and genetic diversity in Lentil (*Lens culinaris* Medik.) germplasm: comparison of ISSR and DAMD marker. *Physiology and Molecular Biology of Plants* 20(4): 495–500. <https://doi.org/10.1007/s12298-014-0253-3>
- Smith JM, Smith NH, O'Rourke M, Spratt BG (1993) How clonal are bacteria? *Proceedings of the National Academy of Sciences* 90(10): 4384–4388. <https://doi.org/10.1073/pnas.90.10.4384>
- Sharma A, Sonah H, Deshmukh RK, Gupta NK, Singh NK, Sharma TR (2011) Analysis of genetic diversity in earthworms using DNA markers. *Zoological Science* 28: 25–31. <https://doi.org/10.2108/zsj.28.25>
- Stürzenbaum SR, Andre J, Kille P, Morgan AJ (2009) Earthworm genomes, genes and proteins: the (re)discovery of Darwin's worms. *Proceeding of the Royal Society B*. 276: 789–797. <https://doi.org/10.1098/rspb.2008.1510>

- Suzuki R, Shimodaira H (2006) Pvcust: an R package for assessing the uncertainty in hierarchical clustering. *Bioinformatics* 22: 1540–1542. <https://doi.org/10.1093/bioinformatics/btl117>
- Taheri S, James S, Roy V, Decaëns T, Williams BW, Anderson F, Rougerie R, Chang CH, Brown G, Cunha L, Stanton DWG, Da Silva E, Chen JH, Lemmon AR, Moriarty Lemmon E, Bartz M, Baretta D, Barois I, Lapied E, Coulis M, Dupont L (2018) Complex taxonomy of the ‘brush tail’ peregrine earthworm *Pontoscolex corethrurus*. *Molecular Phylogenetics and Evolution* 124: 60–70. <https://doi.org/10.1016/j.ympev.2018.02.021>
- Tamura K, Stecher G, Peterson D, Filipski A, Kumar S (2013) MEGA6: Molecular Evolutionary Genetics Analysis version 6.0. *Molecular Biology and Evolution* 30: 2725–2729. <https://doi.org/10.1093/molbev/mst197>
- Terhivuo J, Saura A (1993) Clonal and morphological variation in marginal populations of parthenogenetic earthworms *Octolasion tyrtaeum* and *O. cyaneum* (Oligochaeta, Lumbricidae) from eastern Fennoscandia. *Bolletino di Zoologia* 60: 87–96. <https://doi.org/10.1080/11250009309355796>
- Terhivuo J, Saura A (2006) Dispersal and clonal diversity of North-European parthenogenetic earthworms. *Biological Invasions* 8: 1205–1218. <https://doi.org/10.1007/s10530-006-9015-7>
- Uribe S, Huerta E, Geissen V, Mendoza M, Godoy R, Jarquin A (2012) *Pontoscolex corethrurus* (Annelida: Oligochaeta) indicador de la calidad del suelo en sitios de *Eucalyptus grandis* (Myrtaceae) con manejo tumba y quema. *Revista de Biología Tropical* 60: 1543–552. <https://doi.org/10.15517/rbt.v60i4.2072>
- Vitturi R, Colomba MS, Pirrone AM, Mandrioli M (2002) rDNA (18S–28S and 5S) colocalization and linkage between ribosomal genes and (TTAGGG)(n) telomeric sequence in the earthworm, *Octodrilus complanatus* (Annelida: Oligochaeta: Lumbricidae), revealed by single-and double-color FISH. *Journal of Heredity* 93(4): 279–282. <https://doi.org/10.1093/jhered/93.4.279>

Supplementary material I

Figure S1

Authors: Diana Ortíz-Gamino, Josefát Gregorio, Luis Cunha, Esperanza Martínez-Romero, Carlos Fragosó, Ángel I. Ortíz-Ceballos

Data type: image

Explanation note: Linkage disequilibrium test using \bar{r}_d as implemented in R package Poppr (Kamvar et al. 2014). Visualizations of tests for linkage disequilibrium, where observed values (blue dashed lines) of \bar{r}_d are compared to histograms showing results of 999 permutations..

Copyright notice: This dataset is made available under the Open Database License (<http://opendatacommons.org/licenses/odbl/1.0/>). The Open Database License (ODbL) is a license agreement intended to allow users to freely share, modify, and use this Dataset while maintaining this same freedom for others, provided that the original source and author(s) are credited.

Link: <https://doi.org/10.3897/zookeys.941.49319.suppl1>

Two new genera and species of the Gigantometopini (Hemiptera, Heteroptera, Miridae, Isometopinae) from Borneo with remarks on the distribution of the tribe

Artur Tazsakowski^{1*}, Junggon Kim^{2*}, Claas Damken³, Rodzay A. Wahab³,
Aleksander Herczek¹, Sunghoon Jung^{2,4}

1 Institute of Biology, Biotechnology and Environmental Protection, Faculty of Natural Sciences, University of Silesia in Katowice, Bankowa 9, 40-007 Katowice, Poland **2** Laboratory of Systematic Entomology, Department of Applied Biology, College of Agriculture and Life Sciences, Chungnam National University, Daejeon, South Korea **3** Institute for Biodiversity and Environmental Research, Universiti Brunei Darussalam, Jalan Universiti, BE1410, Darussalam, Brunei **4** Department of Smart Agriculture Systems, College of Agriculture and Life Sciences, Chungnam National University, Daejeon, South Korea

Corresponding author: Artur Tazsakowski (artur.tazsakowski@us.edu.pl); Sunghoon Jung (jung@cnu.ac.kr)

Academic editor: F. Konstantinov | Received 21 October 2019 | Accepted 2 May 2020 | Published 16 June 2020

<http://zoobank.org/B3C9A4BA-B098-4D73-A60C-240051C72124>

Citation: Tazsakowski A, Kim J, Damken C, Wahab RA, Herczek A, Jung S (2020) Two new genera and species of the Gigantometopini (Hemiptera, Heteroptera, Miridae, Isometopinae) from Borneo with remarks on the distribution of the tribe. ZooKeys 941: 71–89. <https://doi.org/10.3897/zookeys.941.47432>

Abstract

Two new genera, each represented by a single new species, *Planicapitus luteus* Tazsakowski, Kim & Herczek, **gen. et sp. nov.** and *Bruneimetopus simulans* Tazsakowski, Kim & Herczek, **gen. et sp. nov.**, are described from Borneo. Detailed photographs of male habitus and genital structures are presented. The checklist with distributional records for all known taxa of Gigantometopini is also provided.

Keywords

Asia, biodiversity, distribution, jumping tree bugs, plant bugs, true bugs

* Contributed equally as the first authors.

Introduction

The Isometopinae are a highly autapomorphic group possessing paired ocelli which are absent in all other members of the plant bug family Miridae (Herczek 1993, Namyatova and Cassis 2016, Yasunaga et al. 2017). This subfamily was considered as the sister group to all other subfamilies based on morphology (Schuh 1974, 1976), but recent works using molecular data do not support this hypothesis (Schuh et al. 2009, Jung and Lee 2012). Therefore, additional works are needed to understand phylogenetic position of this subfamily.

The group has a worldwide distribution, but the majority of known taxa are thermophilic, and occur in the tropics, subtropics, and warm temperate climate zones (Eyles 1971, Schuh 2002–2013, Cassis and Schuh 2012, Namyatova and Cassis 2016, Yasunaga et al. 2017). Due to scarce information on habits, biology, and food preference, the representatives are relatively rare in collections with many species known from singletons or only a handful of specimens (Eyles 1971, Namyatova and Cassis 2016, Herczek et al. 2018). Currently, six tribes, 45 genera and more than 250 species of Isometopinae are known (Namyatova and Cassis 2016, Yasunaga et al. 2016, 2017, Krüger 2018, Herczek et al. 2018) of which 19 species are fossil taxa (Herczek 1993, Schuh 2002–2013, Herczek and Popov 2012, 2014). The Isometopini and Myiommini are the most species-rich isometopine tribes known worldwide (Namyatova and Cassis 2016). The Electromyiommini is an extinct tribe and contains four genera and 14 species; all were described from Baltic amber (Herczek 1993). The Diphlebiini includes only a single genus, *Diphleps* Bergroth, 1924 (Schuh 2002–2013). Yasunaga et al. (2017) created the new tribe Sophianini comprising two genera previously classified within Myiommini: *Alcecoris* McAtee & Malloch, 1924 and *Sophianus* Distant, 1904. Sophianini includes ten species (Yasunaga et al. 2017).

The last tribe is Gigantometopini created by Herczek (1993) to accommodate a single species *Gigantometopus rossi* Schwartz & Schuh, 1990. In 2002 *Isometopidea gryllocephala* Miyamoto, Yasunaga & Hayashi, 1996 was transferred to a newly created genus *Astroscopometopus* Yasunaga & Hayashi and its inclusion to the tribe Gigantometopini was suggested (Yasunaga and Hayashi 2002). In 2004 another species of *Isometopidea* was described, *Isometopidea formosana* Lin, and the next year it was transferred to the genus *Astroscopometopus* (Lin 2005). The same year Yasunaga (2005) described a new species, representing a new genus, *Kohnometopus fraxini* Yasunaga, 2005 in the tribe Myiommini Bergroth, 1924. Next, Akingbohunge (2012) described the second representative of the genus *Gigantometopus*, *G. schuhi* Akingbohunge, 2012. Yasunaga et al. (2017) transferred *Isometopidea yangi* (Lin 2005) to the genus *Kohnometopus*, suggested that this genus seemed better placed in Gigantometopini rather than in Myiommini, and also proposed to place the genus *Isometopidea* Poppius, 1913 (with the single species *Isometopidea lieweni* Poppius, 1913) in the tribe Gigantometopini. Moreover, it was found that the identity of the specimen of *I. lieweni* from Taiwan (Lin and Yang 2004) was based on a misidentification and it is a representative of an undescribed species. Subsequently Herczek et al. (2018) described one more genus and species within Gigantometopini, *Sulawesimetopus henryi* Herczek, Gorczyca & Tazsakowski.

The most characteristic feature of Gigantometopini distinguishing it from other tribes is the large numbers of trichobothria (five or six on both mesofemur and metafe-mur) (Yasunaga et al. 2017).

In this paper, two new genera and species *Planicapitus luteus* gen. et sp. nov. and *Bruneimetopus simulans* gen. et sp. nov. are diagnosed and described; photographic im-ages of habitus and genital structures, as well as scanning electron micrographs of the selected structures of both species are provided.

Materials and methods

The specimens were imaged by the following equipment: Leica M205C stereo mi-croscope with high diffuse dome illumination Leica LED5000 HDI, Leica DFC495 digital camera and Leica application suite 4.9.0 software; Leica DM 3000 upright light microscope with Leica MC 190 HD digital camera and Leica Application Suite 4.12.0 software. SEM photographs were obtained using Phenom XL field emission scanning electron microscope at 5 and 10 kV accelerating voltage with a BackScatter Detector (BSD). Graphic editor Adobe Photoshop CS6 was used to prepare the figures. In case of legs, the preparations for SEM were made with methods traditionally used in mor-phological studies (e.g. Kanturski et al. 2015, Herczek et al. 2018). In contrast, during preparation of other photographs, steps that can damage the specimen e.g., washing, dehydration and sputter-coating with a film of electrically conducting material, have not been applied. Specimens on original glue boards were only cleaned with a brush and mounted on aluminium stubs with double-sided adhesive carbon tape. Next, the specimens were covered with anti-static spray.

Map was prepared in SAGA GIS 7.1.1 (<http://www.saga-gis.org>) using WGS84 datum and EPSG: 3395 (World Mercator cylindrical projection).

Measurements were made with Leica application suite 4.9.0 software and are presented in millimetres (mm). Terminology of morphological structures mainly fol-lows Herczek et al. (2018) and Kim and Jung (2019). Dissections of male genitalia were performed using Kerzhner and Konstantinov's (1999) technique. The termi-nology for genital structures follows Konstantinov (2003). The study was based on material deposited in the collection of the Royal Belgian Institute of Natural Sci-ences (RBINS) and material recently collected by Claas Damken during an exten-sive survey of the Heteroptera fauna of Brunei Darussalam, deposited at Universiti Brunei Darussalam Museum, Brunei Darussalam (UBDM). From 2013 to 2015, sampling took place at different locations and forest types across the Bornean Sul-tanate using a range of methods (e.g., generator-powered light traps, sweep netting, collecting by hand, litter sifting, pitfall traps, Malaise traps, examination of bycatch from other studies). During this field survey, more than 400 species of Heterop-tera were collected, including several species of Isometopinae (<https://tinyurl.com/Brunei-Isometopinae>).

Taxonomy

Planicapitus Tazakowski, Kim & Herczek, gen. nov.

<http://zoobank.org/E38884A2-CDD1-4C4F-95A5-E8AA1F979AA5>

Type species. *Planicapitus luteus* Tazakowski, Kim & Herczek, sp. nov.

Diagnosis. Distinguished by vertical, flattened head, not punctured but wrinkled and distinctly higher than wide, dorsally extending to level of highest point of pronotum; vertex convex, protruding above eye level; width of vertex slightly larger than eye width; dorsum and pleurites of thorax with deep and dense punctures; calli slightly marked, tarsi two segmented, claw without subapical tooth; labium reaching third abdominal segment; right paramere very small, short, dagger-shaped; left paramere ca. 2.5 times as long as right one.

Description. Male. Body oval, slightly elongated (Fig. 1A). Head clearly higher than wide, dorsally extending to highest point of pronotum, flattened, impunctate but wrinkled; Antenna thin (particularly segments III and IV). Labium reaching third abdominal segment (Fig. 1B). Pronotal collar with row of punctures. Pronotum distinctly punctuate, distinctly carinate at sides, with slightly upturned lateral margins; calli slightly marked, separated by shallow fossa. Scutellum convex, wider than long, basomedially clearly depressed. Thoracic pleura distinctly punctate (Fig. 1C). Ostiolar peritreme small, strongly convex and covered with fine spines (Fig. 4A–C). Mesofemora with five trichobothria (Fig. 3C, D). Tarsi two segmented, claws without apical tooth (Fig. 3 E–G). Genitalia: genital capsule trapeziform, with two longitudinal sutures at sides (Fig. 5A, B); aedeagus delicate, membranous, with weakly sclerotized dorsal wall of phallosome, endosoma sacciform and membranous, weakly sclerotized (Fig. 5A, B, E). Left paramere scythe-shaped, sensory lobe with several long setae, apical process elongate (Fig. 5A–C); right paramere very small, short, dagger-shaped (Fig. 5A, B, D).

Remarks. Affiliation of *Planicapitus luteus* to the Gigantometopini is clearly confirmed by the following features: compound eyes relatively small, significantly separated from each other, pronotum deeply punctate and elongate, calli separated by shallow fossa, pronotal collar demarcated by row of punctures, inflated scutellum, and five mesofemoral trichobothria (Herczek 1993, Yasunaga et al. 2017).

Set of features mentioned in the diagnosis clearly differ the new genus from other genera belonging to Gigantometopini. *Planicapitus luteus* belongs to the smallest representatives of tribe. The new genus is similar in size to *Isometopidea lieweni* which body length of the only known specimen equals to 3.0 mm. It is a female, so probably (like other representatives of tribe) males reach a smaller body size (Poppius 1913, Yasunaga 2005, Herczek et al. 2018). *Isometopidea* further differs from newly described genus by the structure of the head, which is not higher than wide, somewhat rounded and not strongly flattened in front. *Sulawesimetopus*, the second comparatively small-sized genus of the Gigantometopini, is slightly larger and can be distinguished from the new genus by the three segmented tarsi and punctured head. Other representatives of Gigantometopini are a way larger than the new genus in body size.

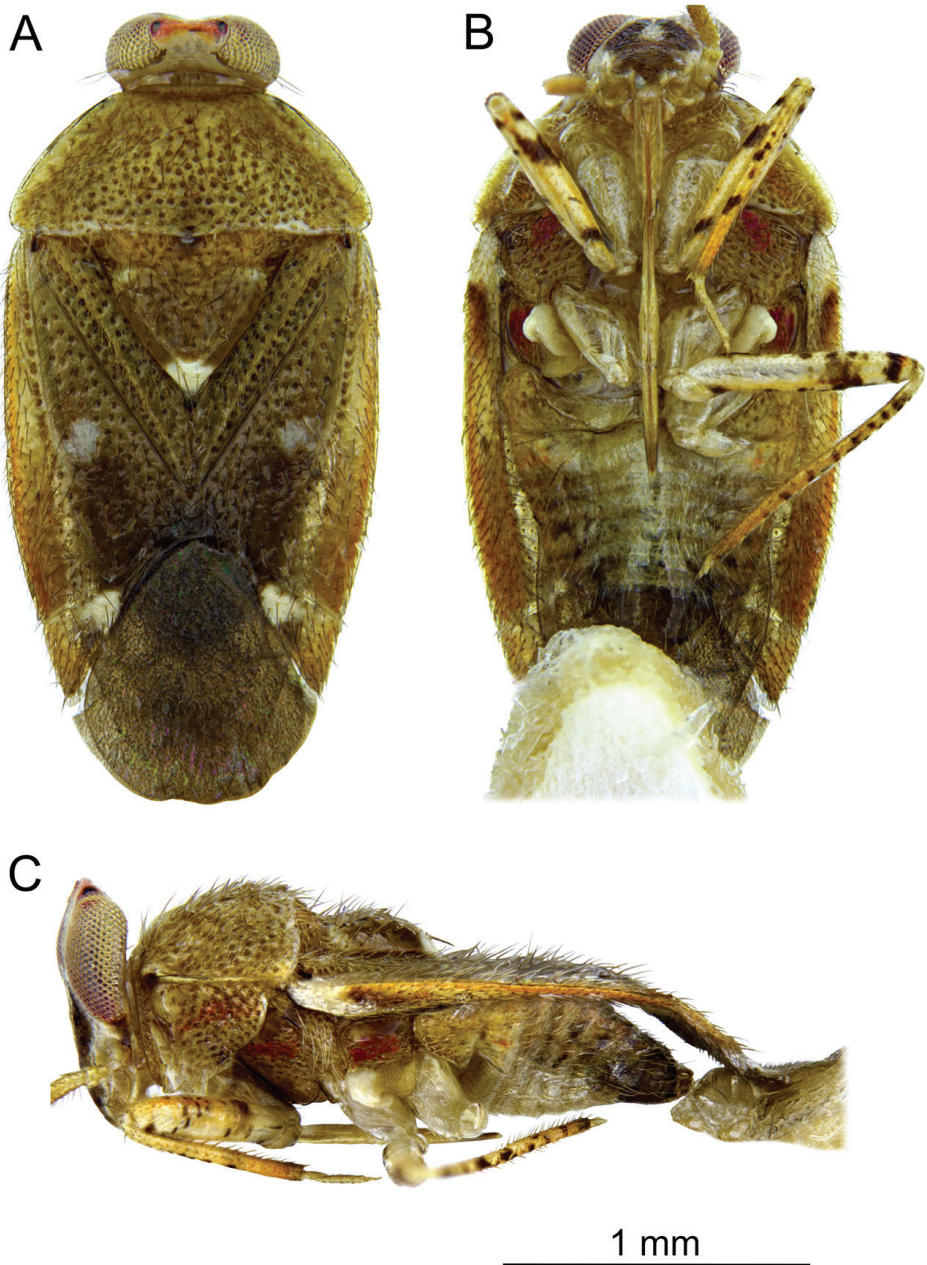


Figure 1. *Planicapitus luteus*: dorsal (A), ventral (B) and lateral (C) views.

Etymology. Combined from Latin adjective: *planus*, flat and noun: *caput, capitis*, head; gender masculine.

***Planicapitus luteus* Tazsakowski, Kim & Herczek, sp. nov.**

<http://zoobank.org/F66DC352-A83C-4661-897A-D101551CDC2C>

Figures 1–5

Diagnosis. See generic diagnosis.

Description. Male. Body shiny, yellow-brownish, covered by semi-erect pale-brown seta (Fig. 1A–C). **Head:** yellow-whitish, 1.5 times as high as wide, compound eyes reddish yellow, vertex orange, convex, 1.3 times as wide as eye width in dorsal view. Frons whitish, with two small dark brown spots ventrally extending into large Y-shaped brown macula; gena whitish yellow (Figs 1C, 2A, B). Antenna yellowish. Labium shiny, yellowish, segment IV with brown apex (Fig. 1B). **Thorax:** pronotum yellow, semi-transparent laterally; exposed part of mesoscutum yellow, scutellum yellowish brown, with apex white and lateral angles narrowly whitish, 0.7 as long as wide. Pleura yellowish brown, with red stripe from propleuron to episternum (Fig. 1B, C). Ostiolar peritreme ivory, evaporative area yellow (Fig. 1B, C). Claval commissure 0.6 times as long as scutellum. **Hemelytron:** in various shades of yellow, median part with

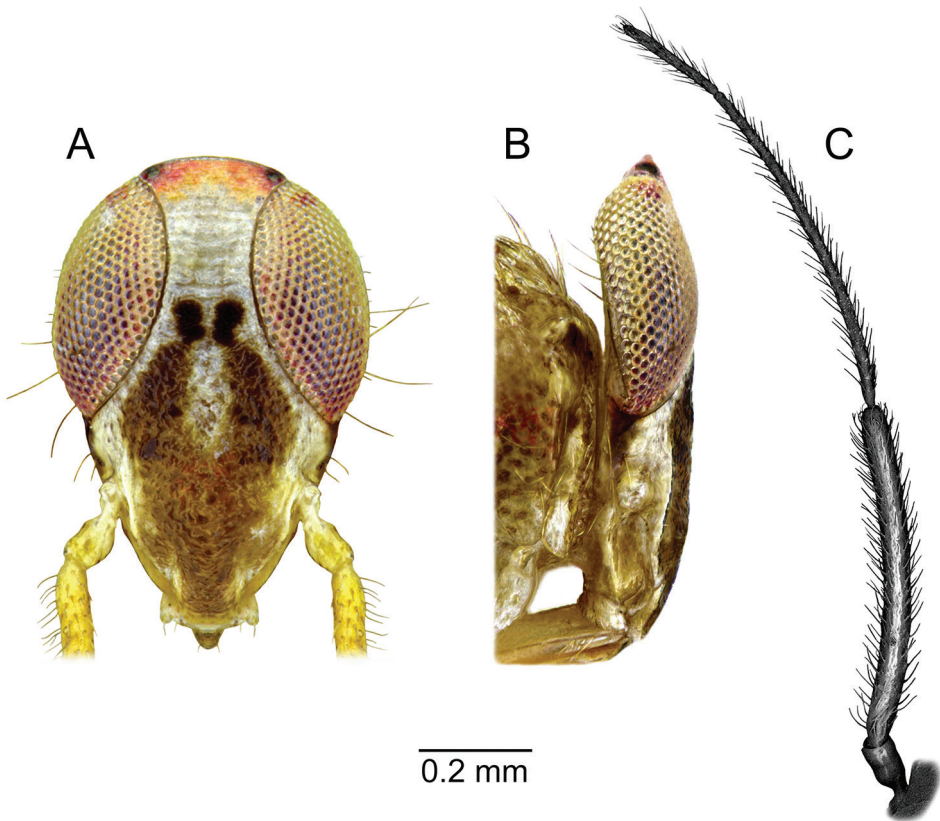


Figure 2. *Planicapitus luteus*: head in frontal view (A), lateral view of head (B), left antenna (C).

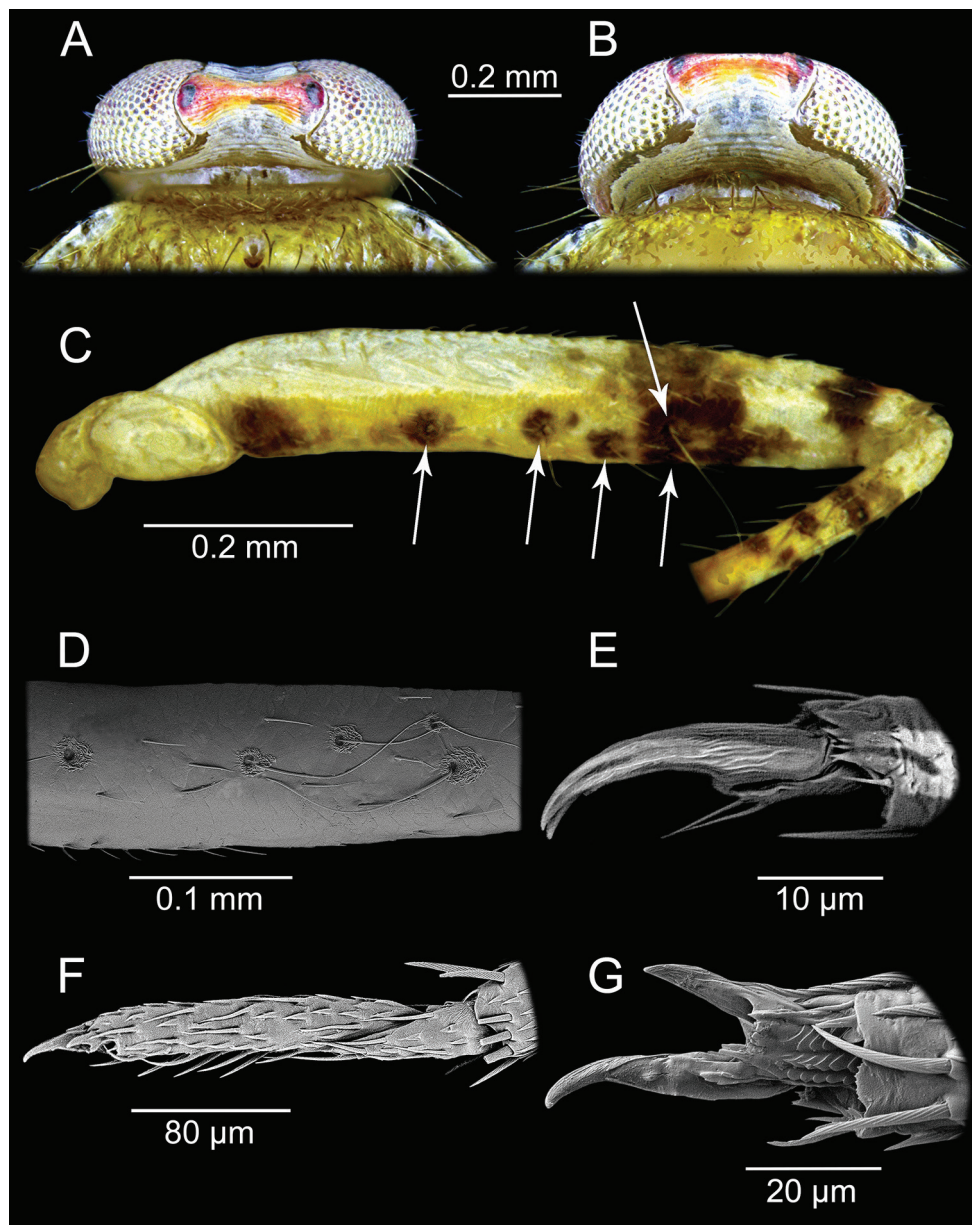


Figure 3. *Planicapitus luteus*: head in dorsal view (A, B), femur of middle leg in ventrolateral view, showing trichobothrial pattern (C, D), pretarsus of foreleg, lateral view (E), tarsus of middle leg, lateral view (F), pretarsus of middle leg, ventral view (G).

two whitish spots. Cuneus 0.9 times as long as wide, yellowish, with white spot in basal inner corner. Membrane pale grey, semi-transparent, with two cells. **Legs:** coxae pale, almost white, femora yellow-white (Fig. 1B, C), with brown spots, tibiae yellow with

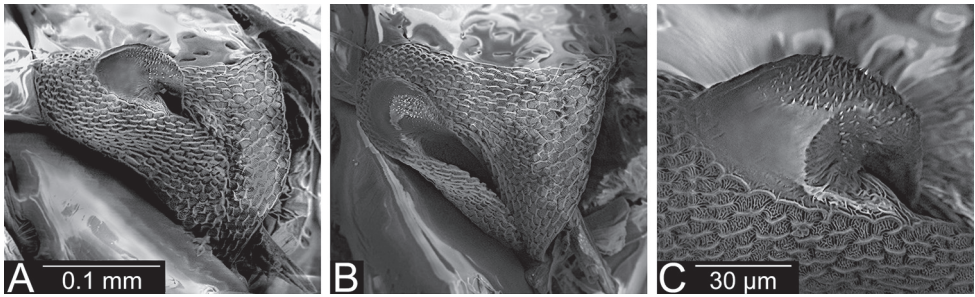


Figure 4. Scent gland, evaporatory area (**A, B**) and peritreme (**C**) of *Planicapitus luteus*.

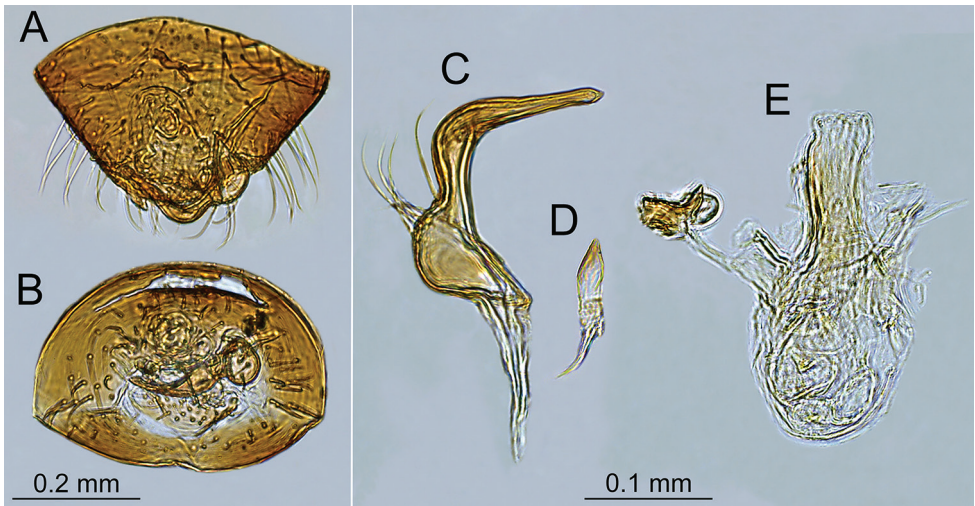


Figure 5. Male genitalia of *Planicapitus luteus*: genital capsule in dorsal (**A**) and caudal (**B**) views, left paramere (**C**), right paramere (**D**), aedeagus in dorsal view (**E**).

dark brown spots, tarsi yellow (Fig. 1B, C). **Abdomen:** bicoloured, dark brown, except for pale yellow genital segment (Fig. 1B, C). **Genitalia:** as described above. **Measurements:** given in the Table 1.

Etymology. From Latin adjective *luteus*, yellow.

Biology. Unknown.

Material examined. **Holotype** (♂): ‘BORNEO, Sabah / DANUM VALLEY / 70km W Lahad Datu / M.J. & J.P. Duffels // East Ridge Trail / 150m / 2.XII.1989 // sample Sab. 53 / understory rainforest, / at light’. The holotype is deposited in RBINS.

***Bruneimetopus* Tazakowski, Kim & Herczek, gen. nov.**

<http://zoobank.org/63C3A9E7-12A1-4CB7-AB92-6F702663401D>

Type species. *Bruneimetopus simulans* Tazakowski, Kim & Herczek, sp. nov.

Diagnosis. Distinguished by vertical, slightly flattened head, not punctured but wrinkled and higher than wide, dorsally not extending to level of highest point of pronotum; vertex slightly convex, protruding above eye level, width of vertex equal to eye width; dorsum and pleurites of thorax with deep and dense punctures; calli slightly marked, tarsi two segmented, claw with very small, barely noticeable apical tooth; labium reaching third abdominal segment, right paramere well developed, with knee-shaped sensory lobe; left paramere ca. 1.5 times as long as right one.

Description. Male. Body oval, slightly elongate (Fig. 6A). Head higher than wide, dorsally not extending to highest point of pronotum, slightly flattened, impunctate but wrinkled. Antenna thin (particularly segments III and IV). Labium reaching third abdominal segment. Pronotal collar with row of punctures posteriorly. Pronotum distinctly punctuate, calli slightly marked, separated by shallow fossa. Scutellum slightly convex, baso-medially clearly depressed. Thoracic pleura distinctly punctate. Ostiolar peritreme small, moderately convex and covered with very fine spines (Fig. 8). Mesofemora with five, metafemora with six trichobothria (Fig. 7F, G). Tarsi two segmented, claws with very small, barely noticeable apical tooth (Fig. 7D, E). Genitalia: genital capsule trapeziform (Fig. 9A), aedeagus delicate, endosoma sacciform and membranous, very weakly sclerotized inside, outer subapical and apical part more sclerotic, clothed with dense spinules (Fig. 9A, D). Left paramere scythe-shaped, sensory lobe with several long setae, apical process elongated (Fig. 9A, B); right paramere left paramere ca. 1.5 times as long as right one, with knee-shaped sensory lobe (Fig. 9C).

Remarks. Affiliation of *Bruneimetopus* to the Gigantometopini is clearly confirmed by the same set of features as for *Planicapitus* (see above). It is also indicated by presence of six metafemoral trichobothria (the specimen of *Planicapitus luteus* is devoid of hindlegs).

As in the case of *Planicapitus*, set of features mentioned in the diagnosis clearly differ the new genus from other genera belonging to Gigantometopini. The newly described genera are very similar morphologically to each other. However, in addition to small differences in the proportions of body parts and coloration, they can easily be distinguished by the completely different shape and size of the right paramere. This was a premise to describe them in separate genera.

Etymology. Name combines Brunei (the type locality) with part of the generic name *Isometopus*, the type genus of the subfamily.

***Bruneimetopus simulans* Tazsakowski, Kim & Herczek, sp. nov.**

<http://zoobank.org/40B3C1AB-7913-4AA4-9AE1-82B098AE5B23>

Figures 6–9

Diagnosis. See generic diagnosis.

Description. Male. Body shiny, in various shades of yellow and brown, covered by semi-erect pale brown and brown setae (Fig. 6A–C). **Head:** brownish yellow, 1.4

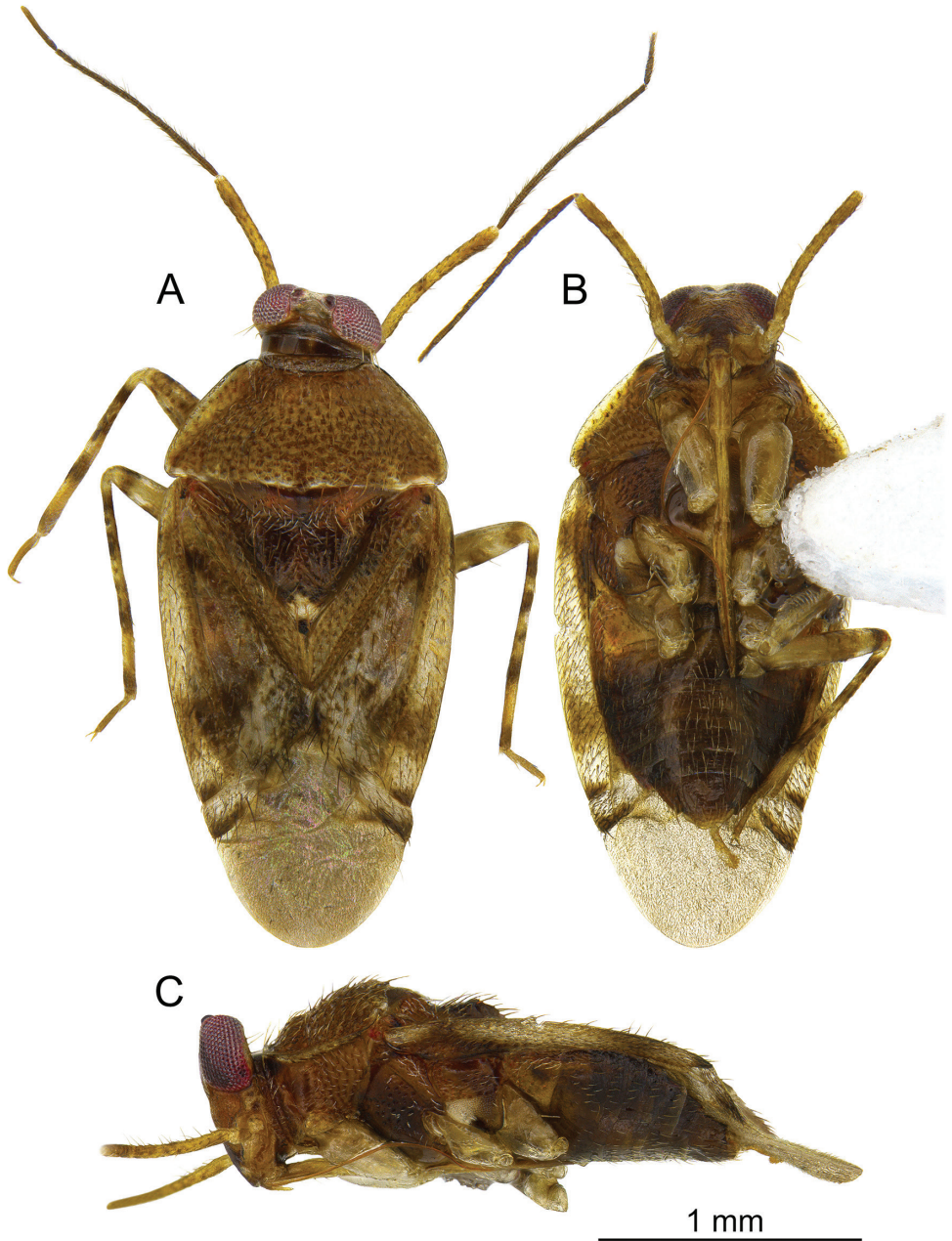


Figure 6. *Bruneimetopus simulans*: holotype: dorsal (A), ventral (B) and lateral (C) views.

times as high as wide, compound eyes reddish, vertex white, slightly convex, as wide as eye in dorsal view. Frons dark brown between eyes, yellowish below inferior margin of eyes; clypeus brown; gena yellow (Fig. 7A–C). Antenna yellowish, segments III and IV

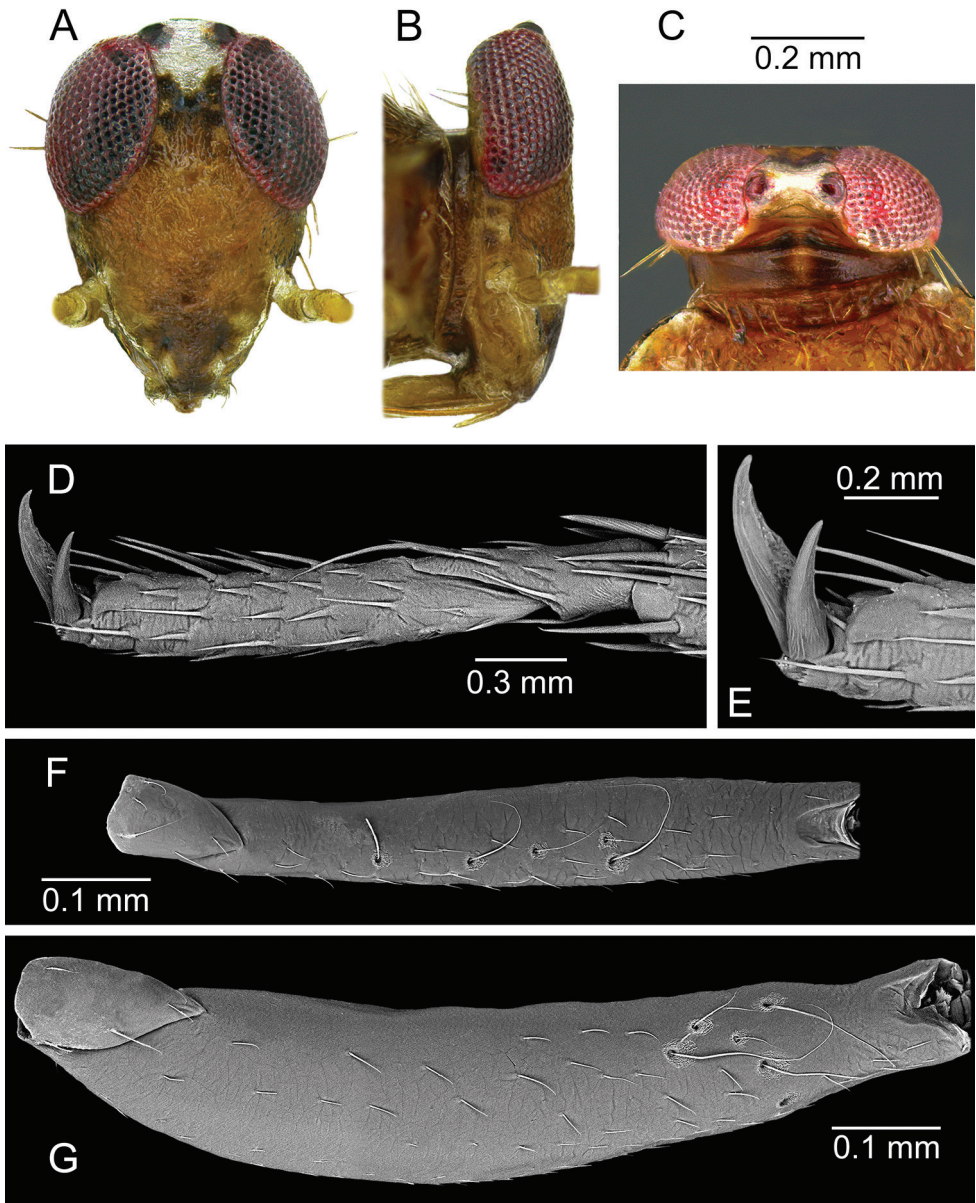


Figure 7. *Bruneimetopus simulans*: holotype: head in frontal view (A), lateral view of head (B), head in dorsal view (C), tarsus of middle leg, lateral view (D), pretarsus of middle leg, lateral view (E), paratype: femur of middle leg in ventral view, showing trichobothrial pattern (F), femur of hind leg in ventral view, showing trichobothrial pattern (G).

darker. Labium shiny, yellowish, segment IV brown (Fig. 6B). **Thorax:** pronotum dark yellow, lateral margins semi-transparent and slightly raised, slightly wider at front; posterior margin whitish. Exposed part of mesoscutum brown with yellow tinge. Scutel-

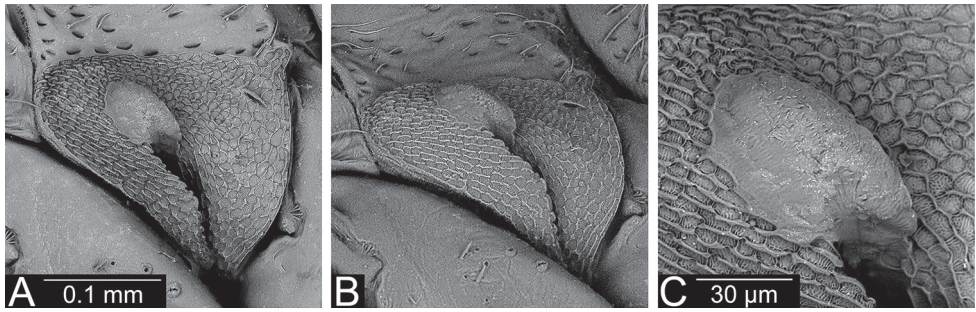


Figure 8. *Bruneimetopus simulans* (holotype) scent gland, evaporatory area (**A, B**) and peritreme (**C**).

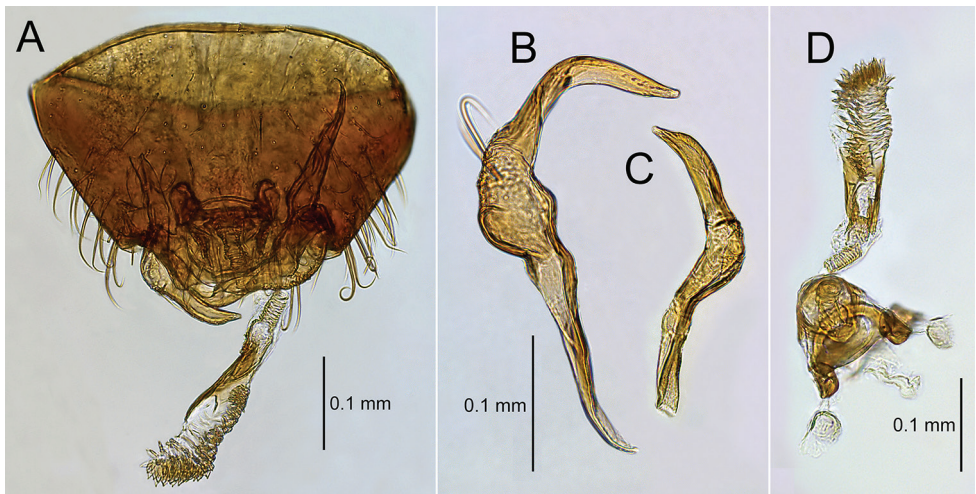


Figure 9. Male genitalia of *Bruneimetopus simulans*: holotype: genital capsule in dorsal view (**A**), left paramere (**B**), right paramere (**C**), aedeagus (**D**).

lum dark brown, with white apical part and black extreme apex, 0.6 times as long as wide, covered by semi-erect setae. Propleuron dark yellow, meso- and metapleurons dark brown with dark yellow tinge. Ostiolar peritreme ivory, evaporative area yellow-brown (Fig. 4D–F). Claval commissure comparatively long, 0.5 times as long as scutellum. **Hemelytron:** in various yellow and brown shades: median, posterior part and cuneus in 2/3 of their length semi-transparent, whitish yellow, base of hemelytra and clavus yellow-brown, part neighbouring with cuneal fracture and 1/3 length of cuneus dark brown. Cuneus 0.9 as long as wide. Membrane pale grey, semi-transparent, with two cells. **Legs:** coxae yellowish pale, femora yellow-white, with brown spots apically, tibiae yellow with four or five dark brown, irregular rings, tarsi yellow (Fig. 6A, B). **Abdomen:** bicolored: first two segments yellowish to brown, others dark brown (Fig. 6B, C). **Genitalia:** as described above. **Measurements:** given in the Table 1.

Table I. Comparison of metric features of *Planicapitus luteus* and *Bruneimetopus simulans*.

	<i>P. luteus</i>	<i>B. simulans</i> holotype	<i>B. simulans</i> paratype	<i>B. simulans</i> average
Body length	2.61	2.52	2.47	2.50
Body width	1.24	1.13	–	1.13
Head length	0.22	0.19	0.19	0.19
Head width	0.58	0.51	0.52	0.52
Head height	0.86	0.71	0.68	0.71
Dorsal width of eye	0.20	0.17	0.19	0.18
Vertex width	0.26	0.17	0.19	0.18
Antennal segments I:II:III:IV	0.10:0.62:0.67:0.21	0.10:0.59:0.78:0.20	0.09:0.60:0.82:0.20	0.10:0.60:0.80:0.20
Labium length	1.30	1.26	–	1.26
Labial segments I:II:III:IV	0.35:0.26:0.30:0.37	0.34:0.36:0.23:0.39	–	0.34:0.36:0.23:0.39
Pronotum length	0.52	0.48	0.43	0.46
Anterior width of pronotum	0.51	0.48	0.44	0.46
Posterior width of pronotum	1.19	1.07	1.07	1.07
Mesoscutum length	0.10	0.12	0.10	0.11
Scutellum length	0.42	0.42	0.49	0.46
Scutellum width	0.61	0.68	0.59	0.64
Claval commissure	0.27	0.23	–	0.23
1 st femur length	0.73	0.64	0.68	0.66
1 st tibia length	0.76	0.73	0.76	0.75
1 st length of tarsus I: II	0.09:0.22	0.08:0.17	0.08:0.17	0.08:0.17
2 nd femur length	0.86	0.73	0.73	0.73
2 nd tibia length	0.96	0.84	0.88	0.86
2 nd length of tarsus I: II	0.21	0.19	0.19	0.19
2 nd length of tarsus I: II	0.08:0.18	0.08:0.16	0.07:0.15	0.08:0.16
3 rd femur length	–	–	0.92	0.92
3 rd femur width	–	–	0.23	0.23
3 rd tibia length	–	–	1.28	1.28
3 rd tarsus length	–	–	0.22	0.22
3 rd length of tarsus I: II	–	–	0.09:0.15	0.09:0.15
Heme length	1.99	1.84	–	1.84
Corium length	1.55	1.25	–	1.25
Cuneus length	0.29	0.23	–	0.23
Cuneus width	0.33	0.27	–	0.27

Etymology. The species name *simulans* (resembling) is the present participle of the Latin verb *simulo* (to make like or to assume the appearance of anything), in allusion to the resemblance of this species to *Planicapitus luteus*.

Biology. Unknown. Two specimens were collected in a mangrove forest (Fig. 10) by a Malaise trap, together with several other specimens of Isometopinae.

Material examined. *Holotype* (♂): 'BORNEO, BRUNEI, Tutong // Tutong area, mangroves forest / small stream near water edge, Malaise / trap 1; 16.viii.2014, leg: C. Dam-



Figure 10. Malaise trap at the collecting site of holotype of *Bruneimetopus simulans*.

ken / 4°46'9.54"N, 114°36'20.64"E // ID code: tutong.mangroves.01780'; **Paratype** (♂): Borneo, BRUNEI, Labu FR. / mangrove forest, Malaise trap ID4 / 06.viii.2018; leg: C. Damken / 4°50'53.11"N, 117°7'45.65"E // ID code: labu.mangroves.01777'. The holotype and paratype are deposited in the UBDM.

Distributional remarks

In total, only 49 imagines of Gigantometopini representing eleven species were ever recorded. Four species are known only from the holotype: *Gigantometopus rossi*, *Gigantometopus schuhi*, *Isometopidea lieweni*, and *Planicapitus luteus*. Below we present the complete checklist of Gigantometopini with distributional records (Fig. 11) and biological information (following Poppius 1913, Schwartz and Schuh 1990, Miyamoto et al. 1996, Yasunaga and Hayashi 1996, Lin and Yang 2004, Yasunaga 2005, Akingbohungbe 2012, Yasunaga et al. 2017, Herczek et al. 2018):

Gigantometopini Herczek, 1993
Astrosopometopus Yasunaga & Hayashi, 2002
***Astrosopometopus formosanus* (Lin, 2004)**
Isometopidea formosana Lin, 2004

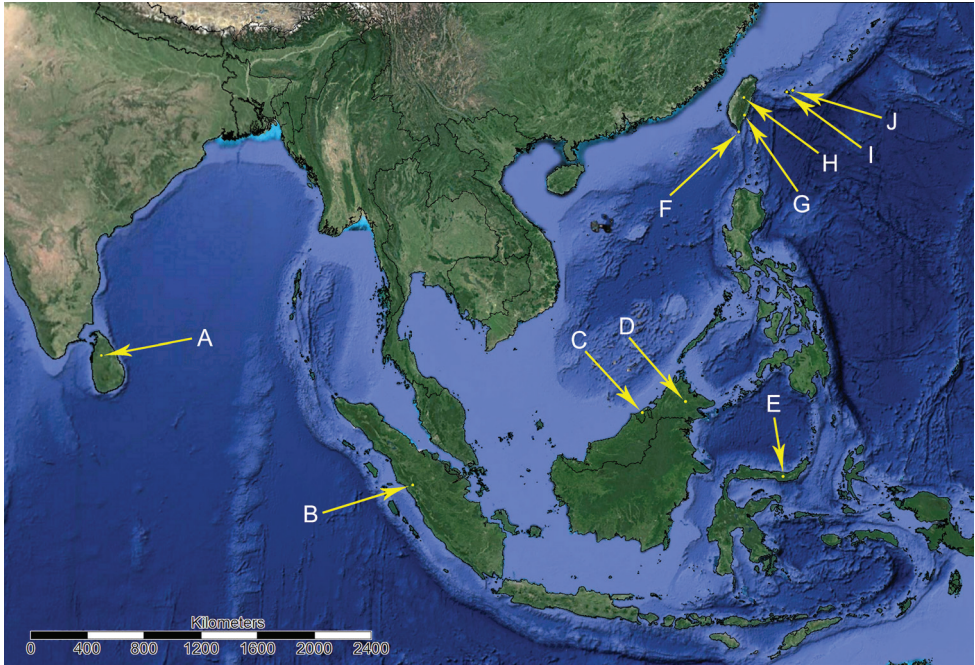


Figure 11. Distribution of Gigantometopini: **A** *I. lieweni* **B** *G. rossi* **C** *G. schuhi* and *B. simulans* **D** *P. luteus* **E** *S. henryi* **F** *A. formosanus* **G** *K. yangi* **H** *A. formosanus* and *I. lieweni* nec **I** *A. gryllocephalus* **J** *A. gryllocephalus* and *K. fraxini*

1♂, Taiwan, Nantou, Chunyang (Fig. 11H), 11 Jun–9 Jul 2002, malaise trap

1♂, Taiwan, Pingtung, Hengchun, Kenting National Park (Fig. 11F), 10 Mar–14 Apr 2005, malaise trap

***Astroscoptometus gryllocephalus* (Miyamoto, Yasunaga, & Hayashi, 1996)**

Isometopidea gryllocephala Miyamoto, Yasunaga, & Hayashi, 1996

1♀, Japan, Ryukyu Arc., Ishigaki Is., Shiramizu (Fig. 11J), 19 Mar 1993, sweeping, grasses growing on the subtropical jungle floor near a montane stream.

1♀, Japan, Ryukyu Arc., Ishigaki Is., Mt. Yarabudake (Fig. 11J), 10 Mar 1999, the bark of the subtropical ash, *Fraxinus griffithii*

1♂, 8 final instar nymphs, Japan, Ryukyu Arc., Ishigaki Is., Mt. Fukami-Omoto (Fig. 11J), 18 Mar 2000, the bark of the subtropical ash, *Fraxinus griffithii*

1♀, Japan, Ryukyu Arc., Iriomote Is. (Fig. 11I), 2 Mar 2002, root of an unidentified broadleaved tree

Gigantometopus Schwartz & Schuh, 1990

***Gigantometopus rossi* Schwartz & Schuh, 1990**

1♀, Indonesia, Sumatra, Sumatera Barat, Mangani, mine near Kota Tinggi, 700 m a.s.l. (Fig. 11B), 20 Jul 1983

***Gigantometopus* cf. *rossi* Schwartz & Schuh, 1990**

1♀, South India

***Gigantometopus schubi* Akingbohungbe, 2012**

1♂, Brunei, Borneo, Bukit Sulang near Lamunin (Fig. 11C), 20 Aug–10 Sep 1982, insecticide fogging on *Shorea macrocarpa*

Isometopidea Poppius, 1913

***Isometopidea lieweni* Poppius, 1913**

1♀, Sri Lanka, Anuradhapura (Fig. 11A), 21 Dec

Isometopidea lieweni nec Poppius, 1913

1♀, Taiwan, Nantou, Lienhachi (Fig. 11H), Nov 1984, malaise trap

Kohnometopus Yasunaga, 2005

***Kohnometopus fraxini* Yasunaga, 2005**

1♂, Japan, Ryukyu Arc., Ishigaki Is., Mt. Fukami-Omoto (Fig. 11J), 28 Sep 2002; 6♀♀, 22 May 2002

1♀, Japan, Ryukyu Arc., Ishigaki Is., Mt. Yarabudake (Fig. 11J), 1 Jun 2002; 2♂♂, 6♀♀, 28 Nov 2002; 1♀, 2 Oct 2002; all specimens of this species were collected on two trees of *Fraxinus griffithii*

***Kohnometopus yangi* (Lin, 2005)**

Isometopidea yangi Lin 2005

1♂, Taiwan, Taitung, Peinan Panchiu Station (Fig. 11G), 19 Nov–16 Dec 2004, malaise trap; 2♂♂, 2♀♀, 19 Nov–16 Dec 2004, malaise trap; 1♀, 7 Oct–19 Nov 2004, malaise trap; 3♂♂, 1♀, 16 Dec 2004–17 Feb 2005, malaise trap

Sulawesimetopus Herczek, Gorczyca & Tazakowski, 2018

***Sulawesimetopus henryi* Herczek, Gorczyca & Tazakowski, 2018**

3♂♂, Indonesia, Sulawesi Utara (Fig. 11E), 8–18 Nov 1985

5♂♂, 1♀, Indonesia, Sulawesi Utara, Dumonga-Bone National Park, Hogg's Back Subcamp, 660 m. a.s.l. (Fig. 11E), 15 Nov 1985

Planicapitus Tazakowski, Kim & Herczek, gen. nov.

***Planicapitus luteus* Tazakowski, Kim & Herczek, sp. nov.**

1♂, Malaysia, Borneo, Sabah Danum Valley, East Ridge Trail, 150 m. a.s.l., (Fig. 11D), 2 Dec 1989, understory rainforest, at light

Bruneimetopus Tazakowski, Kim & Herczek, gen. nov.

***Bruneimetopus simulans* Tazakowski, Kim & Herczek, sp. nov.**

1♂, Brunei, Borneo, Tutong area (Fig. 11C), 16 Aug 2014, mangroves forest (Fig. 10), malaise trap

1♂, Brunei, Borneo, Labu FR. (Fig. 11C), 6 Aug 2018, mangroves forest, malaise trap

Acknowledgements

We are greatly indebted to Dr Jerome Constant from the Royal Belgian Institute of Natural Sciences, Prof Dominik Chłond (University of Silesia in Katowice) for a loan and the assistance with the loan material and Dr Agnieszka Bugaj-Nawrocka (University of Silesia in Katowice) for help in making the map. Claas Damken gratefully acknowledges the support by Ulmar Grafe (Universiti Brunei Darussalam) during the

fieldwork and research on the Heteroptera of Brunei Darussalam. The authors also thank Brunei Forestry Department and Ministry of Primary Resources and Tourism for permission to conduct field work in Brunei Darussalam. The Biodiversity Research and Innovation Centre provided export permits. We also want to thank the reviewers as well as the editors for all the comments that improved this manuscript.

We wanted to apologize to Dr Anna Namyatova for misquoting the work she co-authored in our latest publication. Correct title: Namyatova AA, Cassis G (2016) Review of the seven new species of Isometopinae (Heteroptera: Miridae) in Australia and discussion of distribution and host plant associations of the subfamily on the worldwide basis. *Austral Entomology* 55: 392–422. <https://doi.org/10.1111/aen.12202>

This work was supported by Korea Environment Industry & Technology Institute (KEITI) through Exotic Invasive Species Management Program, funded by Korea Ministry of Environment (MOE)(2018002270005).

The research was supported by the Basic Science Research Program through the National Research Foundation of Korea (NRF) funded by the Ministry of Education (2018R1A6A3A01013374), and was funded through the UBD postdoctoral fellowship (Research and export permit file no: UBD/CAN-387(b)(SAA); UBD/ADM/R3(z)Pt.; UBD/PNC2/2/RG/1(293)).

References

- Akingbohunge AE (2012) A note on *Gigantometopus* Schwartz and Schuh (Heteroptera: Miridae: Isometopinae) with the description of a new species from Borneo. *Entomologica Americana* 118(1/4): 130–132. <https://doi.org/10.1664/12-RA-015.1>
- Cassis G, Schuh RT (2012) Systematics, biodiversity, biogeography, and host associations of the Miridae (Insecta: Hemiptera: Heteroptera: Cimicomorpha). *Annual Review of Entomology* 57: 377–404. <https://doi.org/10.1146/annurev-ento-121510-133533>
- Eyles AC (1971) List of Isometopidae (Heteroptera: Cimicoidea). *New Zealand Journal of Science* 14, 940–944.
- Herczek A, Popov YA (2012) A new peculiar isometopine genus (Hemiptera: Heteroptera: Miridae) from the Eocene Baltic amber. *Zootaxa* 3196: 64–68. <https://doi.org/10.11646/zootaxa.3196.1.4>
- Herczek A (1993) Systematic position of Isometopinae Fieb. (Miridae, Heteroptera) and their intrarelationships. *Prace Naukowe Uniwersytetu Śląskiego, Katowice*, 1357: 1–86.
- Herczek A, Górczyca J, Taszakowski A (2018) *Sulawesimetopus henryi*, a new genus and species of Isometopinae (Hemiptera, Heteroptera, Miridae) from Sulawesi. In: Wheeler Jr AG (Ed.) *A Festschrift Recognizing Thomas J. Henry for a Lifetime of Contributions to Heteropteran Systematics*. *ZooKeys* 796: 147–161. <https://doi.org/10.3897/zookeys.796.21273>
- Jung S, Lee S (2012) Molecular phylogeny of the plant bugs (Heteroptera: Miridae) and the evolution of feeding habits. *Cladistics* 28: 50–79. <https://doi.org/10.1111/j.1096-0031.2011.00365.x>

- Kanturski M, Karcz J, Wiczołek K (2015) Morphology of the European species of the aphid genus *Eulachmus* (Hemiptera: Aphididae: Lachninae) – a SEM comparative and integrative study. *Micron* 76: 23–36. <https://doi.org/10.1016/j.micron.2015.05.004>
- Kerzhner IM, Konstantinov FV (1999) Structure of the aedeagus in Miridae (Heteroptera) and its bearing to suprageneric classification. *Acta Societatis Zoologicae Bohemicae* 63: 117–137.
- Konstantinov FV (2003) Male genitalia in Miridae (Heteroptera) and their significance for suprageneric classification of the family. Part I: general review, Isometopinae and Psallopinae. *Belgian Journal of Entomology* 5: 3–36.
- Kim J, Jung S (2019) Phylogeny of the plant bug subfamily Mirinae (Hemiptera: Heteroptera: Cimicomorpha: Miridae) based on total evidence analysis. *Systematic Entomology* 44, 686–698. <https://doi.org/10.1111/syen.12348>
- Lin CS (2004) Seven new species of Isometopinae (Hemiptera: Miridae) from Taiwan. *Formosan Entomologist* 24: 317–326.
- Lin CS (2005) New or little-known Isometopinae from Taiwan (Hemiptera: Miridae). *Formosan Entomologist* 25: 195–201.
- Lin CS, Yang CT (2004) Isometopinae (Hemiptera: Miridae) from Taiwan. *Formosan Entomologist* 24: 27–42.
- Miyamoto S, Yasunaga T, Hayashi M (1996) Description of a new isometopine plant bug, *Isometopidea gryllocephala*, found on Ishigaki Island, Japan (Insecta, Heteroptera, Miridae). *Species Diversity* 1: 107–110. <https://doi.org/10.12782/specdiv.1.107>
- Namyatova AA, Cassis G (2016) Review of the seven new species of Isometopinae (Heteroptera: Miridae) in Australia and discussion of distribution and host plant associations of the subfamily on a worldwide basis. *Austral Entomology* 55: 392–422. <https://doi.org/10.1111/aen.12202>
- Poppius B (1913) Zur Kenntnis der Miriden, Isometopiden, Anthocoriden, Nabiden und Schizopteriden Ceylon's. *Entomologisk Tidskrift* 34: 239–260. <https://doi.org/10.5962/bhl.part.1634>
- SAGA Development Team (2019) System for Automated Geoscientific Analyses (SAGA) (Version 7.1.1) Institute of Geography at the University of Hamburg, Germany. <http://www.saga-gis.org> [Accessed: 6 February 2019]
- Schuh RT (1974) The Orthotylinae and Phylinae (Hemiptera: Miridae) of South Africa with a phylogenetic analysis of the antmimetic tribes of the two subfamilies for the world. *Entomologica Americana* 47: 1–332.
- Schuh RT (1976) Pretarsal structure in the Miridae (Hemiptera) with a cladistic analysis of relationships within the family. *American Museum Novitates* 2601: 1–39.
- Schuh RT (2002–2013) On-line systematic catalog of plant bugs (Insecta: Heteroptera: Miridae). <http://research.amnh.org/pbi/catalog> [Accessed 19 February 2019]
- Schuh RT, Weirauch C, Wheeler WC (2009) Phylogenetic relationships within the Cimicomorpha (Hemiptera: Heteroptera): a total-evidence analysis. *Systematic Entomology* 34: 15–48. <https://doi.org/10.1111/j.1365-3113.2008.00436.x>
- Schwartz MD, Schuh RT (1990) The world's largest Isometopine, *Gigantometopus rossi*, new genus and new species (Heteroptera: Miridae). *Journal New York Entomological Society* 98(1): 9–13.

- Yasunaga T (2005) Isometopinae plant bugs (Heteroptera: Miridae) preferably inhabiting *Fraxinus griffithii* on Ishigaki Island of the Ryukyus, Japan. *Tijdschrift voor Entomologie* 148: 341–349. <https://doi.org/10.1163/22119434-900000179>
- Yasunaga T, Yamada K, Tsai JF (2017) Taxonomic review of the plant bug subfamily Isometopinae for Taiwan and Japanese Southwest Islands, with descriptions of new taxa (Hemiptera: Heteroptera: Miridae: Isometopinae). *Zootaxa* 4365(4): 421–439
- Yasunaga T, Duangthisan J, Yamada K, Artchawakom T (2016) Further records of the plant bug subfamily Isometopinae from Thailand (Heteroptera: Miridae) with description of three new species. *Tijdschrift voor Entomologie* 159: 89–96. <https://doi.org/10.1163/22119434-15902003>
- Yasunaga T, Hayashi M (2002) New or little known isometopine plant bugs from Japan (Heteroptera: Miridae). *Tijdschrift voor Entomologie* 145: 95–101. <https://doi.org/10.1163/22119434-900000103>

Hyphalus shiyuensis sp. nov. from Xisha Islands, China (Coleoptera, Limnichidae, Hyphalinae)

Zhen-Hua Liu^{1,2}, Qiang Xie¹, Feng-Long Jia¹

1 Institute of Entomology, School of Life Sciences, Sun Yat-sen University, Guangzhou, 510275, Guangdong, China **2** Australian National Insect Collection, CSIRO, GPO Box 1700, Canberra, ACT 2601, Australia

Corresponding author: Feng-Long Jia (lssjfl@mail.sysu.edu.cn; fenglongjia@aliyun.com)

Academic editor: Mariano Michat | Received 28 November 2019 | Accepted 9 May 2020 | Published 16 June 2020

<http://zoobank.org/D14E105C-0B0A-40C6-938B-A2326DEC207F>

Citation: Liu Z-H, Xie Q, Jia F-L (2020) *Hyphalus shiyuensis* sp. nov. from Xisha Islands, China (Coleoptera, Limnichidae, Hyphalinae). ZooKeys 941: 91–99. <https://doi.org/10.3897/zookeys.941.48873>

Abstract

Hyphalus shiyuensis sp. nov. is described from Xisha Islands of China, which represents the ninth species and provides new distribution information for this unique intertidal genus. Brief comparisons between the new species and the known species are given. An updated key to the species of genus *Hyphalus* is provided.

Keywords

Hyphalus, intertidal zone, new species, Oriental Region, taxonomy

Introduction

Hyphalus Britton, 1971 is a poorly known group of intertidal limnichid beetles and the sole genus in the subfamily Hyphalinae, which has a body shape more similar to Byrrhidae rather than Limnichidae. It was described by Britton (1971) from Heron Island, Australia, and suggested to be a group associated with Limnichidae, Dryopidae, and Elmidae. The reason that Britton included it in Limnichidae as a subfamily was that “I think it undesirable to add the number of families in the Dryopoidea where the family separation is already less marked than is usual” (Britton 1971). Since then seven more species of this genus were described from New Zealand, Japan, and Seychelles (Britton 1973, 1977;

Satô 1997; Hernando and Ribera 2000, 2004). All these species are known to live in the intertidal zone, and the larva of *Hyphalus insularis* was reported to be more active in sea water (Britton, 1971), which is extremely rare for beetles and even for insects in general.

Recently, we found three specimens collected from Xisha Islands, China, which perfectly fit in the genus *Hyphalus* and are diagnosed as a new species, based on these specimens. We also present an updated key to the species of *Hyphalus*.

Materials and methods

All the studied specimens of the new species are deposited in the Museum of Biology, Sun Yat-sen University (SYSU). Specimens of described species examined in the study are deposited in the Australian National Insect Collection (ANIC). Specimens for dissection were prepared in 10% KOH for ca 12 hours, then dissected in glycerol on an open slide under a Leica Sapo stereomicroscope. Habitus was photographed using a Nikon DS-Ri2 mounted on a Nikon SMZ25; layers were captured and aligned in the NIS-Elements software. Individual structures in glycerol were photographed using a Zeiss AxioCam HRc mounted on a Zeiss AX10 microscope with the Axio Vision SE64 software. These images were then aligned in Helicon focus (v7.0.2). SEM images were taken using a Phenom Pro, then also aligned in Helicon focus. All the images were processed and plates were made in Photoshop CC 2019.

The terms used in morphological descriptions follow Lawrence and Ślipiński (2013). Measurements were made as follows: body length from apical edge of clypeus to apex of elytra; body width and elytral width are the maximum width of elytra; pronotal length is the median line from anterior margin to posterior margin; pronotal width is the maximum width of pronotum; elytral length is the length along the elytral suture.

Systematic classification

Genus *Hyphalus* Britton, 1971

Hyphalus Britton, 1971: 88. Type species: *Hyphalus insularis* Britton, 1971, by original designation.

Checklist of the described species:

Hyphalus crowsoni Hernando & Ribera, 2000: 240.

Distribution: Seychelles, Aldabra Atoll.

Hyphalus insularis Britton, 1971: 90.

Distribution: Australia, Queensland, Heron Island.

Hyphalus kuscheli Britton, 1977: 82.

Distribution: New Zealand, North Island.

Hyphalus madli Hernando & Ribera, 2004: 413.

Distribution: Seychelles, Silhouette Island.

Hyphalus prolixus Britton, 1977: 85.

Distribution: New Zealand, North Island.

Hyphalus taekoae Satô, 1997: 110.

Distribution: Japan, Ryukyus; China, Taiwan.

Hyphalus ultimus Britton, 1977: 85.

Distribution: New Zealand, North Island.

Hyphalus wisei Britton, 1973: 121.

Distribution: New Zealand, North Island.

***Hyphalus shiyuensis* sp. nov.**

<http://zoobank.org/B0F44404-362F-4045-A42C-177A595BE010>

Figures 1–14

Material examined. *Holotype*: male, CHINA, Hainan Province, Xisha, Shiyu Reef, in a small salty pool (中国, 海南, 西沙, 石屿), 16°32'42"N, 111°44'53"E, alt. 0 m, 30.viii.2018, Qiang Xie leg. (SYSU). *Paratypes*: same data as holotype (2 males, SYSU).

Additional material examined.

Hyphalus insularis Britton, 1971. *Holotype*: Herron I. Gt. Barrier Reef, Q. 24.xi.1968, beneath rocks below high-water mark. E. Britton, S. Misko (ANIC). *Paratypes*: same data as holotype (75 specimens, ANIC).

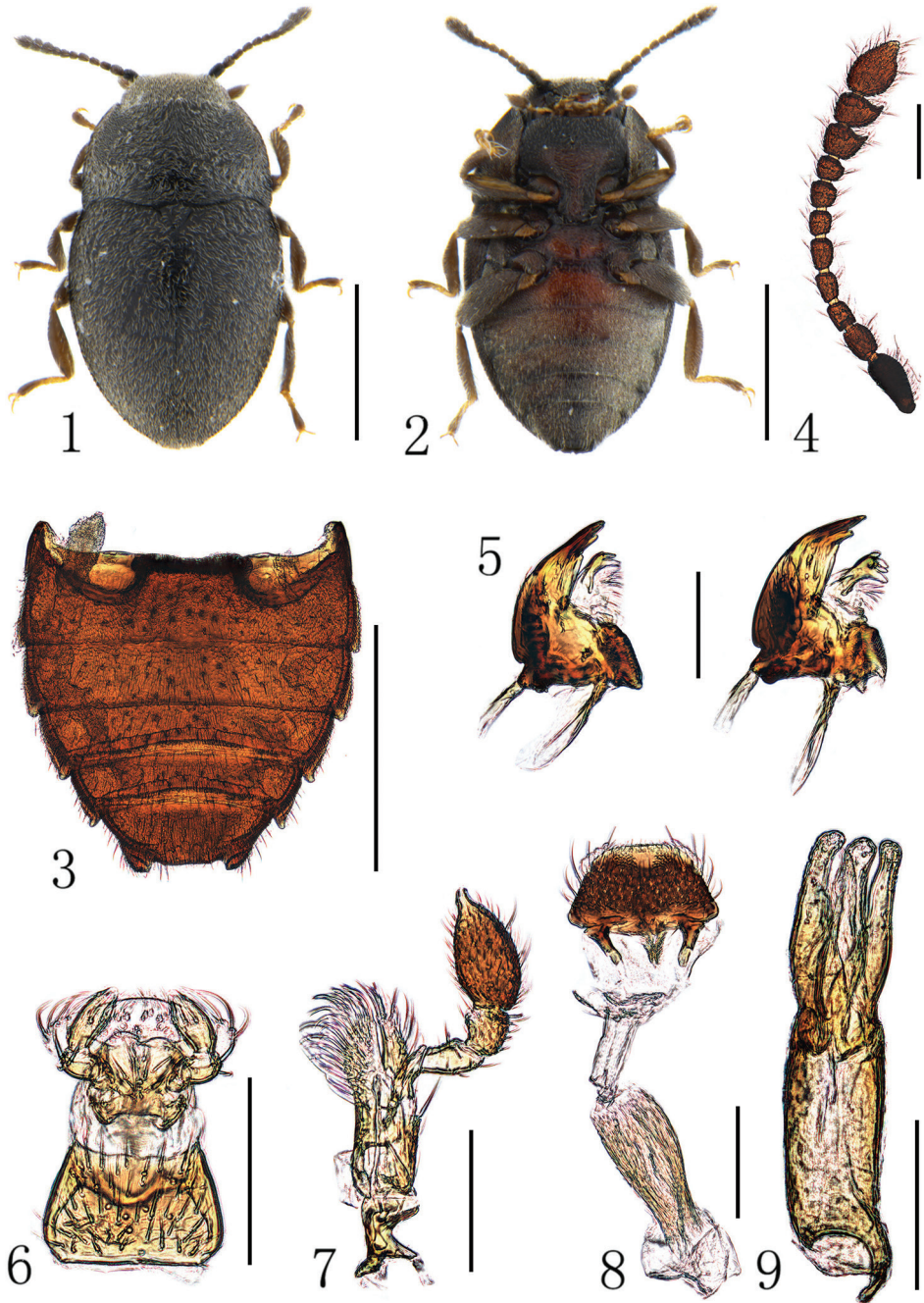
Hyphalus wisei Britton, 1973. *Paratype*: NEW ZEALAND Cape Rodney, North I. exposed rock platform opposite Goat I., N. of Leigh 5.xii.68, K.A.J. Wise (dissected for SEM photograph, ANIC). None types: Leigh, NZ G. Kuschel/ *Hyphalus wisei* Britton ♂ (1 male, ANIC).

Hyphalus kuscheli Britton, 1977. *Paratypes*: In rock crevice at H. W. M. Napier Bay 6. III. 1945 J. M. GURR/ Bay of Islands Co. North I. ANIC); In rock crevice at H. W. M. below recent spring H. W. M. Napier Bay 6. III. 1948 J. M. GURR/ Bay of Islands Co. North I. (ANIC).

Hyphalus prolixus Britton, 1977. *Paratypes*: In rock crevice below H. W. M. Otupoho Bay, Moturua, I. 26. III. 1945 J. M. GURR/ Bay of Islands Co. North I. (4 specimens, ANIC).

Diagnosis. The new species can be separated from the New Zealand species by the broadly ovate body shape. Additionally, the median lobe of aedeagus of *H. shiyuensis* sp. nov. is the same length as the parameres (Fig. 9), thus differing from Seychellois *H. crowsoni* and *H. madli*. It can also be distinguished from the Australian *H. insularis* and Japanese *H. taekoae* by the curved basal projection of the phallobase, which is similar to *H. madli* (Hernando and Ribera 2004: fig. 1).

Description. Length 1.10–1.22 mm, width 0.62–0.69 mm. Body compact and nearly ovate (Fig. 1), dorsum black, venter brown to brownish red, slightly convex both dorsally and ventrally. Vestiture of short and dense silver setae (Fig. 2).

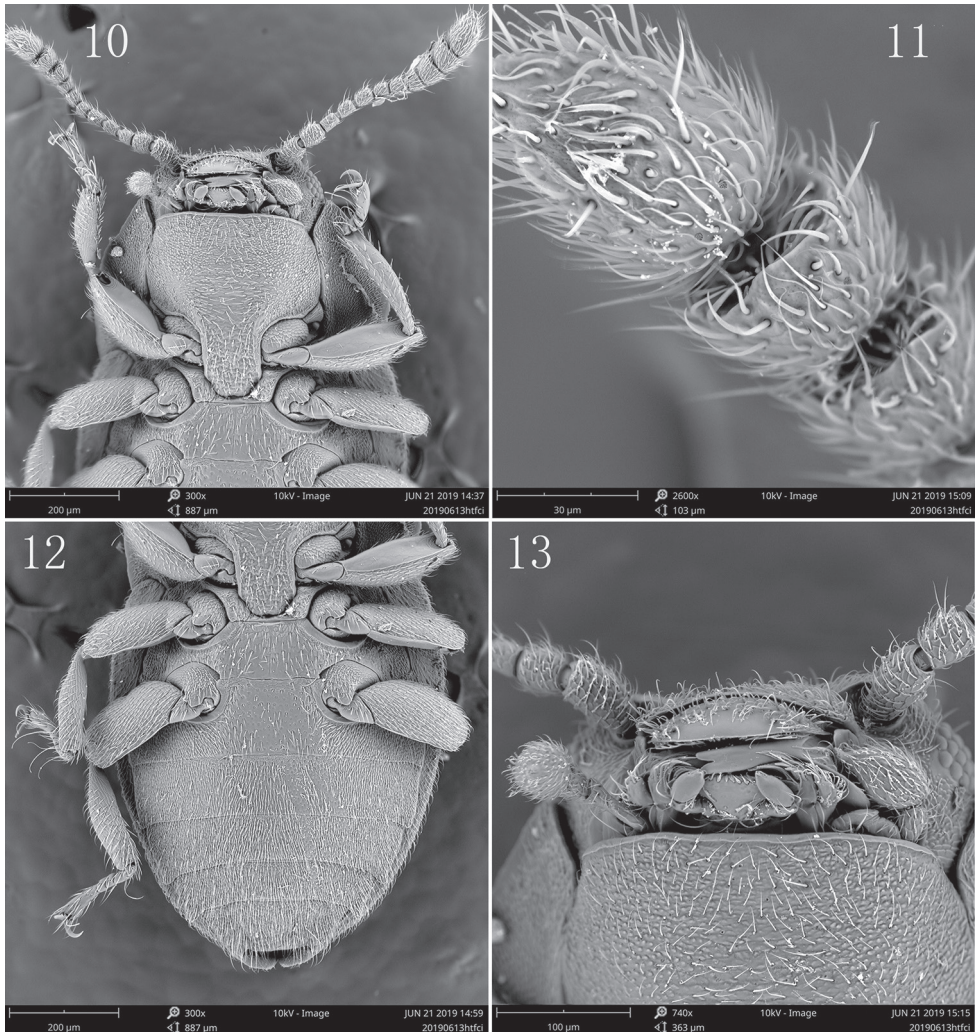


Figures 1–9. *Hyphalus shiyuensis* sp. nov. **1** habitus, dorsum **2** habitus, venter **3** abdomen, venter **4** antenna **5** Mandibles **6** labium **7** maxilla **8** labrum **9** aedeagus. Scale bars: 0.5 mm for (1–3); 0.1 mm for (4–9).

Head sub-rectangular, partly retracted in prothorax, not constricted behind eyes; lateral margins slightly curved, posterior margin slightly emarginated; vertex line and occipital incisions absent. Eyes small and very slightly protruding laterally, finely faceted. Antennae closely inserted in front of eyes; insertions concealed by small frontal expansions laterally. Antennae (Fig. 4) 11-segmented with a 3-segmented antennal club, scape elongate and slightly enlarged apically, pedicel smaller and cylindrical, basal two antennomeres of antennal club with small angulate projection at outer apical corner, terminal segment dilated and fusiform; antennomeres with sparse alveolate sensorium on the surfaces (Fig. 11). Frontoclypeal suture present and straight; clypeus rectangular with apical margin very slightly emarginate; labrum (Fig. 8) large and sub-trapezoid, exposed from dorsal side and freely articulated with clypeus. Mandibles (Fig. 5) sub-triangular with broad base and narrow apex, lateral margins curved with three apical teeth, dorsal surface with a lateral tubercle at base; prosthema sclerotized and elongated with several apical setae; mola present. Maxillae (Figs 7, 13) with 4-segmented palps, first palpomere shortest, second palpomere elongate and slightly enlarged apically, third palpomere transverse and short, terminal palpomere enlarged and ovate with pointed apex; galea not narrower than lacinia, apex acute; lacinia with dense long setae along the inner edge. Labium (Fig. 6) small, labial palps 3-segmented, ligula present and broad. Ventral side of head without sub-antennal suture; gular suture widely separated and diverging posteriorly, gula area short. Cervical sclerites present and large.

Pronotum transverse, ca 0.6 times as long as wide, widest just before posterior angles, lateral margins slightly curved, posterior margin bisinuate, anterior angles acute and extending forwardly, posterior angles acute and extending posteriorly; disc convex, with dense and fine punctations; lateral carinae complete, pronotal epipleuron wide. Prosternum with area before procoxae longer than prosternal process, anterior margin broadly curved; prosternal process broad and parallel sided, apex narrowed with truncate apical margin, extending into the cavities on mesoventrite (Fig. 10). Notosternal suture complete. Procoxae slightly transverse with exposed trochantins (Fig. 10), widely separated; procoxal cavities sub-rectangular, externally and internally open.

Scutellum small and triangular. Elytra relatively broad, ca 1.1 times as long as wide, widest at about anterior third, lateral margins crenulate, apex with quadrangular projection that fits into incision of last ventrite. Dorsal surface weakly convex with fine punctations; epipleuron broad at base, extending to the apical projection. Hind wings absent. Mesoventrite short with pair of lateral depressions anteriorly and a large central concavity to receive the prosternal process, mesoventral process broad with posterior margin truncate; metaventrite short and nearly flattened, metanepisternum broad, meso-metaventral junction simple, of straight line; metendosternite with short and very broad strut, lateral arms slender, laminae and anterior tendons absent. Mesocoxae ovate and widely separated, trochantins exposed; mesocoxal cavities laterally open to mesepimeron, distance between cavities larger than width of cavities. Metacoxae ovate and widely separated, only a little wider than length. Legs all with brown enlarged fem-



Figures 10–13. *Hyphalus shiyuensis* sp. nov. SEM images **10** head, prothorax and mesothorax, venter **11** terminal antennomeres **12** pterothorax and abdomen, venter **13** mouthparts.

ora, trochanters triangular and yellowish; tibiae flattened and expanded; tarsal formula 4-4-4, first three tarsomeres short and yellowish, last tarsomere elongate and enlarged apically with a pair of falciform claws, all with sparse long hairs underneath.

Abdomen (Figs 3, 12) with five ventrites, gradually narrowed posteriorly, covered with dense short depressed setae which are longer on apex; each segment with pair of small posterolateral projections protruding posteriorly, first three ventrites fused and almost equal in length; intercoxal process of first ventrite broad with anterior margin truncate, fourth ventrite shortest, last ventrite sub-trapezoid with pair of small incisions besides posterolateral projections.

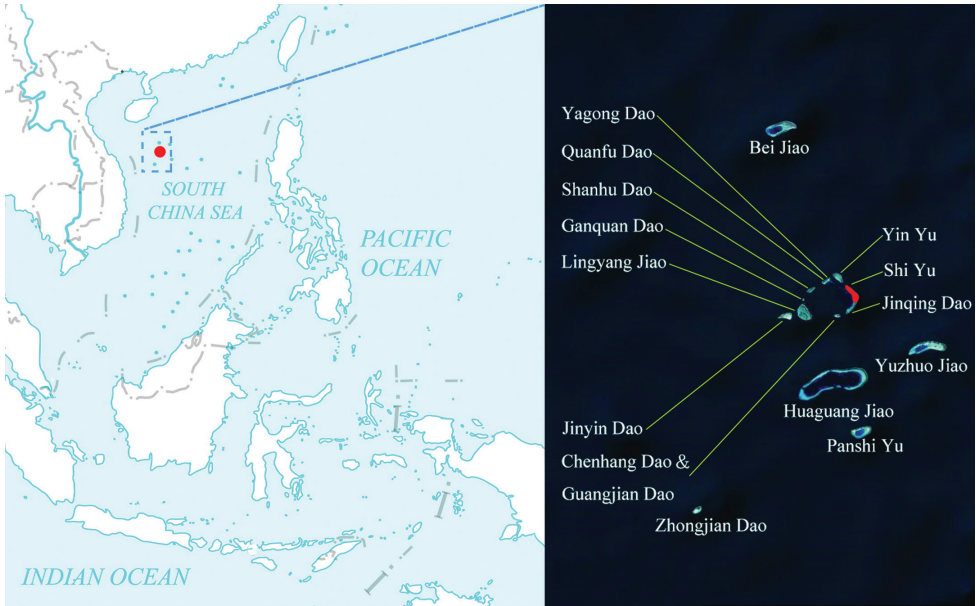


Figure 14. Distribution of *Hyphalus shiyuensis* sp. nov.

Male genitalia with aedeagus trilobate (Fig. 9), phallobase long and sub-cylindrical with a small basal projection, parameres slender with rounded apex, median lobe bowl-shaped with apex slight enlarged, nearly the same length as parameres.

Female unknown.

Habitat. Living in a small pool filled with sea water on a reef.

Etymology. The new species is named after Shiyu Reef, the type locality. The species name is an adjective.

Distribution. Only known from the type locality (Fig. 14).

A key to the species of genus *Hyphalus* (modified from Britton 1977)

- 1 Length more than 1.92 times as long as width 2
- Length less than 1.87 times as long as width 5
- 2 Posterior angles of the pronotum acute 3
- Posterior angles of the pronotum obtuse 4
- 3 Surface of pronotum and elytra bearing obvious tubercles *H. kuscheli*
- Surface of pronotum and elytra without obvious tubercles *H. ultimus*
- 4 Antennomeres 4 and 5 longer than wide, setae on the base of pronotum in front of the scutellum directed obliquely backwards and outwards *H. prolixus*
- Antennomeres 4 and 5 almost of the same length as width, setae on the base of pronotum in front of the scutellum directed obliquely backwards and inwards *H. wisei*

- 5 Median lobe of aedeagus shorter than parameres, body length more than 1.8 times width..... **6**
- Median lobe of aedeagus almost the same length as parameres, body length less than 1.8 times width..... **8**
- 6 Antennomeres 8–11 distinctly asymmetric, antennomeres 8–10 each with a prominent denticle on the anterior inner side (Hernando and Ribera 2000: fig. 1)..... **7**
- Antennomeres 8–11 slightly asymmetric, each without prominent denticle on the anterior inner side..... ***H. insularis***
- 7 Elytra with tubercles on the whole surface, parameres of aedeagus strongly curved, median lobe narrowed pre-apically (Hernando and Ribera 2004: figs 1, 2)..... ***H. madli***
- Elytra with tubercles on the apical region, parameres of aedeagus straight, median lobe not narrowed (Hernando and Ribera 2000: fig. 3) ***H. crowsoni***
- 8 Denticle on the anterior inner side of antennomere 8 distinctly smaller than that on the antennomere 9 (Satô 1997: fig. 2), phallobase of aedeagus with a broad and less curved projection at base (Satô 1997: fig. 4)..... ***H. taekoae***
- Denticle on the anterior inner side of antennomere 8 nearly the same size as that on the antennomere 9 (Fig. 4), phallobase of aedeagus with a slender and strongly curved projection at base (Fig. 9)..... ***H. shiyuensis***

Discussion

Among the nine described species of *Hyphalus*, those from New Zealand are distinctly more elongated. After examining the specimens preserved in ANIC, we have found the antennae of *H. insularis*, *H. wisei*, *H. kuscheli* and *H. prolixus* are more or less asymmetrical rather than symmetrical (Hernando and Ribera 2000) and the elytra of those species have apical tubercles similar to those of the new species. It therefore seems likely that all species of *Hyphalus* have asymmetrical antennal clubs and apical tubercles on elytra, although no specimen of *H. ultimus* was examined in this study. Hence, a more detailed study of the morphology of this genus is still needed.

Hyphalus is only known from Australia, New Zealand, Seychelles, Japan, and China with nine described species until now. The diversity of this genus, however, might be underestimated given the tiny body size and unique habitats of the species. More careful and comprehensive collection of beetles in the intertidal zones is needed to study the biogeography and dispersal methods of these interesting beetles.

Acknowledgements

The authors are grateful to Ignacio Ribera and Carles Hernando for reviewing the manuscript and helpful suggestions. Our thanks also to Dr Adam Slipinski, Austral-

ian National Insect Collection, CSIRO, who improved the English of the manuscript. The Scientific Expedition was organized by South China Sea Research Institute of Sun Yat-sen University. This work was financially supported by National Natural Science Foundation of China (31772494).

References

- Britton EB (1971) A new intertidal beetle (Coleoptera: Limnichidae) from the Great Barrier Reef. *Journal of Entomology Series B, Taxonomy* 40(2): 83–91. <https://doi.org/10.1111/j.1365-3113.1971.tb00108.x>
- Britton EB (1973) *Hyphalus wisei* sp. n., a new intertidal beetle from New Zealand (Coleoptera: Limnichidae). *Records of the Auckland Institute and Museum* 10: 119–122.
- Britton EB (1977) Three new intertidal species of Limnichidae (Coleoptera) from New Zealand. *Records of the Auckland Institute and Museum* 14: 81–85.
- Hernando C, Ribera I (2000) The first species of the intertidal genus *Hyphalus* Britton from the Indian Ocean (Coleoptera: Limnichidae: Hyphalinae). *Annales de la Société entomologique de France* 36(3): 239–243.
- Hernando C, Ribera I (2004) *Hyphalus madli* sp. n., a new intertidal limnichid beetle from the Seychelles. *Koleopterologische Rundschau* 74: 413–417.
- Lawrence JF, Ślipiński A (2013) *Australian Beetles. Vol. 1: Morphology, Classification and Keys*. CSIRO Publishing, Collingwood, Victoria, viii + 561 pp.
- Satō M (1997) Occurrence of a new *Hyphalus* (Coleoptera, Limnichidae) from the Ryukyu Archipelago, Japan. *Elytra* 25(1): 109–112.

First record of the genus *Tetracona* Meyrick (Lepidoptera, Crambidae) from China, with description of a new species

Lu-Lan Jie¹, Jing-Bo Yang¹, Wei-Chun Li¹

¹ College of Agronomy, Jiangxi Agricultural University, Nanchang, 330045, China

Corresponding author: Wei-Chun Li (weichunlee@126.com)

Academic editor: C. Plant | Received 20 December 2019 | Accepted 4 May 2020 | Published 16 June 2020

<http://zoobank.org/9025149F-4264-4690-BA85-132D4E176B93>

Citation: Jie L-L, Yang J-B, Li W-C (2020) First record of the genus *Tetracona* Meyrick (Lepidoptera, Crambidae) from China, with description of a new species. ZooKeys 941: 101–105. <https://doi.org/10.3897/zookeys.941.49559>

Abstract

The genus *Tetracona* has two species with an Australian distribution. The present study aims to record the genus from China for the first time and to add a third species, *T. multispina* Jie & Li, **sp. nov.** to the genus. The new species can be distinguished from the congeners by the antemedial line connecting the postmedial line near the dorsum in the hindwing, and the phallus with a cluster of spine-like cornuti in the male genitalia. Images of the habitus, tympanal organs and male genitalia are provided for the new species.

Keywords

China, Pyraloidea, Spilomelinae, snout moths, *Tetracona*, taxonomy

Introduction

The genus *Tetracona* was erected by Meyrick in 1884 with *Aediodes amathealis* Walker, 1859 as type species (Meyrick 1884). Then it was defined as a junior synonym of *Agrotera* Schrank, 1802 based on the external characters by Hampson (1899). However, the dissected structures of the males provide more effective characters to separate

the two genera. Thus, Chen et al. (2017) removed it from synonymy with *Agrotera* and reinstated it as a valid genus using the male genital characters.

Before this study, the genus contained two species with an Australian distribution (Walker 1859; Meyrick 1884; Warren 1896; Hampson 1899; Chen et al. 2017). In the present paper, we record the genus in the Chinese fauna for the first time and add a new species.

Materials and methods

The specimens were collected at night with a mercury-vapor lamp. The specimens were prepared referring to the method shown in Landry and Landry (1994). The morphological terminology follows Maes (1995). The images of the habitus and genitalia were taken using a digital camera attached to a Zeiss SteREO Discovery V12 microscope and an Optec BK-DM320 microscope, respectively. All the studied specimens are deposited in the Insect Museum, Jiangxi Agricultural University, Nanchang, China (JXAUM).

Taxonomy

Tetracona Meyrick, 1884

Tetracona Meyrick, 1884: 307; Chen et al. 2017: 215. Type species: *Aediodes amathealis* Walker, 1859, by monotypy.

Differential diagnosis. The species of *Tetracona* Meyrick, 1884 are similar to the members of *Agrotera* Schrank, 1802 in their external characters. However, they can be easily distinguished from the latter by using the male genitalia: The uncus of *Tetracona* is lobe-shaped, laterally covered with dense setae; the valvae are basally equipped with a bundle bristles near the middle, and are elliptical with blunt rounded apices. In *Agrotera*, the uncus is short to elongate and conical, set with few setae; the valvae have a large, hook-like process near the base, and are elliptical with narrow and pointed apices (Chen et al. 2017).

Distribution. Australia, China.

Remarks. This genus is recorded from China for the first time herein.

Key to species of *Tetracona* based on wing pattern and male genitalia

- 1 Forewings with basal half yellow and decorated with a brown dot near basal middle (Chen et al. 2017: fig. 16) *T. pictalis*
- Forewings with approximately basal third yellowish white and sprinkled with orange scales, without brown dot 2

- 2 Forewings with a crescent-shaped distal discoidal stigma, postmedial line dentated outwards at approximately dorsal fourth; apical third of valva subtriangular, apex much narrower than valval base, costa concave near middle (Chen et al. 2017: figs 15, 19) *T. amathealis*
- Forewings with an ovate distal discoidal stigma, postmedial line distinctively incurved at approximately dorsal third; apical third of valva subrectangular, apex much wider than valval base, costa straight (Figs 1, 4)
..... *T. multispina* sp. nov.

***Tetracona multispina* Jie & Li, sp. nov.**

<http://zoobank.org/A6316933-1CD5-4AF0-9633-208BFE743B8E>

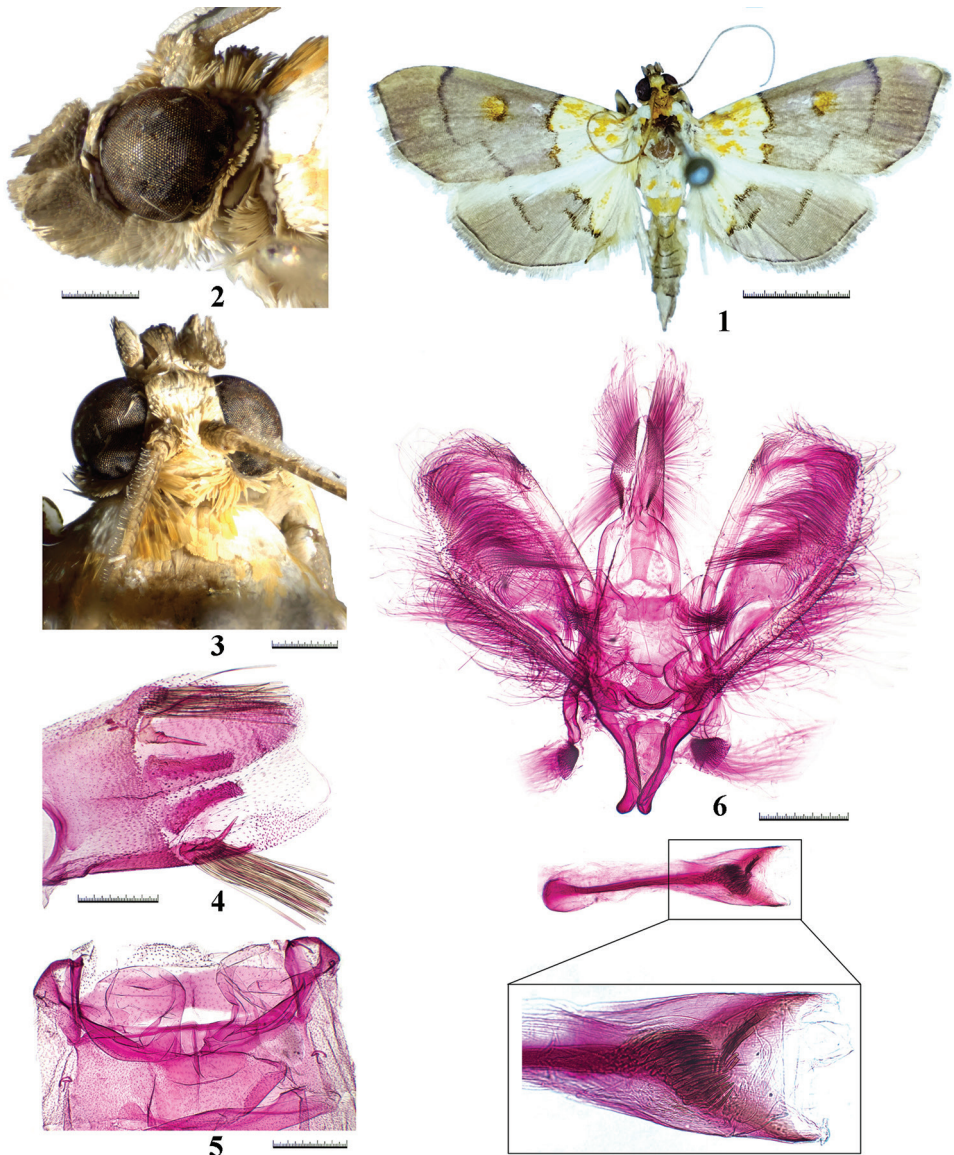
Figures 1–6

Type material. *Holotype* ♂: CHINA: Huangzihao, Fuliang (29°15'N, 117°09'E), Jiangxi Province, 220 m, 26.v.2012, Wei-Chun Li leg., genitalia slide no. JL19103 (JXAUM).

Paratypes: CHINA: 1 ♂, same data as holotype, genitalia slide no. JL16099; 1 ♂, Tongboshan (28°15'N, 117°07'E), Jiangxi Province, 900 m, 30.viii.2012, Wei-Chun Li leg., genitalia slide no. JL16098; 1 ♂, Wuyuan, Shangbao (29°09'N, 117°30.6'E), Jiangxi Province, 23–28.vi.1989, Guang-Pu Shen leg.; 1 ♂, Dabali, Xunwu (29°09'N, 117°30.6'E), Jiangxi Province, 550 m, 22.vii.2007, Yu-Jian Lin leg., genitalia slide no. JL16094; 1 ♂, Doushui (29°09'N, 117°30.6'E), Shangyou, Jiangxi Province, 150 m, 20.x.1991, Yu-Jian Lin leg., genitalia slide no. JL19104; 1 ♂, Shangyou Arboretum (29°09'N, 117°30.6'E), Jiangxi Province, 230 m, 22.x.1991, Yu-Jian Lin leg., genitalia slide no. JL19104 (JXAUM).

Differential diagnosis. This new species can be distinguished from its congeners by the unique characters in the hindwing and male genitalia: its antemedial line connects with the postmedial line near the dorsum and the phallus with a cluster of spine-like cornuti.

Description. *Adult male* (Figs 1–4): Forewing length 10.0–11.0 mm. Frons rounded, pale yellow. Vertex ochreous. Labial palpi upcurved, first segment grey, the remaining brown; second segment ending with truncate tip, third segment with triangular scale tuft. Maxillary palpi upright, ochreous. Thorax yellowish white sprinkled with orange scales. Forewing subtriangular, basal third yellowish white, suffused with irregular orange scales, remaining pale brown; antemedial line blackish brown, dentated inwards near middle; distal discoidal stigma ovate, blackish brown tinged with orange; postmedial line blackish brown, distinctively incurved at approximately dorsal third; terminal margin blackish brown; cilia pale brown mixed with pale yellow. Hindwing basal third yellowish white, suffused with irregular orange scales, remaining pale brown; antemedial line blackish brown, incurve at middle; postmedial line blackish brown, nearly S-shaped, connecting antemedial line near dorsum; terminal margin blackish brown; cilia pale brown. Abdomen with two white basal segments, second segment with two orange lateral stripes; third segment orange, remainder pale



Figures 1–6. *Tetracona multispina* sp. nov. **1** adult in dorsal view, holotype **2** head in lateral view, holotype **3** head in dorsal view, holotype **4** ninth segment of abdomen, paratype **5** tympanal organs in ventral view, paratype **6** male genitalia in ventral view (phallus removed), paratype. Scale bars: 5 mm (**1**), 0.5 mm (**2–6**)

brown mixed with pale yellow except for white distal segment; ninth segment with two well-developed spines and two tufts of culcita. **Tympanal organs** (Fig. 5): Bulla tympani convex on inner margin, more or less concave posteriorly. Saccus tympani extending to about anterior one-fourth of tergite two. Venula secunda absent. **Male genitalia** (Fig. 6): Uncus lobe-shaped, covered with dense setae; distal half narrowed

towards blunted tip. Valva basally narrow, broadened towards distal third, then gently narrowed towards round apex. Saccus weakly sclerotized, thin and long. Saccus basally broad, tapering towards two blunt tips. Juxta nearly fan-shaped. Phallus straight, nearly as long as valva; cornuti composed of multiple spines of various sizes.

Female. Unknown.

Distribution. China (Jiangxi).

Etymology. The specific name is derived from the Latin prefix *multi-* = multiple, and the Latin *spina* = spine, referring to the male genitalia with multiple spine-like cornuti.

Acknowledgements

We extend our cordial thanks to Prof Yu-Jian Lin and Prof Guang-Pu Shen, who generously donated the specimens of the genus *Tetracona* to our insect museum. Special thanks are given to Dr František Slamka for insightful comments on the manuscript. This work is supported by the National Natural Science Foundation of China (No. 31601885).

References

- Chen K, Horak M, Du XC, Zhang DD (2017) Revision of the Australian species of *Agrotera* Schrank (Lepidoptera: Pyraloidea: Crambidae: Spilomelinae). *Zootaxa* 4362(2): 213–224. <https://doi.org/10.11646/zootaxa.4362.2.2>
- Hampson GF (1899) A revision of the moths of the subfamily Pyraustinae and family Pyralidae. Part I. Proceedings of the General Meetings for Scientific Business of the Zoological Society of London, 627–628.
- Landry JF, Landry B (1994) A technique for setting and mounting Microlepidoptera. *Journal of the Lepidopterists' Society* 48(3): 205–227.
- Maes KVN (1995) A comparative morphological study of the adult Crambidae (Lepidoptera, Pyraloidea). *Bulletin et Annales de la Société Royale Belge d'Entomologie* 131: 383–434.
- Meyrick E (1884) On the classification of the Australian Pyralidina. *Transactions of the Entomological Society of London* 32(3): 277–350. <https://doi.org/10.1111/j.1365-2311.1884.tb01610.x>
- Walker F (1859) Pyralides. List of the Specimens of Lepidopterous Insects in the Collection of the British Museum 17: 348–349.
- Warren W (1896) New genera and species of Pyralidae, Thyrididae, and Epiplemidae. *Annals and Magazine of Natural History, including Zoology, Botany and Geology (ser.6)* 17: 139–140. <https://doi.org/10.1080/00222939608680328>

Description of a new *Barsine* Walker, 1854 from India and Nepal (Lepidoptera, Erebidae, Arctiinae, Lithosiini)

Anton V. Volynkin^{1,2}, Navneet Singh³, Jagbir Singh Kirti⁴, Harvinder Singh Datta⁴

1 Altai State University, Lenina Avenue, 61, RF-656049, Barnaul, Russia **2** National Research Tomsk State University, Lenina Avenue, 36, RF-634050, Tomsk, Russia **3** Zoological Survey of India, M-Block, New Alipore, Kolkata, 700053, West Bengal, India **4** Department of Zoology and Environmental Sciences, Punjab University, Patiala, Punjab, 147002, India

Corresponding author: Navneet Singh (nsgill007@gmail.com)

Academic editor: A. Zilli | Received 24 February 2020 | Accepted 26 April 2020 | Published 16 June 2020

<http://zoobank.org/CF545A32-6B77-474C-A8C8-776473CCB7C8>

Citation: Volynkin AV, Singh N, Kirti JS, Datta HS (2020) Description of a new *Barsine* Walker, 1854 from India and Nepal (Lepidoptera, Erebidae, Arctiinae, Lithosiini). ZooKeys 941: 107–120. <https://doi.org/10.3897/zookeys.941.51344>

Abstract

A new species, *B. kirata* Volynkin & N. Singh, **sp. nov.**, similar to *B. germana*, is described from India and Nepal. The existence of two colour forms in some species of the genus *Barsine* Walker, 1854 is revealed. A new synonymy is established for *Barsine germana* (Rothschild, 1913), which includes two forms that were described as three different species: *Barsine germana* (Rothschild, 1913) (the yellow form) = *B. valvalis* Kaleka, 2003, **syn. nov.**, and *B. thomasi* Kaleka, 2003, **syn. nov.** (the red-spotted forms).

Keywords

Asia, *Barsine kirata*, *B. valvalis* Kaleka, *B. thomasi* Kaleka, new species, new synonymy, red and yellow forms

Introduction

Until recently, *Barsine* Walker, 1854 was considered to be a very large and polyphyletic genus including more than a hundred valid species (Holloway 2001; Kaleka 2003,

2018; Černý and Pinratana 2009; Bucsek 2012, 2014; Dubatolov et al. 2012; Dubatolov and Bucsek 2013; Wu et al. 2013; Kirti and Singh 2015, 2016; Černý 2016; Volynkin and Černý 2016a, b, c, 2017a, b, c, d, 2018a, b, 2019; Bayarsaikhan et al. 2018; Huang et al. 2018, 2019; Joshi et al. 2018; Spitsyn et al. 2018; Volynkin 2018; Volynkin et al. 2018, 2019a, b, c, d). Volynkin et al. (2019e) separated several lineages into distinct genera, and now *Barsine* includes 65 species and five subspecies of its type species, *B. defecta* Walker, 1854, having a basal saccular process.

Dissections of numerous specimens of various species of *Barsine* displayed the existence of two colour forms in some of them: the common form having reddish forewing pattern elements together with black ones, and the yellow form lacking reddish forewing pattern elements. The latter, yellow form is usually very rare and has so far been found only in *B. defecta* (Figs 19, 20), *B. orientalis bigamica* Černý, 2009 (illustrated by Bayarsaikhan et al. 2018), *B. gratissima* (de Joannis, 1930), *B. obsoleta* (Reich, 1937), and *B. cacharensis* N. Singh & Kirti, 2016. In some species, intraspecific variation is high and expressed not only in the presence or absence of red pattern elements but also in the shade of the ground colour and red spots, the size of the red and black pattern elements, body size, and even forewing shape (Figs 1–10). Such polymorphism is obvious evidence of a polygenic inheritance, and this matter needs extensive molecular study.

The red and yellow forms of some species have been described as distinct species, as in the case of *Barsine germana* (Rothschild, 1913) (the yellow form; Figs 1–3), and *B. valvalis* Kaleka, 2003 and *B. thomasi* Kaleka, 2003 (the red-spotted form; Figs 4–10). In the present paper, we synonymize *B. valvalis* and *B. thomasi* with *B. germana*. In addition, dissections of red-spotted specimens of this group from various regions of Nepal and India revealed the existence of two species very similar externally but clearly different in their genitalia structures. One of them is described below.

Materials and methods

Abbreviations of the depositories used: **NHMUK** = Natural History Museum (formerly British Museum of Natural History, London, UK); **NZCZSI** = National Zoological Collection, Zoological Survey of India (Kolkata, India); **MWM/ZSM** = The Bavarian State Collection of Zoology (Museum Witt München / Zoologische Staatssammlung München, Munich, Germany); **ZFMK** = Zoological Research Museum Alexander Koenig (Zoologisches Forschungsmuseum Alexander Koenig, Bonn, Germany).

The genitalia of specimens deposited in NHMUK, MWM/ZSM, NZCZSI, and ZFMK collections were dissected, stained with eosin B and mounted in Euparal on glass slides using standard methods of preparation (Lafontaine and Mikkola 1987; Fibiger 2007). Photographs of imagos deposited in NHMUK and MWM/ZSM were taken using a Nikon D3100/AF-S camera equipped with a Nikkor 18–55 mm lens. Genital preparations made by A.V. Volynkin were photographed with the same camera attached to a microscope with an LM-scope adapter.

Taxonomic part

Barsine germana (Rothschild, 1913)

Figs 1–10, 21–24, 29, 30

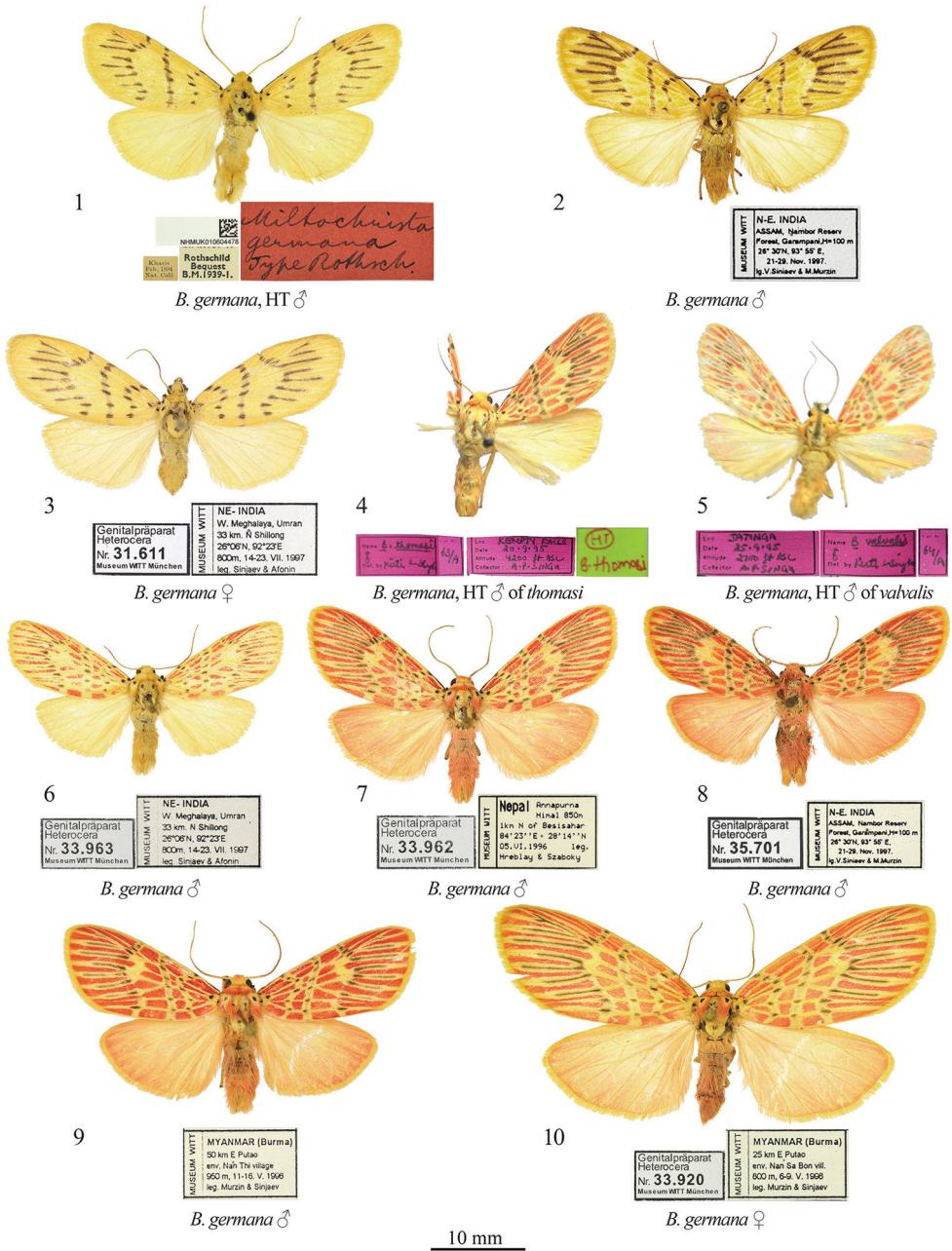
Miltochrista germana Rothschild 1913: 214 (type locality: [India, Meghalaya, the Khasi Hills] “Khasia Hills, Assam”).

Barsine valvalis Kaleka 2003: 97, figs A, 12–19 (type locality: [India] “Assam: North Cachar Hills, Jatinga”), syn. nov.

Barsine thomasi Kaleka 2003: 100, figs B, 25–32 (type locality: [India, Uttarakhand] “Uttar Pradesh: Kempty falls”), syn. nov.

Type material examined. *Holotype* of *Miltochrista germana* (by monotypy) (Fig. 1): male, red handwritten label “*Miltochrista germana* Type Rothsch.” / printed label “Khasis, Feb. 1894, Nat. Coll.” / printed label “Rothschild Bequest B.M. 1939–1.” / printed label with QR-code “NHMUK010604478” (Coll. NHMUK). *Holotype* of *Barsine valvalis* (Figs 5, 24): male, lilac label “Loc. Jatinga | Date 25.9.95 | Altitude 2700 ft. A.S.L. | Collector A.P. Singh” / lilac label “64/ A” / lilac label “Name *B. valvalis* | ♂ | Det. by Kirti & Singh”, gen. prep. by H.S. Datta (Coll. NZCZSI). *Holotype* of *Barsine thomasi* (Figs 4, 23): male, lilac label “Loc. Kempty Falls | Date 20.9.95 | Altitude 4200 ft. A.S.L. | Collector A.P. Singh” / lilac label “63/ A” / lilac label “Name *B. thomasi* | ♂ | Det. by Kirti & Singh” / lettuce green label “HT | *B. thomasi*”, gen. prep. by H.S. Datta (Coll. NZCZSI).

Other material examined. **INDIA.** 1 male, Khasis, Oct. 1896, Nat. Coll., slide NHMUK010313291 Volynkin (Coll. NHMUK); 1 female, Khasia Hills, Assam / Rothschild Bequest B.M. 1939–1., slide NHMUK010313292 Volynkin (Coll. NHMUK); 1 female, NE India, W Meghalaya, Garo Hills, Nokrek National Park, 25°40'N, 91°04'E, 1150 m, 2–13.VII.1997, leg. Afonin & Sinyaev (Coll. MWM/ZSM); 28 males, 19 females, NE India, W Meghalaya, Umran, 33 km N Shillong, 26°06'N, 92°23'E, 800 m, 14–23.VII.1997, leg. Sinyaev & Afonin, slides MWM 31610, MWM 33963 (males), MWM 31611 (female) Volynkin (Coll. MWM/ZSM); 21 males, 11 females, NE India, Assam, Nameri Nat. Park, 40 km N Tezpur, 150 m, 27°20'N, 93°15'E, 24.VII–2.VIII.1997, leg. Sinyaev & Murzin, slides MWM 33964 (male), MWM 33965 (female) Volynkin (Coll. MWM/ZSM); 74 males, 12 females, NE India, Assam, Nambor Reserve Forest, Garampani, h = 100 m, 26°30'N, 93°56'E, 21–29.XI.1997, leg. V. Sinyaev & M. Murzin, slides MWM 31612, MWM 31617, MWM 33922, MWM 35701 (males), MWM 31613, MWM 33923, MWM 35703 (females) Volynkin (Coll. MWM/ZSM); 5 males, NE India, Arunachal Pr., Etalin vicinity, 28°36'56"N, 95°53'21"E, 700m, 12–25.V.2012, L. Dembický & O. Šauša leg., slide MWM 35704 Volynkin (Coll. MWM/ZSM); 4 males, [NE India] Assam: Haflong: Jatinga, 01.X.[19]95 (Coll. NZCZSI). **NEPAL:** 21 males, 2 females, Nepal, Annapurna Himal, Geirigan village, 1340 m, 28°20'N, 83°45'E, 25.VI.1996, leg. Gy. M. László & G. Ronkay, slides MWM 33949 (male), MWM 33950 (female) Volynkin



Figures 1–10. *Barsine germana*: adults **1** holotype male, NE India (NHMUK) **2** male, northeastern India (MWM/ZSM) **3** female, northeastern India (MWM/ZSM) **4** Holotype male of *B. thomasi* (NZC-ZSI) **5** holotype male of *B. valvalis* (NZCZSI) **6** male, northeastern India (MWM/ZSM) **7** male, C Nepal (MWM/ZSM) **8** male, northeastern India (MWM/ZSM) **9** male, northern Myanmar (MWM/ZSM) **10** female, northern Myanmar (MWM/ZSM).

(Coll. MWM/ZSM); 6 males, 1 female, Nepal, Annapurna Himal, 1000m, 1 km S of Bahundanda, 28°20'N, 84°25'E, 06.VI.1996, leg. Hreblay & Szaboky (Coll. MWM/ZSM); 1 male, Nepal, Annapurna Himal, Ulleri, 1900 m, 28°23'N, 83°43'E, 3.X.1994, leg. Csorba & Ronkay (Coll. MWM/ZSM); 1 male, Nepal, Annapurna Himal, 850 m, 1 km N of Besisahar, 28°14'N, 84°23'E, 05.VI.1996, leg. Hreblay & Szaboky, slide MWM 33962 Volynkin (Coll. MWM/ZSM). **MYANMAR:** 45 males, 18 females, Myanmar (Burma), 50 km E Putao, env. Nan Thi village, 950 m, 11–16.V.1998, leg. Murzin & Sinyaev, slide MWM 33921 (male) Volynkin (Coll. MWM/ZSM); 53 males, 17 females, Myanmar (Burma), 25 km E Putao, env. Nan Sa Bon village, 800 m, 6–9.V.1998, leg. Murzin & Sinyaev, slides MWM 33919 (male), MWM 33920 (female) Volynkin (Coll. MWM/ZSM); 21 male, 2 females, Myanmar (Burma), 21 km E Putao Nan Sa Bon village 550 m, 1–5.V.1998, leg. Murzin & Sinyaev (Coll. MWM/ZSM).

Remarks. Joshi et al. (2018) considered this species to consist only of yellow-patterned individuals matching the holotype (Figs 1–3). Nonetheless, dissections of similarly patterned red-spotted syntopic specimens (Figs 4–10) revealed these two color forms to be conspecific. The red-patterned form had been described twice before by Kaleka (2003) as *B. thomasi* Kaleka, 2003 (Figs 4, 23) and as *B. valvalis* Kaleka, 2003 (Figs 5, 24). These names are therefore synonymized here with *B. germana*.

The holotype of *B. germana* is undissected. However, the senior author has microscopically examined the tips of its valvae, which have the distal saccular process structure identical to those in the holotypes of *B. valvalis* and *B. thomasi*. The holotype is also externally similar to specimens from the same region of India, and clearly different from *B. kirata*, sp. nov. A detailed comparison of *B. germana* with *B. kirata* sp. nov. is provided below.

Barsine germana varies considerably in its size: the forewing length is 13–17 mm in males and 16–23 mm in females.

Distribution. Northern (Uttarakhand) and northeastern India (Meghalaya, Assam, Arunachal Pradesh) (Rothschild 1913; Kaleka 2003; Joshi et al. 2018), eastern Nepal, and northern Myanmar (Kachin state).

***Barsine kirata* Volynkin & N. Singh, sp. nov.**

<http://zoobank.org/487A79AB-5ACC-44D7-BDE8-DBB8187FFB41>

Figs 11–18, 25–28, 31, 32

Type material. Holotype (Figs 11, 25): male, “N-E. India, Assam, Nambor Reserv[e] Forest, Garampani, H = 100 m, 26°20'N, 93°55'E, 21–20. Nov. [IX] 1997, leg. V. Siniaev & M. Murzin”, slide MWM 35702 Volynkin (Coll. MWM/ZSM).

Paratypes. **INDIA:** 1 male, same data as in the holotype (Coll. MWM/ZSM); 6 males, India, Andhra Pradesh, Visakhapatnam, Paderu, 08.IX.2018, leg. Navneet Singh & Party, gen. preps by H.S. Datta (Coll. NZCZSI); **NEPAL:** 1 male, Nepal, Tana-



11

Genitalpräparat
Heterocera
Nr. 35.702
Museum WITT München

MUSEUM WITT
N-E. INDIA
ASSAM, Karatoli Reserve
Forest, Garapani, H=100 m
26.30'N, 93.55' E
21-29. Nov. 1987
Dr. V. Srinivas & M. Murzin

B. kirata sp. n., HT ♂



12

Genitalpräparat
Heterocera
Nr. 33.918
Museum WITT München

MUSEUM WITT
NEPAL, Ganesh Himal
valley of Trisuli River
2km. S. of Betrawati
930m., 25-IX-1995, leg.
L. Németh

B. kirata sp. n., PT ♂



13

Genitalpräparat
Heterocera
Nr. 33.937
Museum WITT München

NEPAL, valley of Ta-
mea Kosi River, 5km.
S. of Piguti, 950m., 8/9-
X-1995, leg.: L. Németh

B. kirata sp. n., PT ♂



14

Genitalpräparat
Heterocera
Nr. 33.938
Museum WITT München

NEPAL, valley of Ta-
mea Kosi River, 1km.
N of Dolakha, 1700m.
12-X-1995, leg.: L. Né-
meth

B. kirata sp. n., PT ♀



15

Genitalpräparat
Heterocera
Nr. 33.943
Museum WITT München

NEPAL, Lapchi Kang Range
1 km S of Chitre (Signal)
1200m (86°10' E, 27°42' N)
08.09.1995, leg. Chenga Sherpa
MUSEUM WITT

B. kirata sp. n., PT ♂



16

Genitalpräparat
Heterocera
Nr. 33.944
Museum WITT München

NEPAL, Lapchi Kang Range
1 km S of Chitre (Signal)
1200m (86°10' E, 27°42' N)
08.09.1995, leg. Chenga Sherpa
MUSEUM WITT

B. kirata sp. n., PT ♀



17

INDIA, Andhra Pradesh
Loc. Visakhapatnam,
Padara
Date: 8. ix. 2018
Coll. Navneet Singh &
Fany

B. kirata sp. n., PT ♂



18

INDIA, Andhra Pradesh
Loc. Visakhapatnam,
Padara
Date: 8. ix. 2018
Coll. Navneet Singh &
Fany

B. kirata sp. n., PT ♂



19

INDIA, Andhra Pradesh
Loc. Visakhapatnam,
Padara
Date: 8. ix. 2018
Coll. Navneet Singh &
Fany

B. defecta ♂



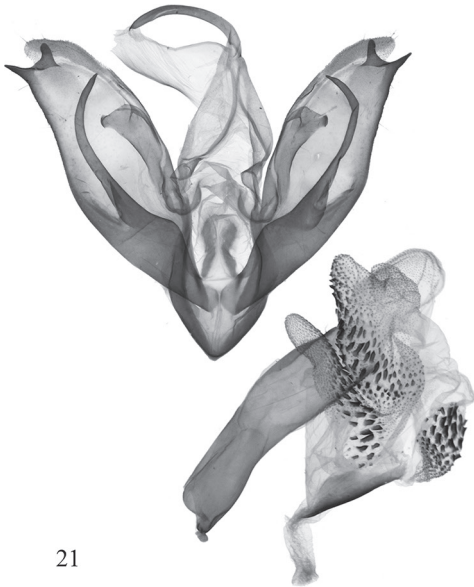
20

INDIA, Karnataka
Kumthala, Kerala
Bhim Tal 1500m
Srinagar, Mysore
coll. Dr. H. Tomlin
Museum WITT München
23. 8. 74

B. defecta ♂

10 mm

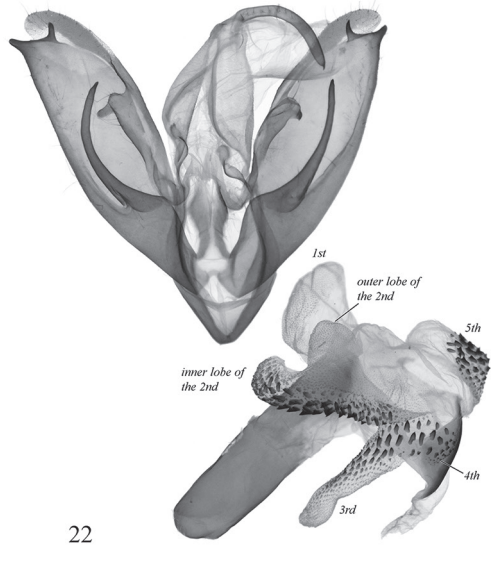
Figures 11–20. *Barsine* spp.: adults 11–18 *B. kirata* sp. nov. 11 holotype male, northeastern India (MWM/ZSM) 12 paratype male, Nepal (MWM/ZSM) 13 paratype male, Nepal (MWM/ZSM) 14 paratype female, Nepal (MWM/ZSM) 15 paratype male, Nepal (MWM/ZSM) 16 paratype female, Nepal (MWM/ZSM) 17 paratype male, southeastern India (NZCZSI) 18 paratype male, southeastern India (NZCZSI) 19, 20 *B. defecta*: 19 male, N India (MWM/ZSM) 20 male, N India (MWM/ZSM).



21

B. germana

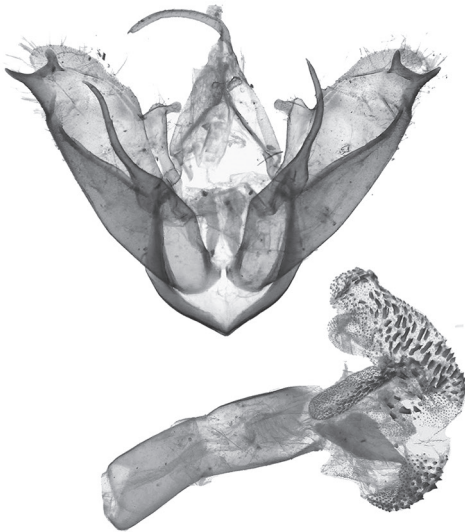
NE India, Assam, Nameri, slide MWM 33964



22

B. germana

Nepal, Annapurna Himal, slide MWM 33962



23

B. germana*, HT of *thomasi

N India, Uttarakhand, Kempty Falls, gen. prep. H.S. Datta



24

B. germana*, HT of *valvalis

NE India, Assam, Jatinga, gen. prep. H.S. Datta

Figures 21–24. *Barsine germana*: male genitalia **21** northeastern India, slide MWM 33964 Volynkin **22** Nepal, slide MWM 33962 Volynkin **23** holotype of *B. thomasi*, northern India, prep. H.S. Datta **24** holotype of *B. valvalis*, northeastern India, prep. H.S. Datta.

houn distr., Baisakhe Ghat, 10 km W Duleguunda, 630 m, 10.X.1994, leg. Csorba & Ronkay, slide MWM 33961 Volynkin (Coll. MWM/ZSM); 2 females, Nepal, valley of Tamea Kosi River, 1 km N of Dolakha, 1700 m, 12.X.1995, leg. L. Németh, slide MWM 33938 Volynkin (Coll. MWM/ZSM); 1 male, Nepal, valley of Tamea Kosi River, 5 km S of Piguti, 950m, 8/9.X.1995, leg.: L. Németh, slide MWM 33937 Volynkin (Coll. MWM/ZSM); 2 males, 19 females, Nepal, Lapchi Kang Range, 1 km S of Chitre (Signati), 1200m, (27°42'N, 86°10'E), 08.09.1995, leg. Chenga Sherpa, Museum Witt, slides MWM 33943 (male), MWM 33944 (female) Volynkin (Coll. MWM/ZSM); 3 males, 5 females, Nepal, Tanahoun distr., Bimalnager village, 530 m, 12.X.1994, leg. Csorba & Ronkay (Coll. MWM/ZSM); 7 males, 1 female, Nepal, Ganesh Himal, valley of Trisuli River, 2 km S of Betrawati, 930 m, 25.IX.1995, leg. L. Németh, slide MWM 33918 (male) Volynkin (Coll. MWM/ZSM); 2 males, Nepal, Ganesh Himal, 1040 m, Mailung Khola, ca 20 km NE Trisuli, 28°04'5"N, 85°12'5"E, 24.IX.1995, leg. B. Herczig & Gy. M. László (Coll. MWM/ZSM); 1 male, Nepal, Royal Chitwan National Park, Island Jungle Resort, 240 m, 21–23.VI.1993, leg. M. Hreblay, G. Csorba (Coll. MWM/ZSM).

Remarks. Kirti and Singh (2016) erroneously recorded this species from India as *B. orientalis bigamica* Černý, 2009. Like *B. germana*, *B. kirata* sp. nov. is dimorphic, but the yellow form (Figs 17, 18) is rare, and, so far, known only from the state of Andhra Pradesh (southeast India).

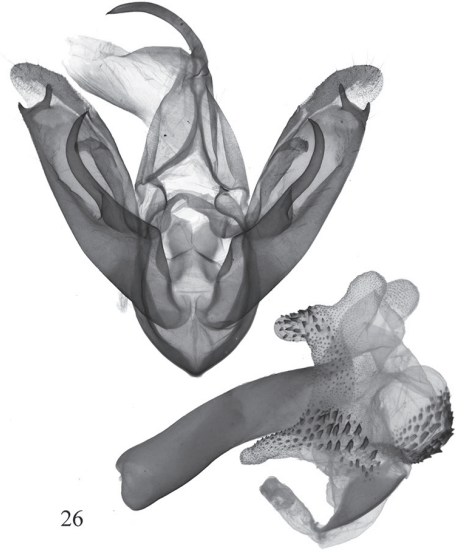
Diagnosis. The new species (Figs 11–18) is very similar externally to *B. germana* (Figs 1–10) and can be distinguished from it by its less wavy antemedial transverse line. The male genital capsule of the new species (Figs 25–28) differs clearly from that of *B. germana* (Figs 21–24) by the distal ventral process of the valva having a short distal lobe directed dorso-distally and the longer dorsal lobe dorsally directed, while in *B. germana* the distal lobe is more elongated and distally directed and the dorsal lobe is dorso-distally directed. Additionally, in *B. kirata* sp. nov. the juxta is broader than that of *B. germana*, the basal saccular process is stouter and more curved, the distal lobe of valva is larger, and the distal part of the distal ventral process of valva is more robust. The vesica of *B. kirata* sp. nov. differs from that of *B. germana* by its slightly narrower 1st medial diverticulum, the smaller cornuti on the 2nd medial diverticulum, and the slightly less elongated 3rd medial diverticulum. The female genitalia of the new species (Figs 31, 32) clearly differ from those of *B. germana* (29, 30) by the significantly shorter ductus bursae with shorter subostial folds, the wrinkled posterior sclerotised section of corpus bursae, the slightly smaller signum, the presence of the second, band-like signum in the anterior section of corpus bursae (absent in *B. germana*), and the slightly smaller lateral membranous protrusion of the corpus bursae.

Description. External morphology of adults (Figs 11–18). Wingspan 14.5–16 mm in males (15 mm in holotype) and 18–20 mm in females. Male antennae ciliate, female antennae filiform, pale ochreous in both sexes. Head crimson with yellow spot on frons. Thorax yellow, with three black dots; collar and tegulae yellow with crimson margins. Forewing broad with slightly elongated and rounded apex. Forewing ground colour yellow, with a pattern of black dots and strokes and various-



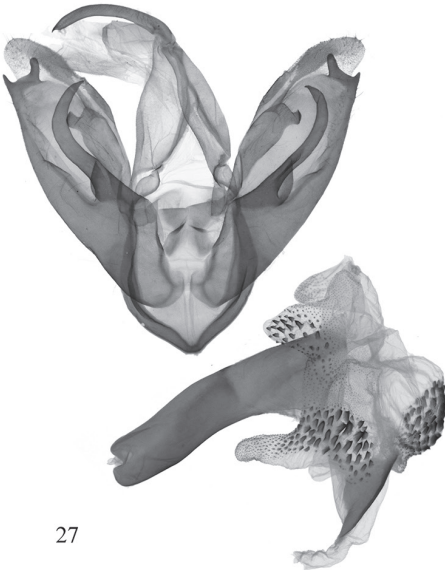
25

B. kirata sp. n., HT
NE India, Assam, Nambor, slide MWM 35702



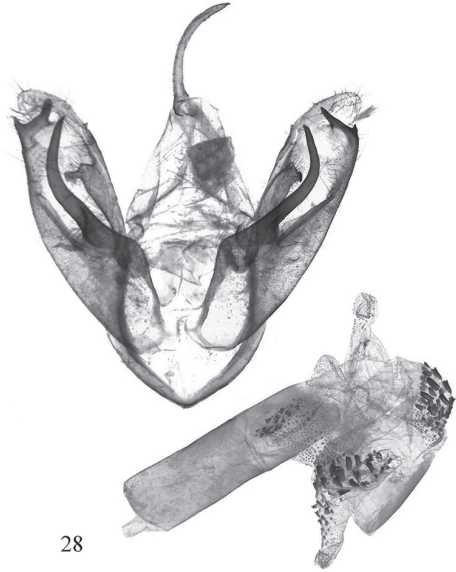
26

B. kirata sp. n., PT
E Nepal, Tamea Kosi River vall., slide MWM 33937



27

B. kirata sp. n., PT
north of C Nepal, Ganesh Himal, slide MWM 33918

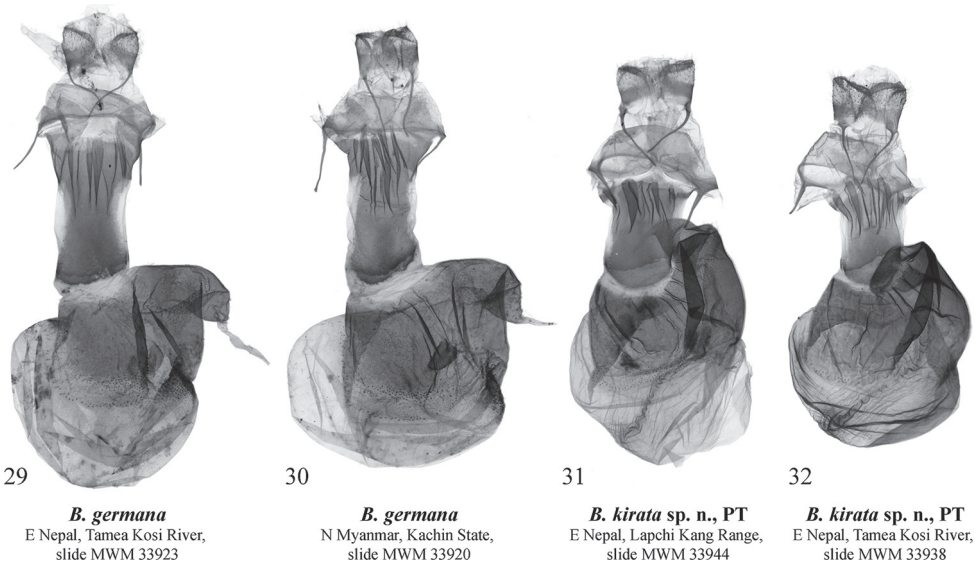


28

B. kirata sp. n., PT
SE India, Andhra Pradesh, Visakhapatnam, prep. H.S. Datta

Figures 25–28. *Barsine kirata* sp. nov., male genitalia **25** holotype, northeastern India, slide MWM 35702 Volynkin **26** paratype, eastern Nepal, slide MWM 33937 Volynkin **27** paratype, central Nepal, slide MWM 33918 Volynkin **28** paratype, southeastern India, prep. H.S. Datta.

shaped crimson spots and strokes between veins; costa between base and antemedial line black; basal spot very small, black; subbasal spot black, round; antemedial line W-like wavy, black, interrupted into a series of variously shaped, small spots on veins;



Figures 29–32. *Barsine* spp.: female genitalia **29** *B. germana*, Nepal, slide MWM 33923 Volyntin **30** *B. germana*, northern Myanmar, slide MWM 33920 Volyntin **31** *B. kirata* sp. nov., paratype, Nepal, slide MWM 33944 Volyntin **32** *B. kirata* sp. nov., paratype, Nepal, slide MWM 33938 Volyntin.

medial line almost straight, angled inwards at costa, interrupted into a series of variously shaped small spots on veins; postmedial line smoothly curved outwards medially, presented as a series of black thin strokes of different lengths between veins; cilia amber yellow. Hindwing pale pink with yellowish suffusion along veins; cilia amber yellow along outer margin and apex, and pink along anal margin. Yellow form of species lacks all reddish pattern elements. Abdomen pink with admixture of yellow scales. **Male genitalia** (Figs 25–28). Tegumen moderately broad, shorter than valva; vinculum short but robust, V-shaped with convex lateral margins. Valva massive, with almost parallel margins; medial costal process broadly trigonal, with convex outer margin and slightly broadened and blunted tip; distal costal process very small, tubercle-shaped; distal lobe of valva large, oblique; sacculus broad, its basal process robust, broad, curved dorsally, apically rounded, reaches the distal costal process; distal ventral process broad, bilobate, its dorsal lobe approximately two 2 times longer than distal lobe, narrow, apically blunted, directed dorsally; distal lobe short, thorn-shaped, directed dorso-distally. Uncus narrow, laterally flattened, curved, medially broadened, with claw-like tip; tuba analis broad. Scaphium narrow, weakly sclerotized. Juxta weakly sclerotized, X-shaped, with broader apical lobes. Aedeagus elongated, narrow, slightly curved medially and broadened distally. Vesica membranous, short and broad, with several diverticula: 1st medial diverticulum elongated, sack-like with rounded tip, its distal half weakly granulated; 2nd medial diverticulum bilobate, its inner lobe covered with numerous variously sized short but robust cornuti, outer lobe weakly granulated; 3rd medial diverticulum long, covered with numerous vari-

ously sized short but robust trigonal cornuti; 4th medial diverticulum small, globular, covered with small trigonal cornuti; 5th medial diverticulum broadly globular, its outer surface with broad cluster of small, trigonal cornuti of various sizes; basal diverticulum absent; distal plate of vesica broad, trigonal with slightly convex outer margin, heavily sclerotized. **Female genitalia** (Figs 31, 32). Ostium bursae broad. Ductus bursae dorso-ventrally flattened, sclerotized, its lateral margins more weakly sclerotized than medial part; posterior section of ductus bursae slightly broadened, with several narrow longitudinal subostial folds. Corpus bursae broad, sac-like, with posterior section moderately sclerotized with wrinkled posterior margin ventrally, and reniform signum dorsally; border between posterior and anterior sections of corpus bursae weakly sclerotized, with a band of short scobination; anterior section of corpus bursae thick and membranous, with a band-like signum surrounded by a rugose area. Appendix bursae weakly sclerotized and granulated, short, conical, situated postero-laterally, directed posteriorly and curved inwards. Apophyses long and thin, apophyses posteriores thinner and ca 1.8 times longer than apophyses anteriores. Papillae anales broad, trapezoidal, weakly setose.

Distribution. The new species is known from northeastern India (Sikkim, Darjeeling, and Assam) (Kirti and Singh 2016, as *B. orientalis bigamica*), southeastern India, and Nepal (present study).

Etymology. The Kirata are the people inhabiting the Himalayas and northeastern India.

Acknowledgements

We express our sincere thanks to the following colleagues for their kind assistance provided during senior author's studies at their institutions: Dr Axel Hausmann, Dr Wolfgang Speidel and Mr Ulf Buchsbaum (ZSM, Munich, Germany); Dr Thomas J. Witt (†) (MWM/ZSM, Munich, Germany); Dr Alberto Zilli and Mr Geoff Martin (NHMUK); and Dr Marianne Espeland (ZFMK). Second, third, and fourth authors thank the Director of the Zoological Survey of India and Head of the Department of Zoology and Environmental Sciences for providing necessary facilities.

References

- Bayarsaikhan U, Lee DJ, Bae YS (2018) A review of *Barsine* Walker, 1854 (Lepidoptera: Erebiidae, Arctiinae) in Cambodia, with a new record. *Journal of Asia-Pacific Biodiversity* 11(3): 377–385. <https://doi.org/10.1016/j.japb.2018.05.003>
- Bucsek K (2012) Erebiidae, Arctiinae (Lithosiini, Arctiini) of Malaya Peninsula-Malaysia. Institute of Zoology SAS, Bratislava, 170 pp.
- Bucsek K (2014) Erebiidae, Arctiinae (Lithosiini, Arctiini) of Malaya Peninsula-Malaysia (Supplementum). Institute of Zoology SAS, Bratislava, 45 pp.

- Černý K (2016) A contribution to the knowledge of the *Miltochrista-Lyclene* genus group in South East Asia (Lepidoptera, Erebidae, Arctiinae, Lithosiini). *Nachrichten des Entomologischen Vereins Apollo*, N.F. 37(2/3): 93–107.
- Černý K, Pinratana A (2009) Moths of Thailand (Vol. 6). Arctiidae. Brothers of Saint Gabriel in Thailand, Bangkok, 283 pp.
- Dubatolov VV, Kishida Y, Min W (2012) New records of lichen-moth from the Nanling Mts., Guangdong, South China, with descriptions of new genera and species (Lepidoptera, Arctiidae: Lithosiinae). *Tinea* 22(1): 25–52.
- Dubatolov VV, Bucsek K (2013) New species of lichen-moths from South-East Asia (Lepidoptera, Noctuoidea, Lithosiini). *Tinea* 22(4): 279–291.
- Fibiger M (1997) Noctuidae III. Noctuidae Europaeae (Vol. 3). Entomological Press, Sorø, 418 pp.
- Joannis Jde (1930) Lépidoptères hétérocères du Tonkin. 3e partie. *Annales de la Société entomologique de France* 99 (Supplément): 559–835.
- Holloway JD (2001) The Moths of Borneo: Family Arctiidae, Subfamily Lithosiinae. *Malayan Nature Journal* 7: 279–486.
- Huang SY, Ji SQ, Wang M, Fan XL (2018) *Barsine paraprominens* sp. nov. (Lepidoptera, Erebidae, Arctiinae, Lithosiini) from China, with notes on four new records. *Zootaxa* 4457(1): 189–196. <https://doi.org/10.11646/zootaxa.4457.1.11>
- Huang SY, Volynkin AV, Černý K, Wang M, Fan XL (2019) Contribution to the knowledge on the genus *Barsine* Walker, 1854 from mainland China and Indochina, with description of a new species (Lepidoptera, Erebidae, Arctiinae, Lithosiini). *Zootaxa* 4711(3): 495–516. <https://doi.org/10.11646/zootaxa.4711.3.4>
- Joshi R, Singh N, Volynkin AV (2018) New data on the genus *Barsine* Walker, 1854 from India, with description of a new species (Lepidoptera: Erebidae: Arctiinae: Lithosiini). *Zootaxa* 4425(3): 456–470. <https://doi.org/10.11646/zootaxa.4425.3.2>
- Kaleka APS (2003) Revival of genus *Barsine* Walker (Lithosiinae: Arctiidae: Lepidoptera) along with description of two new species from India. *Journal of Entomological Research* 27(2): 93–103.
- Kaleka APS (2018) Further studies on genus *Barsine* Walker (Arctiidae: Lepidoptera) along with addition of two species from India. *Journal of Entomological Research* 42(4): 595–600. <https://doi.org/10.5958/0974-4576.2018.00101.9>
- Kirti JS, Singh N (2015) Arctiid Moths of India (Vol. 1). Nature Books India, New Delhi, 205 pp.
- Kirti JS, Singh N (2016) Arctiid Moths of India (Vol. 2). Nature Books India, New Delhi, 225 pp.
- Lafontaine JD, Mikkola K (1987) Lock-and-key system in the inner genitalia of Noctuidae (Lepidoptera) as taxonomic character. *Entomologiske Meddelelser* 55: 161–167.
- Reich P (1937) Die Arctiidae der Chinaausbeute des Herrn Hermann Höne in Shanghai. *Deutsche entomologische Zeitschrift Iris* 51: 113–130.
- Rothschild W (1913) New Lithosianae. *Novitates Zoologicae* 20(1): 192–226.
- Spitsyn VM, Kondakov AV, Tomilova AA, Pham NT, Bolotov IN (2018) *Barsine vinhphucensis* sp. nov. from Vietnam (Lepidoptera: Erebidae: Arctiinae: Lithosiini). *Ecologica Montenegro* 18: 18–25. <https://doi.org/10.37828/em.2018.18.3>
- Volynkin AV (2018) Four new species of the genus *Barsine* Walker, 1854 (Lepidoptera, Erebidae, Arctiinae) from Oriental Region. *Far Eastern Entomologist* 358: 1–18. <https://doi.org/10.25221/fee.358.1>

- Volynkin AV, Černý K (2016a) *Barsine amaculata*, a new species from Vietnam (Lepidoptera, Erebidae, Arctiinae). *Zootaxa* 4200(2): 345–350. <https://doi.org/10.11646/zootaxa.4200.2.11>
- Volynkin AV, Černý K (2016b) A review of the *Barsine flammealis* species-complex with description of a new species from Himalaya (Lepidoptera, Erebidae, Arctiinae). *Biological Bulletin of Bogdan Chmelniński Melitopol State Pedagogical University* 6(3): 303–310. <https://doi.org/10.15421/201699>
- Volynkin AV, Černý K (2016c) *Barsine deliciosa*, a new species from China (Lepidoptera, Erebidae, Arctiinae). *Zootaxa* 4200(1): 181–191. <https://doi.org/10.11646/zootaxa.4200.1.9>
- Volynkin AV, Černý K (2017a) A review of the *Barsine obsoleta* species-group with description of a new species from Vietnam. *Zootaxa* 4254(2): 188–200. <https://doi.org/10.11646/zootaxa.4254.2.2>
- Volynkin AV, Černý K (2017b) On the taxonomy of the *Barsine delineata* species-complex (Lepidoptera, Erebidae, Arctiinae). *Zootaxa* 4258(2): 138–144. <https://doi.org/10.11646/zootaxa.4258.2.3>
- Volynkin AV, Černý K (2017c) Revision of the *Barsine cardinalis-anomala* ‘species-complex’ (Lepidoptera, Erebidae, Arctiinae). *Zootaxa* 4358(3): 441–461. <https://doi.org/10.11646/zootaxa.4358.3.3>
- Volynkin AV, Černý K (2017d) On the taxonomy of the genus *Barsine* Walker, 1854 (Lepidoptera, Erebidae, Arctiinae). *Far Eastern Entomologist* 346: 17–32. <https://doi.org/10.25221/fee.346.3>
- Volynkin AV, Černý K (2018a) Revision of the *Barsine zebrina* species-complex, with description of three new species (Lepidoptera, Erebidae, Arctiinae, Lithosiini). *Zootaxa* 4402(2): 339–352. <https://doi.org/10.11646/zootaxa.4402.2.6>
- Volynkin AV, Černý K (2018b) Two new dark colored species of the genus *Barsine* Walker, 1854 from China and Indochina (Lepidoptera, Erebidae, Arctiinae, Lithosiini). *Ecologica Montenegrina* 19: 61–68. <https://doi.org/10.37828/em.2018.19.7>
- Volynkin AV, Černý K (2019) A review of the *Barsine inflexa* Moore, 1878 and the *B. flavodiscalis* (Talbot, 1926) species-groups, with descriptions of six new species from Indochina, India and China (Lepidoptera, Erebidae, Arctiinae). *Zootaxa* 4668(4): 543–561. <https://doi.org/10.11646/zootaxa.4668.4.7>
- Volynkin AV, Černý K, Ivanova MS (2018) Revision of the *Barsine punicea* Moore, 1878 species-group, with descriptions of two new species and two new subspecies (Lepidoptera, Erebidae, Arctiinae). *Journal of Asia-Pacific Entomology* 21: 999–1008. <https://doi.org/10.1016/j.aspen.2018.07.020>
- Volynkin AV, Černý K, Huang SY (2019a) A review of the *Barsine hypoprepioides* (Walker, 1862) species-group, with descriptions of fifteen new species and a new subspecies (Lepidoptera, Erebidae, Arctiinae). *Zootaxa* 4618(1): 1–82. <https://doi.org/10.11646/zootaxa.4618.1.1>
- Volynkin AV, Černý K, Huang SY (2019b) A review of the *Barsine perpallida*-*B. yuennanensis* species-group, with descriptions of six new species (Lepidoptera: Erebidae: Arctiinae). *Acta Entomologica Musei Nationalis Pragae* 59(1): 273–293. <https://doi.org/10.2478/aemnp-2019-0022>
- Volynkin AV, Huang SY, Dubatolov VV, Kishida Y (2019c) *Barsine wangi*, a new species from Guangdong, southern China (Lepidoptera, Erebidae, Arctiinae). *Zootaxa* 4664(3): 445–450. <https://doi.org/10.11646/zootaxa.4664.3.12>

- Volynkin AV, Černý K, Im KH, Bae YS, Bayarsaikhan U (2019d) *Barsine insolita*, a new species from Indochina and India (Lepidoptera, Erebidae, Arctiinae). *Zootaxa* 4700(4): 494–500. <https://doi.org/10.11646/zootaxa.4700.4.8>
- Volynkin AV, Huang SY, Ivanova MS (2019e) An overview of genera and subgenera of the *Asura* / *Miltochrista* generic complex (Lepidoptera, Erebidae, Arctiinae). Part 1. *Barsine* Walker, 1854 sensu lato, *Asura* Walker, 1854 and related genera, with descriptions of twenty new genera, ten new subgenera and a check list of taxa of the *Asura/Miltochrista* generic complex. *Ecologica Montenegrina* 26: 14–92. <https://doi.org/10.37828/em.2019.26.3>
- Walker F (1854) List of the Specimens of Lepidopterous Insects in the Collection of the British Museum. Part I.—Lepidoptera Heterocera. The Trustees of the British Museum, London, 278 pp. <https://doi.org/10.5962/bhl.title.58221>
- Wu Sh, Fu Ch M, Chang W Ch, Shih L Ch (2013) Arctiinae. In: Fu CM, Ronkay L, Lin HH (Eds) Moths of Hehuanshan. Endemic Species Research Institute, Nantou, 308–333.

A conservation checklist of the herpetofauna of Morelos, with comparisons with adjoining states

Julio A. Lemos-Espinal¹, Geoffrey R. Smith²

1 *Laboratorio de Ecología-UBIPRO, FES Iztacala UNAM, Avenida los Barrios 1, Los Reyes Iztacala, Tlalnepantla, edo. de México, 54090, México* **2** *Department of Biology, Denison University, Granville, Ohio 43023, USA*

Corresponding author: Julio A. Lemos-Espinal (lemos@unam.mx)

Academic editor: A. Herrel | Received 12 March 2020 | Accepted 2 May 2020 | Published 16 June 2020

<http://zoobank.org/8B313148-40DC-4DD5-AB8D-206A45727041>

Citation: Lemos-Espinal JA, Smith GR (2020) A conservation checklist of the herpetofauna of Morelos, with comparisons with adjoining states. *ZooKeys* 941: 121–144. <https://doi.org/10.3897/zookeys.941.52011>

Abstract

Despite being one of the smallest states in Mexico, the high diversity of habitats in Morelos has led to the development of a rich biota made up of a mixture of species typical of the Neovolcanic Axis and the Sierra Madre del Sur. However, recent expansion of cities in Morelos is likely to have consequences for the state's herpetofauna. Here a checklist of the amphibians and reptiles of Morelos is provided with a summary of their conservation status and overlap with its neighboring states. Morelos is home to 139 species of amphibians and reptiles representing 32 families and 75 genera. Twenty-six of the 38 species of amphibians and 70 of the 101 species of reptiles that inhabit Morelos are endemic to Mexico. Fourteen species of amphibians and reptiles from Morelos are IUCN listed (i.e., Vulnerable, Near Threatened, or Endangered), 22 are placed in a protected category by SEMARNAT, and 41 are categorized as high risk by the EVS. The Tropical Deciduous Forest vegetation type hosts the greatest number of amphibian and reptile species in Morelos (84 species). Morelos shares the largest proportion of its herpetofauna with the State of Mexico (79.3%), Puebla (77.0%), and Guerrero (74.8%).

Keywords

amphibians, frogs, lizards, reptiles, salamanders, snakes, turtles

Introduction

Morelos is one of the smallest states in Mexico; however, its high diversity of habitats has led to the development of a rich biota represented by a mixture of species typical of the Neovolcanic Axis and the Sierra Madre del Sur. The contrast in the habitat found in Morelos can be seen by the altitudinal gradient that occurs in its 4,961 km² where altitude reaches a maximum of 5,380 m on the Popocatepetl Volcano, and a minimum of 800 m in the Río Amacuzac (INEGI 2017). In addition, Cuernavaca, the state capital located in northwestern Morelos, is known as the city of eternal spring for its pleasant and benign climate with little variation between seasons. This condition is not exclusive to Cuernavaca but prevails in most of the state, due to this and the proximity of Morelos to the metropolitan area of Mexico City, Morelos has become one of the favorite places for inhabitants of the Mexico City to spend weekends or vacations. This has also led to the growth of cities such as Cuernavaca, Jiutepec, Temixco, and Cuautla. As in other states, this population growth results in environmental degradation, including the clearing of forests, garbage generation, air and water pollution, and fragmentation of natural habitats. For example, in the dry forest of Morelos, the effects of grazing and timber harvesting have had significant effects on the vegetation of this habitat type resulting in fewer trees and a change in the herbaceous layer (de la O-Toris et al. 2012). In addition, many of the tropical dry forests and deciduous forests of Morelos are being lost to deforestation (García-Estrada et al. 2002; Navar et al. 2010). Indeed one study estimated that 60% of the original vegetation in Morelos had been removed by 1990 and only 19% was forested (Trejo and Dirzo 2000); however, the rate of deforestation appears to have slowed but not stopped, yet the forests have not recovered (Sotello-Caro et al. 2015). Such deforestation has increased habitat fragmentation with negative consequences for vertebrates (García-Estrada et al. 2002). Such changes in Morelos are likely to have consequences for the state's fauna, including the amphibians and reptiles. It would be useful to develop an up-to-date inventory of such species as well as their conservation status as a first effort to understanding how to conserve and manage these species. Here we provide an up-to-date checklist of the amphibians and reptiles of Morelos and summarize their conservation status and overlap with species in its neighboring states.

Physiographic characteristics of the state

Morelos has an area of 4,961 km² which represents only 0.2% of the total area of Mexico. Morelos is located in central-southern Mexico, between 19°07'54"N and 18°19'56"N and -98°37'58"W and -99°29'39"W. It is bordered by the State of Mexico and Mexico City to the north, Puebla to the east and southeast, Guerrero to the south and southwest, and the State of Mexico to the west (Fig. 1; INEGI 2017).

Morelos contains portions of two physiographic provinces: the Neovolcanic Axis with one subprovince (Lagos y Volcanes de Anáhuac) and the Sierra Madre del Sur



Figure 1. Map of Mexico with the state of Morelos shown in red (modified from INEGI, 2018).

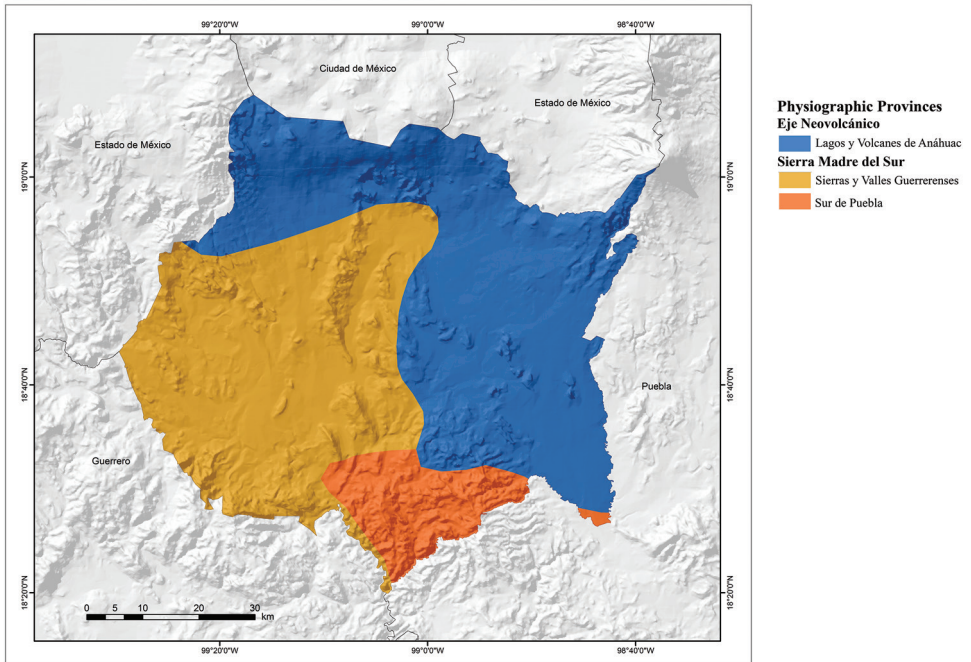


Figure 2. Physiographic provinces of the state of Morelos, Mexico (modified from Cervantes-Zamora et al. 1990).

with two subprovinces (Sierras y Valles Guerrerenses and Sur de Puebla) (Fig. 2). The Neovolcanic Axis covers most of the state, from north to southeast, and the Sierra Madre del Sur covers the central and southwestern parts of the state (INEGI 2017). However, according to Aguilar (1990) the geological and physiographic characteristics of the northern part of Morelos are different from the plains of the east, so they should not be seen as the same province, and the southwestern part of the state is also not located within the Sierra Madre del Sur, but rather within the Balsas Basin. Thus, Morelos can be considered to include the physiographic provinces of the Neovolcanic Axis in the northern part of the state above 1,600 m asl, and the Balsas Basin found in the central and southern parts of the state (Contreras-MacBeath et al. 2006a).

According to Monroy and Colin (1991), Morelos is divided into three ecological regions: the mountainous region of the north, the intermontane valley, and the mountainous region of the south (Fig. 3). The mountainous region of the north is characterized by temperate forest, both pine and oak, and some broadleaved associations. This region is found in the Neovolcanic Axis province. The intermontane valley is located in the central part of the state. Its natural resources have suffered a serious qualitative

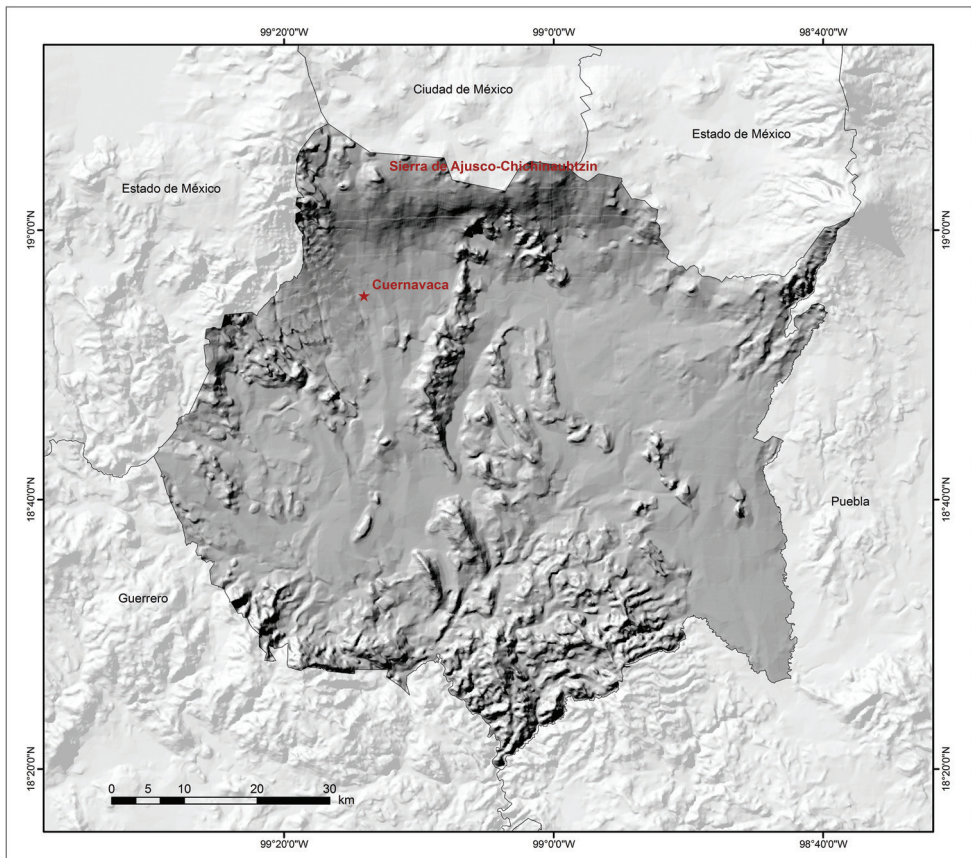


Figure 3. Topographical map of the state of Morelos, Mexico (INEGI 2009).

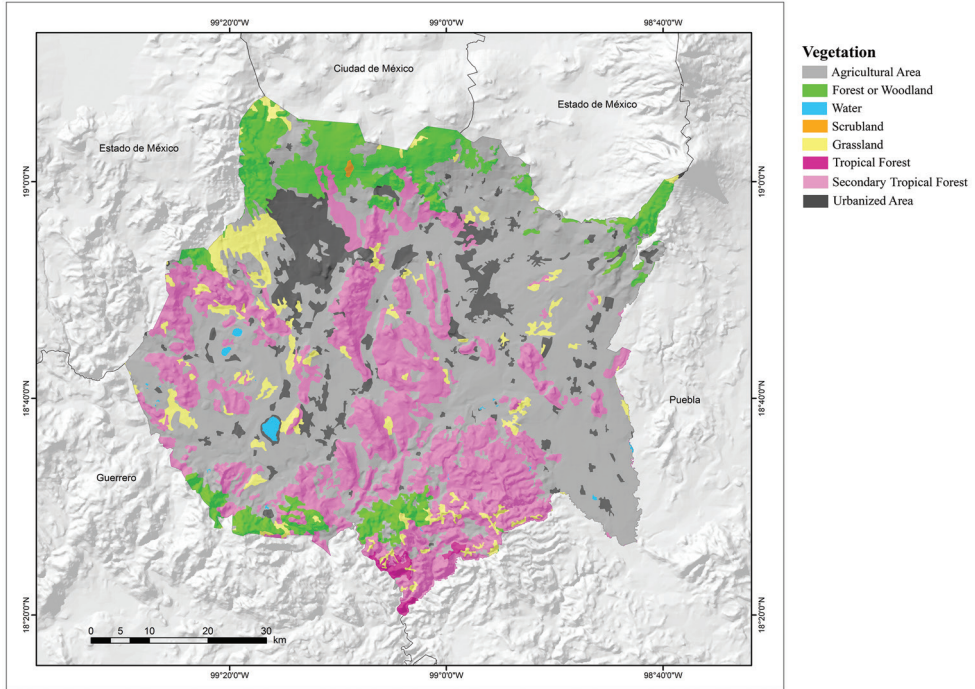


Figure 4. Vegetation map of the state of Morelos, Mexico (modified from Dirección General de Geografía – INEGI 2013).

and quantitative decline due to the expansion of urban areas on the one hand and by pollution of the soil, water, and air on the other. In this region, most of the agricultural crops produced in the state are cultivated, although some patches of disturbed tropical deciduous forest can also be found here. The mountainous region of the south is in the Balsas Basin province, and is characterized by tropical deciduous forest, still preserved in some parts of the state (Contreras-MacBeath et al. 2006b).

The vegetation of Morelos is a product of the great heterogeneity of environmental conditions present in the state, and so it hosts a wide variety of vegetation types that for the purpose of this paper can be divided into three types, in addition to agricultural areas and areas devoid of vegetation (Fig. 4; INEGI 2017). These vegetation types are: Forests or Woodland (Oak, Pine-oak, Pine, and *Abies* Forests), Tropical Deciduous Forest, and Grasslands. The Woodlands can be divided in Coniferous Forest and Oak Forest. The Coniferous Forest is the most important of the forested areas that occupy the high elevations of the Neovolcanic Axis, mainly between 1,500 and 4,000 m a.s.l. This is a more or less dense community formed by a tree stratum that varies from 8 to 35 m high, with a broad floristic representation in the herbaceous and shrubby strata. This type of vegetation includes the following communities: a) pine-oak forest, b) pine forest, and c) *Abies* forest. The Oak Forest is distributed in the northern, southern, and southwestern parts of the state. Woodlands cover 11.45% of the total surface of

Morelos (INEGI 2017). The Tropical Deciduous Forest develops in warm and semi-warm sub-humid climates. The largest area of this vegetation type is in the mountains of central and southern Morelos, between 900 and 1,600 m a.s.l. It is characterized by trees that lose their leaves almost completely during the dry season, between December and June, and produce their foliage and flowers in the rainy season. Tropical Deciduous Forest covers 27.61% of the total area of Morelos (INEGI 2017). The Grasslands are distributed in small areas, mainly in warm and subhumid semi-warm climates. They are located in flat areas or rolling hills. Alpine grassland is distributed in the highest mountain areas in northern Morelos, generally above 3,500 m a.s.l. (Contreras-MacBeath et al. 2006b). In Morelos Grasslands cover 4.29% of the surface area. The remaining 56.58% of the surface territory of Morelos is covered by agricultural areas and areas devoid of vegetation (INEGI 2017).

Several climates (based on the classification of Köppen modified by García 1998) are found in Morelos (Fig. 5). Cold subhumid occurs in the highest parts of the Popocatepetl Volcano and to the northeast along the border with the State of Mexico and Mexico City and is characterized by an average annual temperature of less than 5 °C, with a high incidence of frost (Contreras-MacBeath et al. 2006a). According to the climatic units defined by Boyás (1992), this climate type only occurs in about 0.2% of the state. The semicold subhumid climate type is characterized by a long summer, with an average annual temperature between 5 and 12 °C and is located in the northern

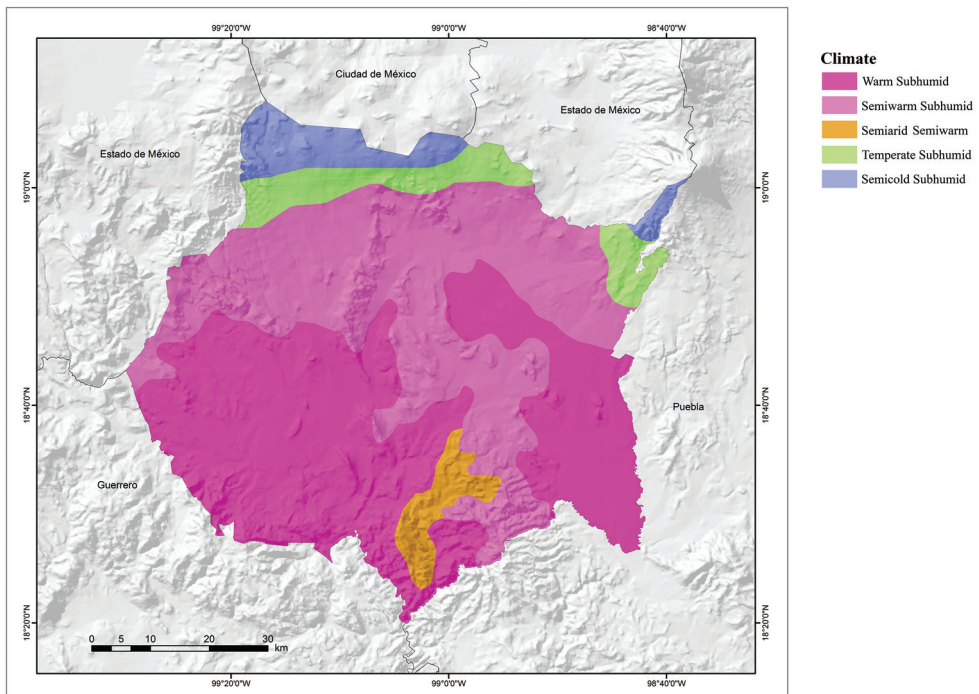


Figure 5. Climate map of the state of Morelos, Mexico (modified from García – Comisión Nacional para el Conocimiento y Uso de la Biodiversidad 1998).

part of the state and south of the Sierra del Ajusco (Contreras-MacBeath et al. 2006a). According to the climatic units defined by Boyás (1992), this type of climate is found in 2% of the state. The temperate subhumid climate type has summer rains and is the wettest of the subhumid climates, with an average annual temperature between 5 and 12 °C, a long summer with the warmest months being April and May, and January the coldest. It is located in the northern part of the state (Contreras-MacBeath et al. 2006a). According to Boyás (1992 in Contreras-MacBeath et al. 2006a) this type of climate occurs in 10% of the state. The semihumid subhumid climate type is characterized by an average annual temperature between 18 and 22 °C, with summer rains and winter rains making up < 5% of the total annual rainfall (Contreras-MacBeath et al. 2006a). It is found in the northern part of Morelos and covers 16% of the state. The warm subhumid climate type is located throughout most of Morelos, but mainly in the central and southern parts. It is characterized by an average annual temperature > 22 °C, summer rains (from May to October), and a dry winter (< 5% of the total annual rainfall) (Contreras-MacBeath et al. 2006a). It covers 72% of the state area.

Materials and methods

We compiled our list of amphibians and reptiles of Morelos from: (1) our field work; (2) a thorough examination of the available literature on amphibians and reptiles in the state; (3) amphibian and reptile records for Morelos in VertNet.org; and 4) amphibian and reptile records for Morelos in Servicio de Descarga de Ejemplares del Sistema Nacional de Información sobre Biodiversidad (SNIB-CONABIO), data bases Amphibians state of Morelos and Reptiles state of Morelos.

We follow Frost (2020) and AmphibiaWeb (2019) (<http://amphibiaweb.org>) for amphibian names and Uetz and Hošek (2019) for reptile names. We included species in the list if we could confirm records, either by direct observation or through documented museum records or vouchers. We do not include previously reported species for Morelos whose distribution is doubtful in the state because of a large gap between the currently known distributions of these species and the reports for Morelos. These species are: *Rana maculata* reported by Castro-Franco et al. (2006), which is distributed from eastern Oaxaca in the Isthmus of Tehuantepec, extending southeast to the central part of Nicaragua (Frost 2020); *Rana pustulosa* Boulenger, 1883 reported by Castro-Franco et al. (2006), which is distributed from southeastern Sonora and western Chihuahua extending south along the western slope of the Sierra Madre Occidental to Colima and Michoacán (Frost, 2020), the populations in Morelos previously considered as *R. pustulosa* are included in *R. zweifeli* (Hillis et al. 1984); *Rana vailanti* Brocchi, 1877 reported by Castro-Franco et al. (2006) which is distributed from northern Veracruz and northern Oaxaca on the Atlantic slope and from southeastern Oaxaca and northwestern Chiapas on the Pacific slope, extending south through much of Central America, to southwestern Colombia and northwestern Ecuador (Frost 2020); and *Thamnophis sirtalis* (Linnaeus, 1758), reported by Castro-Franco

and Bustos-Zagal (1994) as *T. dorsalis* (Baird & Girard, 1853) which is distributed from southeastern Alaska east to Nova Scotia and south across much of the United States, with isolated populations in Texas, New Mexico, and Chihuahua in northwestern Mexico (Fitch 1980). The southernmost record is reported in western Chihuahua, such that we consider it unlikely that this species occurs in Morelos. However, we did not examine any of the specimens used by Castro-Franco et al. (2006) to report these species, so we include them in the list of species that probably occur in Morelos (Table 2). On the other hand, there is a record of *Craugastor pygmaeus* (AMNH A-57809) collected in July 1953, by R. Ruibal at Tepozteco, and a record of *Eleutherodactylus verruculatus* (MVZ:Herp:36573) collected in July 1941, by Robert W. Storer, 12 mi S of Cuernavaca. We were unable to confirm the identity of these two specimens, so we do not include them in the species list for the state but we include them in the list of species that probably occurs in Morelos. Although we believe there is a high probability that *Ambystoma velasci* inhabits the eastern end of Morelos and there are seven records of this species for the state reported in Vertnet.org (MCZ A-24844-50: Museum of Comparative Zoology, Harvard University, Subset of data for VERTNET. Record ID: MCZ:Herp:A-24844. Source: http://digir.mcz.harvard.edu/ipt/resource.do?r=mcz_subset_for_vertnet) the locality reported in six of these records (24845-50) seems to place them in Puebla (circa 224-5 km from Mexico, Puebla, Mexico), and another (24844) is doubtful (circa 62 km S of Mexico, DF). Because of this, we decided not to include this species in the list of species presented here, but do include it in the list of species that probably occur in Morelos (see below).

We generated species accumulation curves for the total herpetofauna, amphibians, and reptiles using the year of the first recorded observation for each species. Such species accumulation curves can estimate potential species richness of amphibians and reptiles (see Raxworthy et al. 2012). In addition, we recorded the conservation status of each species based on the IUCN Red List 2019-2 (IUCN 2019); listing in SEMARNAT (2010); Environmental Vulnerability Scores from Wilson et al. (2013a, b) and Johnson et al. (2015).

The number of overlapping species with the three states and Mexico City that neighbor Morelos, was determined using recent check lists (Mexico City, Lemos-Espinal and Smith unpubl.; State of Mexico, Lemos-Espinal and Smith unpubl.; Guerrero, Palacios-Aguilar and Flores-Villela 2018; Puebla, Woolrich-Piña et al. 2017).

Results and discussion

Morelos is home to 139 species of amphibians and reptiles representing 32 families (three of which are introduced: Gekkonidae, Typhlopidae, and Tryonidae) and 75 genera (three of which are introduced: *Hemidactylus*, *Indotyphlops*, and *Apalone*) (Tables 1, 2). These include 38 species of amphibians (31 anurans [one introduced] and seven salamanders), and 101 reptiles (42 lizards [one introduced], 55 snakes [one introduced], and four turtles [one introduced]). The four introduced species are: the American Bullfrog

Table 1. Amphibians and reptiles of the state of Morelos with distributional and conservation status. Vegetation Type (VT): (1= Oak Forest; 2= Pine-oak Forest; 3= Pine Forest; 4= *Abies* Forest; 5= Tropical Deciduous Forest; 6= Grassland) according to Contreras-MacBeath et al. (2006b) and INEGI (2017). IUCN Status: (DD = Data Deficient; LC = Least Concern, VU = Vulnerable, NT = Near Threatened; EN = Endangered; CR = Critically Endangered; NE = not Evaluated) according to the IUCN Red List (The IUCN Red List of Threatened Species, Version 2019–2(www.iucnredlist.org; accessed 29November 2019); conservation status in Mexico according to SEMARNAT (2010) (CSM): (P = in danger of extinction, A = threatened, Pr = subject to special protection, NL – not listed); Environmental Vulnerability Score: (EVS – the higher the score the greater the vulnerability: low (L) vulnerability species (EVS of 3–9); medium (M) vulnerability species (EVS of 10–13); and high (H) vulnerability species (EVS of 14–20) from Wilson et al. (2013a,b) and Johnson et al. (2015); Global Distribution: 1= Endemic to Mexico; 2= Shared between the US and Mexico; 3= widely distributed from Mexico to Central or South America; 4= widely distributed from the US to Central or South America; IN = Introduced to Morelos. Date in which the first record appeared (1st); and Source of the first record.

	VT	IUCN	CSM	EVS	Global	1 st	Source
CLASS AMPHIBIA							
ORDER ANURA							
FAMILY BUFONIDAE							
<i>Anaxyrus compactilis</i> (Wiegmann, 1833)	1,2,6	LC	NL	H (14)	1	1950	TCWC 6276
<i>Incilius marmoratus</i> (Wiegmann, 1833)	6	LC	NL	M (13)	1	1957	UAZ 11664
<i>Incilius occidentalis</i> (Camerano, 1879)	1,2,3,6	LC	NL	M (11)	1	1903	FMNH 17123
<i>Incilius perplexus</i> (Taylor, 1943)	5	EN	NL	M (11)	1	1936	FMNH 126950
<i>Rhinella horribilis</i> (Wiegmann, 1833)	5	LC	NL	L (3)	4	1901	FMNH 1620
FAMILY CENTROLENIDAE							
<i>Hyalinobatrachium fleischmanni</i> (Boettger, 1893)	5	LC	NL	M (10)	3	1999	CARUM 2742
FAMILY CRAUGASTORIDAE							
<i>Craugastor augusti</i> (Dugès, 1879)	1,2,3,6	LC	NL	L (8)	2	1972	LACM 106766
<i>Craugastor hobartsmithi</i> (Taylor, 1937)	1,5	EN	NL	H (15)	1	1975	MZFC 1089
<i>Craugastor rhodopis</i> (Cope, 1867)	1,5	VU	NL	H (14)	1	1930	FMNH 103253
<i>Craugastor rugulosus</i> (Cope, 1870)	3	LC	NL	M (13)	1	2004	Valenzuela-Galván et al. 2004a
FAMILY ELEUTHERODACTYLIDAE							
<i>Eleutherodactylus angustidigitorum</i> (Taylor, 1940)	1,2,3	VU	Pr	H (17)	1	1956	UCM 9223
<i>Eleutherodactylus maurus</i> Hedges, 1989	3	DD	Pr	H (17)	1	1953	AMNH A-57810
<i>Eleutherodactylus nitidus</i> (Peters, 1870)	5	LC	NL	M (12)	1	1938	FMNH 104455
FAMILY HYLIDAE							
<i>Dryophytes arenicolor</i> (Cope, 1886)	1,2,3,4,5,6	LC	NL	L (7)	2	1936	FMNH 99459
<i>Dryophytes eximius</i> (Baird, 1854)	1,2,3,4	LC	NL	M (10)	1	1932	FMNH 99712
<i>Dryophytes plicatus</i> (Brocchi, 1877)	1,2,3,4	LC	A	M (11)	1	1936	FMNH 27067
<i>Exerodonta smaragdina</i> (Taylor, 1940)	5	LC	Pr	M (12)	1	1943	Taylor 1943
<i>Sarcohyala bistrincta</i> (Cope, 1877)	1,2,3	LC	Pr	L (9)	1	1936	CAS 87826
<i>Scinax staufferi</i> (Cope, 1865)	5	LC	NL	L (4)	3	1960	TCWC 16645
<i>Smilisca baudinii</i> (Duméril & Bibron, 1841)	5	LC	NL	L (3)	4	1949	TCWC 3576
<i>Tlalocobyla smithii</i> (Boulenger, 1902)	3,5	LC	NL	M (11)	1	1902	Boulenger, 1902
FAMILY MICROHYLIDAE							
<i>Gastrophryne olivacea</i> (Hallowell, 1856)	5	LC	Pr	L (9)	2	1938	FMNH 104397
<i>Hypopachus ustus</i> (Cope, 1866)	2,5	LC	Pr	L (7)	3	2004	Valenzuela-Galván et al. 2004b
<i>Hypopachus variolosus</i> (Cope, 1866)	2,5	LC	NL	L (4)	4	1936	FMNH 100572
FAMILY PHYLLOMEDUSIDAE							
<i>Agalychnis dacnicolor</i> (Cope, 1864)	5	LC	NL	M (13)	1	1905	USNM 57554
FAMILY RANIDAE							
<i>Rana catesbeiana</i> Shaw, 1802	IN	IN	IN	IN	IN	1971	ENCB 6943
<i>Rana forreri</i> Boulenger, 1883	5	LC	Pr	L (3)	3	1939	USNM 113856

	VT	IUCN	CSM	EVS	Global	I*	Source
<i>Rana montezumae</i> Baird, 1854	1,2,3,5	LC	Pr	M (13)	1	1983	KU KUH 195251
<i>Rana spectabilis</i> Hillis & Frost, 1985	1,2,3,5	LC	NL	M (12)	1	1938	FMNH 107767
<i>Rana zweifeli</i> Hillis, Frost & Webb, 1984	1,2,3,5	LC	NL	M (11)	1	1892	USNM 20165
FAMILY SCAPHIOPODIDAE							
<i>Spea multiplicata</i> (Cope, 1863)	1,2,5	LC	NL	L (3)	2	1930	FMNH 99013
ORDER CAUDATA							
FAMILY AMBYSTOMATIDAE							
<i>Ambystoma altamirani</i> Dugès, 1895	1,2,3,6	EN	A	M (13)	1	1939	USNM 116614
FAMILY PLETHODONTIDAE							
<i>Aquiloerycea cephalica</i> (Cope, 1865)	1,2,3,4	NT	A	H (14)	1	1936	FMNH 114426
<i>Chiropterotriton orculus</i> (Cope, 1865)	1,2,3,4	VU	NL	H (18)	1	1902	Günther 1901
<i>Isthmura belli</i> (Gray, 1850)	1,2,3,4,6	VU	A	M (12)	1	1950	TCWC 6110
<i>Pseudoerycea altamontana</i> (Taylor, 1939)	1,2,3,4	EN	Pr	H (17)	1	1939	Taylor 1939
<i>Pseudoerycea leprosa</i> (Cope, 1869)	1,2,3,4	LC	A	H (16)	1	1933	FMNH 106158
<i>Pseudoerycea tillicixil</i> Lara-Góngora, 2003	1,2,3,4	EN	NL	H (17)	1	1979	CNAR w/o #
CLASS REPTILIA							
ORDER SQUAMATA							
SUBORDER LACERTILIA							
FAMILY ANGUIDAE							
<i>Abronia deppii</i> (Wiegmann, 1828)	2	EN	A	H (16)	1	1981	MZFC 20215
<i>Barisia imbricata</i> (Wiegmann, 1828)	1,2,3,4,6	LC	Pr	H (14)	1	1936	FMNH 105770
<i>Barisia rudicollis</i> (Wiegmann, 1828)	1,2,3,5	EN	P	H (15)	1	1987	CARUM 508
<i>Gerrhonotus liocephalus</i> Wiegmann, 1828	5	LC	Pr	L (6)	1	1964	MSUM 6999
FAMILY DACTYLOIDAE							
<i>Anolis nebulosus</i> (Wiegmann, 1834)	1,2,5	LC	NL	M (13)	1	1892	USNM 20182
FAMILY EUBLEPHARIDAE							
<i>Coleonyx elegans</i> Gray, 1845	5	LC	A	L (9)	3	1950	TCWC 6548
FAMILY GEKKONIDAE							
<i>Hemidactylus frenatus</i> Duméril & Bribon, 1836	IN	IN	IN	IN	IN	2014	CARUM 2499
FAMILY HELODERMATIDAE							
<i>Heloderma horridum</i> (Wiegmann, 1829)	5	LC	A	M (11)	3	1932	FMNH 103953
FAMILY IGUANIDAE							
<i>Ctenosaura pectinata</i> (Wiegmann, 1834)	5	NE	A	H (15)	1	1939	CNAR 459
FAMILY PHRYNOSOMATIDAE							
<i>Phrynosoma asio</i> Cope, 1864	5	LC	Pr	M (11)	1	2004	Castro-Franco and Bustos Zagal 2004
<i>Phrynosoma orbiculare</i> (Linnaeus, 1758)	1,2,3	LC	A	M (12)	1	1932	FMNH 102370
<i>Phrynosoma taurus</i> Bocourt, 1870	5	LC	A	M (12)	1	1998	CARUM 2622
<i>Sceloporus aeneus</i> Wiegmann, 1828	6	LC	NL	M (13)	1	1931	MCZ R-33914
<i>Sceloporus gadoviae</i> Boulenger, 1905	5	LC	NL	M (11)	1	1932	FMNH 32580
<i>Sceloporus grammicus</i> Wiegmann, 1828	1,2,3,4	LC	Pr	L (9)	1	1903	FMNH 1280
<i>Sceloporus horridus</i> Wiegmann, 1834	5	LC	NL	M (11)	1	1903	FMNH 1281
<i>Sceloporus melanorhinus</i> Bocourt, 1876	5	LC	NL	L (9)	3	1997	CARUM 2580
<i>Sceloporus mucronatus</i> Cope, 1885	1,2,3,4	LC	NL	M (13)	1	1970	BYU 36233
<i>Sceloporus ochoterenae</i> Smith, 1934	5	LC	NL	M (12)	1	1936	FMNH 33398
<i>Sceloporus palaciosi</i> Lara-Góngora, 1983	1,2,3,4	LC	NL	H (15)	1	1949	TCWC 3868
<i>Sceloporus scalaris</i> Wiegmann, 1828	1,2,4,6	LC	NL	M (12)	1	1890	Günther 1901
<i>Sceloporus siniferus</i> Cope, 1870	5	LC	NL	M (11)	3	1977	CNAR 2375
<i>Sceloporus spinosus</i> Wiegmann, 1828	5	LC	NL	M (12)	1	1931	MCZ R-33912
<i>Sceloporus sugillatus</i> Smith, 1942	1,2,3	LC	NL	H (16)	1	1939	MCZ R-46762
<i>Sceloporus torquatus</i> Wiegmann, 1828	1,2,3	LC	NL	M (11)	1	1932	FMNH 32737
<i>Sceloporus utiformis</i> Cope, 1864	5	LC	NL	H (15)	1	2004	Castro-Franco and Bustos Zagal 2004
<i>Urosaurus bicarinatus</i> (Duméril, 1856)	5	LC	NL	M (12)	1	1899	CAS 3795
FAMILY PHYLLODACTYLIDAE							
<i>Phyllodactylus bordai</i> Taylor, 1942	1,5	LC	Pr	M (13)	1	1966	UAZ 55033
<i>Phyllodactylus lanei</i> Smith, 1935	1,5	LC	NL	H (15)	1	2008	Aréchaga-Ocampo et al. 2008

	VT	IUCN	CSM	EVS	Global	I*	Source
<i>Phyllodactylus tuberculosus</i> Wiegmann, 1834	1,5	LC	NL	L (8)	3	1997	CARUM 2385
FAMILY SCINCIDAE							
<i>Marisora brachypoda</i> (Taylor, 1956)	5	LC	NL	L (6)	3	1931	MCZ R-33689
<i>Plestiodon brevirostris</i> (Günther, 1860)	1,2,3	LC	NL	M (11)	1	1936	FMNH 114200
<i>Plestiodon copei</i> (Taylor, 1933)	1,2,3	LC	Pr	H (14)	1	1936	FMNH 114293
<i>Plestiodon indubitus</i> (Taylor, 1933)	1,2,3	NE	NL	H (15)	1	1933	Taylor, 1933
<i>Plestiodon lotus</i> Pavón-Vázquez, Nieto Montes de Oca, Mendoza-Hernández, Centenero-Alcalá, Santa Cruz-Padilla, & Jiménez-Arcos, 2017	1,5	NE	NL	NE	1	2017	Pavón-Vázquez et al. 2017
FAMILY TEIIDAE							
<i>Aspidoscelis communis</i> (Cope, 1878)	5	LC	Pr	H (14)	1	2004	Castro-Franco and Bustos Zagal 2004
<i>Aspidoscelis costatus</i> (Cope, 1878)	5	LC	Pr	M (11)	1	1906	NHMUK 1906.7.19.24-26
<i>Aspidoscelis deppii</i> (Wiegmann, 1834)	5	LC	NL	L (8)	3	1941	MVZ 36595
<i>Aspidoscelis guttatus</i> (Wiegmann, 1834)	5	LC	NL	M (12)	1	1980	CARUM 1255
<i>Aspidoscelis lineatissimus</i> (Cope, 1878)	5	LC	Pr	H (14)	1	1953	Davis and Smith 1953b
<i>Aspidoscelis sackii</i> (Wiegmann, 1834)	5	LC	NL	H (14)	1	1901	FMNH 1016
<i>Holcosus sinister</i> (Wiegmann, 1834)	5	NE	NL	M (13)	1	1956	USNM 139373
SUBORDER SERPENTES							
FAMILY BOIDAE							
<i>Boa sigma</i> Smith, 1943	5	NE	NL	H (15)	1	1949	TCWC 7401
FAMILY COLUBRIDAE							
<i>Conopsis biserialis</i> (Taylor & Smith, 1942)	1,2,3,4,6	LC	A	M (13)	1	1932	FMNH 126813
<i>Conopsis lineata</i> (Kennicott, 1859)	1,2,3,4,6	LC	NL	M (13)	1	1953	Davis and Smith 1953a
<i>Conopsis nasus</i> (Günther, 1858)	1,2,3,4,6	LC	NL	M (11)	1	1970	MCZ R-167269
<i>Drymarchon melanurus</i> (Duméril, Bibron & Duméril, 1854)	5	LC	NL	L (6)	3	1949	TCWC 4112
<i>Drymobius margaritiferus</i> (Schlegel, 1837)	5	LC	NL	L (6)	3	1903	USNM 46545
<i>Ficimia publia</i> (Cope, 1866)	5	LC	NL	L (9)	3	2004	Castro-Franco and Bustos Zagal 2004
<i>Lampropeltis polyzona</i> Cope, 1860	5	LC	NL	L (7)	1	1950	TCWC 7312
<i>Leptophis diplotropis</i> (Günther, 1872)	5	LC	A	H (14)	1	1953	Davis and Smith 1953a
<i>Masticophis mentovarius</i> (Duméril, Bibron & Duméril, 1854)	2,5	LC	A	L (6)	3	1938	FMNH 106202
<i>Mastigodryas melanolomus</i> (Cope, 1868)	5	LC	NL	L (6)	3	1974	CUMV R-0009974
<i>Oxybelis aeneus</i> (Wagler, 1824)	5	LC	NL	L (5)	4	1945	USNM 122059
<i>Pituophis deppei</i> (Duméril, 1853)	1,2,3,5	LC	A	H (14)	1	1949	UMMZ 101931
<i>Pituophis lineaticollis</i> (Cope, 1861)	2,3	LC	NL	L (8)	3	1940	Taylor 1940a
<i>Pseudoficimia frontalis</i> (Cope, 1864)	5	LC	NL	M (13)	1	1938	FMNH 106367
<i>Salvadora bairdi</i> Jan & Sordelli, 1860	1,2,3,5	LC	Pr	H (15)	1	1953	Davis and Smith 1953a
<i>Salvadora mexicana</i> (Duméril, Bibron & Duméril, 1854)	5	LC	Pr	H (15)	1	1938	Taylor 1940
<i>Senticolis triaspis</i> (Cope, 1866)	1,2,5,6	LC	NL	L (6)	4	1860	CUMV R-0009673
<i>Sonora michoacanensis</i> (Dugès, 1884)	5	LC	NL	H (14)	1	1956	UCM 9080
<i>Tantilla bocourti</i> (Günther, 1895)	1,2,6	LC	NL	L (9)	1	1936	FMNH 111093
<i>Tantilla calamarina</i> Cope, 1866	1,2,3,6	LC	Pr	M (12)	1	1938	Taylor 1940
<i>Tantilla deppei</i> (Bocourt, 1883)	1,2,3,6	LC	A	M (13)	1	1949	TCWC 7350
<i>Trimorphodon biscutatus</i> (Duméril, Bibron & Duméril, 1854)	5	NE	NL	L (7)	3	1938	FMNH 106205
<i>Trimorphodon tau</i> Cope, 1870	5	LC	NL	M (13)	1	1938	FMNH 105287
FAMILY DIPSADIDAE							
<i>Coniophanes lateritius</i> Cope, 1862	3	DD	NL	M (13)	1	1945	Smith and Taylor 1945
<i>Coniophanes piceivittis</i> Cope, 1870	5	LC	NL	L (7)	3	1970	LSUMZ 73757

	VT	IUCN	CSM	EVS	Global	I*	Source
<i>Conophis vittatus</i> Peters, 1860	5	LC	NL	M (11)	3	1936	FMNH 104949
<i>Enulius flavitorques</i> (Cope, 1868)	5	LC	NL	L (5)	3	1939	Taylor, 1940a
<i>Hypsiglena torquata</i> (Günther, 1860)	5	LC	Pr	L (8)	1	1938	FMNH 105174
<i>Imantodes gemmistratus</i> (Cope, 1861)	5	LC	Pr	L (6)	3	1938	FMNH 125551
<i>Leptodeira maculata</i> (Hallowell, 1861)	5,6	LC	Pr	L (7)	1	2008	Aréchaga-Ocampo et al. 2008
<i>Leptodeira splendida</i> Günther, 1895	2,5	LC	NL	H (14)	1	1936	FMNH 105352
<i>Pseudoleptodeira latifasciata</i> (Günther, 1894)	5	LC	Pr	H (14)	1	1938	FMNH 99670
<i>Rhadinaea hesperia</i> Bailey, 1940	5	LC	Pr	M (10)	1	1892	USNM 20166
<i>Rhadinaea laureata</i> (Günther, 1868)	1,2,3	LC	NL	M (12)	1	1953	Davis and Smith 1953a
<i>Rhadinaea taeniata</i> (Peters, 1863)	1,2,3	LC	NL	M (13)	1	1932	USNM 110373
<i>Tropidodipsas zueifeli</i> (Liner & Wilson, 1970)	5	NE	Pr	H (16)	1	1966	AMNH R-115572
FAMILY ELAPIDAE							
<i>Micrurus laticollaris</i> Peters, 1870	5	LC	Pr	H (14)	1	1892	USNM 20167
<i>Micrurus tener</i> Baird & Girard, 1953	1,5	LC	NL	M (11)	2	1939	USNM 11334
FAMILY LEPTOTYPHLOPIDAE							
<i>Rena maxima</i> (Loveridge, 1932)	5	LC	NL	M (11)	1	1949	TCWC 4109
FAMILY LOXOCEMIDAE							
<i>Loxocemus bicolor</i> Cope, 1861	5	LC	Pr	M (10)	3	1938	Taylor 1940
FAMILY NATRICIDAE							
<i>Adelophis copei</i> Dugès, 1879	5	VU	Pr	H (15)	1	1940	USNM 110335
<i>Storeria storerioides</i> (Cope, 1866)	1,2,3	LC	NL	M (11)	1	1950	TCWC 7386
<i>Thamnophis cyrtopsis</i> (Kennicott, 1860)	1,2,3	LC	A	L (7)	4	1953	Davis and Smith 1953a
<i>Thamnophis eques</i> (Reuss, 1834)	1,2,3,4	LC	A	L (8)	2	1936	FMNH 106041
<i>Thamnophis scalaris</i> Cope, 1861	1,2,3,4	LC	A	H (14)	1	1936	FMNH 106285
FAMILY TYPHLOPIDAE							
<i>Indotyphlops braminus</i> (Daudin, 1803)	IN	IN	IN	IN	IN	1965	FMNH 154799
FAMILY VIPERIDAE							
<i>Aegistrodon bilineatus</i> Günther, 1863	5	NT	Pr	M (11)	3	1953	Davis and Smith 1953a
<i>Crotalus culminatus</i> Klauber, 1952	1,2,5	NE	NL	H (15)	1	1939	USNM 110610
<i>Crotalus molossus</i> Baird & Girard, 1853	1,2,3,4	LC	Pr	L (8)	2	1970	ENCB 6595
<i>Crotalus polyicticus</i> (Cope, 1865)	1,2,3,4	LC	Pr	H (16)	1	1999	CNAR 19243
<i>Crotalus ravus</i> Cope, 1865	1,2,3	LC	A	H (14)	1	1953	Davis and Smith 1953a
<i>Crotalus tlaloci</i> Bryson, Linkem, Dorcas, Lathrop, Jones, Alvarado-Díaz, Grünwald & Murphy, 2014	1,2,3	NE	NL	H (16)	1	2014	Bryson et al. 2014
<i>Crotalus transversus</i> Taylor, 1944	4	LC	P	H (17)	1	1944	Taylor 1944
<i>Crotalus triseriatus</i> (Wagler, 1830)	1,2,3	LC	NL	H (16)	1	1949	TCWC 4131
ORDER TESTUDINES							
FAMILY KINOSTERNIDAE							
<i>Kinosternon birtipes</i> (Wagler, 1830)	2,5	LC	Pr	M (10)	2	1892	USNM 20188
<i>Kinosternon integrum</i> LeConte, 1854	2,5	LC	Pr	M (11)	1	1936	UMMZ 80790
<i>Kinosternon scorpioides</i> (Linnaeus, 1766)	2,5	NE	Pr	M (10)	3	1964	TNHC 32286
TRIONYCHIDAE							
<i>Apalone spinifera</i> (Le Sueur, 1827)	IN	IN	IN	IN	IN	2004	Castro-Franco and Bustos Zagal 2004

(*Rana catesbeiana*), the Common House Gecko (*Hemidactylus frenatus*), the Brahminy Blindsnake (*Indotyphlops braminus*), and the Spiny Softshell (*Apalone spinifera*). The most speciose families of amphibians are Hylidae and Plethodontidae, whereas the most speciose families of reptiles are Phrynosomatidae and Colubridae (Tables 1, 2).

Table 2. Summary of native species present in Morelos by Family, Order or Suborder, and Class. Status summary indicates the number of species found in each IUCN conservation status in the order DD, LC, VU, NT, EN, CE (see Table 1 for abbreviations; in some cases species have not been assigned a status by the IUCN and therefore these may not add up to the total number of species in a taxon). Mean EVS is the mean Environmental Vulnerability Score, scores ≥ 14 are considered high vulnerability (Wilson et al. 2013a, b) and conservation status in Mexico according to SEMARNAT (2010) in the order NL, Pr, A, P (see Table 1 for abbreviations).

Scientific name	Numbers of genera	Numbers of species	IUCN DD, LC, VU, NT, EN, CE	\bar{x} EVS	SEMARNAT NL, Pr, A, P
CLASS AMPHIBIA					
ORDER ANURA	17	30	1,25,2,0,2,0	10	21,8,1,0
Bufo	3	5	0,4,0,0,1,0	10.4	5,0,0,0
Centrolenidae	1	1	0,1,0,0,0,0	10	1,0,0,0
Craugastoridae	1	4	0,2,1,0,1,0	12.5	4,0,0,0
Eleutherodactylidae	1	3	1,1,1,0,0,0	15.3	1,2,0,0
Hylidae	6	8	0,8,0,0,0,0	8.4	5,2,1,0
Microhylidae	2	3	0,3,0,0,0,0	6.7	1,2,0,0
Phyllomedusidae	1	1	0,1,0,0,0,0	13	1,0,0,0
Ranidae	1	4	0,4,0,0,0,0	9.8	2,2,0,0
Scaphiropodidae	1	1	0,1,0,0,0,0	3	1,0,0,0
ORDER CAUDATA	5	7	0,1,2,1,3,0	15.3	2,1,4,0
Ambystomatidae	1	1	0,0,0,0,1,0	13	0,0,1,0
Plethodontidae	4	6	0,1,2,1,2,0	15.7	2,1,3,0
SUBTOTAL	22	37	1,26,4,1,5,0	11.0	23,9,5,0
CLASS REPTILIA					
ORDER SQUAMATA	49	95	1,80,1,1,2,0	11.6	54,24,15,2
SUBORDER LACERTILIA	15	41	0,35,0,0,2,0	12.1	25,9,6,1
Anguillidae	3	4	0,2,0,0,2,0	12.8	0,2,1,1
Dactyloidae	1	1	0,1,0,0,0,0	13	1,0,0,0
Eublepharidae	1	1	0,1,0,0,0,0	9	0,0,1,0
Helodermatidae	1	1	0,1,0,0,0,0	11	0,0,1,0
Iguanidae	1	1	0,0,0,0,0,0	15	0,0,1,0
Phrynosomatidae	3	18	0,18,0,0,0,0	12.1	14,2,2,0
Phyllodactylidae	1	3	0,3,0,0,0,0	12	2,1,0,0
Scincidae	2	5	0,3,0,0,0,0	11.5	4,1,0,0
Teiidae	2	7	0,6,0,0,0,0	12.3	4,3,0,0
SUBORDER SERPENTES	34	54	1,45,1,1,0,0	11.1	29,15,9,1
Boidae	1	1	0,0,0,0,0,0	15	1,0,0,0
Colubridae	16	23	0,21,0,0,0,0	10.2	15,3,5,0
Dipsadidae	9	13	1,11,0,0,0,0	10.5	7,6,0,0
Elapidae	1	2	0,2,0,0,0,0	12.5	1,1,0,0
Leptotyphlopidae	1	1	0,1,0,0,0,0	11	1,0,0,0
Loxocemidae	1	1	0,1,0,0,0,0	10	0,1,0,0
Natricidae	3	6	0,4,1,0,0,0	11	2,1,3,0
Viperidae	2	8	0,5,0,1,0,0	14.1	3,3,1,1
ORDER TESTUDINES	1	3	0,2,0,0,0,0	10.3	0,3,0,0
Kinosternidae	1	3	0,2,0,0,0,0	10.3	0,3,0,0
SUBTOTAL	50	98	1,82,1,1,2,0	11.5	54,27,15,2
TOTAL	72	135	2,108,5,2,7,0	11.4	77,36,20,2

We compiled a list of 21 species (eight amphibians, 13 reptiles) that we believe potentially occur in Morelos (Table 3). We created this list from species that are distributed near the border with Morelos in southern Mexico City, west-central State of Mexico, northern Guerrero, and southwestern Puebla. The distributional records we

Table 3. List of amphibian and reptile species that potentially occur in Morelos

	Likely to occur in:
CLASS AMPHIBIA	
ORDER ANURA	
FAMILY CRAUGASTORIDAE	
<i>Craugastor pygmaeus</i> (Taylor, 1937)	recorded at Tepozteco (AMNH A-57809)
FAMILY ELEUTHERODACTYLIDAE	
<i>Eleutherodactylus verruculatus</i> (Peters, 1870)	recorded at 12mi S of Cuernavaca (MVZ 36573)
FAMILY LEPTODACTYLIDAE	
<i>Leptodactylus fragilis</i> (Brocchi, 1877)	western and/or eastern Morelos
<i>Leptodactylus melanonotus</i> (Hallowell, 1861)	western, southern, and/or eastern Morelos
FAMILY RANIDAE	
<i>Rana maculata</i> Brocchi, 1877	reported by Castro-Franco et al. (2006)
<i>Rana pustulosa</i> Boulenger, 1883	reported by Castro-Franco et al. (2006)
<i>Rana vaillanti</i> Brocchi, 1877	reported by Castro-Franco et al. (2006)
ORDER CAUDATA	
FAMILY AMBYSTOMATIDAE	
<i>Ambystoma velasci</i> Dugès, 1888	eastern Morelos
CLASS REPTILIA	
SUBORDER LACERTILIA	
FAMILY PHRYNOSOMATIDAE	
<i>Sceloporus anahuacus</i> Lara-Góngora, 1983	northern Morelos
<i>Sceloporus pyrocephalus</i> Cope, 1864	western Morelos
FAMILY SCINCIDAE	
<i>Plestiodon lynxe</i> (Wiegmann, 1834)	northern and/or western Morelos
SUBORDER SERPENTES	
FAMILY COLUBRIDAE	
<i>Tantilla rubra</i> Cope, 1875	eastern Morelos
FAMILY DIPSADIDAE	
<i>Diadophis punctatus</i> (Linnaeus, 1766)	northern Morelos
<i>Geophis bicolor</i> Günther, 1868	northern Morelos
<i>Geophis petersii</i> Boulenger, 1894	northern Morelos
FAMILY ELAPIDAE	
<i>Micrurus browni</i> Schmidt & Smith, 1943	northwestern Morelos
FAMILY NATRICIDAE	
<i>Thamnophis sirtalis</i> (Linnaeus, 1758)	reported as <i>T. dorsalis</i> by Castro-Franco and Bustos-Zagal (1994)
<i>Thamnophis melanogaster</i> (Wiegmann, 1830)	northern Morelos
<i>Thamnophis pulchrilatus</i> (Cope, 1885)	northern Morelos
<i>Thamnophis scaliger</i> (Jan, 1863)	northern Morelos
ORDER TESTUDINES	
FAMILY EMYDIDAE	
<i>Trachemys venusta</i> (Gray, 1855)	eastern Morelos

used to create this list were found in Vertnet.org and Sistema Nacional de Información sobre Biodiversidad (SNIB-CONABIO) for the three neighboring states and Mexico City. We are convinced that as more herpetological work is done near borders with these neighboring states, these “likely to occur” species, will be recorded for Morelos. Indeed, the species accumulation curves suggest that our checklist is likely to underestimate the number of species present in Morelos, especially for reptiles (Fig. 6). In particular, there was a relatively steady increase in species documented in Morelos throughout the 20th Century, and while the rate of species being added to the known herpetofauna in Morelos has slowed more recently, particularly for amphibians, it has continued. We therefore predict that more species will be added to our list as more survey and systematic work in the state and region are completed.

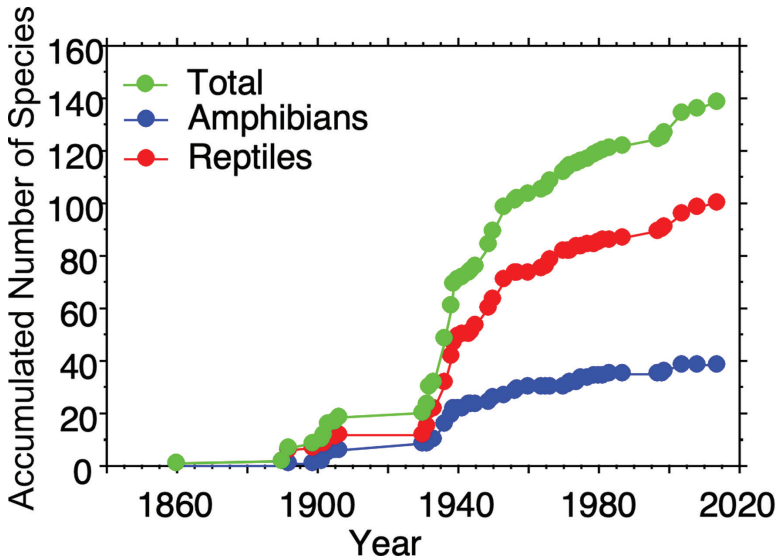


Figure 6. Species accumulation curves for total herpetofauna, amphibians, and reptiles of Morelos, Mexico.

General distribution

Nineteen of the 31 species of anuran that inhabit Morelos are endemic to Mexico. Four of the twelve non-endemic species to Mexico are distributed in the United States and Mexico, another four range from Mexico to Central America, three more are distributed from the United States to Central America or South America, and one is introduced to Morelos. All seven species of salamanders that inhabit Morelos are endemic to Mexico.

Thirty-three of the 42 species of lizards that inhabit Morelos are endemic to Mexico. Of the nine species of lizards not endemic to Mexico, only one is found in the US and Mexico (*Sceloporus grammicus*), another seven range from Mexico to Central America, and the remaining species is introduced to Morelos. Thirty-five of the 55 species of snakes that inhabit Morelos are endemic to Mexico. Three of the 20 non-endemic species to Mexico are found in the US and Mexico, 13 are distributed from Mexico to Central America or South America, three occur from the US to Central America or South America, and one is introduced to Morelos. One of the four species of turtles that inhabit Morelos is endemic to Mexico, one occurs in the US and Mexico, one is distributed from Mexico to South America, and one is introduced to Morelos.

Conservation status

A total of 14 (= 11.2% [14/125]) species of amphibians and reptiles is IUCN listed (i.e., Vulnerable, Near Threatened, or Endangered), 22 (= 16.3% [22/135]) are placed in a protected category (excluding NL and Pr, this last category is equivalent to the LC category of IUCN) by SEMARNAT and 41 species (= 30.6% [41/134]) are categorized as high risk by the EVS (Fig. 7; Table 3). For amphibians, 27.0% [10/37] are IUCN

listed, 13.5% (5/37) are protected by SEMARNAT, and 27.0% [10/37] are at high risk according to the EVS (Fig. 7; Table 3). For reptiles, 4.5% [4/88] are listed by the IUCN, 17.3% [17/98] are protected by SEMARNAT, and 32.0% [31/97] are at high risk according to the EVS (Fig. 7; Table 3). These results suggest that both amphibians and reptiles in the state of Morelos are considered to have relatively low conservation status at global (IUCN) and local (SEMARNAT and EVS) scales. However, although in general the number of species considered in high risk by the EVS is relatively low, this number is greater than that considered in categories of conservation concern by IUCN and SEMARNAT, which is an indicator that the most reliable system to categorize species with some conservation status is the EVS. Although the IUCN evaluation is global, in general it should reflect the conservation status faithfully for the Morelos herpetofauna since 71.1% (96/135) of its species are endemic to the country, so the global evaluation in this case is based in more local or regional evaluations. On the other hand, the Mexican government (SEMARNAT) released a new update in 2019 but it does not appear conservation statuses have been reevaluated since 2010 because all Morelos statuses for amphibians and reptiles have remained the same, so although it is a local evaluation, it might not reflect the current conservation status of the species. The best example of this is the differences that exist in these three evaluation systems in two of the Morelos salamanders: *Chiropoterotriton orculus* is regarded as Vulnerable (VU)

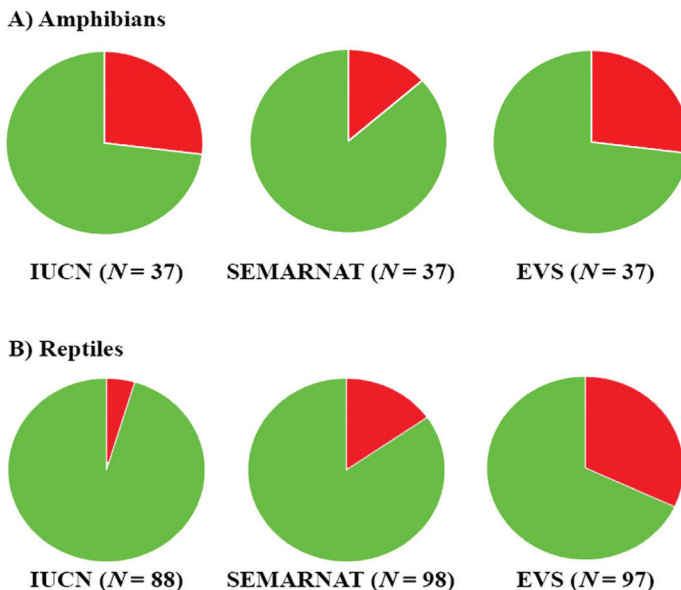


Figure 7. Percent of **A** amphibians and **B** reptiles listed in protected categories on the IUCN Red List and SEMARNAT. Green is percentage in Data Deficient and Least Concern (IUCN); Not Listed and Subject to Special Protection (we regarded the category of Subject to Special Protection in SEMARNAT equivalent to Least Concern in IUCN) (SEMARNAT). Red is percentage in protected categories. N is the number of species assessed by each agency.

by the IUCN, is not considered in any protection category by SEMARNAT, and has a value of 18 (high risk) according to the EVS; and *Pseudoeurycea tlilixitl* is considered Endangered (EN) by the IUCN, is not considered in any protection category by SEMARNAT, and has a value of 17 (high risk) according to the EVS. Similar differences occur in several species of Morelos herpetofauna, suggesting an updated assessment of the conservation of Mexican amphibians and reptiles by SEMARNAT is sorely needed.

Habitat types

The vegetation type that hosts the greatest number of amphibian and reptile species in Morelos is the Tropical Deciduous Forest (Table 4), which represent 63.0% (85/135) of the total number of species. However, it is also the vegetation type that has the lowest percentage of species protected by the IUCN or SEMARNAT, and except for the Grassland, it is also the type of vegetation with the lowest number of species categorized as high risk by the EVS (Table 5). The vegetation type of Morelos with the second richest herpetofauna is Pine-oak Forest with 62 species (45.9% of the species richness of Morelos), followed by Oak Forest with 60 species (21 amphibians, 39 reptiles: 44.4% of the species richness of Morelos) (Table 4). Although these two vegetation types house fewer species than the Tropical Deciduous Forest, they have much higher percentages of species protected by the IUCN and SEMARNAT or categorized as high risk by the EVS. In fact,

Table 4. Number of amphibian and reptile species in each vegetation type of Morelos

	Oak Forest	Pine-oak Forest	Pine Forest	<i>Abies</i> Forest	Tropical Deciduous Forest	Grassland
Amphibians	21	21	20	9	20	7
Reptiles	39	41	31	13	65	11
Total	60	62	51	22	85	18

Table 5. Number of amphibian and reptile species in each vegetation type of Morelos listed and protected in the IUCN Red List or SEMARNAT list, or with a high EVS. Numbers in parenthesis represent the number of species not evaluated by the IUCN.

	IUCN	SEMARNAT	EVS
Amphibians			
Oak Forest	9	12	12
Pine-oak Forest	7	14	14
Pine Forest	7	13	13
<i>Abies</i> Forest	5	4	4
Tropical Deciduous Forest	3	17	18
Grassland	2	5	6
Reptiles			
Oak Forest	1	34(3)	23
Pine-oak Forest	2	35(4)	25
Pine Forest	1	28(2)	18
<i>Abies</i> Forest	–	13	8
Tropical Deciduous Forest	3	52(9)	45
Grassland	–	11	10

if Grassland is excluded, the two vegetation types with the lowest numbers of amphibian and reptile species, the Pine and *Abies* Forests, are also the two vegetation types with the highest percentages of species protected by the IUCN and SEMARNAT or categorized as high risk by the EVS (Table 5). The small number of species inhabiting the Pine and *Abies* Forest is due to the small areas that these two vegetation types occupy in the state, according to SARH (1994), in Morelos, the Pine Forest occupies 80.7 km² (1.7% of the state area), and the *Abies* Forest occupies 22.7 km² (0.5% of the state area), and both are distributed mainly in the northern part of the state.

Comparison with neighboring states

Morelos shares the largest proportion of its amphibian and reptile species with the State of Mexico; however, this percentage is very similar to that of the species shared with Puebla and Guerrero (Table 6). These high percentages of shared species are due to a combination of the extent of the borders between Morelos and each of these three states, and the territorial size of each of them. Although the State of Mexico is smaller than Puebla and Guerrero, it surrounds almost the entire northern half of Morelos, especially if one considers that Mexico City is essentially a part of the State of Mexico from a herpetofaunal point of view (i.e., one could consider Mexico City as an extension of the State of Mexico in this context) (Fig. 1). This large contact area likely results in a high percentage of shared species. For example, all species of salamanders that inhabit Morelos, are also found in the State of Mexico, and five of the nine families of anurans that inhabit Morelos are fully shared with the State of Mexico. Only five species of Morelos anurans do not inhabit the State of Mexico, resulting in the highest percentage of amphibian species shared in the region and the highest percentage of shared herpetofauna. However, Morelos shares a similar proportion of reptile species with Guerrero, Puebla and the State of Mexico (Table 6). Thus, Morelos shares an almost equal proportion of

Table 6. Summary of the numbers of species shared between Morelos and neighboring Mexican states (not including introduced species). The percent of Morelos species shared by a neighboring state are given in parentheses. Total refers to the total number of species found in Morelos and four neighboring states (i.e., regional species pool) and the number in parentheses in this column is the percent of the regional species pool found in Morelos. – indicates either Morelos or the neighboring state has no species in the taxonomic group, or none of that specific taxon is shared between the states, thus no value for shared species is provided.

TAXON	Morelos	Mexico	Puebla	Guerrero	Mexico City	TOTAL
CLASS AMPHIBIA	37	32(86.5)	28(75.7)	24(64.9)	14(37.8)	150(24.7)
ORDER ANURA	30	25(83.3)	25(83.3)	22(73.3)	7(23.3)	100(30.0)
Bufo	5	5(100)	5(100)	4(80.0)	1(20.0)	10(50.0)
Centrolenidae	1	–	1(100)	1(100)	–	1(100)
Craugastoridae	4	3(75.0)	2(50.0)	3(75.0)	1(25.0)	16(25.0)
Eleutherodactylidae	3	3(100.0)	1(33.3)	1(33.3)	–	11(27.3)
Hylidae	8	7(87.5)	8(100)	7(87.5)	3(37.5)	40(20.0)

TAXON	Morelos	Mexico	Puebla	Guerrero	Mexico City	TOTAL
Leptodactylidae	–	–	–	–	–	2(0)
Microhylidae	3	1(33.3)	2(66.7)	2(66.7)	–	3(100)
Phyllomedusidae	1	1(100)	1(100)	1(100)	–	3(33.3)
Ranidae	4	4(100)	3(75.0)	2(50.0)	1(25.0)	12(33.3)
Rhinophrynidae	–	–	–	–	–	1(0)
Scaphiropodidae	1	1(100)	1(100)	1(100)	1(100)	1(100)
ORDER CAUDATA	7	7(100)	3(42.9)	2(28.6)	7(100)	49(14.3)
Ambystomatidae	1	1(100)	–	–	1(100)	10(10.0)
Plethodontidae	6	6(100)	3(50.0)	2(33.3)	6(100)	38(15.8)
Salamandridae	–	–	–	–	–	1(0)
ORDER GYMNOPIHIONA	–	–	–	–	–	1(0)
Caecilidae	–	–	–	–	–	1(0)
CLASS REPTILIA	98	75(76.5)	76(77.6)	77(78.6)	35(35.7)	294(33.3)
ORDER CROCODYLIA	–	–	–	–	–	1(0)
Crocodylidae	–	–	–	–	–	1(0)
ORDER SQUAMATA	95	73(76.8)	75(78.9)	76(80.0)	33(34.7)	280(33.9)
SUBORDEN AMPHISBAENIA	–	–	–	–	–	2(0)
Bipedidae	–	–	–	–	–	2(0)
SUBORDER LACERTILIA	41	30(73.2)	29(70.7)	35(85.4)	12(29.3)	118(34.7)
Anguidae	4	4(100)	2(50.0)	3(75.0)	1(25.0)	11(36.4)
Corytophanidae	–	–	–	–	–	3(0)
Dactyloidae	1	1(100)	–	1(100)	–	18(5.6)
Diploglossidae	–	–	–	–	–	2(0)
Eublepharidae	1	–	1(100)	1(100)	–	1(100)
Helodermatidae	1	1(100)	1(100)	1(100)	–	1(100)
Iguanidae	1	1(100)	1(100)	1(100)	–	4(25.0)
Phrynosomatidae	18	14(77.8)	15(83.3)	15(83.3)	9(50.0)	36(50.0)
Phyllodactylidae	3	1(33.3)	1(33.3)	3(100)	–	5(60.0)
Scincidae	5	4(80.0)	4(80.0)	4(80.0)	2(40.0)	15(33.3)
Teiidae	7	4(57.1)	4(57.1)	6(85.7)	–	12(58.3)
Xantusidae	–	–	–	–	–	5(0)
Xenosauridae	–	–	–	–	–	5(0)
SUBORDER SERPENTES	54	43(79.6)	46(85.2)	41(75.9)	21(38.9)	160(33.8)
Boidae	1	1(100)	1(100)	–	–	2(50.0)
Colubridae	23	20(87.0)	22(95.7)	20(87.0)	9(39.1)	41(56.1)
Dipsadidae	13	8(61.5)	10(76.9)	11(84.6)	2(15.4)	62(21.0)
Elapidae	2	2(100)	2(100)	1(50.0)	1(50.0)	10(20.0)
Leptotyphlopidae	1	1(100)	1(100)	1(100)	–	6(16.7)
Loxocemidae	1	–	–	1(100)	–	1(100)
Natricidae	5	4(80.0)	4(80.0)	3(60.0)	4(80.0)	16(31.3)
Typhlopidae	–	–	–	–	–	1(0)
Viperidae	8	7(87.5)	6(75.0)	4(50.0)	5(62.5)	21(38.1)
ORDER TESTUDINES	3	2(66.7)	1(33.3)	1(33.3)	2(66.7)	13(23.1)
Cheloniidae	–	–	–	–	–	3(0)
Dermochelyidae	–	–	–	–	–	1(0)
Emydidae	–	–	–	–	–	2(0)
Geoemydidae	–	–	–	–	–	2(0)
Kinosternidae	3	2(66.7)	1(33.3)	1(33.3)	2(66.7)	5(60.0)
TOTAL	135	107(79.3)	104(77.0)	101(74.8)	49(36.3)	444(30.4)

amphibian and reptile species with these three states, and an explanation for the difference in the species shared with each of them is found in the large number of salamanders that Morelos shares with the State of Mexico. This is due to the fact that these two states share the temperate habitats of northern Morelos, which host this unique assortment of salamander species, since the number of reptile species that Morelos shares with each of these three states is virtually the same, regardless of size of the state.

Acknowledgments

We thank Jesús Sigala for very helpful comments that greatly improved the manuscript. Support for this study was provided by Dirección General de Asuntos del Personal Académico, Programa de Apoyo a Proyectos de Investigación e Innovación Tecnológica (DGAPA-PAPIIT) through the Project IN215418. We are grateful to A. Núñez Merchand from the National Commission for the Understanding and Use of Biodiversity (CONABIO) for kindly creating and providing the municipality, topographic, physiographic, climate, and vegetation maps used in this publication, and to I. Cruz, also from CONABIO, for providing the satellite imagen of the state of Morelos. We are grateful to A. Resetar and J. Mata from the Field Museum of Natural History, Chicago, Illinois; E.M. Braker from the University of Colorado Museum, University of Colorado at Boulder; J. McGuire, C. Spencer, and D. Wake from the Museum of Vertebrate Zoology at Berkeley, University of California at Berkeley; and D. Dickey and D.A. Kizirian from the American Museum of Natural History, New York.

References

- Aguilar BS (1990) Dimensiones ecológicas del estado de Morelos. Centro Regional de Investigaciones Multidisciplinarias, UNAM, 221 pp.
- Alcaraz-Cruz H, Chávez-Juárez J, Valenzuela D (2004) *Coniophanes lateritius*. Herpetological Review 35: 190.
- Aréchaga-Ocampo S, Montalbán-Huidobro CA, Castro-Franco R (2008) Nuevos registros y ampliación de la distribución de anfibios y reptiles en el estado de Morelos, México. Acta Zoológica Mexicana (nueva serie) 24: 311–233. <https://doi.org/10.21829/azm.2008.242720>
- Boulenger GA (1902) Reptilia and Batrachia (1901). Zoological Record 38: 1–35.
- Boyás DJC (1992) Determinación de la composición, estructura y productividad de las comunidades arbóreas del estado de Morelos en base a unidades ecológicas. Doctoral Thesis. Facultad de Ciencias, UNAM.
- Bryson RW, Linkem CW, Dorcas ME, Lathrop A, Jones JM, Alvarado-Díaz J, Grünwald CI, Murphy RW (2014) Multilocus species delimitation in the *Crotalus triseriatus* species group (Serpentes: Viperidae: Crotalinae), with the description of two new species. Zootaxa 3826: 475–496. <https://doi.org/10.11646/zootaxa.3826.3.3>

- Castro-Franco R, Bustos Zagal MG (1994) List of reptiles of Morelos, Mexico, and their distribution in relation to vegetation types. *Southwestern Naturalist* 39: 171–174. <https://doi.org/10.2307/3672243>
- Castro-Franco R, Bustos Zagal MG (2004) Additional records and range extensions of reptiles of Morelos, Mexico. *Herpetological Review* 35: 196–197.
- Castro-Franco R, Vergara García GG, Bustos Zagal MG, Mena Arizmendi W (2006) Diversidad y distribución de anfibios del estado de Morelos, Mexico. *Acta Zoológica Mexicana* 22: 95–101.
- Cervantes-Zamora Y, Cornejo-Olgín SL, Lucero-Márquez R, Espinoza-Rodríguez JM, Miranda-Viquez E, Pineda-Velázquez A (1990) Provincias Fisiográficas de México – Extraído de Clasificación de Regiones Naturales de México II, IV.10.2. Atlas Nacional de México. Vol. 85 II. Escala 1:4000000. Instituto de Geografía, UNAM, México. http://www.conabio.gob.mx/informacion/metadatos/gis/rfisio4mgw.xml?_httpcache=yes&_xsl=/db/metadatos/xsl/fgde_html.xsl&_indent=no
- Contreras-MacBeath T, Boyás-Delgado JC, Martínez-Thomas JI, Taboada-Salgado M, Pöhle-Morales OM, Herrera-Ascencio P, Saldaña-Favela P, Oliver-Guadarrama R (2006a) Marco de Referencia Físico. En: CONABIO y UAEM (2006) La diversidad biológica en Morelos: Estudio del Estado. Contreras-MacBeath T, Boyás-Delgado JC, Jaramillo F (editores) Comisión Nacional para el Conocimiento y Uso de la Biodiversidad y Universidad Autónoma del Estado de Morelos, 7–20.
- Contreras-MacBeath T, Bonilla-Barbosa JR, Boyás-Delgado JC, Bustos-Zagal G, Caspeta-Mandujado JM, Castro-Franco R, Lozano-García MA, Martínez-Thomas JI, Mejía-Mojica H, Ortiz-Villaseñor AL, Portugal-Portugal D, Trejo-Albarrán R, Trejo-Loyo A, Urbina-Torres F (2006b) Biodiversidad. En: CONABIO y UAEM (2006b) La diversidad biológica en Morelos: Estudio del Estado. Contreras-MacBeath T, Boyás-Delgado JC, Jaramillo F (editores) Comisión Nacional para el Conocimiento y Uso de la Biodiversidad y Universidad Autónoma del Estado de Morelos, 31–58.
- Davis WB, Smith HM (1953a) Snakes of the Mexican State of Morelos. *Herpetologica* 8: 133–143.
- Davis WB, Smith HM (1953b) Lizards and Turtles of the Mexican State of Morelos. *Herpetologica* 9: 100–108.
- De la O-Toris J, Maldonado B, Martínez-Garza C (2012) Efecto de la perturbación en la comunidad de herbáceas nativas y ruderales de una selva estacional Mexicana. *Botanical Sciences* 90: 469–480. <https://doi.org/10.17129/botsci.475>
- Fitch HS (1980) *Thamnophis sirtalis* (Linnaeus). Common garter snake. *Catalogue of American Amphibians and Reptiles* 270: 1–4.
- Frost DR (2020) Amphibian Species of the World: an Online Reference. Version 6.0 (4 January 2020). Electronic Database accessible at <http://research.amnh.org/herpetology/amphibia/index.html>. American Museum of Natural History, New York.
- García E (1998) Modificaciones al sistema de clasificación climática de Köppen. Instituto de Geografía – UNAM, 90 pp.
- García E, Comisión Nacional para el Conocimiento y Uso de la Biodiversidad (CONABIO) (1998). “Climas (Clasificación de Köppen, modificado por García)”. Escala 1:1 000 000. Mexico.

- García-Estrada C, Romero-Almaraz M, Sanchez-Hernández C (2002) Comparison of rodent communities in sites with different degrees of disturbance in deciduous forest of southeastern Morelos, Mexico. *Acta Zoologica Mexicana Nueva Serie* 85: 153–168.
- Günther ACLG (1901) Reptilia and Batrachia. Part 165. Salvin O, Godman FD (eds.), *Biologia Centrali Americana*. Volume 7, Porter RH and Dulau & Co., London, 261–268.
- Hillis DM, Frost JS, Webb RG (1984) A new species of frog of the *Rana tarahumarae* group from southwestern Mexico. *Copeia* 1984: 398–403. <https://doi.org/10.2307/1445197>
- INEGI (2009). ‘Modelo digital de terreno, escala: 1:250000. Instituto Nacional de Estadística y Geografía. Aguascalientes, Aguascalientes.
- INEGI (2013). ‘Conjunto de datos vectoriales de uso de suelo y vegetación escala 1:250 000, serie V (capa unión)’, escala: 1:250000. edición: 2a. Instituto Nacional de Estadística y Geografía. Aguascalientes, Aguascalientes.
- INEGI (2017). Anuario estadístico y geográfico de Morelos 2017 / Instituto Nacional de Estadística y Geografía. Mexico: INEGI, 475 pp.
- INEGI (2018) ‘Áreas Geoestadísticas Estatales’, escala: 1:250000. edición: 1. Instituto Nacional de Estadística y Geografía. Aguascalientes, Mexico.
- IUCN (2019) IUCN Red List of Threatened Species, Version 2019.2. [Downloaded on 24 October 2019]
- Johnson JD, Mata-Silva V, Wilson LD (2015) A conservation reassessment of the Central American herpetofauna based on the EVS measure. *Amphibian & Reptile Conservation* 9: 1–94.
- Monroy R, Colin H (1991) Perspectiva ecológica integral del estado de Morelos. In: Tapia UM (Ed.) Primeras jornadas de investigación en el estado de Morelos. Centro Regional de Investigaciones multidisciplinarias, Universidad Nacional Autónoma de México. Cuernavaca, Morelos, Mexico, 45–52.
- Navar J, Estrada-Salvador A, Estrada-Castrillon E (2010) The effect of land use change in the tropical dry forests of Morelos, Mexico on carbon stocks and fluxes. *Journal of Tropical Forest Science* 22: 295–307.
- Palacios-Aguilar RI, Flores-Villela O (2018) An updated checklist of the herpetofauna from Guerrero, Mexico. *Zootaxa* 4422: 1–24. <https://doi.org/10.11646/zootaxa.4422.1.1>
- Pavón-Vázquez CJ, Nieto Montes de Oca A, Mendoza-Hernández AA, Centenero-Alcalá E, Santa Cruz-Padilla SA, Jiménez-Arcos VH (2017) A new species of *Plestiodon* (Squamata: Scincidae) from the Balsas Basin, Mexico. *Zootaxa* 4365: 149–172. <https://doi.org/10.11646/zootaxa.4365.2.3>
- Raxworthy CJ, Ananjeva N, Orlov NC (2012) Complete species inventories. In: McDiarmid RW, Foster MS, Guyer C, Gibbons JW, Chernoff N (Eds) *Reptile Biodiversity: Standard Methods for Inventory and Monitoring*. University of California Press, Berkeley, 209–215.
- SARH [Secretaría de Agricultura y Recursos Hidráulicos] (1994) *Inventario Nacional Periódico, Memoria Nacional, Subsecretaría Forestal y de Fauna Silvestre*, SARH, México.
- SEMARNAT [Secretaría de Medio Ambiente y Recursos Naturales] (2010) Norma Oficial Mexicana NOM-059-Ecol-2010. Protección ambiental-Especies nativas de Mexico de flora y fauna silvestres-Categorías de riesgo y especificaciones para su inclusión, exclusión o cambio-Lista de especies en riesgo. Diario oficial (Segunda Sección, 30-dic), 77 pp. http://www.profepa.gob.mx/innovaportal/file/435/1/NOM_059_SEMARNAT_2010.pdf

- Smith HM, Taylor EH (1945) An annotated checklist and keys to the snakes of Mexico. Bulletin of the US National Museum, 187: 1–239. <https://doi.org/10.5479/si.03629236.187.1>
- Sotello-Caro O, Chichia-González J, Sorani V, Flores-Palacios A (2015) Changes in the deforestation dynamics of a river sub-basin of Mexico: non-recovery of primary habitats following cessation of deforestation. *Revista de Geografía Norte Grande* 61: 205–219. <https://doi.org/10.4067/S0718-34022015000200011>
- Taylor EH (1933) A new species of lizard from Mexico. *University of Kansas Science Bulletin* 21: 257–262.
- Taylor EH (1939 “1938”) Concerning Mexican salamanders. *University of Kansas Science Bulletin* 25: 259–313. <https://doi.org/10.5962/bhl.part.1703>
- Taylor EH (1940 “1939”) Some Mexican Serpentes. *University of Kansas Science Bulletin* 26: 445–487.
- Taylor EH (1943) A new *Hylella* from Mexico. *Proceedings of the Biological Society of Washington* 56: 49–52.
- Taylor EH (1944) Two new species of Crotalid snakes from Mexico. *University of Kansas Science Bulletin* 30: 47–56. <https://doi.org/10.5962/bhl.part.6501>
- Trejo I, Dirzo R (2000) Deforestation of seasonally dry tropical forest: A national and local analysis in Mexico. *Biological Conservation* 94: 133–142.
- Valenzuela Galván D, Chávez-Juárez J, Alcaraz-Cruz H (2004a) *Eleutherodactylus rugulosus*. *Herpetological Review* 35: 184.
- Valenzuela Galván D, Chávez-Juárez J, Alcaraz-Cruz H (2004b) *Gastrophryne usta*. *Herpetological Review* 35: 184.
- Uetz P, Hošek J (2019) The Reptile Database. <http://www.reptile-database.org> [accessed 24 October 2019]
- Wilson LD, Johnson JD, Mata-Silva V (2013a) A conservation reassessment of the amphibians of Mexico based on the EVS measure. *Amphibian & Reptile Conservation* 7: 97–127.
- Wilson LD, Mata-Silva V, Johnson JD (2013b) A conservation reassessment of the reptiles of Mexico based on the EVS measure. *Amphibian & Reptile Conservation* 7: 1–47.
- Woolrich-Piña GA, García-Padilla E, DeSantis DL, Johnson JD, Mata-Silva V, Wilson LD (2017) The herpetofauna of Puebla, Mexico: composition, distribution, and conservation status. *Mesoamerican Herpetology* 4: 791–884.

Appendix I

Museum collections included in the VertNet.org database records of Morelos amphibians and reptiles that house specimens of the first record of a species in Morelos.

- AMNH** Collection of Herpetology, Herpetology Department, American Museum of Natural History
- NHMK** Zoological Collection, British Museum of Natural History, London
- BYU** Herpetology Collection, Monte L. Bean Museum, Brigham Young University
- CNAR** Colección Nacional de Anfibios y Reptiles, Instituto de Biología, Universidad Nacional Autónoma de México

- CUMV** Amphibian and Reptile Collection, Cornell University Museum of Vertebrates
- CARUM** Colección de Anfibios y Reptiles, Universidad Autónoma del Estado de Morelos
- CAS** Collection of Herpetology, Herpetology Department, California Academy of Sciences
- ENCB** Escuela Nacional de Ciencias Biológicas, Instituto Politécnico Nacional
- FMNH** Division of Amphibians and Reptiles, Field Museum of Natural History
- KU KUH** Herpetology Collection, University of Kansas Biodiversity Institute
- LACM** Collection of Herpetology, Herpetology Section, Natural History Museum of Los Angeles County
- LSUMZ** Collection of Reptiles and Amphibians, Louisiana State University Museum of Natural Science
- MCZ** Collection of Herpetology, Museum of Comparative Zoology, Harvard University Cambridge
- MSUM** Ichthyology and Herpetology Collections, Michigan State University Museum
- MVZ** Herpetological Collection, Museum of Vertebrate Zoology at Berkeley
- MZFC** Colección Herpetológica, Museo de Zoología Alfonso L. Herrera, Facultad de Ciencias, UNAM
- TCWC** Collection of Herpetology, Texas Cooperative Wildlife Collection, Texas A&M University
- TNHC** Collection of Herpetology, Texas Natural History Collection, University of Texas Austin
- UAZ** Amphibians and Reptiles Collections, University of Arizona
- UCM** Collection of Herpetology, University of Colorado Museum
- UMMZ** Collection of Herpetology, Museum of Zoology, University of Michigan Ann Arbor
- USNM** Collection of Herpetology, Department of Vertebrate Zoology, National Museum of Natural History, Smithsonian Institution

Two new species of *Plectranthias* (Teleostei, Serranidae, Anthiaginae) from mesophotic coral ecosystems in the tropical Central Pacific

Bart Shepherd¹, Tyler A. Y. Phelps^{2,3}, Hudson T. Pinheiro²,
Claudia R. Rocha², Luiz A. Rocha²

1 *Steinhart Aquarium, California Academy of Sciences, San Francisco, CA 94118, USA* **2** *Department of Ichthyology, California Academy of Sciences, San Francisco, CA 94118, USA* **3** *Department of Biology, San Francisco State University, San Francisco, CA 94132, USA*

Corresponding author: Bart Shepherd (bshepherd@calacademy.org)

Academic editor: D. Morgan | Received 17 January 2020 | Accepted 14 April 2020 | Published 16 June 2020

<http://zoobank.org/57CFFFDD-5493-4AD1-9C3C-D727231AF29E>

Citation: Shepherd B, Phelps TAY, Pinheiro HT, Rocha CR, Rocha LA (2020) Two new species of *Plectranthias* (Teleostei, Serranidae, Anthiaginae) from mesophotic coral ecosystems in the tropical Central Pacific. ZooKeys 941: 145–161. <https://doi.org/10.3897/zookeys.941.50243>

Abstract

Two new species of *Plectranthias* perchlets are described, collected from mesophotic coral ecosystems in French Polynesia and the Republic of the Marshall Islands, in the tropical Central Pacific. *Plectranthias polygonius* **sp. nov.** was collected at a depth of 105 m in Tahiti, French Polynesia, and 120 m in Maloelap Atoll, Republic of the Marshall Islands. It was also observed in Moorea and Rangiroa (French Polynesia), and at Majuro and Erikub Atolls, Republic of the Marshall Islands. *Plectranthias hinano* **sp. nov.** was collected at a depth of 90–98 m in Tahiti, French Polynesia, and observed in Moorea. The barcode fragment of the cytochrome oxidase I gene of *Plectranthias polygonius* **sp. nov.** does not closely match any published sequence of *Plectranthias*, with approximately 15% uncorrected divergence from several species. *Plectranthias polygonius* **sp. nov.** can be distinguished from all of its congeners by coloration and morphology. The barcode fragment of the COI gene of *Plectranthias hinano* **sp. nov.** is closest to *Plectranthias bennetti*, with 5.4% uncorrected divergence. *Plectranthias hinano* **sp. nov.** is also distinguished from all of its congeners by morphology, and a coloration that includes two indistinct black spots along the base of the dorsal-fin, and transparent yellow dorsal and anal fin membranes. With this publication, the genus *Plectranthias* now comprises 58 valid species, with representatives from tropical to temperate waters of the Atlantic, Pacific, and Indian oceans. These two new discoveries add to the growing body of research highlighting the rich biodiversity of mesophotic ecosystems.

Keywords

biodiversity, closed-circuit rebreather, coral-reef twilight zone, ichthyology, perchlet, reef fish, taxonomy

Introduction

The anthiadine genus *Plectranthias* Bleeker, 1873, currently comprises 56 valid species from tropical to temperate waters in the Atlantic, Pacific, and Indian oceans (Fricke et al. 2019). Most of these fishes are found in relatively deep habitats (depths of 90–420 m) with complex rocky formations (Allen and Walsh 2015; Gill et al. 2016). In general, they are small (20 cm max length, but most in the 5–10 cm range), benthic, feed on small mobile invertebrates, and hide in crevices and holes on the reef (Kuitert 2004). Due to their small size and cryptic habits, they are poorly represented in museum collections, and most species have been described based on a single or a small number of specimens (Randall 1980; Heemstra and Randall 2008; Bineesh et al. 2014; Allen and Walsh 2015; Gill et al. 2016; Shepherd et al. 2018; Gill and Roberts 2020; Wada et al. 2020).

Mesophotic coral ecosystems (MCEs) are coral reef habitats found at depths of 30–150 m, and are also known as the coral reef “twilight zone” (Rocha et al. 2018). While conducting ichthyological and ecological surveys of MCEs at various locations across the wider tropical Pacific region, our team has encountered many new species, especially reef fishes within the family Serranidae. In this paper, we describe two new anthiadine fishes within the genus *Plectranthias* from French Polynesia and the Republic of the Marshall Islands. These two new perchlets represent the 57th and 58th species of *Plectranthias*, adding to the spate of recent new species from MCEs.

Materials and methods

All specimens were collected with hand nets while diving on mixed-gas closed-circuit rebreather (Hollis Prism 2) in French Polynesia (Tahiti, Moorea) and Micronesia (Majuro, Republic of Marshall Islands). Specimens were collected and immediately transported to a field laboratory, where they were photographed, tissues sampled, fixed in 10% formalin, and preserved in 75% ethanol. The preserved specimens were later measured and x-radiographed at the California Academy of Sciences. Measurements were taken with digital calipers to the nearest 0.01 mm and rounded to one decimal place, following the conventions described in Anderson and Heemstra (2012), Williams et al. (2013), and Gill and Roberts (2020). Principal caudal rays are those associated with hypurals, as described in Gill et al. (2016). Procurrent caudal-fin rays are those dorsal and ventral to the principal rays. Principal and procurrent caudal-fin ray counts are presented as upper + lower. Vertebral counts are presented as precaudal + caudal. The anterior-most vertebra with a haemal spine was counted as the first cau-

dal vertebra, the urostylar complex the last. Gill raker counts are presented as upper (epibranchial) + lower (ceratobranchial) rakers on the anterior face of the first arch; the angle raker is included in the second count. The anterior supraneural-dorsal ray-pterygiophore-neural spine interdigitation pattern is presented as a formula with “0” representing a supraneural, “/” a neural spine, and numerals indicating the number of spines borne by each pterygiophore (Anderson and Heemstra 2012; Williams et al. 2013). Morphometric and meristic data for the holotypes and paratypes are presented in Table 1. Measurements in the text are proportions of standard length (SL), unless otherwise noted. Values in parentheses represent ranges for paratypes, when different from the holotypes. The holotypes were deposited at the California Academy of Sciences ichthyological collection (CAS), and the paratypes were deposited at the Smithsonian Institution, National Museum of Natural History ichthyological collection (USNM).

Mitochondrial cytochrome c oxidase subunit I (COI) DNA was sequenced and analyzed for the new species. DNA extraction and PCR amplification of the COI gene were performed following protocols detailed in Weigt et al. (2012). DNA sequences were compared to the fourteen *Plectranthias* species available in GenBank (*P. abiahiata* Shepherd, Phelps, Pinheiro, Perez-Matus & Rocha, 2018: MH025944; *P. alleni* Randall, 1980: FOAO1479; *P. bennetti* Allen & Walsh, 2015: KT601636; *P. flammeus* Williams, Delrieu-Trottin & Planes, 2013: KC565477–KC565480; *P. fourmanoiri* Randall, 1980: KC567662, KC567663; *P. japonicus* Steindachner, 1883: JQ681323, JQ681324; *P. kamii* Randall, 1980: KU943548; *P. kelloggi* Jordan & Evermann, 1903: KP267643; *P. longimanus* Weber, 1913: JF494178; *P. maculicauda* Regan, 1914: FNZ095; *P. nanus* Randall, 1980: JQ432001–JQ432004, KC565481, KC567661; *P. randalli* Fourmanoir & Rivaton, 1980: KP267613; *P. retrofasciatus* Fourmanoir & Randall, 1979: JN313133; *P. winniensis* Tyler, 1966: KC565482, KC565483). Alignments of DNA sequences were done using a standard Geneious global alignment with free end gaps and 65% similarity in the program Geneious Prime 2020.0.3 (Biomatters, Auckland; Kearse et al. 2012).

Taxonomy

Plectranthias polygonius sp. nov.

<http://zoobank.org/12603BD5-EA0F-4826-AA9C-A380A594F316>

Figures 1, 2A, Table 1

Polygon Perchlet

Type locality. Tahiti, French Polynesia.

Holotype. CAS 247193, field code: HTP906, GenBank MN922331. 29.5 mm SL, Tahiti, French Polynesia, 17°29'27"S, 149°28'01"W, depth of collection 105 m, collected with hand nets by B Shepherd, HT Pinheiro, TAY Phelps, MV Bell, and LA Rocha, 03 March 2019.

Table 1. Proportional measurements of type specimens of *Plectranthias polygonius* sp. nov., and *Plectranthias hinano* sp. nov. expressed as a percentage of the standard length.

	<i>Plectranthias polygonius</i> sp. nov.		<i>Plectranthias hinano</i> sp. nov.	
	Holotype	Paratype	Holotype	Paratype
	CAS 247193	USNM 445722	CAS 247195	USNM 445723
Standard length (mm)	29.5	32.3	49.6	28.0
Head length	31.3	32.3	42.1	39.8
Greatest body depth	29.5	31.6	34.0	33.2
Body width	11.1	13.5	16.5	13.9
Snout length	9.3	9.0	14.2	12.3
Postorbital of head	21.0	21.1	18.6	17.9
Bony interorbital width	5.9	7.1	4.0	5.4
Orbit diameter	11.2	11.5	11.5	11.4
Upper jaw length	17.6	19.1	19.0	19.1
Maxilla width	5.6	6.2	5.9	5.6
Caudal peduncle length	8.7	8.1	10.6	9.7
Caudal peduncle depth	12.3	13.0	11.4	11.8
Predorsal length	38.0	41.4	41.8	41.0
Preanal length	70.0	70.6	68.4	67.4
Prepelvic length	35.9	38.7	42.5	39.9
Dorsal-fin base length	48.7	52.9	48.5	53.7
First dorsal spine	5.6	6.3	5.7	10.7
Longest dorsal spine (number)	18.8 (3rd)	20.0 (3rd)	18.2 (4th)	15.7 (3rd)
First segmented dorsal ray	17.1	15.6	14.9	16.4
Longest segmented dorsal ray (number)	17.3 (2nd)	15.6 (1st)	15.3 (2nd)	19.8 (3rd)
Anal fin base length	15.8	15.4	16.0	18.8
First anal spine	7.6	8.0	6.3	8.0
Second anal spine	19.0	19.6	20.6	20.8
Third anal spine	13.2	13.7	15.9	15.4
First segmented anal ray	17.5	17.7	16.1	17.7
Longest anal spine (number)	25.8 (2nd)	23.5 (2nd)	15.4 (2nd)	27.1 (2nd)
Longest segmented anal ray (number)	23.6 (4th)	21.5 (4th)	14.0 (2nd)	24.8 (2nd)
Caudal-fin length	20.9	21.7	32.5	27.9
Pectoral-fin length	26.2	29.7	35.7	38.7
Pelvic spine length	16.0	16.5	17.4	17.4
Pelvic-fin length	21.8	23.6	21.5	24.9

Paratype. USNM 445722, field code: HTP942, GenBank MN922330. 32.3 mm SL, Maloelap Atoll, Republic of the Marshall Islands, 8°37'42"N, 170°59'58"E, depth of collection 120 m, collected with hand nets by HT Pinheiro, TAY Phelps, MV Bell, and LA Rocha, 13 August 2019.

Diagnosis. *Plectranthias polygonius* sp. nov. can be distinguished from all of its congeners by live coloration, in particular the two rows of orange rhomboid-shaped polygons on the lateral part of the body and an elongated yellow and white third dorsal spine (Fig. 1A, D), and by the following combination of characters: dorsal-fin rays X, 16; pectoral-fin rays 14, all unbranched; vertebrae 10+16; continuous lateral line with 27–30 tubed scales; circumpeduncular scales 10 or 11; absence of antrorse spines on the preopercle.

Description. Proportional measurements for the type specimens are presented in Table 1. Dorsal rays X, 16, the last soft ray branched to base and counted as one; first

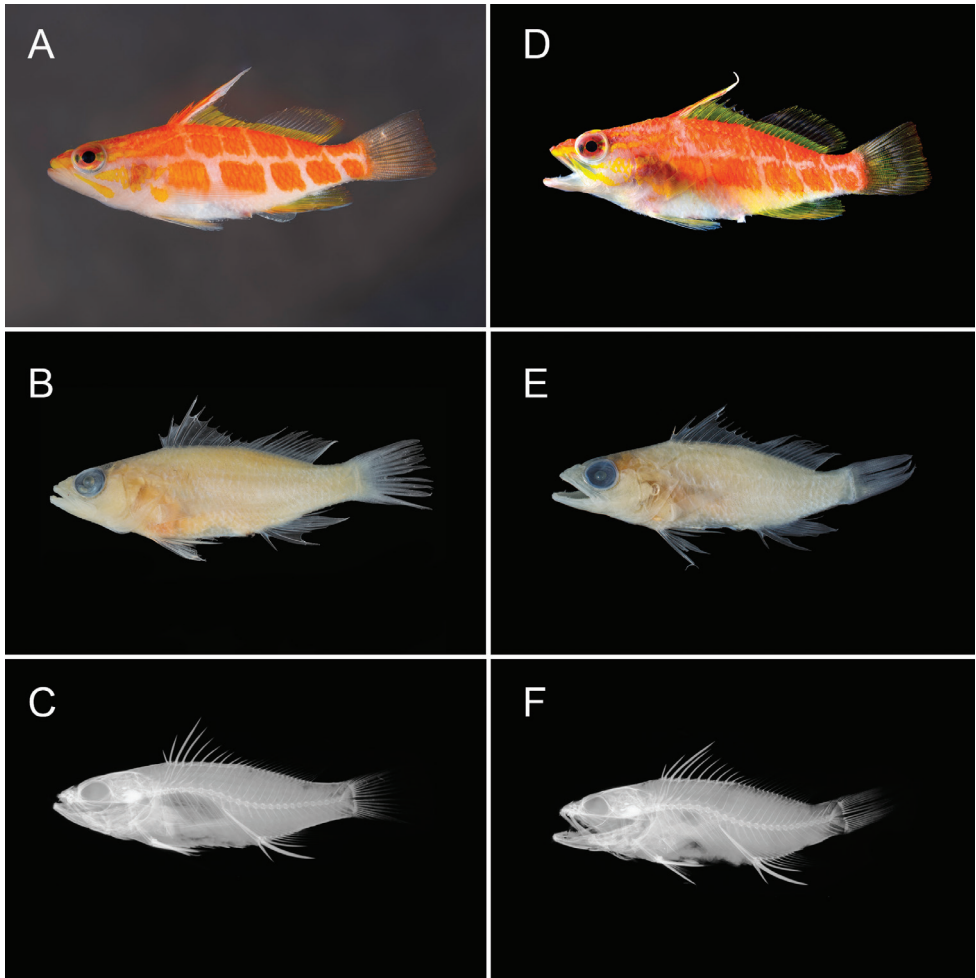


Figure 1. *Plectranthias polygonius* sp. nov. holotype **A** shortly after death **B** preserved **C** radiograph, and paratype **D** shortly after death **E** preserved **F** radiograph. Photographs by LA Rocha (**A**), A Gaisiner (**B**, **E**), J Fong (**C**, **F**), and T Sinclair-Taylor (**D**).

dorsal spine short, 18.0 in SL (15.8); third dorsal spine longest, 1.7 in HL (1.6) with flag-like extension; dorsal-fin base length 2.1 in SL (1.9); anal-fin rays III, 7, last soft ray branched to base and counted as one; anal-fin base length 6.3 in SL (6.5); second anal spine longest and stoutest at 1.6 in HL; anal-fin origin at vertical beneath fourth dorsal-fin ray; pectoral-fin rays 14, all unbranched, length 3.8 in SL (3.4); pelvic fin I, 5; pelvic-fin length 4.6 in SL (4.2); pelvic-spine length 2.0 in HL; procurrent caudal-fin rays 7+6 (6+5); principal caudal-fin rays 9+8.

Body moderately elongate, laterally compressed; depth of body 3.4 in SL (3.2); width of body 2.7 in depth (2.3); head length 3.2 in SL (3.1); snout length 3.4 in HL (3.6); bony interorbital width 1.6 in snout length (1.3); orbit diameter 2.8 in HL;

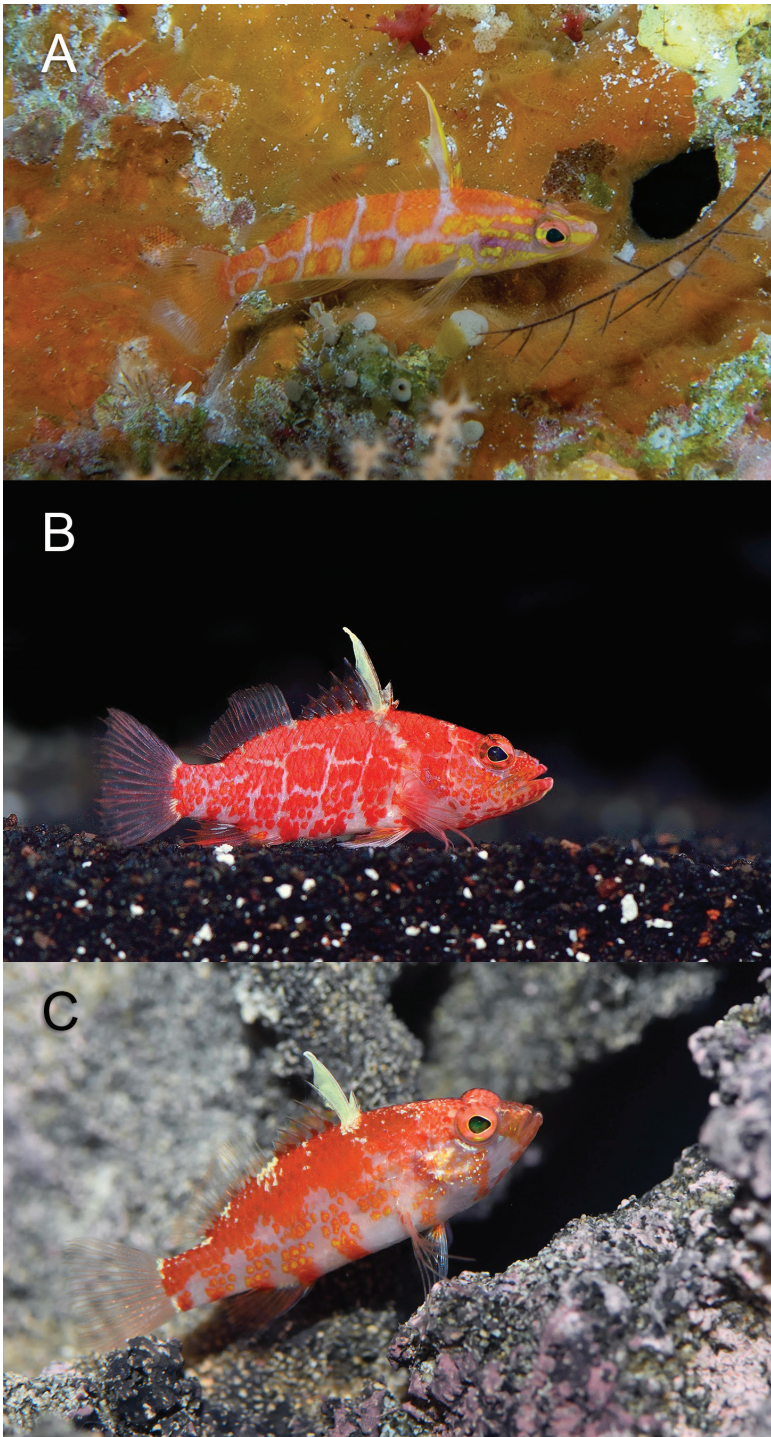


Figure 2. *Plectranthias polygonius* sp. nov. at Erikub Atoll, Republic of the Marshall Islands, at a depth of 120 m (**A**), aquarium photos of *P. inermis* (**B**), and *P. altipinnatus* (**C**). Photographs by LA Rocha (**A**) and YK Tea (**B, C**).

post-orbital head length 4.8 in SL (4.7); least depth of caudal-peduncle 2.5 in HL; caudal peduncle length 3.6 in HL (4.0).

Scales ctenoid; lateral line complete and broadly arched over pectoral fin following body contour; 30 (27) tubed scales; scales above lateral line to origin of dorsal fin 2; scales above lateral line to base of middle dorsal spine 2; scales below lateral line to origin of anal fin 9 (10); diagonal rows of scales on cheek 5; scales on top of head extending anteriorly to vertical from anterior margin of pupil; no scales on chin, maxilla, or snout; circumpeduncular scales 10 (11); gill rakers 5+13 (6+13); vertebrae 10+16; supraneurals 3; anterior supraneural-dorsal ray-pterygiophore-neural spine interdigitation pattern: 0/0+0/2/1+1/1.

Mouth large and terminal, slightly upturned; lower jaw protrudes slightly; maxilla expanded posteriorly, extending to below the posterior edge of eye; dorsal profile of head almost straight; upper jaw with one fixed, stout canine on either side of symphysis; upper canines flanked internally by villiform band with four or five rows of depressible, smaller, sharp-tipped teeth; inner rows become progressively longer, innermost row with largest teeth; lower jaw has pair of fixed, short stout canines on either side of symphysis followed by smaller, depressible, sharp-tipped conical teeth in a villiform band of 3–5 rows; lower teeth become progressively longer on inner rows; vomer roughly V-shaped band of two rows of similarly sized, sharp-tipped, conical teeth; palatines with one row of small, sharp-tipped conical teeth; tongue small, slender, pointed, and without teeth.

Opercle with three spines, the middle spine the longest; preopercle with 14 (17) small spines (serrae) along posterior margin; antrorse spines lacking on ventral margin; interopercle with no spines; subopercle smooth, with no spines; anterior nostrils positioned halfway between snout and eye, each with a small rounded flap rising from anterior rim; posterior nostrils an elliptical opening at anterior border of orbit.

Color in life. *Body:* overall white with two rows of bright orange rhomboid-shaped polygons, four to six in each row, arranged in an irregular grid along lateral midline of body; uppermost row of orange polygons proceeds from behind eye to dorsal third of caudal peduncle; lower row starts just dorsal to origin of pectoral fin and continues to ventral half of caudal peduncle; throat and belly white. *Head:* dorsal third of head orange and bottom two thirds pinkish white with two yellow stripes, both originating from the tip of the upper lip. The first extending horizontally across orbit, bifurcating past posterior edge of pupil to approximately edge of opercle. The second from tip of upper lip, tracing obliquely along maxilla and extending to ventral edge of preopercle. Preopercle region with a yellow triangular patch, from lower mid-orbit expanding in width to edge of preopercle with bifurcations to horizontal edge of operculum and pelvic fin bases respectively; orbit mostly orange-red; iris outlined in silver-grey to black with horizontal yellow stripe through middle of anterior portion; posterior portion of iris with two yellow stripes arising from a bifurcation of the anterior yellow stripe; pupil black. *Fins:* first three membranes of spinous portion of dorsal fin mostly orange with yellow highlights; third spine with yellow and white membrane; remaining membranes of spinous portion mostly yellow, with hyaline tips; yellow coloration continues on lower third of soft portion of dorsal fin, with upper two-thirds mostly

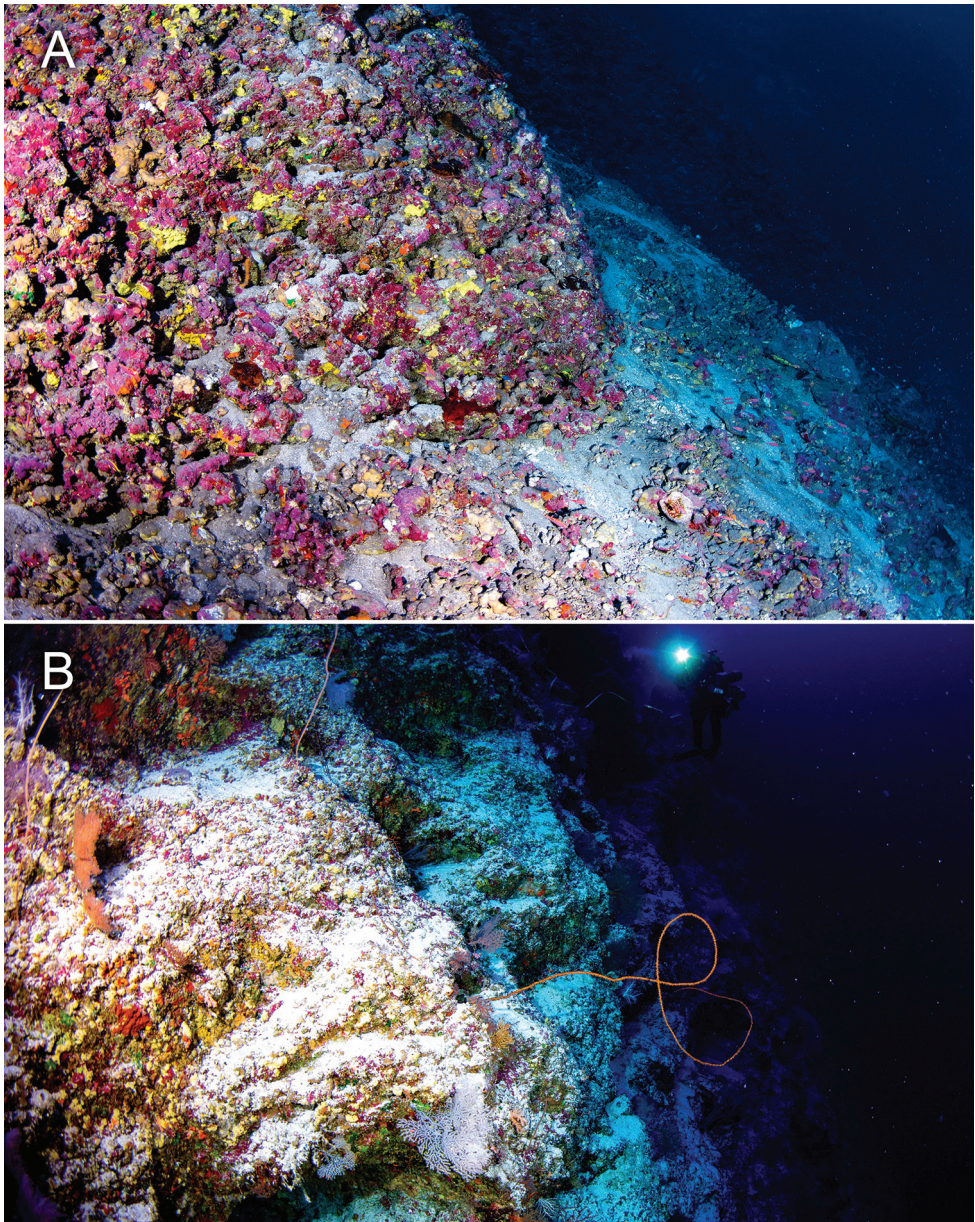


Figure 3. Habitat of *Plectranthias polygonius* sp. nov. and *Plectranthias hinano* sp. nov. in **A** Tahiti, French Polynesia, depth of approximately 100 m, and **B** Erikub Atoll, Republic of the Marshall Islands, depth of approximately 120 m. Photographs by LA Rocha.

hyaline; some yellow and pale orange on tips of soft dorsal and membranes of last four to five rays; caudal fin hyaline with white and orange rays; anal fin mostly yellow, with white margin; pelvic fins mostly white distally, with yellow rays proximally; pectoral fins hyaline. Living specimen photographed in the Marshall Islands exhibits more yel-

low coloration on head, within rhomboid-shaped polygons on lateral midline, and on first three membranes of spinous dorsal fin (Fig. 2A).

Color in alcohol. Light tan overall, with no visible markings.

Etymology. *Plectranthias polygonius* sp. nov. is named for the orange rhomboid-shaped polygons arranged in parallel rows along the lateral midline that distinguish it from all other known species within the genus. To be treated as a noun in apposition.

Distribution and habitat. *Plectranthias polygonius* sp. nov. appears to be the same species as an undescribed *Plectranthias* species that was photographed off Rangiroa, French Polynesia, at a depth of 65 m (Williams et al. 2013). However, some superficial differences exist between our specimen and the one in Williams et al. (2013), including the thickness of the white lines on the upper body and the color of the iris. These may be due to individual variability. The two specimens described in this paper were collected in highly complex reefs predominantly covered by coralline algae and sponges in Tahiti (Fig. 3A) and crevices of steep reef walls in the Marshall Islands (Fig. 3B), indicating that this species probably has a wider Pacific distribution. All known individuals have been observed or collected at mesophotic depths, suggesting that *Plectranthias polygonius* sp. nov., as with most of its congeners, does not inhabit shallow coral reef habitats.

Comparisons. The general body shape, color, and prolongation of the third dorsal-fin spine in *Plectranthias polygonius* sp. nov. resemble *P. inermis* and *P. altipinnatus* (Fig. 2B, C); however, the barcode fragment of the COI gene of *P. polygonius* sp. nov. is not close to any published barcode sequence of *Plectranthias*, with approximately 15% uncorrected pairwise genetic distance from several species in the genus. Morphologically, it can easily be distinguished from *P. inermis* by having ten circumpeduncular scales (vs. 14 or 15 in *P. inermis*); canine teeth on the lower jaw (lacking in *P. inermis*); and 14–17 spines on the posterior edge of the preopercle (spines lacking in *P. inermis*; feebly serrated in *P. altipinnatus*). The new species differs from *P. altipinnatus* by having X, 16 dorsal-fin rays (X, 18 in *P. altipinnatus*), a shallower body (3.2–3.4 in SL vs. 2.8 in *P. altipinnatus*), smaller head (3.1–3.2 in SL vs. 2.2 in *P. altipinnatus*), and a larger eye (2.8 in HL vs. 4.75 in *P. altipinnatus*).

***Plectranthias hinano* sp. nov.**

<http://zoobank.org/84A5C4AA-577B-4D79-BE21-8973EFDF7BE9>

Figures 4, 5, Table 1

Hinano's Perchlet

Type locality. Tahiti, French Polynesia

Holotype. CAS 247195, field code: HTP909, GenBank MN922329. 49.6 mm SL, Tahiti, French Polynesia, 17°29'27"S, 149°28'01"W, depth of collection 98 m, collected with hand nets by B Shepherd, HT Pinheiro, TAY Phelps, MV Bell, and LA Rocha, 03 March 2019 (Fig. 4).

Paratype. USNM 445723, field code: TAH007, GenBank MN922328. 28.0 mm SL, Tahiti, French Polynesia, 17°36'59"S, 149°37'13"W, depth of collection 90 m,

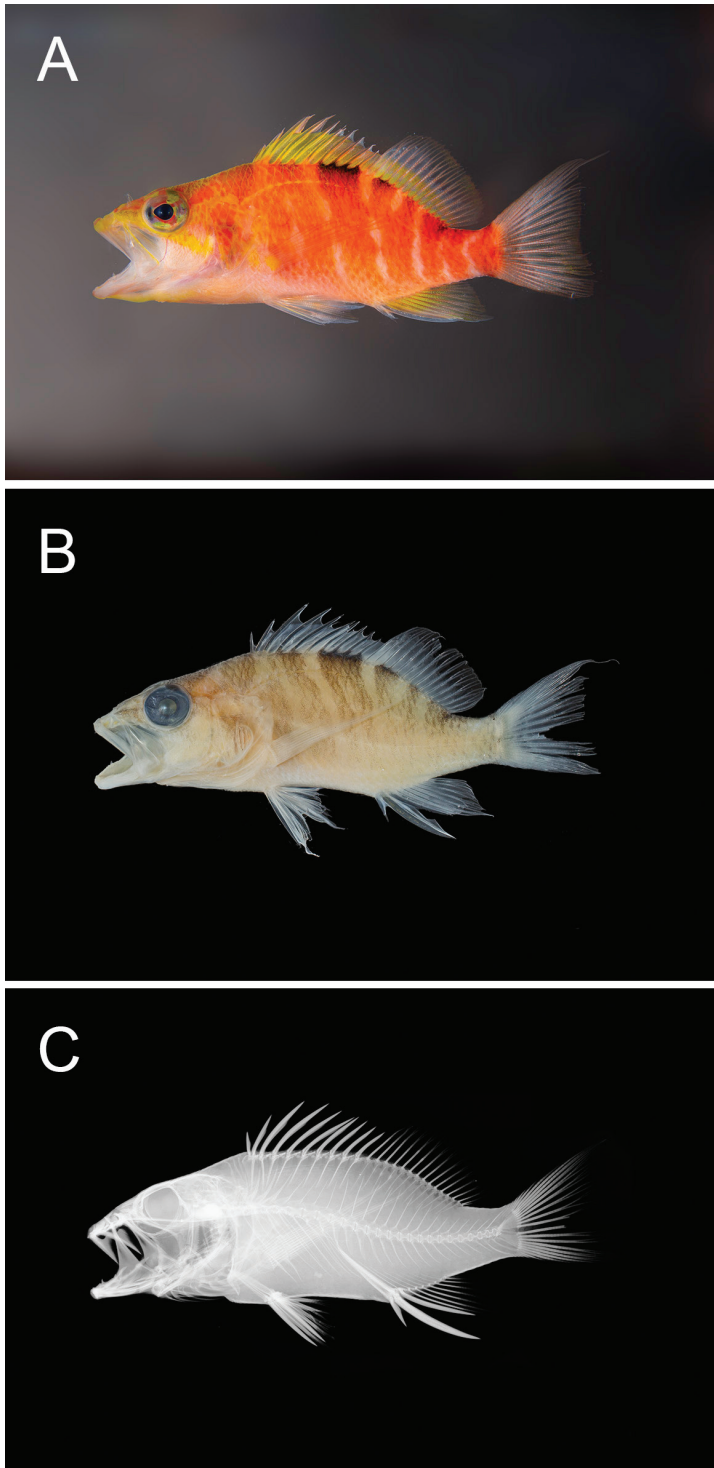


Figure 4. *Plectranthias hinano* sp. nov. holotype **A** shortly after death **B** preserved specimen **C** radiograph. Photographs by LA Rocha (**A**), A Gaisiner (**B**), and J Fong (**C**).

collected with hand nets by B Shepherd, HT Pinheiro, TAY Phelps, MV Bell, and LA Rocha, 28 February 2019.

Diagnosis. *Plectranthias hinano* sp. nov. can be distinguished from all of its congeners by the following combination of characters: dorsal-fin rays X, 15, the last branched to base and counted as one; pectoral fin rays 11 or 12; vertebrae 10+16; lateral line complete with 29–30 tubed scales; gill rakers 7–8+12–13; ventral margin of preopercle with three antrorse spines; snout moderately long, 3.0–3.2 in HL, 12.3–14.2% SL, overall red coloration with two indistinct black spots along the base of dorsal fin, translucent yellow dorsal and anal-fin membranes.

Description. Proportional measurements for the type specimens are presented in Table 1. Dorsal-fin rays X, 15; last soft ray branched to base and counted as one; first dorsal spine very short, 17.6 in SL (9.4); fourth dorsal spine longest, 5.5 in SL (third dorsal spine longest, 6.4 in SL); dorsal-fin base length 2.1 in SL (1.9); anal-fin rays III, 7; last soft ray branched to base and counted as one; anal-fin base 6.2 in SL (5.3); second anal spine longest and stoutest at 2.0 in HL (2.1); anal-fin origin at vertical beneath fourth dorsal-fin ray; pectoral-fin rays 11 (12), all unbranched, length 2.8 in SL (2.6); pelvic fin I, 5; pelvic-fin length 4.6 in SL (4.0); pelvic-spine length 2.4 in HL (2.3); caudal-fin procurvent rays 6+5; caudal-fin principal rays 9+8.

Body moderately elongate, laterally compressed; depth of body 2.9 in SL (3.0); width of body 2.1 in depth (2.4); head length 2.4 in SL (2.5); snout length 3.0 in HL (3.2); bony interorbital width 3.5 in snout length (2.3); orbit diameter 3.7 in HL (3.5); post-orbital head length 5.4 in SL (5.6); least depth of caudal-peduncle 3.7 in HL (3.4); caudal-peduncle length 4.0 in SL (4.1).

Scales ctenoid; lateral line complete and broadly arched over pectoral fin following body contour; 29 (30) tubed scales; scales above lateral line to origin of dorsal fin 3; scales above lateral line to base of middle dorsal spine 2; scales below lateral line to origin of anal fin 12; diagonal rows of scales on cheek 4; scales on top of head extending anteriorly to vertical from center of eye; area on top of head between eyes with scales; no scales on chin, maxilla, or snout; circumpeduncular scales 12; gill rakers 8+13 (7+12); vertebrae 10+16; supraneurals 3; anterior supraneural-dorsal ray-pterygiophore-neural spine interdigitation pattern: 0/0+0/2/1+1/1.

Mouth large and terminal, slightly upturned; lower jaw protrudes slightly; maxilla expanded posteriorly, extending to below the posterior edge of pupil; upper jaw with one fixed, stout canine on either side of symphysis; upper canines flanked internally by villiform band with 7–9 irregular rows of depressible, smaller, sharp-tipped teeth; inner rows become progressively longer, innermost row with largest teeth; lower jaw has one large, fixed canine on either side of lower jaw, roughly at midpoint, followed by smaller, depressible, sharp-tipped conical teeth in a villiform band of 4–6 irregular rows, innermost teeth same size as outer rows; vomer roughly V-shaped band of two rows of similarly-sized, sharp-tipped, conical teeth; palatines with one row of small, sharp-tipped conical teeth anteriorly, two rows posteriorly; tongue small, slender, pointed, and without teeth.

Opercle with three flat spines, the middle spine the longest; preopercle with 22 (12) small spines (serrae) along posterior margin; ventral (inferior) margin of preoper-

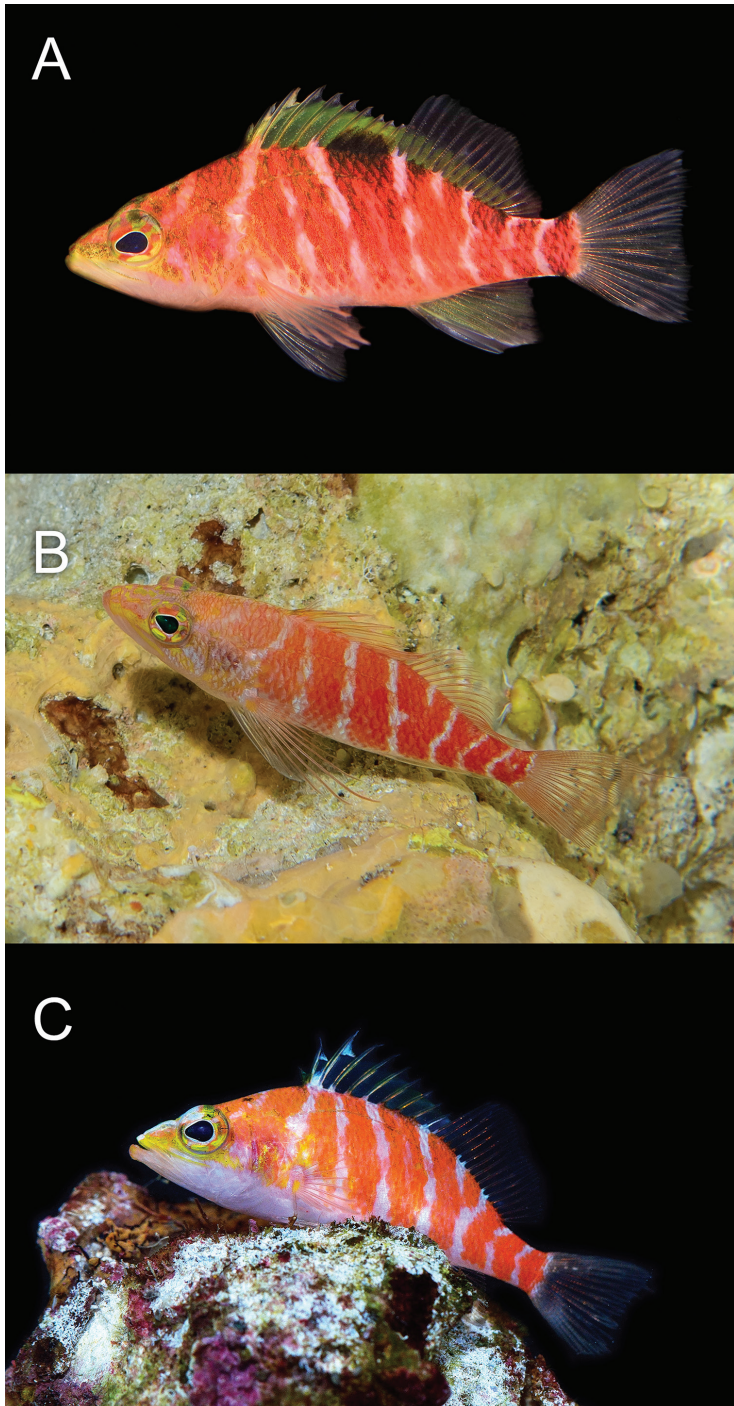


Figure 5. Living specimens of **A** *Plectranthias hinano* sp. nov. at Steinhart Aquarium, California Academy of Sciences **B** *Plectranthias* cf. *bennetti* photographed at a depth of 120 m at Maloelap Atoll, Republic of the Marshall Islands, and **C** *Plectranthias bennetti* photographed in an aquarium. Photographs by T Wong (**A**), LA Rocha (**B**), and YK Tea (**C**).

cle with three antrorse spines; interopercle with no spines; subopercle smooth, with one spine on inferior margin; anterior nostrils positioned closer to eye than to snout, each with a small rounded flap rising from anterior rim; posterior nostrils an elliptical opening at anterior border of orbit.

Color in life. *Body:* overall light red in color; chest and belly mostly light red to pink; dorsal portion of body darker red with yellow along scale margins and lateral line; series of 8–12 pink to white incomplete bars on the body, originating just behind orbit and continuing to base of caudal fin; bars are approximately 20 degrees off of vertical anteriorly, becoming near vertical as they approach base of caudal fin; black spot, almost twice the diameter of orbit, at base of spinous dorsal-fin spines 7–10 and soft rays 1–5, continuing slightly more than halfway up membrane of spinous dorsal; black spot is interrupted by the near-vertical white bar originating below soft rays 1 or 2; smaller second black spot, slightly smaller than orbit, located at base of soft dorsal rays 11–15. *Head:* snout, throat, anterior portion of lower lip, maxilla, and operculum mostly light pink; yellow stripe originating at snout, proceeding across maxilla, below orbit to preopercle; lattice-like network of indistinct yellow stripes radiating outward from pupil across iris, between eyes, across top of head, from ventral margin of orbit to origin of lateral line and lower margin of operculum; iris mostly pink with yellow splotches radiating outward from pupil; pupil black and teardrop-shaped, pointed anteriorly. *Fins:* spinous portion of dorsal fin predominantly translucent yellow, with upper half of black spot on membrane between spines 7–10; lower third of soft dorsal fin mostly translucent yellow, upper two-thirds hyaline; caudal-fin membranes mostly hyaline with some regions a faint transparent yellow, fin rays white with red margins; pelvic fins hyaline with faint yellow on rays; anal fin mostly translucent yellow with hyaline margins; pectoral fins hyaline with rays outlined in pink; base of pectoral fins yellow. Freshly dead specimens exhibit similar coloration, with slightly more yellow on head, body, and fins (Fig. 4A).

Color in alcohol. Light tan overall, with dark brown stippling in vertical bands along lateral sides of body, darkest brown along base of dorsal fin at location of black spots.

Etymology. *Plectranthias hinano* sp. nov. is named after Teurumeariki Hinano Teavai Murphy, former associate director of the University of California Berkeley Gump Research Station and president of the cultural association Te Pu Atitia, in honor of the significant contributions she has made supporting Polynesian biocultural heritage and field research in Moorea, French Polynesia. The name is a noun in the genitive case.

Distribution and habitat. The two specimens described in this paper, plus an individual that was retained for public aquarium exhibition, were collected respectively in Tahiti and Moorea, French Polynesia. A similar species was photographed at 120 m depth in Erikub Atoll, Republic of Marshall Islands, however specimens were not retained (Fig. 5B). The Marshall Islands specimens lack the black markings along the dorsal-fin base, and thus more closely resemble *Plectranthias bennetti* (Fig. 5C), indicating that the latter may have a wider Pacific distribution and not just be restricted to the Coral Sea. All known individuals of *P. hinano* sp. nov. have been observed or col-

lected in highly complex habitats on walls and ledges within MCEs (Fig. 3), suggesting that the species does not inhabit shallow coral reefs.

Comparisons. The most similar barcode fragment of the mtDNA COI gene to *Plectranthias hinano* sp. nov. is *P. bennetti* from the Coral Sea (5.5% uncorrected pairwise genetic distance). Morphologically, it can be distinguished from *P. bennetti* by having a longer snout (3.0–3.2 in HL vs. 4.4 in *P. bennetti*), a larger orbit (3.5–3.7 in HL vs. 4.1 in *P. bennetti*), in the number of circumpeduncular scales (12 vs. 14 in *P. bennetti*), the number of gill rakers (7–8 + 12–13, vs. 5+13 in *P. bennetti*), and in coloration (by having two indistinct black spots along the base of the dorsal fin, and yellow dorsal and anal fin membranes).

Discussion

Species within the genus *Plectranthias* appear to be common and conspicuous inhabitants of MCEs, and we have regularly observed them in highly complex, rocky habitats with abundant coralline algae, sponges, and black corals (Fig. 3). They are usually sampled with the use of hand nets and closed-circuit rebreather technical diving. As with much of the Anthiadae, the genus *Plectranthias* is in need of revision, as it is not currently defined on the basis of synapomorphies, and there is high variation within many of the defining characters (Anderson and Heemstra 2012; Gill et al. 2016). Hence, placement of the two new species presented here should be regarded as provisional. We expect that the known diversity within *Plectranthias* will continue to expand with further MCE exploration, and that future sampling, comparative work, and genetic analysis will unravel some of the taxonomic confusion within this genus.

More than 70% of all research on MCEs has been published in the past seven years (Pyle and Copus 2019), and undoubtedly these discoveries will continue as several teams lead expeditions to global biodiversity hotspots and regions where MCEs have not been previously surveyed. Continued research on mesophotic coral ecosystems (MCEs), whether using submarines, closed-circuit rebreathers or ROVs, is documenting many new species and range extensions for fishes found at depths between 60–150 m (Pyle 2000; Baldwin et al. 2016; Pinheiro et al. 2016, 2019; Pyle et al. 2016; Rocha et al. 2017; Shepherd et al. 2018; Arango et al. 2019; Shepherd et al. 2019). Discovery rates of new species are as high as two new species per hour of exploration (Pinheiro et al. 2019). This, coupled with ecological observations, has led to the conclusion that mesophotic coral reefs are unique and threatened (Baldwin et al. 2018; Rocha et al. 2018). Through research expeditions using technical diving and closed-circuit rebreathers to systematically survey habitats down to 150 m depth across tropical regions of the world, the California Academy of Sciences' Hope for Reefs initiative is advancing the knowledge of the biodiversity and ecology of MCEs. Our goals are not only to document undiscovered species diversity, but also to raise awareness of the need

to protect MCEs from anthropogenic impacts such as climate change, unsustainable fishing practices, plastic pollution, and sedimentation.

Comparative material

Plectranthias inermis. CAS 241326. Philippines, Batangas, 28 April 2015.

P. japonicus. CAS 33555, 1. Philippines, Batangas, 23 June 1966.

P. longimanus. CAS 213185, 3. Fiji, Viti Levu Island, 31 May 1999.

P. sagamiensis. CAS 235596, 1. Philippines, Luzon Island, 02 June 2011.

P. winniensis. CAS 219169, 1. Fiji, Vanua Levu Island, 27 May 2003.

Acknowledgements

This work was funded by the generous support of donors to the California Academy of Sciences' Hope for Reefs Initiative. Our research in French Polynesia was conducted under permit number USR 3278 from the Ministry of Fisheries, and in the Republic of the Marshall Islands under permit from the Marshall Islands Marine Resources Authority. We are grateful to many colleagues who helped in the field, lab, and with discussions: MV Bell, M Bozinovic, C Castillo, D Catania, K de Brum, J Fong, E Kabua-Tibon, M Lane, A Mecho, JE McCosker, A Shafer, G Siu, B Stockwell, YK Tea, H Teavai-Murphy, M White, N Yim, and S Yong. Logistics, equipment, and technical diving support was provided by Hollis Rebreathers LLC, G Siu, L Roattino, C Ciccuto, SubTecnologie, and Indies Trader. We would like to thank J Fong for taking the radiographs, A Gaisiner for photographing the preserved types, T Sinclair-Taylor for photographing the Marshall Islands specimen and field support, T Wong for photographing the living specimen at Steinhart Aquarium, and YK Tea for providing photographs of closely related species and valuable suggestions to improve the manuscript.

References

- Allen GR, Walsh F (2015) *Plectranthias bennetti*, a new species of anthiine fish (Pisces: Serranidae) from the Coral Sea, Australia. *Journal of the Ocean Science Foundation* 16: 82–89. <http://oceansciencefoundation.org/josf/josf16d.pdf>
- Anderson WD, Heemstra PC (2012) Review of Atlantic and eastern Pacific Anthiine fishes (Teleostei: Perciformes: Serranidae), with descriptions of two new genera. *Transactions of the American Philosophical Society, New Series* 102(2): 1–173. <http://www.jstor.org/stable/41507695>
- Arango BG, Pinheiro HT, Rocha C, Greene BD, Pyle RL, Copus JM, Shepherd B, Rocha LA (2019) Three new species of *Chromis* (Teleostei, Pomacentridae) from mesophotic

- coral ecosystems of the Philippines. *ZooKeys* 835: 1–15. <https://doi.org/10.3897/zookeys.835.27528>
- Baldwin CC, Robertson DR, Nonaka A, Tornabene L (2016) Two new deep-reef basslets (Teleostei, Grammatidae, *Lipogramma*), with comments on the eco-evolutionary relationships of the genus. *ZooKeys* 638: 45–82. <https://doi.org/10.3897/zookeys.638.10455>
- Baldwin CC, Tornabene L, Robertson DR (2018) Below the mesophotic. *Scientific Reports* 8 (4920): 1–13. <https://doi.org/10.1038/s41598-018-23067-1>
- Bineesh KK, Akhilesh KV, Gopalakrishnan A, Jena JK (2014) *Plectranthias alcocki*, a new anthiine fish species (Perciformes: Serranidae) from the Arabian Sea, off southwest India. *Zootaxa* 3785: 490–496. <https://doi.org/10.11646/zootaxa.3785.3.10>
- Fricke R, Eschmeyer WN, van der Laan R [Eds] (2019) Eschmeyer's Catalog of Fishes: Genera, Species, References. <http://researcharchive.calacademy.org/research/ichthyology/catalog/fishcatmain.asp>
- Gill AC, Tea YK, Senou H (2016) *Plectranthias takasei*, new species of anthiadine fish from southern Japan (Teleostei: Serranidae). *Zootaxa* 4205(4): 349–356. <https://doi.org/10.11646/zootaxa.4205.4.3>
- Gill AC, Roberts CD (2020) *Plectranthias cruentus*, a new species of anthiadine perchlet (Teleostei: Serranidae) from the Lord Howe Rise, Tasman Sea. *Zootaxa* 4750(4): 560–566. <https://doi.org/10.11646/zootaxa.4750.4.6>
- Heemstra PC, Randall JE (2008) A review of the anthiine fish genus *Plectranthias* (Perciformes: Serranidae) of the Western Indian Ocean, with description of a new species, and a key to the species. *Smithiana Bulletin* 10: 3–17.
- Kearse M, Moir R, Wilson A, Stones-Havas S, Cheung M, Sturrock S, Buxton S, Cooper A, Markowitz S, Duran C, Thierer T, Ashton B, Meintjes P, Drummond A (2012) Geneious Basic: An integrated and extendable desktop software platform for the organization and analysis of sequence data. *Bioinformatics* 28: 1647–1649. <https://doi.org/10.1093/bioinformatics/bts199>
- Kuiter RH (2004) Serranidae & Plesiopidae: A Comprehensive Guide to Basslets, Hamlets, Longfins & relatives. Aquatic Photographics, Seaford, Australia, 108 pp.
- Pinheiro HT, Goodbody-Gringley G, Jessup ME, Shepherd B, Chequer AD, Rocha LA (2016) Upper and lower mesophotic coral reef fish communities evaluated by underwater visual censuses in two Caribbean locations. *Coral Reefs* 35(1): 139–151. <https://doi.org/10.1007/s00338-015-1381-0>
- Pinheiro HT, Shepherd B, Castillo C, Abesamis RA, Copus JM, Pyle RL, Greene BD, Coleman RR, Whitton RK, Thillainath E, Bucol AA, Birt M, Catania D, Rocha LA (2019) Deep reef fishes in the world's epicenter of marine biodiversity. *Coral Reefs* 38: 985–995. <https://doi.org/10.1007/s00338-019-01825-5>
- Pyle RL (2000) Assessing Undiscovered Fish Biodiversity on Deep Coral Reefs Using Advanced Self-Contained Diving Technology. *Marine Technology Society Journal* 34(4): 82–91. <https://doi.org/10.4031/MTSJ.34.4.11>
- Pyle RL, Copus JM (2019) Mesophotic Coral Ecosystems: Introduction and Overview. In: Loya Y, Puglise KA, Bridge Tom CL (Eds) *Mesophotic Coral Ecosystems*. Springer, New York, 1003 pp. <https://doi.org/10.1007/978-3-319-92735-0>

- Pyle RL, Greene BD, Kosaki RK (2016) *Tosanooides obama*, a new basslet (Perciformes, Percoidae, Serranidae) from deep coral reefs in the Northwestern Hawaiian Islands. *ZooKeys* 641: 165–181. <https://doi.org/10.3897/zookeys.641.11500>
- Randall JE (1980) Revision of the genus *Plectranthias* (Serranidae: Anthiinae) with descriptions of 13 new species. *Micronesica* 16(1): 101–187.
- Rocha LA, Pinheiro HT, Wandell M, Rocha CR, Shepherd B (2017) *Roa rumsfeldi*, a new butterflyfish (Teleostei, Chaetodontidae) from mesophotic coral ecosystems of the Philippines. *ZooKeys* 709: 127–134. <https://doi.org/10.3897/zookeys.709.20404>
- Rocha LA, Pinheiro HT, Shepherd B, Papastamatiou YP, Luiz OJ, Pyle RL, Bongaerts P (2018) Mesophotic coral ecosystems are threatened and ecologically distinct from shallow water reefs. *Science* 361: 281–284. <https://doi.org/10.1126/science.aag1614>
- Shepherd B, Phelps T, Pinheiro HT, Pérez-Matus A, Rocha LA (2018) *Plectranthias abiahiata*, a new species of perchlet from a mesophotic ecosystem at Rapa Nui (Easter Island) (Teleostei, Serranidae, Anthiinae). *ZooKeys* 762: 105–116. <https://doi.org/10.3897/zookeys.762.24618>
- Shepherd B, Pinheiro HT, Phelps T, Pérez-Matus A, Rocha LA (2019) *Luzonichthys kiomeamea* (Teleostei: Serranidae: Anthiinae), a new species from a mesophotic coral ecosystem of Rapa Nui (Easter Island). *Journal of the Ocean Science Foundation* 33: 17–27. <https://doi.org/10.5281/zenodo.3237914>
- Wada H, Suzuki T, Senou H, Motomura H (2020) *Plectranthias ryukyuensis*, a new species of perchlet from the Ryukyu Islands, Japan, with a key to the Japanese species of *Plectranthias* (Serranidae: Anthiinae). *Ichthyological Research*. <https://doi.org/10.1007/s10228-019-00725-6>
- Weigt LA, Baldwin CC, Driskell A, Smith DG, Ormos A, Reyier EA (2012) Using DNA Barcoding to Assess Caribbean Reef Fish Biodiversity: Expanding Taxonomic and Geographic Coverage. *PLoS ONE* 7: e41059. <https://doi.org/10.1371/journal.pone.0041059>
- Williams JT, Delrieu-Trottin E, Planes S (2013) Two new fish species of the subfamily Anthiinae (Perciformes, Serranidae) from the Marquesas. *Zootaxa* 3647(1): 167–180. <https://doi.org/10.11646/zootaxa.3647.1.8>

